

UNCLASSIFIED

AD NUMBER
AD835378
NEW LIMITATION CHANGE
TO Approved for public release, distribution unlimited
FROM Distribution authorized to U.S. Gov't. agencies and their contractors; Critical Technology; MAY 1968. Other requests shall be referred to Air Force Materials Laboratory, ATTN: MATC, Wright-Patterson AFB, OH 45433.
AUTHORITY
AFSC ltr dtd 26 May 1972

THIS PAGE IS UNCLASSIFIED

AD885378

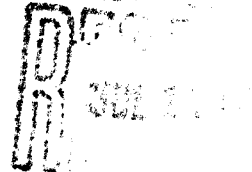
AFML-TR-68-138

MANUFACTURING METHODS FOR HIGH TEMPERATURE COATING OF LARGE COLUMBIUM PARTS

H. A. FISCH
J. D. GADD
TRW Inc.
Cleveland, Ohio



**TECHNICAL REPORT AFML-TR-68-138
MAY 1968**



This document is subject to special export controls and each transmittal to foreign governments or foreign nationals may be made only with prior approval of the Air Force Materials Laboratory (MATC), Wright-Patterson Air Force Base, Ohio 45433.

**AIR FORCE MATERIALS LABORATORY
AIR FORCE SYSTEMS COMMAND
WRIGHT-PATTERSON AIR FORCE BASE, OHIO**

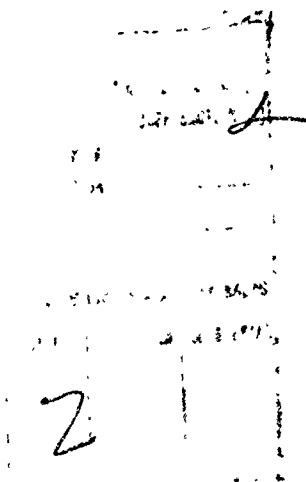
NOTICES

When U.S. Government Drawings, Specifications, or other data, are used for any purpose other than a definitely related Government procurement operation, the Government thereby incurs no responsibility nor any obligation whatsoever; and the fact that the Government may have formulated, furnished, or in any way supplied the said drawings, specifications, or other data, is not to be regarded by implication or otherwise, as in any manner licensing the holder or any other person or corporation, or conveying any rights or permission to manufacture, use or sell any patented invention that may in any way be related thereto.

Reproduction in whole or in part is prohibited except with the permission of the Manufacturing Technology Division. However, DDC is authorized to reproduce the document for "U.S. Governmental Purposes".

Do not return this copy unless return is requested by security considerations, contractual obligations, or notice on a specific document.

This document is subject to special export controls and each transmittal to foreign governments or foreign nationals may be made only with prior approval of the Air Force Materials Laboratory (MATC), Wright-Patterson Air Force Base, Ohio 45433.



AFML-TR-68-134

MANUFACTURING METHODS FOR
HIGH TEMPERATURE COATING OF
LARGE COLUMBIUM PARTS

H. A. Fisch
J. D. Gadd

TRW INC.
Cleveland, Ohio

TECHNICAL REPORT AFML-TR-68-134

May 1968

This document is subject to special export controls and each transmittal to foreign governments or foreign nationals may be made only with prior approval of the Air Force Materials Laboratory (MATC), Wright-Patterson Air Force Base, Ohio 45433.

Air Force Materials Laboratory
Air Force Systems Command
Wright-Patterson Air Force Base, Ohio

FOREWORD

This Final Technical Report was prepared by the Equipment Laboratories Division of TRW, Inc., Cleveland, Ohio. The work was initiated by the Chemical Processing Branch (MATC) of the Manufacturing Technology Division, Air Force Materials Laboratory under Contract AF 33(615)-2018, Project 3-183. The program was accomplished under the technical direction of Mr. G. E. Eichelman and Mr. W. P. Johnson, Chemical Processing Branch, Manufacturing Technology Division, Wright-Patterson Air Force Base, Ohio. The manuscript was released by the authors 30 April 1968.

The work described, to develop manufacturing methods for providing a high temperature coating for large columbium parts, was performed during the period from 1 December 1964 to 1 April 1968. The contract was managed by Dr. J.D. Gadd, Manager, Coatings; Dr. S. Baranow and Dr. E. Roland. Significant contributions were made by Dr. H. A. Fisch, Principal Engineer, R. A. Jefferys, O. Heighton, Dr. A. Nemy and A. Bond. The report has been given corporation internal number ER-7268.

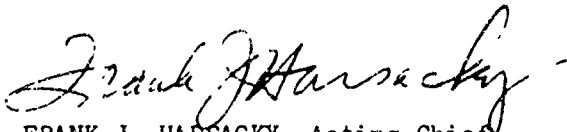
Closely related efforts were covered under MMP Projects 8-264, "Refractory Metal Coatings by Chemical Vapor Deposition"; 8-346, "Refractory Metal Coatings by the Fused Salt Method"; 8-184, "Fluidized Bed Techniques for Coating Refractory Metals" and 8-344, "Electrophoretic Deposition of Refractory Metal Coatings".

This project has been accomplished as a part of the Air Force Manufacturing Methods Program, the primary objective of which is to develop, on a timely basis, manufacturing processes, techniques and equipment for use in economical production of USAF materials and components. The program encompasses the following technical areas:

- Chemical - Propellant, Coating, Ceramics, Graphite, Nonmetallics
- Electronic - Solid State, Materials & Special Techniques, Thermionics
- Fabrication - Forming, Material Removal, Joining, Components
- Metallurgy - Rolling, Forging, Extruding, Casting, Fiber, Powder

Suggestions concerning additional manufacturing methods development required on this or other subjects will be appreciated.

This technical report has been reviewed and is approved.



FRANK J. HARSACKY, Acting Chief
Chemical Processing Branch
Manufacturing Technology Division
Air Force Materials Laboratory

ABSTRACT

A program was conducted to develop a manufacturing method for producing the high temperature oxidation resistant Cr-Ti-Si coating on large columbium parts. The program was accomplished in three principle development areas: 1) scale-up of the diffusion pack process for producing the Cr-Ti-Si coatings, 2) scale-up of the slurry diffusion process for producing this coating, and 3) production proof of the slurry diffusion process. A vacuum furnace with hearth dimensions of 42" diameter X 48" high was constructed and successfully adapted to application of the Cr-Ti-Si coating. Cr-Ti-Si coatings formed in the production-scale furnace by both the vacuum pack and slurry-diffusion methods reliably protected columbium alloys from oxidation for times greater than 125 hours at 1800°F and 50 hours at 2600°F.

Three secondary areas of investigation were also undertaken: 1) an investigation of the effects of edge preparation and edge radius on the protection offered by the Cr-Ti-Si coating system 2) a development using fused silicides locally applied and fired either in argon or air for repairing defects in unoxidized and oxidized coatings, and 3) an evaluation of the effect of the Cr-Ti-Si coating system on the tensile properties of 0.018 inch Cb752 alloy sheet.

This document is subject to special export controls and each transmittal to foreign governments or foreign nationals may be made only with prior approval of the Air Force Materials Laboratory (MATC), Wright-Patterson Air Force Base, Ohio 45433.

TABLE OF CONTENTS

<u>Section</u>	<u>Page</u>
1 INTRODUCTION -----	1
2 SUMMARY -----	2
MATERIALS AND TEST PROCEDURES -----	7
3.1 Materials -----	7
3.2 Coating Test Procedures -----	7
3.3 Construction of the Production-Scale Furnace ---	9
4 VACUUM-PACK PROCESS DEVELOPMENT -----	15
4.1 Heat Transfer Studies -----	15
4.2 Pilot Scale Coating Process Studies -----	24
4.2.1 Cr-Ti Coating Conditions -----	25
4.2.2 Silicon Coating Conditions -----	29
4.2.3 Coating Oxidation Test Results -----	29
4.2.4 Conclusions from the Pilot-Scale Studies -----	55
4.3 Coating Studies in the Production-Scale Furnace -----	59
4.4 Coating Process Reproducibility Studies -----	63
4.5 Preliminary Production Proof -----	76
4.5.1 Oxidation Testing of Cr-Ti-Si Coated Segmented Structures -----	83
5 SLURRY DIFFUSION PROCESS DEVELOPMENT -----	93
5.1 Laboratory Investigation -----	93
5.1.1 Bisque Thickness -----	94
5.1.2 Slurry Application Technique -----	94
5.1.3 Gettering Techniques -----	94
5.1.4 Support Method -----	97
5.1.5 Effect of Slurry Variables on Coating Cr-Ti Coating Characteristics --	99
5.1.6 Evaluation of Coating Process Parameters -----	99
5.2 Coating Process Reproducibility Studies -----	111
5.3 Preliminary Production Proof -----	115
5.3.1 Oxidation Testing of Slurry-Diffusion Cr-Ti-Si Coated Segmented Structures ---	124
6. PRODUCTION PROOF -----	133

<u>Section</u>	<u>Page</u>
7. EDGE EFFECT AND COATING DEFECT REPAIR STUDIES -----	149
7.1 Edge Effect Studies -----	149
7.1.1 Edge Effect with Diffusion-Pack Coated Coupons -----	151
7.1.2 Edge Effect with Slurry Diffusion Coated Coupons -----	156
7.2 Coating Defect Repair Studies -----	156
7.2.1 Repair of Defects in Unoxidized Coatings -----	159
7.2.2 Repair of Defects in Oxidized Coatings -----	165
8. TENSILE PROPERTIES OF Cr-Ti-Si COATED Cb-752 ALLOY SHEET -----	175
9. CONCLUSIONS -----	179
10. BIBLIOGRAPHY -----	181

APPENDICES

<u>APPENDIX</u>	<u>Page</u>
I Cr-Ti and Si Weight Gains on Columbium Alloys - Coupons Coated in Module Runs 1-15 as a Function of Pack Position -----	182
II Oxidation Lives of Module Vacuum-Pack Coated Coupons as a Function of Pack Position -----	189
III Oxidation Lives of Module Vacuum-Pack Coated Coupons as a Function of Alloy Composition -----	219
IV Summary of Oxidation Lives of Coupons Coated in Module Runs -----	249
V Results of Module Studies in the Production-Scale Furnace -----	263
VI Oxidation Test Results from the Vacuum-Pack Reproducibility Study -----	276
VII Oxidation Performance Data of Slurry-Diffusion Coated Coupons Evaluated in the Factorial Experiments -----	283

LIST OF ILLUSTRATIONS

<u>Figure No.</u>		<u>Page</u>
1	Cr-Ti-Si Coated Columbium Alloy - As Coated -----	10
2	Schematic Layout of the Production Scale Bell Furnace -----	12
3	Cross Sectional View of the Production Scale Bell Furnace -----	13
4	Photograph of the Production Scale Facility -----	14
5	Graph of $\alpha t/S^2$ Vs. θ_o/θ_i For a Cylinder of Infinite Length. Wall Temperature Suddenly Changed -----	17
6	Thermal Diffusivity Test Apparatus -----	19
7	Typical Time-Temperature Graph for 60Cr-40Ti Pack at 100 to 150 Torr Helium Pressure -----	20
8	Typical Time-Temperature Graph for a Silicon Pack at 100 to 150 Torr Helium Pressure -----	21
9	Thermal Diffusivity of 60Cr-40Ti Powder as a Function of Gaseous Environment, Pressure, and Temperature -----	22
10	Thermal Diffusivity of Silicon Powder as a Function of Gaseous Environment, Pressure, and Temperature -----	23
11	Key to Positioning of Columbium Alloy Specimens in Module -----	26
12	Time-Temperature Relationships for Cr-Ti Coating Deposition -----	28
13	Time-Temperature Relationships for Silicon Coating Deposition -----	30
14	Time-Temperature Relationships for Silicon Coating Deposition -----	31
15	Wrinkling on Cr-Ti-Si Coated Columbium Alloys -----	39
16	Section Through a Small "Wrinkle" B-66 Alloy Heated 1 Hour in Vacuum at 2700°F -----	40
17	Section Through a Large "Wrinkle" B-66 Alloy Heated 1 Hour in Vacuum at 2700°F -----	41

LIST OF ILLUSTRATIONS (continued)

Figure No.		Page
18	B-66 Alloy Specimen After 9 Hours at 2700°F -----	42
19	Percent Cumulative Failure Vs. Cyclic Oxidation Life at 2700°F for B-66 and D-43 Alloy Specimens -----	44
20	Hours to Failure Vs. Ratio $\Delta W_{Cr-Ti}/\Delta W_{Si}$ For Cr-Ti-Si Coated Cb Specimens Oxidation Tested at 1800°F-----	45
21	Hours to Failure Vs. Ratio $\Delta W_{Cr-Ti}/\Delta W_{Si}$ For Cr-Ti-Si Coated Cb Specimens Oxidation Tested at 2500°F -----	46
22	Cr-Ti Coated B-66 Alloy Specimens, Module Run 1 -----	48
23	Cr-Ti Coated B-66 Alloy Specimens, Module Run 4 -----	49
24	Cr-Ti-Si Coated B-66 Alloy Specimens, Module Run 1 -----	50
25	Cr-Ti-Si Coated B-66 Alloy Specimens, Module Run 4 -----	51
26	Cr-Ti-Si Coated B-66 Alloy Specimens, Module Run 10 -----	52
27	Cr-Ti-Si Coated B-66 Alloy Specimens, Module Run 15 -----	53
28	Photomicrograph of Cr-Ti Coated B-66 Alloy Specimens from Module Run 3 and Module Run 13 Showing the Random Thinning and Disappearances of the Cr-Ti Coating -----	54
29	Average Cr-Ti Weight Gain Vs. Total Amount of Activator for All Coating Runs Using the Module Retort and 60Cr- 40Ti Powder -----	57
30	Cr-Ti-Si Coated Cb-752 Alloy Specimens from Vacuum Pack Reproducibility Run A -----	67
31	Cr-Ti-Si Coated Cb-752 Alloy Specimens from Vacuum Pack Reproducibility Run B -----	68
32	Cr-Ti-Si Coated Cb-752 Alloy Specimens from Vacuum Pack Reproducibility Run C -----	69
33	Cr-Ti Coatings on Cb-752 Columbium Alloy Formed from Used (Depleted) and New 60Cr-40Ti Alloy Pack Material -----	70
34	EMP Images of Cr-Ti Coating on Cb-752 Columbium Alloy Formed from New 60Cr-40Ti Alloy Pack Media -----	72

LIST OF ILLUSTRATIONS (continued)

Table No.		Page
35	EMP Images of Cr-Ti Coating on Cb-752 Columbian Alloy Formed from Used (Depleted) 60Cr-40Ti Alloy Pack Media -----	73
36	Photomicrograph and EMP X-Ray Images from Cross Section of Used (Depleted) Nominal 60Cr-40Ti Alloy Pack Particle -----	75
37	Cr-Ti Coating Weight Gain at Various Positions in the 12-inch Diameter Retort -----	77
38	Silicon Coating Weight Gain at Various Positions in the 12-inch Diameter Retort -----	78
39	Diffusion Pack Cr-Ti-Si Coated Cb-752 Alloy Segmented Structures -----	80
40	Photomicrographs of the Cr-Ti-Si Coating on a Control Coupon from the Diffusion-Pack Preliminary Production Proof -----	82
41	Simulated Flight Temperature Profile Used for Cyclic Oxidation Testing Coated Structures -----	84
42	Diffusion Pack Cr-Ti-Si Coated Cb-752 Alloy Corrugated Panel After Oxidation Testing -----	86
43	Diffusion Pack Cr-Ti-Si Coated Cb-752 Alloy Box Panels After Oxidation Testing -----	87
44	Diffusion Pack Cr-Ti-Si Coated Cb-753 Alloy Cylinders After Oxidation Testing -----	88
45	Diffusion Pack Cr-Ti-Si Coated Cb-752 Alloy Sheet Panels After Oxidation Testing -----	89
46	Diffusion Pack Cr-Ti-Si Coated B-66 Alloy Sheet Panels After Oxidation Testing -----	90
47	Diffusion Pack Cr-Ti-Si Coated C129Y Alloy Sheet Panels After Oxidation Testing -----	91
48	Slurry Coated Specimen Showing Bisque Finish and Edge Coverage -----	96
49	Schematic Sketch of the Columbian Coating Retort Showing the Cr-Ti Getter Seal -----	98

LIST OF ILLUSTRATIONS (continued)

<u>Figure No.</u>		<u>Page</u>
50	Cr-Ti Coated Cb-752 Alloy Specimens Showing the Effect of Varying the System Pressure -----	100
51	Summary of Cr-Ti Coatings on B-66 and D-43 Alloys by the Slip Pack Technique -----	101
52	Cr-Ti Coating Cycle -----	113
53	Silicon Coating Cycle -----	114
54	Cr-Ti-Si Coated Columbium Alloy Specimens from Slurry-Diffusion Process Reproducibility Run A -----	117
55	Cr-Ti-Si Coated Columbium Alloy Specimens from Slurry-Diffusion Process Reproducibility Run B -----	118
56	Cr-Ti-Si Coated Columbium Alloy Specimens from Slurry-Diffusion Process Reproducibility Run C -----	119
57	Non-Uniform Cr-Ti Coating on B-66 Alloy Sheet Panel -----	120
58	Photomicrographs of Cr-Ti Coating on B-66 Alloy Sheet Panel -----	121
59	Cr-Ti-Si Coating on Cb-752 Coupon from Slurry-Diffusion Preliminary Proof Run -----	123
60	Segmented Structure Parts Cr-Ti-Si Coated Using the Slurry Diffusion Process - Preliminary Production Procf Run -----	125
61	Columbium Alloy Sheet Panels Cr-Ti-Si Coated Using the Slurry Diffusion Process - Preliminary Production Proof Run -----	126
62	Slurry Diffusion Cr-Ti-Si Coated Corrugated Panel After Oxidation Testing -----	128
63	Slurry Diffusion Cr-Ti-Si Coated Cylinders After Oxidation Testing -----	129
64	Slurry Diffusion Cr-Ti-Si Coated Box Panels After Oxidation Testing -----	130
65	Slurry Diffusion Coated Cb-752 Alloy Sheet Panels After Oxidation Testing -----	131

LIST OF ILLUSTRATIONS (continued)

Figure No.		Page
66	Slurry Diffusion Coated C129Y Alloy Sheet Panels After Oxidation Testing -----	132
67	As Received Cb-752 Alloy Nose Cone -----	135
68	As Received Cb-752 Alloy Equipment Support Ring -----	136
69	Cb-752 Alloy Ring and Cone Sections Before Cr-Ti-Si Coating -----	137
70	Silicon Bisque on Nose Cone After Silicon Coating Cycle -----	139
71	Nose Cone and Silicon Bisque After Bisque Removal -----	140
72	Ring Section 1 with Silicon Bisque After Coating -----	141
73	Ring Section 2 with Silicon Bisque After Coating -----	142
74	Ring Section 2 with a Portion of the Silicon Bisque Removed After Completion of the Coating Cycle -----	143
75	Cr-Ti-Si Coated Nose Cone and Ring Sections -----	144
76	Microstructures of the Cr-Ti-Si Coating on Production Proof Test Control Specimens Cb-752 Alloy -----	146
77	Columbium Alloy Sheet Panels After Ten Simulated Flight Temperature Cycles -----	148
78	Typical Edge Finishes on 0.030 Inch Thick Cb-752 Alloy Coupons -----	150
79	Cr-Ti-Si Coated 0.020 Inch Thick Edge Effect Coupons -----	154
80	Failure Modes on Cr-Ti-Si Coated Cb-752 Alloy Coupons -----	157
81	Cb-752 Coupon Edges After Air Oxidation for One Hour at 2600°F -----	162
82	Edge and Surface Defect Repairs on Cb-752 Alloy Using Fused Slurry Silicides - Argon - 2600°F - 1 Hour -----	163
83	Edge Repair on Cb-752 Alloy Coupon Made With Fused Si-20Cr-20Fe-10VSi ₂ Slurry -----	164

LIST OF ILLUSTRATIONS (continued)

<u>Figure No.</u>		<u>Page</u>
84	Repaired Surface Defects on Cr-Ti-Si Coated Cb-752 Alloy - After Oxidation Testing -----	166
85	Repaired Surface Defects in Cr-Ti-Si Coated Cb-752 Alloy - After Oxidation Testing at 1800°F -----	167
86	Repaired Surface Defects in Cr-Ti-Si Coated Cb-752 Alloy - After Oxidation Testing at 2600°F -----	168
87	Repaired and 1800°F Oxidation Tested Defects in Preoxidized Coupons -----	171
88	Repaired and 1800°F Oxidation Tested Defects in Preoxidized Coupons -----	172

LIST OF TABLES

<u>Table No.</u>		<u>Page</u>
1	CHEMICAL COMPOSITION OF COATING POWDERS -----	8
2	MODULE RUN PROCESSING PARAMETERS -----	27
3	COMPILATION OF WEIGHT GAIN AND OXIDATION PERFORMANCE ----	32
4	PRODUCTION SCALE FURNACE PROCESS DEVELOPMENT PARAMETERS -	60
5	COMPILATION OF WEIGHT GAIN AND OXIDATION PERFORMANCE-----	61
6	PARAMETERS USED FOR THE VACUUM PACK REPRODUCIBILITY RUNS -----	64
7	COMPILATION OF RESULTS FOR THE VACUUM PACK REPRODUCIBILITY COATING RUNS -----	66
8	OXIDATION TEST RESULTS-PRELIMINARY PRODUCTION PROOF COUPONS -----	81
9	VACUUM-PACK Cr-Ti-Si COATED HARDWARE-OXIDATION TEST RESULTS -----	85
10	OBSERVATIONS REGARDING SLURRY APPLICATION METHODS -----	95
11	RANDOMIZED FRACTIONAL FACTORIAL EXPERIMENT -----	105
12	COMPILATION OF MAIN EFFECTS AND INTERACTIONS CALCULABLE FOR THE Cr-Ti COATING CYCLE BY THE ANALYSIS OF VARIANCE METHOD -----	106
13	COATING PARAMETERS FOR SLURRY-DIFFUSION REPRODUCIBILITY RUNS -----	112
14	COMPILATION OF RESULTS FROM THE SLURRY-DIFFUSION REPRODUCIBILITY COATING RUN -----	116
15	SLURRY-DIFFUSION COATED COUPON OXIDATION TEST RESULTS ---	124
16	SLURRY-DIFFUSION Cr-Ti-Si COATED HARDWARE OXIDATION TEST RESULTS -----	127
17	COMPARISON BETWEEN VACUUM-PACK AND SLURRY-DIFFUSION COATING PROCESSES -----	134
18	SLURRY-DIFFUSION COATING PARAMETERS FOR PRODUCTION PROOF -----	138

LIST OF TABLES (continued)

<u>Table No.</u>		<u>Page</u>
19	PRODUCTION PROOF COATING WEIGHT GAINS-CONTROL COUPONS -----	145
20	OXIDATION PERFORMANCE OF CONTROL COUPONS FROM THE PRODUCTION PROOF -----	147
21	COMPILATION OF HOURS TO FAILURE AND FAILURE MODE OF EDGE STUDY COUPONS PACK COATED WITH TITANIUM DEPLETED 60Cr-40Ti AND SILICON-OXIDATION TESTED AT 1800°F-----	152
22	COMPILATION OF HOURS TO FAILURE AND FAILURE MODE OF EDGE STUDY COUPONS PACK COATED WITH TITANIUM DEPLETED 60Cr-40Ti AND SILICON-OXIDATION TESTED AT 2600°F-----	153
23	COMPILATION OF HOURS TO FAILURE AND FAILURE MODE OF EDGE STUDY COUPONS PACK COATED WITH 60Cr-40Ti ALLOY AND SILICON OXIDATION TESTED AT 2500°F-----	155
24	COMPILATION OF HOURS TO FAILURE AND FAILURE MODE OF EDGE STUDY COUPONS DIFFUSION-PACK COATED WITH 50Cr-50Ti ALLOY AND SILICON OXIDATION TESTED AT 2600°F-----	158
25	SUMMARY OF RESULTS FOR EDGE DEFECT STUDY -----	160
26	OXIDATION PERFORMANCE OF REPAIRS TO DEFECTS IN Cr-Ti-Si COATED Cb-752 COUPONS -----	169
27	OXIDATION PERFORMANCE OF REPAIRS TO DEFECTS IN PREOXIDIZED Cr-Ti-Si COATED Cb-752 COUPONS -----	173
28	TENSILE PROPERTIES OF AS RECEIVED AND Cr-Ti-Si COATED 0.018 INCH Cb-752 SHEET -----	176
29	TENSILE PROPERTIES OF Cb-752 SHEET -----	177

1 INTRODUCTION

The development of the vacuum pack process for Cr-Ti-Si diffusion alloy coating originated in 1958, when TRW made the initial development of the process to coat columbium alloy aircraft gas turbine components. By 1960, Air Force support was provided for the further development of the coating and process for use in aerospace reentry applications under Contract AF 33(616)-7215, and since that time under Contract AF 33(657)-7396.

During this time the Cr-Ti-Si vacuum-pack coating process advanced from a laboratory method to a pilot-scale operation, Air Force contractors requiring columbium coatings for structure development programs provided further impetus to the process scale-up effort. The first requirement came with the Air Force-McDonnell Aircraft columbium alloy fin and rudder structures program, AF 33(616)-6578, which required coatings on several thousand threaded fasteners and other components too large for the then available small laboratory coating furnace. Solely on the basis of development information, the vacuum pack process was scaled up from a 3 inch diameter by 8 inch long retort to a 7-1/2-inch diameter by 18 inch long retort. The vacuum-pack process for this retort and furnace was further improved and optimized for use with the Air Force-McDonnell Aircraft ASSET program AF 33(616)-6106. As the requirements for larger parts on the ASSET program and the Air Force-Martin brazed honeycomb panel program, AF 33(657)-7276, became apparent, the vacuum-pack process was again scaled up, this time to a pack retort size of 24 x 24 x 8 inches.

The goals of the program summarized in this report were to construct a production scale coating facility, and to develop a reproducible method for applying the Cr-Ti-Si coating to large columbium alloy parts. Two processes for applying the Cr-Ti-Si coating were developed: a vacuum-pack process and a slip-pack process. In addition to these process development activities, investigations were made regarding the effect of edge preparation and sheet thickness on cyclic oxidation life of the Cr-Ti-Si coating at 1800 and 2600°F. Coating defect repair techniques were also developed utilizing a fused silicide approach, and the effect of the coating on the tensile properties of Cb752 alloy sheet was evaluated.

2 SUMMARY

This report presents the results of a 40 month effort under Contract AF 33(615)-2018. The program followed four principal areas: (1) construction of manufacturing-scale vacuum furnace, (2) scale-up of the diffusion pack process for producing the Cr-Ti-Si coating on columbium alloys Cb752, B66 and C129Y, (3) scale-up of the slurry diffusion process for producing this coating, and (4) a production proof utilizing the slurry diffusion process. Three secondary areas of investigation were also undertaken: (1) an investigation of the effects of edge preparation and edge radius on the protection offered by the Cr-Ti-Si coating system, (2) the development of a technique for repairing defects in unoxidized and oxidized Cr-Ti-Si coatings, and (3) an evaluation of the effects of the Cr-Ti-Si coating system on the tensile properties of 0.018 inch thick Cb752 alloy sheet.

A production-scale vacuum furnace with a hot zone 42 inches diameter and 48 inches high was built during the first phase of the program. Concurrent with this effort, the heat transfer characteristics of the Cr-Ti-Si coating were developed in a pilot-scale facility. The results of these latter two activities were employed to develop the following process parameters for use in the production-scale furnace:

	<u>Cr-Ti Coating</u>	<u>Silicon Coating</u>
Powder Composition (w/o)	60Cr-40Ti	100 Si
Particle Size (mesh)	-8 + 30	-8 + 30
Activator 2 CrCl ₃ : 1NaF (w/o)	0.75	
KF (w/o)		0.25
Coating Temperature (°F)	2300	1900
Coating Time (hours)	8	3.5-4
System Pressure (helium, torr)	10	1

In order to demonstrate the vacuum-pack process reproducibility, three Cr-Ti-Si coating runs were made using the production furnace. Coupons of Cb752 alloy were coated in each run. The criteria of reproducibility were that the coatings demonstrate 90 percent reliable lives, based on a Weibull analysis, of at least 125 hours at 1800°F, 50 ± 10 hours at 2600°F, and that the Weibull shape factor be greater than unity. The oxidation protection afforded by these coatings exceeded these performance criteria.

As a preliminary proof of the vacuum pack coating process, a segmented structure, which simulated an aerospace configuration, was fabricated using joint designs currently employed for aerospace structures. The structures were fabricated from 0.018 inch thick Cb752 alloy sheet. The

Cr-Ti-Si coating was to be formed on these structures using the parameters established in the reproducibility runs. However, prior to this experiment, it was found by chemical analysis that the Cr-Ti powder which had been used for the reproducibility trials was depleted in titanium. A new lot of 60Cr-40Ti alloy powder was therefore procured for use in the preliminary production proof run. Since the reproducibility parameters were established with titanium deficient 60Cr-40Ti alloy powder, an adjustment in these parameters was necessary to account for the increased titanium concentration in the new powder source. Decreasing the system pressure was known to decrease the available titanium in the pack vapor phase. Therefore, the Cr-Ti cycle of the preliminary production proof was performed at a pressure of 1×10^{-2} torr, rather than 10 torr, and the lower vapor pressure NaF was employed for activation rather than the CrCl_3 -NaF mixture. All other coating parameters for the Cr-Ti and the subsequent siliciding cycle were those used for the reproducibility runs. The oxidation performance criteria were that the structures survive 50 hours of life testing at 2600°F, and 10 simulated flight temperature cycles from room temperature to 2600°F. In oxidation testing this hardware, the only coating failures were at faying surfaces, regions where the coating was accidentally damaged by handling, and on welds where unalloyed columbium was inadvertently used as filler. The coating produced under the above processing conditions was not optimum for unalloyed columbium. On properly fabricated and tested parts, the oxidation performance of the Cr-Ti-Si coated structures met or exceeded the target requirements for both tests. Coupons also coated in these runs and oxidation life tested at 1800, 2200, 2600 and 2800°F showed 90 percent reliable oxidation lives of 690, 500, 60 and 20 hours, respectively.

The slurry-diffusion process was also scaled up for use in the production size furnace. In order to establish coating parameters for this process, a series of 16 statistically designed Cr-Ti-Si coating experiments was made in a laboratory scale furnace. These runs produced coated coupons which were oxidation life tested at 1800 and 2600°F. The significant coating parameters and interactions, and their relationships to Cr-Ti coating weight gain, were evaluated by an analysis of variance technique. The relationships of Cr-Ti and silicon weight gains to 1800 and 2600°F oxidation lives were subsequently evaluated by a multiple regression analysis. The results of these analyses were the basis for the selection of slurry-diffusion parameters for three Cr-Ti-Si coating reproducibility runs. The parameters for these runs were as follows:

	<u>Cr-Ti Coating</u>	<u>Silicon Coating</u>
Powder Composition (w/o)	50Cr-50Ti	100 Si
Particle Size (mesh)	-250 + 325	-250 + 325
Activator NaF (w/o)	2	
KF (w/o)		2
Bisque Weight (gm/cm ²)	0.2	0.2
Coating Temperature (°F)	2350	2000
Coating Time (hours)	10	2
System Pressure (argon, torr)	100	100

In each reproducibility run, coupons made of three columbium alloys, Cb752, B66 and C129Y, were Cr-Ti-Si coated and oxidation tested at 1800 and 2600°F. The criteria for satisfactory oxidation performance were the same as those specified for the diffusion pack coating reproducibility run. These performance criteria were attained by all three alloys coated in each run. Before performing the slurry-diffusion preliminary proof it was determined experimentally that the total surface area of the hardware being slurry coated exerted a profound influence on the coating element deposition process. Increasing the hardware surface area increased the total quantity of bisque and activator in the system; and with 50Cr-50Ti alloy in the bisque the result was excessive titanium transfer to the coating. In this case, a reduction in the titanium content of the Cr-Ti powder was warranted, and the preliminary production proof was made using 60Cr-40Ti alloy powder. The hardware configurations and oxidation test procedures were the same as those used for the vacuum pack preliminary proof. The segmented structures met the oxidation performance criteria, and the 90 percent reliable oxidation lives of test coupons coated with this hardware were as follows: 1800°F - 509 hours, 2200°F - 400 hours, 2600°F - 160 hours, and 2800°F - 22 hours.

Based upon a comparison of oxidation performance, coating appearance, coating microstructure, heat transfer considerations, and other factors, the slurry diffusion process was selected for use in the final production proof phase of the program. Three production proof runs were made using large Cb-752 alloy parts acquired by the Air Force. In the first run, a nose cone section 10.5 inches diameter by 12 inches high was coated. In each of the other two runs, one-half of a 16 inch diameter support ring was coated. Again 60Cr-40Ti powder was used. The coating parameters were the same as those employed in the reproducibility runs, except that the siliconizing cycle was increased to 4 hours to provide additional soaking time for the massive parts. Control coupons cut from the hardware were also Cr-Ti-Si coated in the appropriate coating runs. The large parts were not oxidation tested; however,

the coupons from each of the runs exhibited oxidation lives in excess of 200 hours at 1800°F and 125 hours at 2600°F. It was demonstrated by these three runs that reliable Cr-Ti-Si coatings can be formed on columbium alloy hardware, in the manufacturing scale facility constructed for this program.

Investigations were made regarding the effects of alloy substrate thickness and edge preparation on the oxidation protection afforded by the Cr-Ti-Si coating at 1800 and 2600°F. For sheet thicknesses in the range 0.015 to 0.030 inches, edges were prepared to radii in the range 0.002 to 0.009 inches by grit blasting, tumbling and hand honing. The Cr-Ti-Si coating was applied using both vacuum-pack and slurry-diffusion processes. The vacuum pack coated specimens were oxidation life tested at 1800 and 2600°F. At 1800°F there were no failures after 667 hours of testing of the vacuum-pack coated specimens; also, there were no failures after 802 hours of testing of the slurry diffusion coated specimens at this temperature. At these relatively long exposure times, the tests were stopped and it was concluded that at 1800°F there was no preferential deterioration of the coating at edges or corners. For the vacuum pack coated specimens tested at 2600°F, initial failures occurred as early as 14 hours, while in some cases the failures did not occur until 138 hours of exposure. For slurry diffusion coated coupons, the initial failure times were in the range 79 to 148 hours. However, the test results showed no correlation of failure time and location with edge preparation or edge radius for either the vacuum-pack or slurry-diffusion coated specimens.

Intentional edge and surface defects were prepared by grinding through an unoxidized Cr-Ti-Si coating into the substrate. These defects were covered with either one of two fused slurry silicides, Si-20Cr-20Fe or Si-20Cr-20Fe-10VSi₂, and heated for one hour at 2600°F under a pressure of 150 torr argon. Both slurries produced repairs which were compatible with the substrate and the original coating. These repairs provided oxidation protection for times greater than 794 hours at 1800°F and 150 hours at 2600°F, and both slurries provided essentially equivalent protection.

Localized defect failures which had occurred at edges, corners and on surfaces of Cr-Ti-Si coated specimens exposed to air at 1800 and 2600°F for times from 6 to 60 hours were cleaned by abrasive blasting to remove the oxides, and to expose the substrate and the surrounding unoxidized coating. These regions were covered with each of the slurry coatings. The repaired specimens were then re-exposed to air at 1800 and 2600°F. The compatibility of each slurry with the substrate and the coating was again good, and each slurry was equally effective in affording oxidation protection to the repaired regions. Protective lives greater than 38 hours at both temperatures were found.

Defects in unoxidized Cr-Ti-Si coatings were similarly repaired by firing each of the two slurry silicides in air for one hour at 2600°F.

After heating, both slurries formed adherent fused deposits over the defects. On subsequent oxidation testing these repairs were protective for times greater than 100 hours at 1800°F and 50 hours at 2600°F. Successful repairs to oxidized, damaged coatings were not made using air-fired slurries.

Tensile properties of uncoated and Cr-Ti-Si coated 0.018 inch thick Cb752 alloy sheet were determined at room temperature and 2200°F. At room temperature the U.T.S. and 0.2 percent offset Y.S. of Cb752 were essentially unaffected by the presence of Cr-Ti-Si coatings formed by either the vacuum-pack or slurry-diffusion processes, while the ductility (percent elongation) was sharply reduced. At 2200°F the coating had no adverse effect on the strength or ductility of the alloy.

3 MATERIALS AND TEST PROCEDURES

3.1 Materials

Three columbium-base alloys, B66 (Cb-5Mo-5V-1Zr), C129Y (Cb-10W-10Hf-0.1Y) and Cb752 (Cb-10W-2.5Zr) were used in the process development. These alloys were of ordinary commercial composition. The as received analyses of the alloy powders used to form the Cr-Ti and silicon coatings are given in Table I. The variations in the powder compositions had no apparent effect on the coatings.

3.2 Coating Test Procedures

The recommendations of the Materials Advisory Board (1) were used as a guide for the oxidation test procedures. At temperatures below 1800°F the specimens were removed from the furnace, cooled in ambient air to room temperature, and examined at 4 hour intervals for the first 200 hours of exposure. Subsequently, examination was made after each of two 4-hour exposures and one 16-hour exposure in each 24 hour period. At higher temperatures to 2700°F, specimens were examined after each hour of exposure for the first 100 hours, and subsequently, after each of five 1-hour exposures and one 16-hour exposure in a 24-hour period. Specimens were considered to have failed when there was evidence of oxide protrusions on the surface, or there were visible defects such as sites of erosion through the coating.

The data were analyzed by the Weibull cumulative frequency function as recommended by Wurst(2). The Weibull function is defined by:

$$F(t) = 1 - \exp (-t/\theta + \alpha/\theta)^\beta$$

Where $F(t)$ = fraction of cumulative failures

t = time

θ = time to failure of 63.2% of the sample population

β = shape parameter

α = the threshold or location parameter (normally equal to zero)

Since each set of test data was represented by less than 50 samples, median range values were used for the graphical plots. The table of median range values relates the percent cumulative failures within a given sample size to the percentage values which would have been obtained had an infinite number of samples been tested. Deviations from a single straight line denote polymodal failure mechanisms or a mixed population sample. The significance of the shape factor, β , is that for $\beta \leq 1$ failure is considered random and is usually due to coating defects. For $\beta > 1$ the failure mechanism is primarily through

TABLE 1

CHEMICAL COMPOSITION OF COATING POWDERS

Composition, Weight Percent (1)

Nominal Composition	Lot No	Cr	Ti	Si	Fe	Ca	C	H	O
70Cr-30Ti	OMC 2391	68.1	29.6	-	0.44	-	0.023	0.0165	0.25
60Cr-40Ti	OMC 2321	58.1	37.5	-	-	-	0.015	1×10^{-4}	0.42
60Cr-40Ti	OMC 2390	57.07	40.46	-	0.50	-	0.027	0.0465	0.49
60Cr-40Ti	OMC 3412	59.0	40.6	-	0.20	-	0.021	0.001	0.13
50Cr-50Ti	OMC 3487	50.5	49.2 (2)	-	.122	-	0.023	0.0143	0.13
100Si	01063	-	-	98.67	0.50	0.07			

(1) Based on vendor's analysis
Cr-Ti powder supplied by Oregon Metallurgical Corporation
Silicon powder supplied by Cerac Incorporated

(2) Composition by difference.

wearout, with $\beta = 3.6$ representing a near normal distribution. Values for β were evaluated graphically following a method described by Nelson (3).

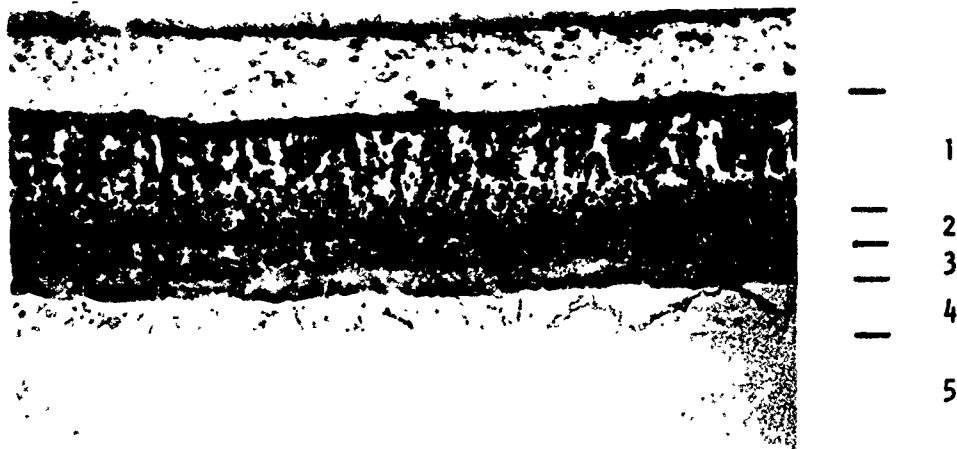
In this program, a considerable portion of the analysis of coating formation and oxidation performance of the Cr-Ti-Si coating system was based on microscopic evaluation of the coatings. For this reason, it is appropriate here to discuss the morphology of an ideal Cr-Ti-Si coating system.

The morphology of the Cr-Ti-Si coating system shown in Figure 1 has been described in detail elsewhere (4), and only the salient features will be mentioned here. The initial Cr-Ti coating cycle forms a Laves phase $(\text{Cb,Ti})\text{Cr}_2$ over a diffusion zone containing chromium and titanium in solid solution. The Cr-Ti-Si coating is a disilicide coating containing concentration gradients of chromium, titanium and columbium across the disilicide region and can be represented as $(\text{Cr,Ti,Cb,X})\text{Si}_2$, where X represents alloying elements in the columbium matrix, e.g., tungsten in Cb752. Two lower silicide regions, $(\text{Cr,Ti,Cb,X})\text{Si}_3$ and $(\text{Cr,Ti,Cb,X})\text{Si}_5$ form beneath the disilicide region. The solid solution region adjacent to the columbium alloy matrix contains chromium, titanium and silicon in solid solution. Formation of the optimum Cr-Ti-Si coating depends upon the proper deposition of the prior Cr-Ti coating. The amount of chromium and titanium in this coating must be sufficient to form, after siliconizing, the three Cr-Ti rich silicide surface regions, as well as a Cr-Ti enriched solid solution substrate diffusion region. An indication that the proper amounts of chromium and titanium have been transferred to the alloy substrate is given by the presence of $(\text{Cb,Ti})\text{Cr}_2$ Laves phase protrusions from the continuous overlay into the solid solution diffusion zone. This transfer occurs along diffusion paths formed by the alloy substrate grain boundaries, and has the appearance of irregular spikes.

Tensile tests were performed on coated and uncoated Cb752 alloy sheet at room temperature and 2200°F. All tests were conducted in an Instron tensile machine in accordance with the test procedures recommended by the Materials Advisory Board. For room temperature tests a crosshead travel of 0.005 in/min was employed to at least 0.6% offset, and then increased to 0.050 in/min thereafter until fracture. At 2200°F the rate of crosshead travel was maintained at 0.050 in/min from zero strain to fracture. Quartz lamp radiant heating was employed in 2200°F air tests of Cr-Ti-Si coated sheet. Specimen temperature was monitored with a Pt vs. Pt10Rh thermocouple. At room temperature a gage extensometer was used to record load-strain curves. However, at the elevated temperatures the load-extension curves based on crosshead travel were used. Original substrate dimensions were used for all stress calculations.

3.3 Construction of the Production-Scale Furnace

As part of this program a production-scale furnace was designed and constructed for coating parts in a vacuum or low-pressure



- 1 (Cr,Ti,Cb,X--) Si_2 Zone Etched 500X
 2 (Cr,Ti,Cb,X--) Si_2 Zone
 3 (Cr,Ti,Cb,X--) Si_3 Zone
 4 Cr,Ti,Si Solid Solution Zone
 5 Columbian Alloy Substrate

Figure 1 Cr-Ti-Si Coated Columbian Alloy - As Coated.

inert gas atmosphere. A schematic of the furnace is presented in Figures 2 and 3, and photographs of the furnace and control panel are shown in Figure 4. The hot zone is 42 inches diameter and 48 inches high, with a total heated volume of about 44 cubic feet. Heat is provided by ten parallel-connected hair-pin shaped elements made from 0.25 inch diameter molybdenum rod. The elements are equally spaced around the circumference of the hot zone and extend vertically to within 6 inches of the top and 0.5 inch of the bottom of the zone. All of the internal brickwork, the furnace wall and the hearth is high purity alumina brick. The cascade water cooled furnace bell is stainless steel. The rumping system consists of an 8-inch diameter oil diffusion pump backed by a 100 cfm. mechanical pump. System pressures are monitored by thermocouple gages in the furnace hearth, the furnace exhaust manifold, diffusion pump inlet line and mechanical pump inlet line. Provision is made for measuring the furnace hot volume temperature at eight different locations using ceramic shielded Pt vs. Pt10Rh thermocouples. These temperatures are recorded on a multipoint recorder and two recorder-controllers. During operation, one of the recorder-controllers is used only as a recorder and serves as a backup controller. The thermocouple connections are completely interchangeable, and any one of the eight thermocouples may be used as the input to either controller. The furnace can be isolated from the pumping system by a gate valve, and provision is made for rapid cool-down by forced gas circulation.

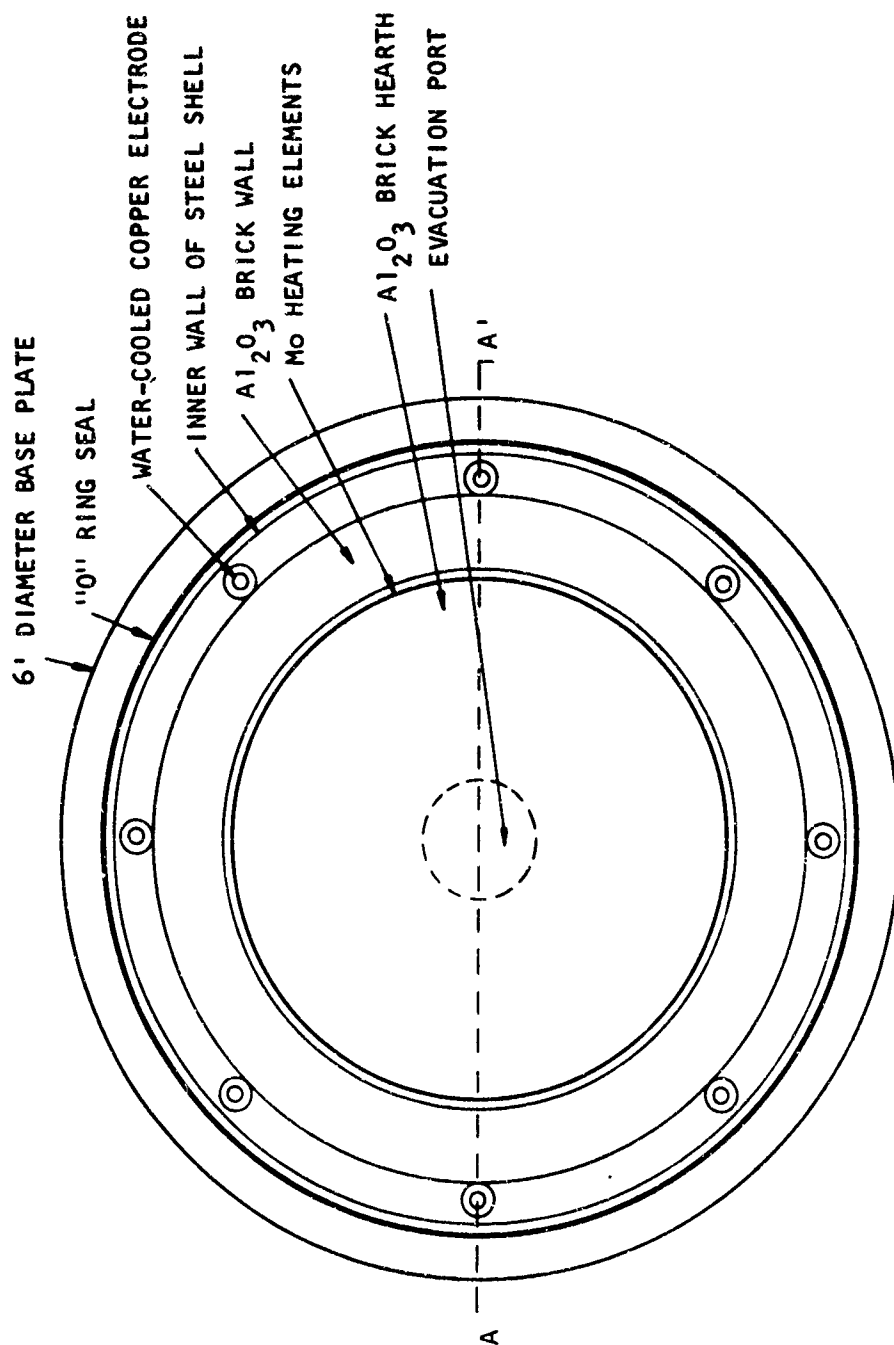


Figure 2 Schematic Layout of the Production Scale Bell Furnace

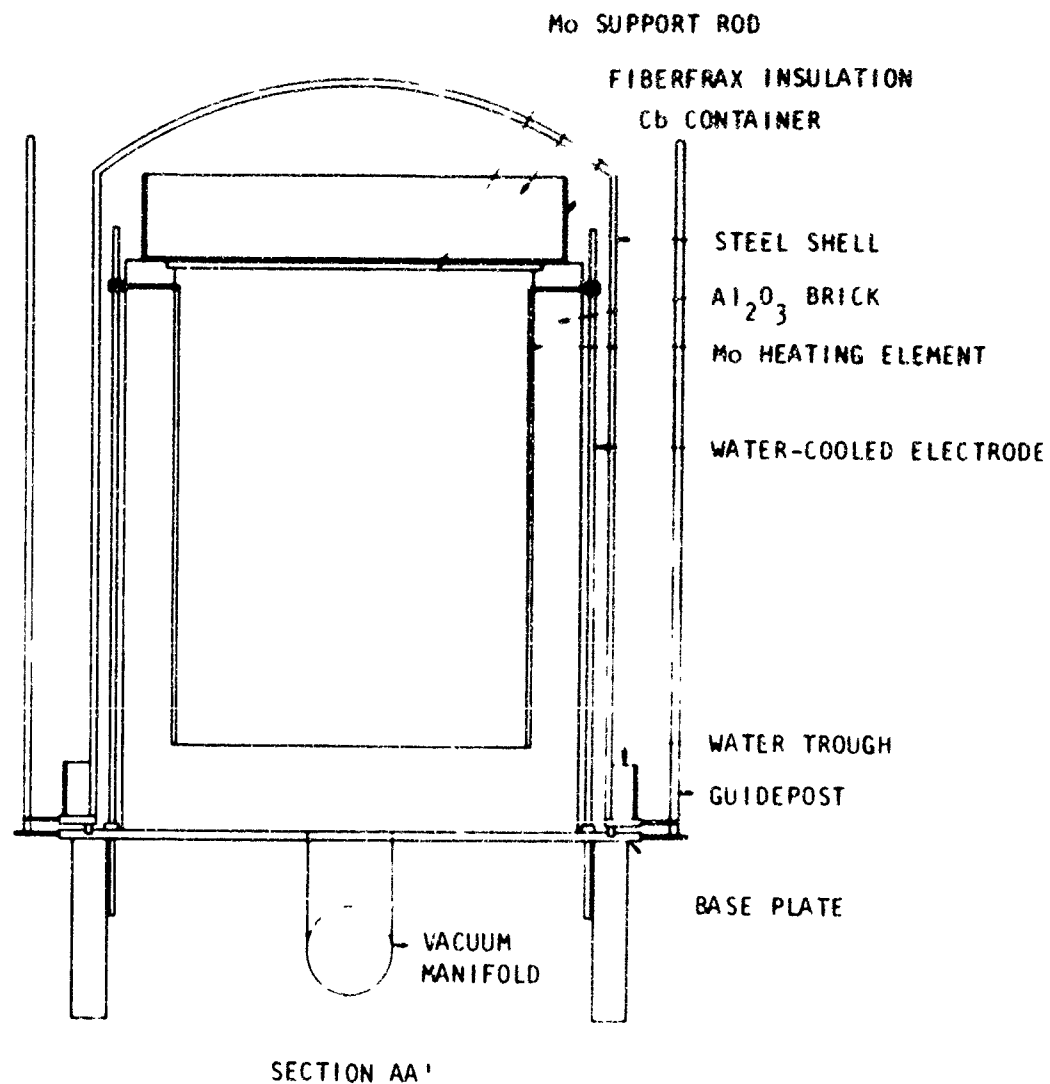


Figure 3 Cross Sectional View of the Production Scale Bell Furnace

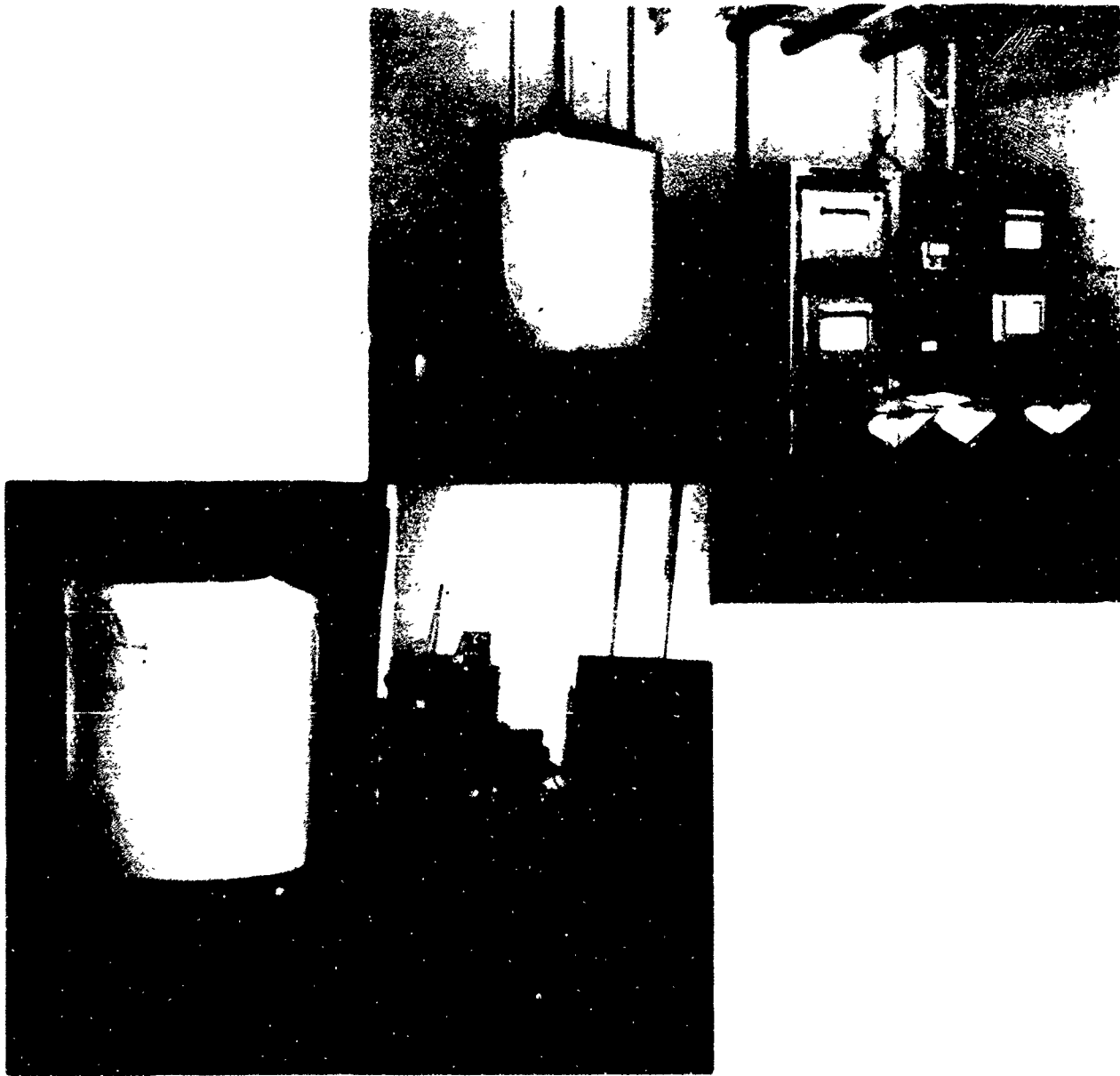


Figure 4. Photograph of the Production Scale Facility

4 VACUUM-PACK PROCESS DEVELOPMENT

Development of the manufacturing scale vacuum pack process was divided into four sequential phases: 1) heat transfer studies, 2) pilot-scale coating process studies, 3) process reproducibility studies in the production furnace, and 4) preliminary production proof.

Heat transfer is an important factor affecting the practicality of the vacuum pack process for coating large parts. In a large pack, temperature gradients exist from the hot retort wall toward the center of the pack. The thermal diffusivity of the Cr-Ti or silicon pack must be known in order to estimate the time-temperature history, and hence the rate of coating formation, at any point within the pack. This information would allow the prediction of coating times and temperatures for different pack sizes.

Process parameters for both the Cr-Ti and silicon cycles were developed in a pilot-scale study. These data were obtained in order to provide information needed for scale-up to the production size furnace, and were obtained during the time when the production furnace was being constructed.

The results from the pilot-scale study led to the selection of Cr-Ti and silicon coating process parameters for use in the production scale furnace. To demonstrate the reproducibility of the coating process in the production scale furnace, three Cr-Ti-Si coating runs were made, and the coated parts were oxidation tested at 1800 and 2600°F.

As a preliminary production proof of the vacuum process, and its applicability to the coating of aerospace structures, a Cr-Ti-Si coating run was performed with fabricated columbium hardware. Three segmented-structural configurations were coated and oxidation tested at 1800 and 2600°F. Coupons were coated along with these structures for oxidation testing at 1800, 2200, 2600 and 2800°F.

4.1 Heat Transfer Studies

The apparent thermal diffusivities of 60Cr-40Ti* and silicon powders as a function of temperature, gaseous environment and pressure were determined in order to analyze the heat transfer data related to the Cr-Ti-Si coating process; and, to predict the time-temperature cycle for the production scale process. The experiments were designed to determine the thermal diffusivity under conditions closely approximating those encountered in a coating cycle.

* In this report nominal compositions will be given in weight percent except when noted.

Calculations of thermal diffusivity from the experimental data were based on the theoretical solution to the problem of unsteady heat flow in a cylinder of infinite length outlined as follows:

The general equation for heat flow in one dimension(s) may be written as:

$$\frac{\partial t}{\partial \tau} = \frac{K}{\rho C_p} \frac{\partial^2 t}{\partial x^2} = \alpha \frac{\partial^2 t}{\partial x^2} \quad (1)$$

Where $\alpha = \frac{K}{\rho C_p}$ thermal diffusivity,
 K = thermal conductivity,
 ρ = density,
 C_p = specific heat at constant pressure,
 τ = time
 t = temperature
 x = distance

For an infinitely long cylinder, initially at a uniform temperature $t = t_i$, and whose surface temperature is suddenly changed (at time $\tau = 0$) to $t = t_s$ and then permanently held at t_s , Equation 1 leads to the following relation:

$$t_o = t_s + (t_i - t_s) \frac{\alpha \tau}{s^2} \quad (2)$$

Where s = radius of the cylinder,
 t_s = temperature of retort wall for $t > 0$
 t_o = temperature of pack center for $t > 0$
 t_i = initial equilibrium temperature of pack for $t > 0$

Equation 2 may be rearranged to

$$\frac{t_o - t_s}{t_s - t_i} = \frac{\Theta_o}{\Theta_i} = \frac{\alpha \tau}{s^2} \quad (3)$$

The relationship⁽⁶⁾ between $\frac{\Theta_o}{\Theta_i}$ and $\frac{\alpha \tau}{s^2}$ is shown in Figure 5.

Thermal diffusivities of 60Cr-40Ti powder and silicon powder in vacuum, helium and argon atmospheres were calculated from Equation 3 using experimentally determined equilibrium values of t_s , t_o , t_i , and Figure 5.

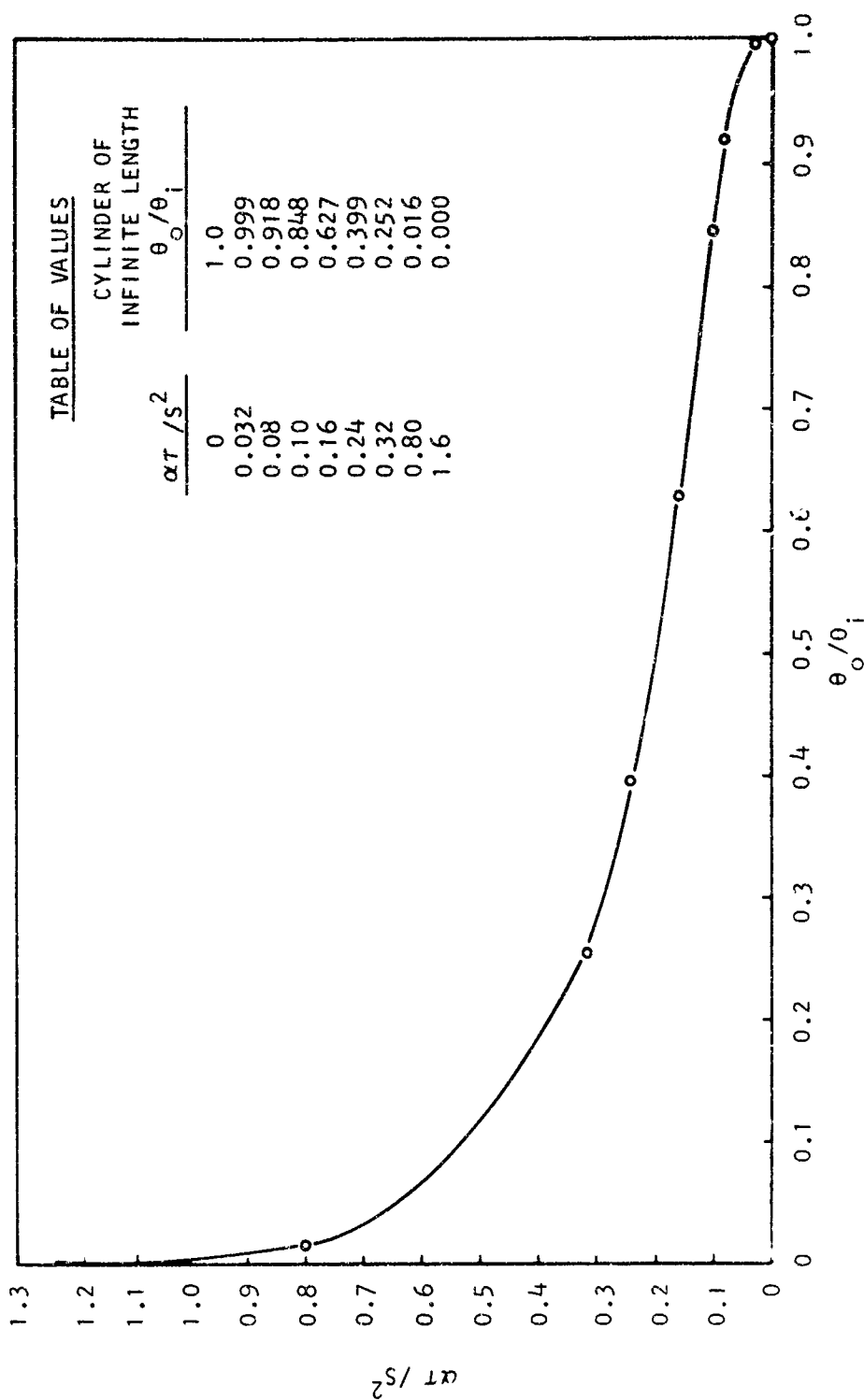


Figure 5 Graph of $\alpha\tau/s^2$ Vs. θ_o/θ_i For a Cylinder of Infinite Length.
Wall Temperature Suddenly Changed

The apparatus used to determine the thermal diffusivities of the 60Cr-40Ti and 100 silicon powder is shown in Figure 6. A columbium container 3.3-inches in diameter x 12-inches high, and having a wall thickness of 0.060-inch, was used as the retort. Prior to filling the retort, two Pt vs Pt10Rh thermocouples were attached to the outside wall exactly 6-inches from the retort bottom and 180° apart. In addition, a tantalum tube 0.375-inch O.D. X 0.0625-inch wall thickness was centered in the retort, and another Pt vs Pt10Rh thermocouple was positioned in the tube to monitor the temperature in the center of the pack, 6-inches from the retort bottom. This tube was of sufficient length to extend completely out of the hot zone when the retort was positioned in the hearth. This was done in order to eliminate contamination of the thermocouple by pack material or coating vapors during the experiment.

The diffusivity apparatus was placed into an induction-heated furnace, and the appropriate vacuum or gas environment was established. The wall temperature was very quickly increased by 300°F, and this temperature was maintained until the pack center temperature reached equilibrium. By successively raising the wall temperature in 300°F increments, and allowing the pack center to come to temperature equilibrium, a range of wall temperature and corresponding pack center temperatures was obtained.

Figures 7 and 8 show graphical representations of the experimental data for a typical experiment using a 60Cr-40Ti pack and a silicon pack at a helium pressure of 100 to 150 torr. From these experimental data, values of θ_0 and θ_i were calculated (equation 3), while $\alpha t/S^2$ values were read from Figure 5. Multiplying $\alpha t/S^2$ by the experimental values of S^2/t yielded a value of α for each value of t_c . The average value of α for each group of measurements was calculated and plotted against the mean temperature $(t_i + t_s)/2$ of the particular series of measurements.

The results of these experiments are presented in Figures 9 and 10. Figure 9 shows values of thermal diffusivity for -6 + 30 mesh size 60Cr-40Ti alloy powder over a temperature range from 200 to 2000°F in helium, argon and vacuum atmospheres. The thermal diffusivity of the Cr-Ti pack for an atmosphere of helium at 100-150 torr increased almost linearly from 0.07 in²/min at room temperature to 0.085 in²/min at 2000°F. The corresponding diffusivity values for an argon atmosphere of 100-150 torr were 0.015 and 0.05 in²/min, respectively. The thermal diffusivity of the Cr-Ti pack with helium gas at 150 torr pressure was 3 to 7 times greater than it was with the pack at a helium pressure of 0.05 torr or lower. Measurements of thermal diffusivity as a function of temperature in the range of 1000°F to 1900°F, at a pressure of 300-400 torr of helium, gave essentially the same values as for 100-150 torr pressure. Fine (-30 mesh) 60Cr-40Ti powder was found to sinter severely

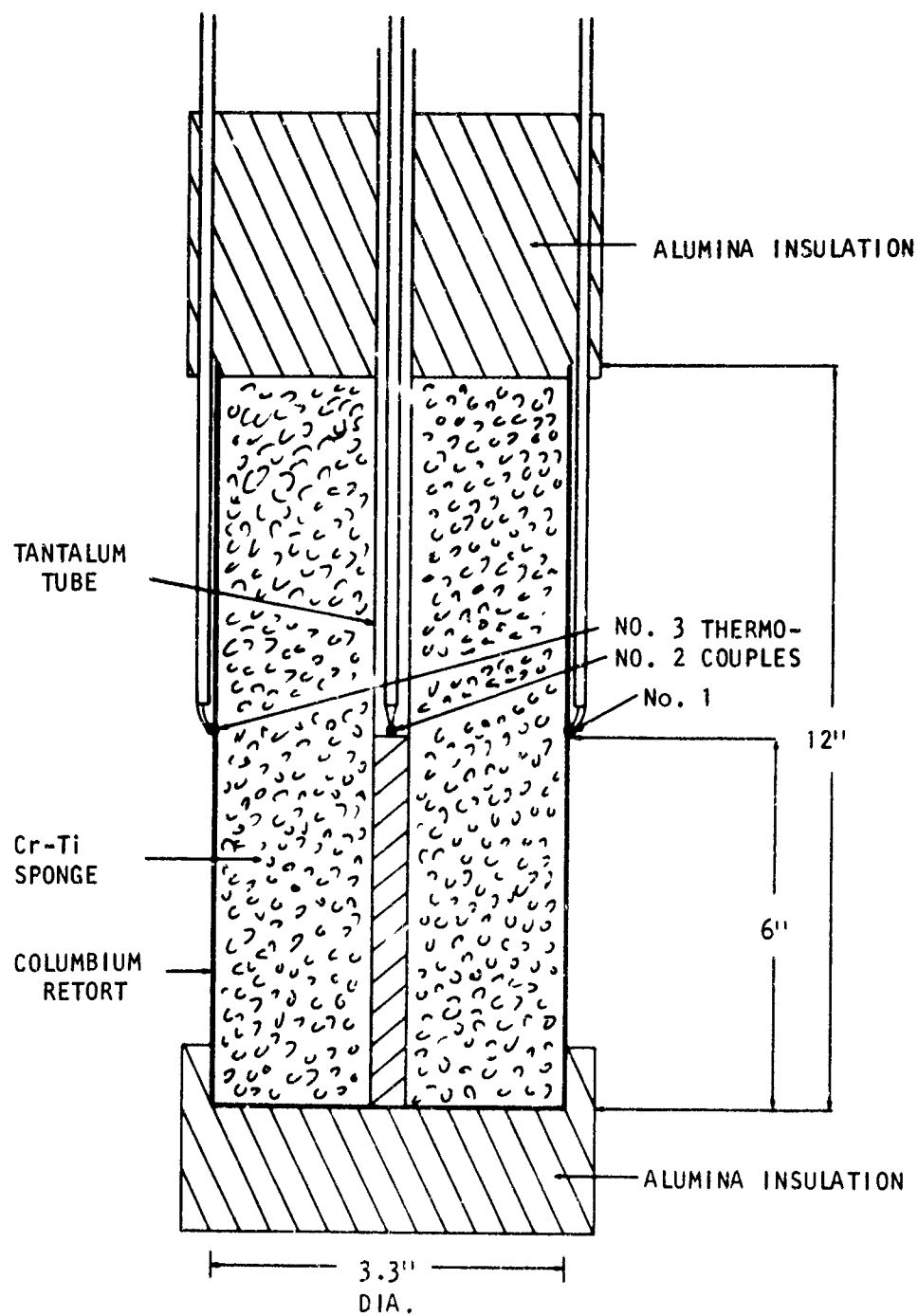


Figure 6 Thermal Diffusivity Test Apparatus

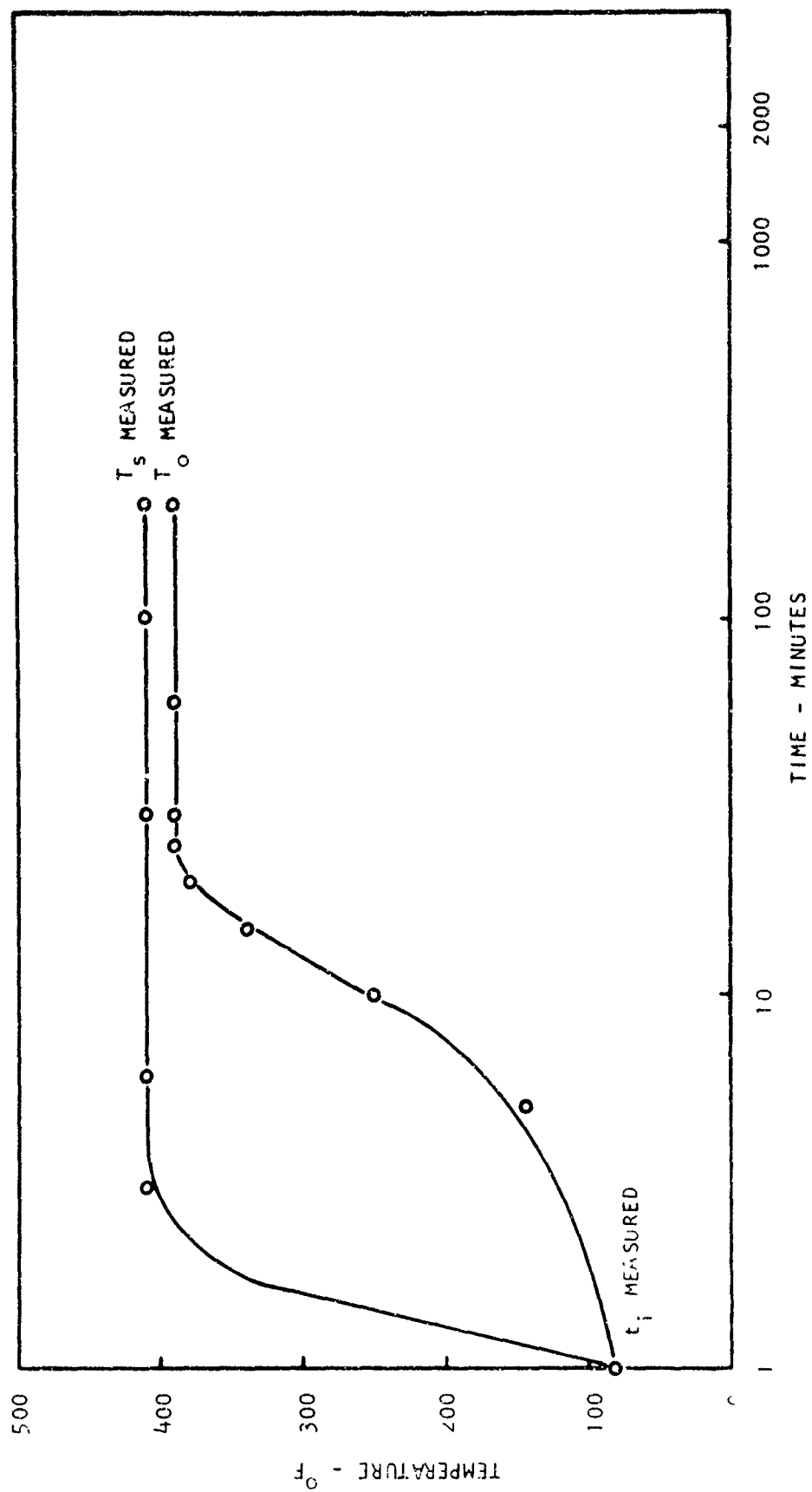


Figure 7 Typical Time-Temperature Graph for 60Cr-40Ti Pack at 100 to 150 Torr Helium Pressure

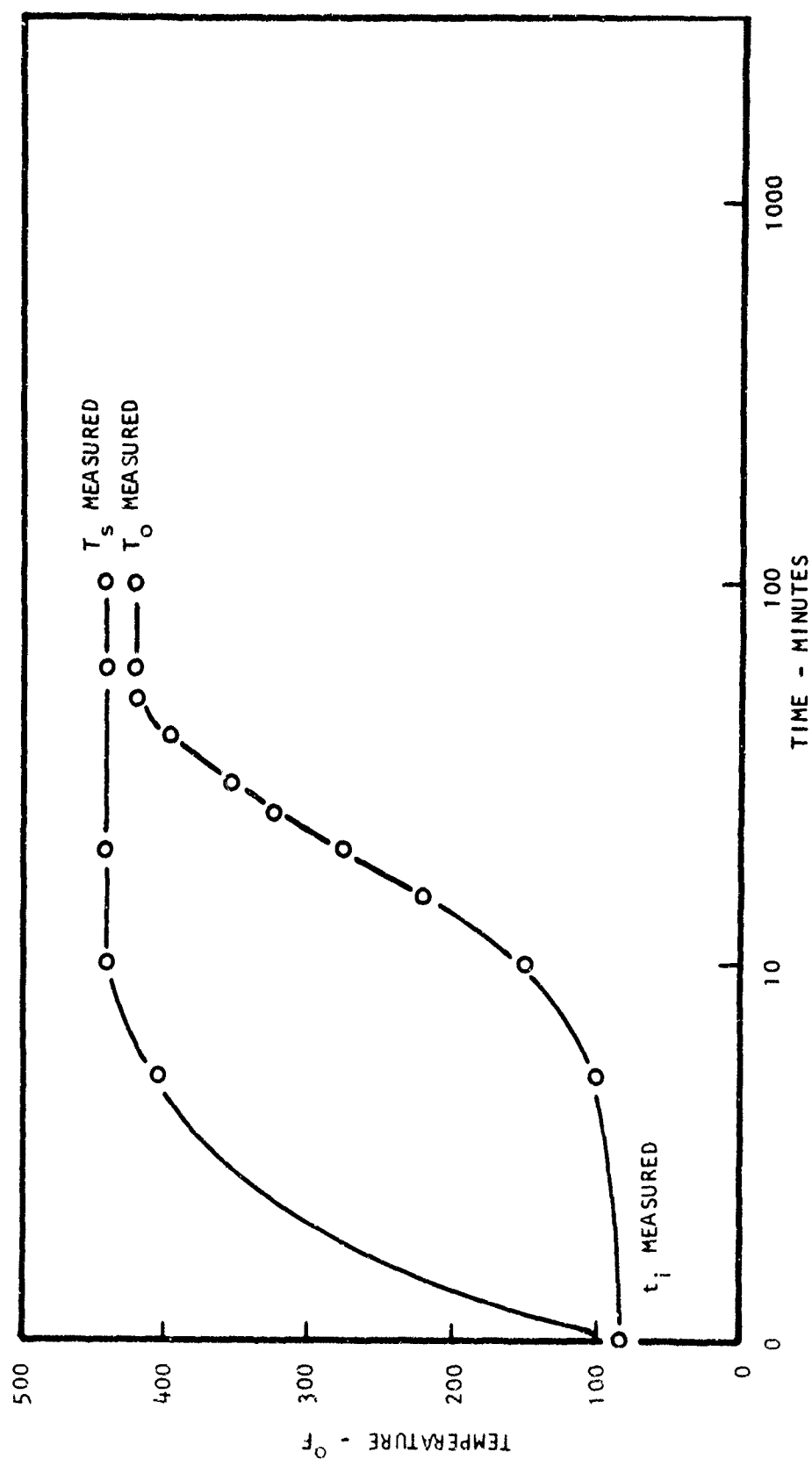


Figure 8 Typical Time-Temperature Graph for a Silicon Pack at 100 to 150 Torr Helium Pressure

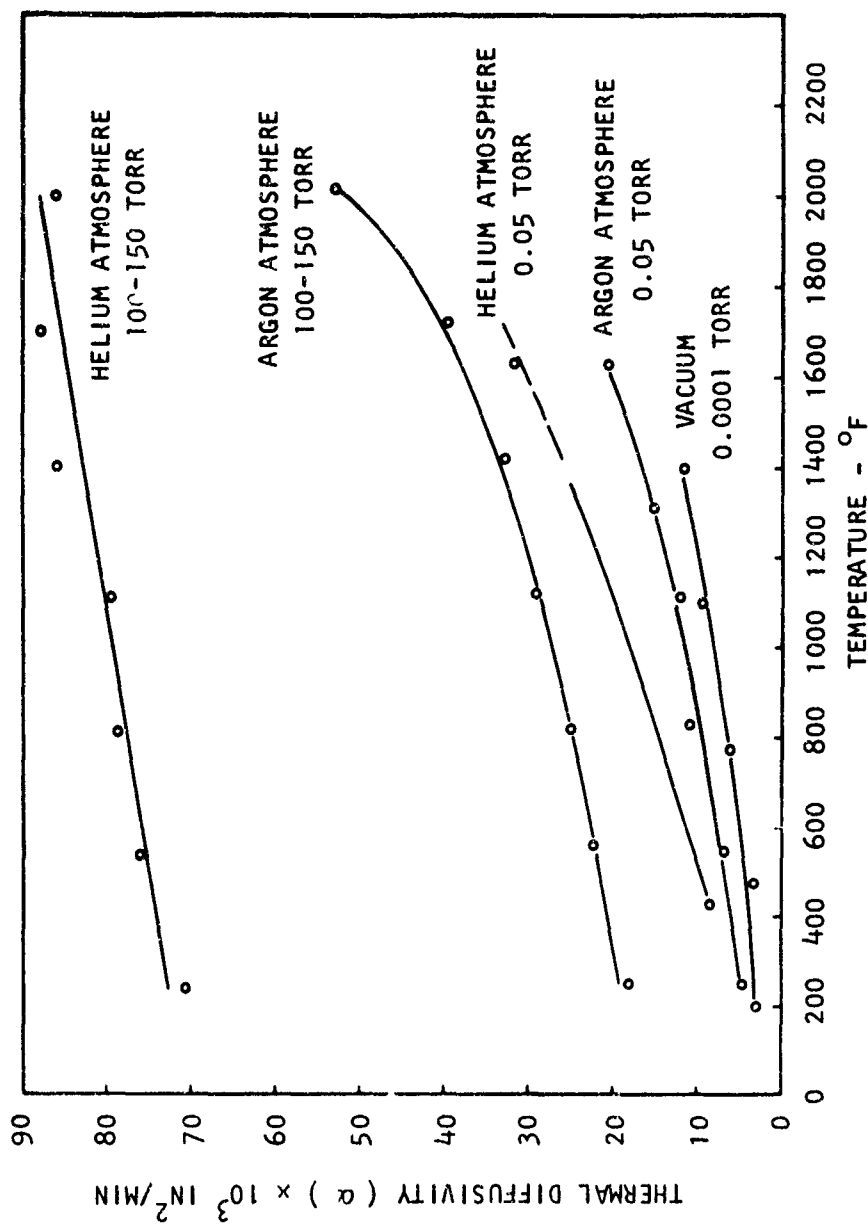


Figure 9 Thermal Diffusivity of 60Cr-40Ti Powder as a Function of Gaseous Environment, Pressure, and Temperature

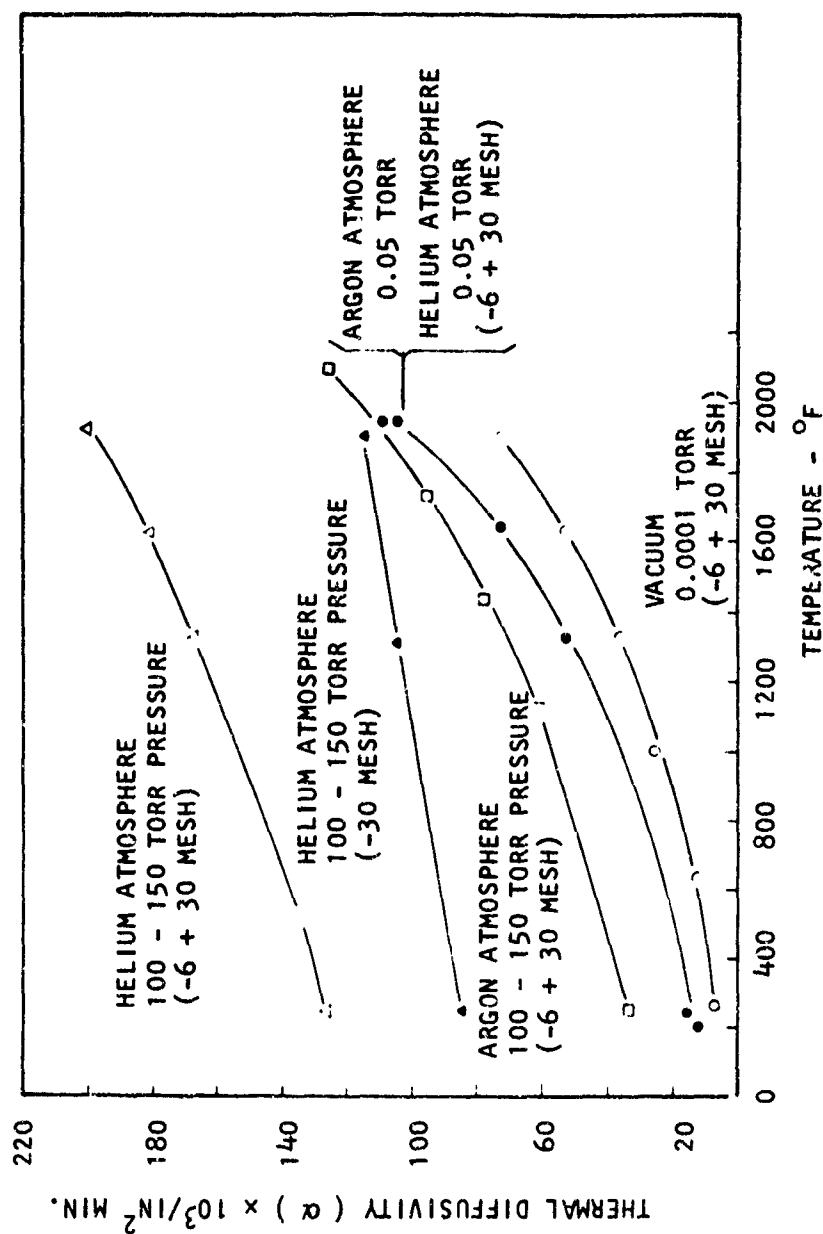


Figure 10 Thermal Diffusivity of Silicon Powder as a Function of Gaseous Environment, Pressure, and Temperature

at 2300°F, and was unsuitable for pack material at normal Cr-Ti coating temperatures. Therefore, its thermal diffusivity was not determined.

Figure 10 shows that the thermal diffusivity of silicon powder, under vacuum, increased from 0.0077 in²/min at a temperature of 265°F to 0.073 in²/min at 1900°F. Under 100-150 torr of helium the thermal diffusivity increased from 0.126 in²/min at 240°F to 0.196 in²/min at 1940°F, while under 100-150 torr pressure of argon the thermal diffusivity increased from 0.033 in²/min at 250°F to 0.125 in²/min at 2040°F. The values for the thermal diffusivity in both argon and helium atmospheres at 0.05 torr pressure varied essentially in the same manner over the temperature range 200 to 1940°F. The thermal diffusivity for the -30 mesh silicon powder under 100-150 torr helium increased linearly from 0.085 in²/min at 260°F to 0.110 in²/min at 1890°F. Finer -30 mesh silicon powder had approximately 2/3 the thermal diffusivity of -6 + 30 mesh powder over the temperature range from 260° to 1890°F.

The effects of using an inert gas environment to increase the thermal diffusivity of the granular metal packs are clearly shown in Figures 9 and 10. The particulate alloy pack material has a low thermal diffusivity, thus the thermal diffusivity of the pack and its gaseous environment is largely governed by the thermal diffusivity of the gas. Since the thermal diffusivity of a gas increases with pressure, the thermal diffusivity of the pack and its gaseous atmosphere also increased with increasing pressure. This increase was more pronounced for the helium atmosphere because helium has a greater thermal diffusivity than argon. Using an inert atmosphere in the pack will reduce the time required to achieve a uniform temperature in large packs, thereby shortening the time required for the coating cycle, along with improving coating uniformity throughout the pack. These thermal diffusivity data were subsequently employed to analyze the time-temperature relationships in large packs used in the development and scale-up of the vacuum-pack process.

4.2 Pilot Scale Coating Process Studies

A major problem in using a large pack is that as the retort size increases, more time is required to bring the center of the pack to the coating temperature. For reasonably short coating times, the temperature gradient in the pack will produce substantially non-uniform coating weight gains on material at various positions in the pack. The comparatively poor thermal conductivity of the granular pack media was improved by introducing helium or argon in-

to the retort, as shown in Section 4.1. However, in order to obtain uniform coating deposition throughout the pack, all regions of the pack must be brought to the coating temperature within a relatively short time span. This problem of coating uniformity was investigated for various furnace sizes, gaseous atmospheres and thermal cycles.

The effect of these temperature gradients was first evaluated in an existing pilot scale coating facility similar in design to the production size furnace, but about 1/3 the volume. Coupons were placed at six different positions in a module pack as shown in Figure 11. Positions designated BC, MC and TC were in the center of the pack, 4, 18 and 32 inches respectively above the square base. Positions designated BO, MO and TO were 4, 18 and 32 inches above the base, and 2 inches from one side of the pack.

Using the above arrangement, the effect of varying Cr-Ti and silicon coating parameters on the respective coating weight gains, and on oxidation resistance of 3 columbium alloys, C129Y, B66 and Cb752, was determined from 15 Cr-Ti-Si coating runs. Each run produced 36 coated coupons which were cyclic oxidation tested for a maximum of 200 hours at 1800 and 2500°F, and for a maximum of 100 hours at 2700°F. Selected coupons were also microscopically examined to evaluate the extent of protection provided to the substrate by the coating. These data were then used to determine the optimum coating parameters for the 3-inch x 8-inch x 36-inch module retort, based on the parameters summarized in Table 2.

4.2.1 Cr-Ti Coating Conditions

All of the Cr-Ti coatings were formed using the same time-temperature conditions. The surface temperature of the retort was brought to 2000°F under a helium pressure of 100 to 150 torr; and held there for one hour. Coating deposition under these conditions is negligible. The temperature was then raised to the coating deposition temperature of 2300°F. Upon reaching 2300°F, the pressure was lowered to the equilibrium pressure given in Table 2, and these conditions were maintained for the 8-hour coating deposition period.

A time vs. temperature relationship which is representative of the Cr-Ti coating deposition runs is shown in Figure 12. The conditions depicted were measured for Module Run 3. This module was fitted with thermocouples in the center of the pack so that this temperature, as well as the retort wall temperatures, was measured. If it is assumed that in a helium atmosphere, pressures in the range 100-150 torr have only a slight effect on the pack

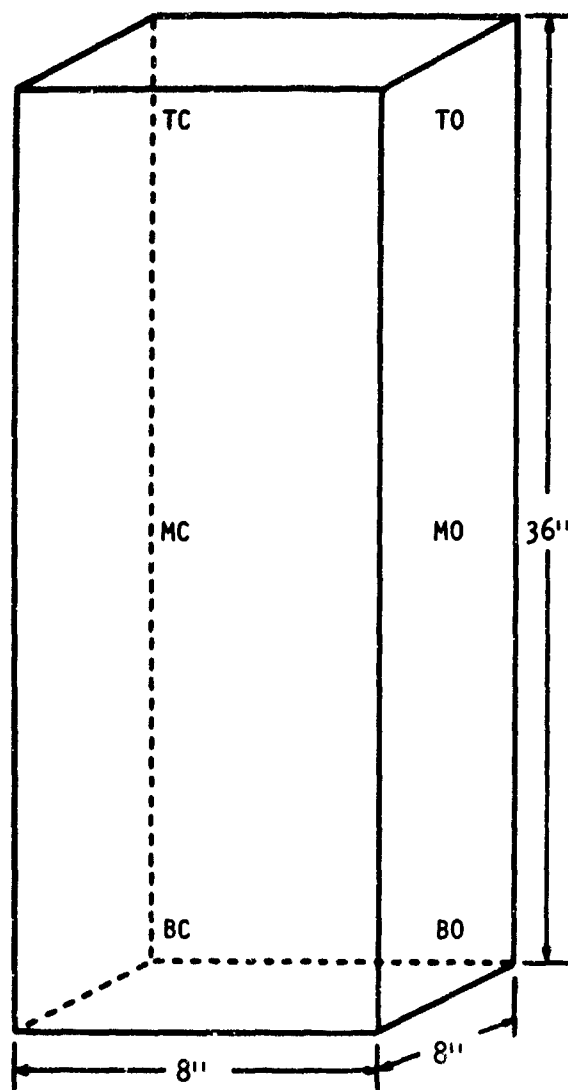


Figure 11 Key to Positioning of Columbian Alloy Specimens in Module

TABLE 2
MODULE RUN PROCESSING PARAMETERS

Mod No	Pack Powder	Cr-Ti Cycle				Silicon Cycle			
		Activator (gms)	Equilibrium Condition		at Temp (Hrs)	Activator (gms)	Equilibrium Condition		Time at Temp (Hrs)
			Press (Torr)	Temp (°F)			Press (Torr)	Temp (°F)	
1	60Cr-40Ti	NaF(125)	0.05	2300	8	KF(125)	0.05(1)	2100	5
2	60Cr-40Ti	CrCl ₃ (45)	1.0	2300	8	CrCl ₃ (45)	1.0(1)	2050	4
3	60Cr-40Ti	CrCl ₃ (45)	10.0	2300	8	SiF ₄	1.0(2)	2000	4
4	60Cr-40Ti	NaF(50)	1.0	2300	8	KF(50)	0.05(1)	2000	4
5	70Cr-30Ti	CrCl ₃ (50)	10.0	2300	8	KF(50)	1.0(1)	2000	4
6	70Cr-30Ti	NaF(50)	1.0	2300	8	KF(25)	1.0(1)	2000	4
7	70Cr-30Ti	NaF(25)	10.0	2300	8	KF(25)	10.0(2)	2000	4
8	60Cr-40Ti	CrCl ₃ (50)	10.0	2300	8	SiF ₄	1.0(2)	2000	4
9	60Cr-40Ti	CrCl ₃ (25)	10.0	2300	8	SiF ₄	5.0(3)	2100	4
10	60Cr-40Ti	CrCl ₃ (25)	1.0	2300	8	KF(50)	1.0(1)	2000	4
11	60Cr-40Ti	CrCl ₃ (100)	10.0	2300	8	KF(50)	1.0(4)	1900	4
12	60Cr-40Ti	CrCl ₃ (100)	10.0	2300	8	KF(25)	1.0(4)	1900	4
13	60Cr-40Ti	CrCl ₃ (100)	10.0	2300	8	KF(25)	1.0(5)	2000	3
14	60Cr-40Ti	CrCl ₃ (200)	10.0	2300	8	KF(50)	0.05(5)	2000	3
15	60Cr-40Ti	CrCl ₃ (100)	1.0	2300	8	KF(50)	0.05(5)	2000	3

- (1) Pressure attained at a retort wall temperature of 1500°F.
 (2) Pressure attained at a retort wall temperature of 2000°F and backfilled with SiF₄ to indicated pressure at this temperature.
 (3) Pressure attained at a retort wall temperature of 2100°F.
 (4) Pressure attained at a retort wall temperature of 1900°F.
 (5) Pressure attained at a retort wall temperature of 2000°F after a 1 hour hold at 1700°F.

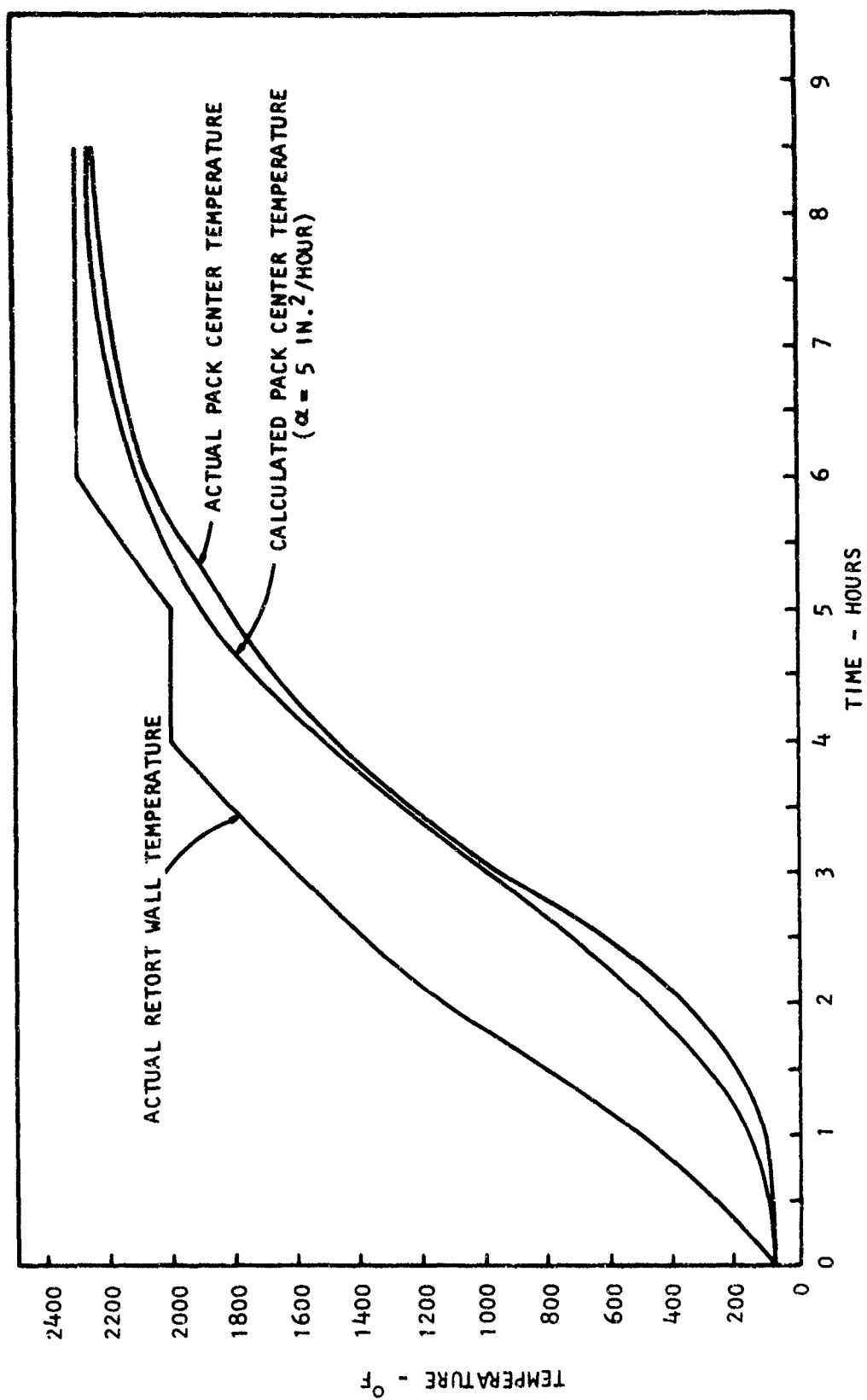


Figure 12 Time-Temperature Relationships for Cr-Ti Coating Deposition

thermal diffusivity, α , then the values of α at 100-150 torr (Figure 9) may be extrapolated to give an approximate value of 5 in²/hr for α at 2300°F. The good agreement between the observed and calculated center pack temperatures, shown in Figure 12, supports this assumption.

4.2.2 Silicon Coating Conditions

Silicon was also deposited by bringing the module retort to temperature at a helium pressure of 150 torr, and then reducing the system pressure. In addition to evaluating the process parameters given in Table 2, the effect of heating rate on silicon weight gain was investigated. This was done by reducing the system pressure, and thereby changing the effective thermal diffusivity of the pack at different retort wall temperatures while approaching the coating deposition temperatures.

Figure 13 shows time vs. temperature relationships for runs made at peak temperatures of 1900, 2050 and 2100°F. Figure 14 shows a representative time vs. temperature relationship for coating runs made at 2000°F, and is based on Run 6 which was instrumented to record the temperature at the center of the pack, as well as at the retort wall. Two values of thermal diffusivity α were used in calculating the pack center temperature. A value of $\alpha = 10$ in²/hr was used until the retort wall temperature reached 1500°F. The pack pressure was then reduced to 1 torr and a value of $\alpha = 7$ in²/hr was used to complete the calculation. These calculations, as well as the previous calculations for the Cr-Ti pack, show that the thermal diffusivity data can be used to predict the temperature rise in a pack.

4.2.3 Coating Oxidation Test Results

Before discussing the various coating deposition parameters, and the selection of the optimum parameters, the oxidation protection performance of the coating produced in the module runs will be summarized. The results of these module tests are presented in Table 3, and data summaries showing coating weight gains and oxidation performance of coupons as functions of test temperature, alloy substrate composition, and pack position are given in Appendices I to IV. On the whole there was no significant relationship between oxidation resistance and substrate composition.

In Module I at 1800°F, only two coupons which had been damaged in handling before oxidation testing did not survive 200 hours exposure, and, the effect of pack position and substrate composition

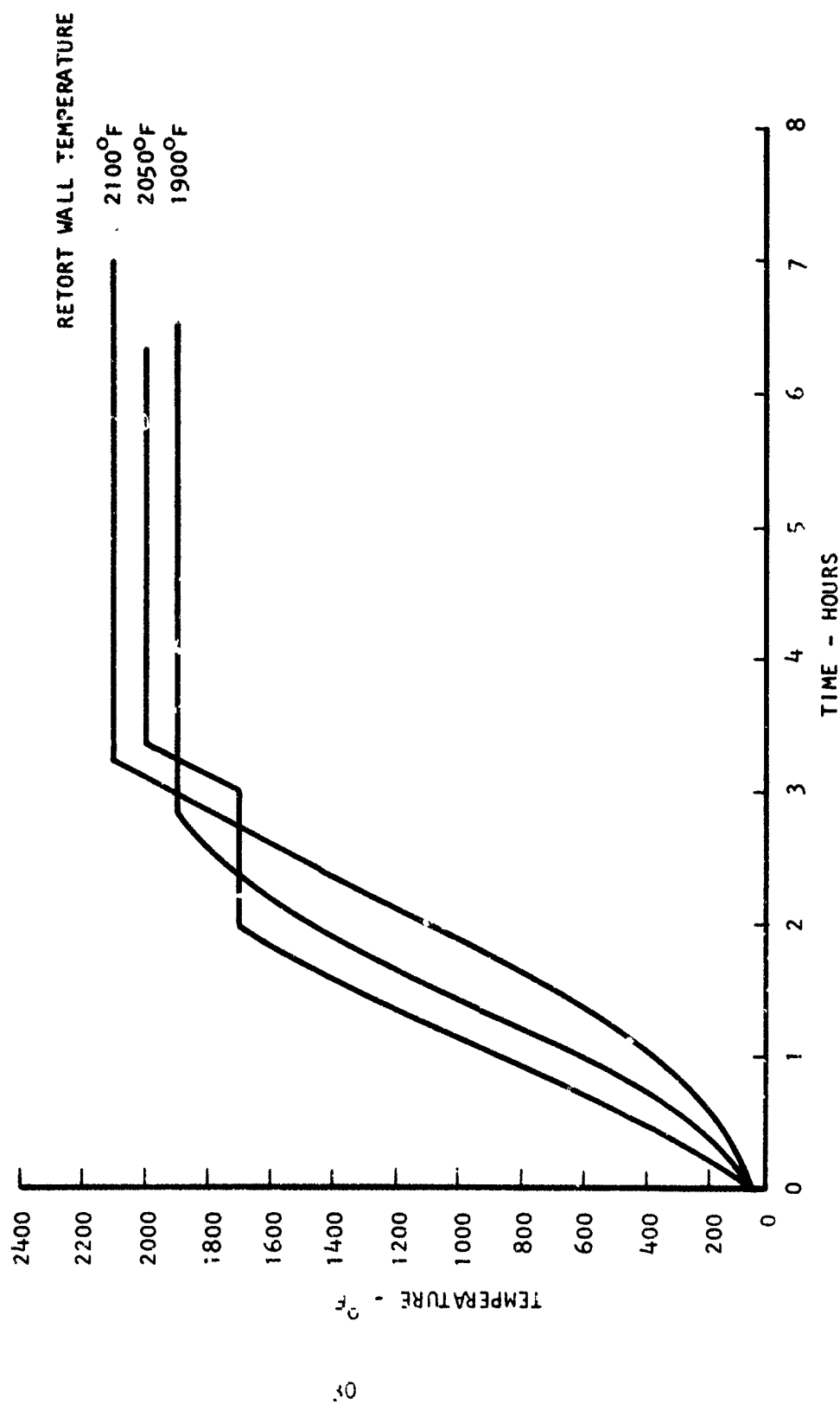


Figure 1; Time-Temperature Relationships for Silicon Coating Deposition

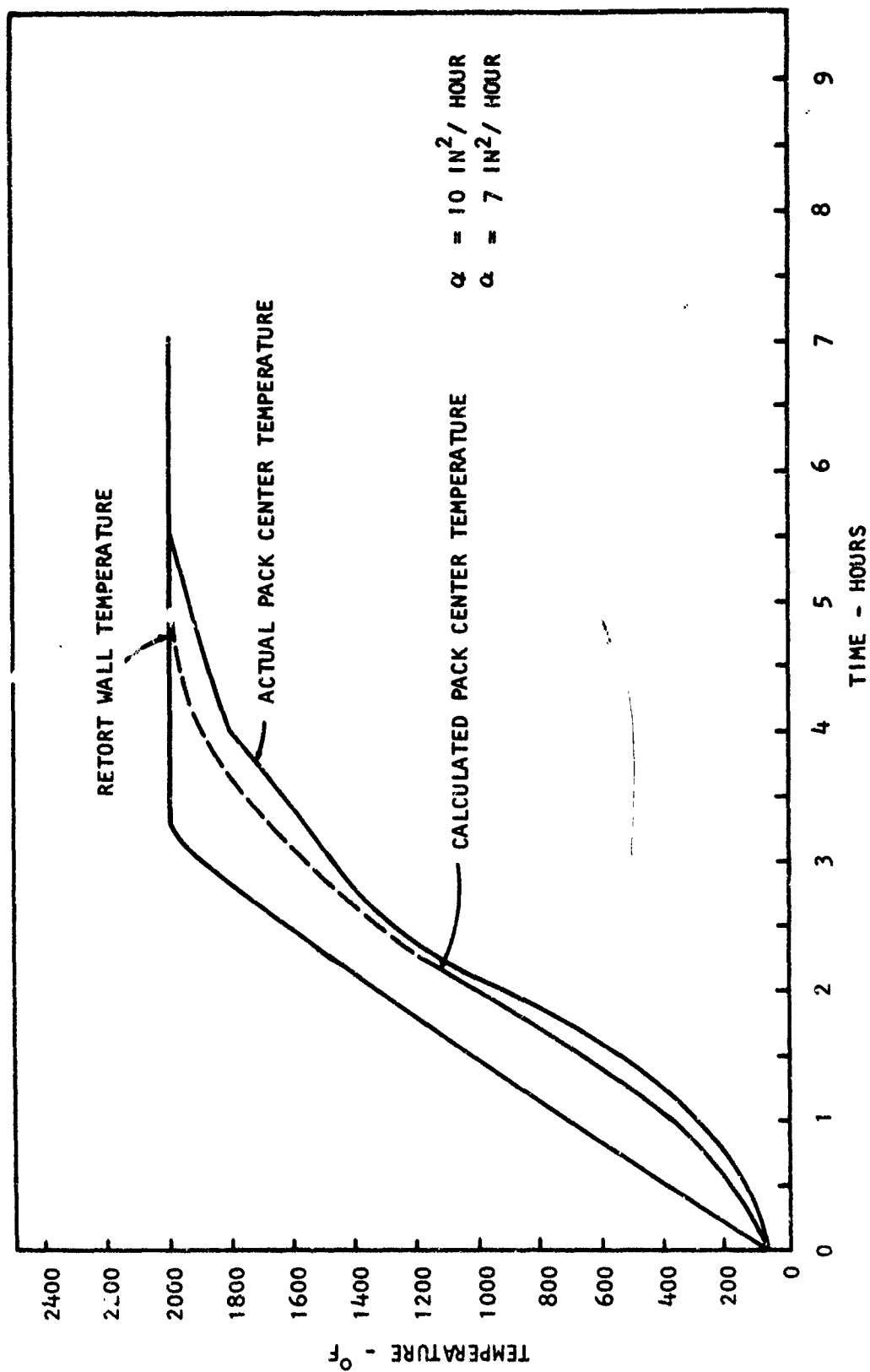


Figure 14 Time-Temperature Relationships for Silicon Coating Deposition

TABLE 3

COMPILATION OF WEIGHT GAIN AND OXIDATION PERFORMANCE

Alloy	Average Coat Weight mg/cm ²	Surface Area cm ²	Weight Gain mg	Pack Position											
				20			30			40			50		
				Coat Weight mg/cm ²	Life hrs.	Coat Weight mg/cm ²	Coat Weight mg/cm ²	Life hrs.	Coat Weight mg/cm ²	Coat Weight mg/cm ²	Life hrs.	Coat Weight mg/cm ²	Coat Weight mg/cm ²	Life hrs.	Coat Weight mg/cm ²
Mod 1	C1207	17.0	1000	14.8	13.1	17.8	17.6	17.6	21.7	17.6	17.6	21.7	18.6	200-200	200-200
			200	112	100	112	112	112	112	112	112	112	112	112	112
			200	112	100	112	112	112	112	112	112	112	112	112	112
			200	112	100	112	112	112	112	112	112	112	112	112	112
Mod 2	B66	17.0	1000	13.6	16.6	17.6	16.3	16.3	21.2	18.9	18.9	21.2	20.2	200-200	200-200
			200	112	100	112	112	112	112	112	112	112	112	112	112
			200	112	100	112	112	112	112	112	112	112	112	112	112
			200	112	100	112	112	112	112	112	112	112	112	112	112
Mod 3	C8752	17.0	1000	11.4	13.1	17.9	15.8	15.8	21.8	16.7	16.7	21.8	19.4	200-200	200-200
			200	112	100	112	112	112	112	112	112	112	112	112	112
			200	112	100	112	112	112	112	112	112	112	112	112	112
			200	112	100	112	112	112	112	112	112	112	112	112	112
Mod 4	C1207	17.8	1000	13.0	2.8	15.6	15.6	15.6	17.6	3.9	3.9	17.6	15.5	200-200	200-200
			200	112	100	112	112	112	112	112	112	112	112	112	112
			200	112	100	112	112	112	112	112	112	112	112	112	112
			200	112	100	112	112	112	112	112	112	112	112	112	112
Mod 5	B66	17.8	1000	13.3	2.6	15.3	16.3	16.3	19.2	2.3	2.3	19.2	16.7	200-200	200-200
			200	112	100	112	112	112	112	112	112	112	112	112	112
			200	112	100	112	112	112	112	112	112	112	112	112	112
			200	112	100	112	112	112	112	112	112	112	112	112	112
Mod 6	C8752	17.8	1000	13.5	3.1	15.9	15.8	15.8	18.0	3.6	3.6	18.0	16.7	200-200	200-200
			200	112	100	112	112	112	112	112	112	112	112	112	112
			200	112	100	112	112	112	112	112	112	112	112	112	112
			200	112	100	112	112	112	112	112	112	112	112	112	112
Mod 7	C1207	22.5	1000	22.9	5.2	24.0	24.0	24.0	25.3	10.1	10.1	25.3	23.1	200-200	200-200
			200	112	100	112	112	112	112	112	112	112	112	112	112
			200	112	100	112	112	112	112	112	112	112	112	112	112
			200	112	100	112	112	112	112	112	112	112	112	112	112
Mod 8	B66	22.5	1000	24.0	4.9	25.1	25.1	25.1	26.9	9.7	9.7	26.9	23.5	200-200	200-200
			200	112	100	112	112	112	112	112	112	112	112	112	112
			200	112	100	112	112	112	112	112	112	112	112	112	112
			200	112	100	112	112	112	112	112	112	112	112	112	112
Mod 9	C8752	22.5	1000	27.4	5.0	22.8	22.8	22.8	25.2	9.8	9.8	25.2	24.3	200-200	200-200
			200	112	100	112	112	112	112	112	112	112	112	112	112
			200	112	100	112	112	112	112	112	112	112	112	112	112
			200	112	100	112	112	112	112	112	112	112	112	112	112
Mod 10	C1207	19.7	1000	16.8	14.3	17.5	17.5	17.5	18.6	19.7	19.7	18.6	22.5	200-200	200-200
			200	112	100	112	112	112	112	112	112	112	112	112	112
			200	112	100	112	112	112	112	112	112	112	112	112	112
			200	112	100	112	112	112	112	112	112	112	112	112	112
Mod 11	B66	19.7	1000	19.1	13.5	20.4	20.4	20.4	22.7	20.1	20.1	22.7	25.7	200-200	200-200
			200	112	100	112	112	112	112	112	112	112	112	112	112
			200	112	100	112	112	112	112	112	112	112	112	112	112
			200	112	100	112	112	112	112	112	112	112	112	112	112
Mod 12	C8752	19.7	1000	17.7	13.7	19.1	19.1	19.1	20.4	17.3	17.3	20.4	25.8	200-200	200-200
			200	112	100	112	112	112	112	112	112	112	112	112	112
			200	112	100	112	112	112	112	112	112	112	112	112	112
			200	112	100	112	112	112	112	112	112	112	112	112	112

TABLE 3
COMPILATION OF WEIGHT GAIN AND OXIDATION PERFORMANCE

Mod	Alloy	Average Coat Weight Gr-Cr mg/cm ²	Airflow liters per hr.	Life hrs.	Peak Position											
					70			80			90			100		
					Coat Weight Gr-Cr mg/cm ²	Gr-Cr mg/cm ²	Life hrs.	Coat Weight Gr-Cr mg/cm ²	Gr-Cr mg/cm ²	Life hrs.	Coat Weight Gr-Cr mg/cm ²	Gr-Cr mg/cm ²	Life hrs.	Coat Weight Gr-Cr mg/cm ²	Gr-Cr mg/cm ²	Life hrs.
Mod 5	C1297	16.5	25.8	2500	15.9	23.5	16.4	25.2	15.8	27.1	17.6	29.0	17.3	23.3	17.2	26.6
	E66	16.5	25.8	2500	17.3	23.4	18.1	26.3	17.8	27.2	18.4	29.5	15.3	23.8	18.4	27.4
	C6752	16.6	25.8	2500	15.4	22.9	16.4	24.7	16.0	26.5	18.2	28.9	13.5	23.1	17.0	24.9
	C1297	14.0	21.1	2500	13.6	17.6	14.0	23.2	13.9	23.3	15.6	24.6	11.7	19.0	13.6	21.4
Mod 6	E66	14.0	21.1	2500	14.8	17.1	15.5	19.5	15.1	22.9	16.9	25.2	12.2	18.4	15.2	22.1
	C6752	14.0	21.1	2500	13.1	18.4	13.1	21.8	13.1	22.1	14.6	25.4	10.8	17.9	14.7	23.2
	C1297	11.2	19.8	2500	11.2	16.7	11.6	17.4	11.3	23.2	12.9	24.3	8.8	19.1	10.7	20.8
	E66	11.2	19.8	2500	11.7	16.4	12.7	17.3	11.9	22.3	13.5	23.7	9.2	18.5	12.2	20.9
Mod 7	C6752	11.2	19.8	2500	10.7	15.2	11.1	16.9	10.6	21.4	11.4	22.7	8.7	17.6	11.0	21.2
	C1297	22.3	2.3	2500	20.8	1.4	22.0	1.7	22.7	2.1	24.3	4.3	19.8	1.8	23.6	3.1
	E66	22.3	2.3	2500	21.0	1.3	22.5	1.7	23.4	1.9	27.3	4.1	20.8	1.7	24.5	2.6
	C1297	22.3	2.3	2500	19.8	1.4	21.5	1.7	22.1	2.0	25.1	3.2	19.2	1.7	21.0	4.2
Mod 8	C1297	22.3	2.3	2500	20.8	1.4	22.0	1.7	22.7	2.1	24.3	4.3	19.8	1.8	23.6	3.1
	E66	22.3	2.3	2500	21.0	1.3	22.5	1.7	23.4	1.9	27.3	4.1	20.8	1.7	24.5	2.6
	C1297	22.3	2.3	2500	19.8	1.4	21.5	1.7	22.1	2.0	25.1	3.2	19.2	1.7	21.0	4.2
	E66	22.3	2.3	2500	21.0	1.3	22.5	1.7	23.4	1.9	27.3	4.1	20.8	1.7	24.5	2.6

TABLE 3

COMPILATION OF WEIGHT GAIN AND OXIDATION PERFORMANCE

Run	Ave. Cost Weight Gain (lb/100 lb Fe)	Oxidation (lb/100 lb Fe)	Weight Gain (lb/100 lb Fe)	Peak Functions									
				20		25		30		35		40	
				Cost Weight Gain (lb/100 lb Fe)	Oxidation (lb/100 lb Fe)	Cost Weight Gain (lb/100 lb Fe)	Oxidation (lb/100 lb Fe)	Cost Weight Gain (lb/100 lb Fe)	Oxidation (lb/100 lb Fe)	Cost Weight Gain (lb/100 lb Fe)	Oxidation (lb/100 lb Fe)	Cost Weight Gain (lb/100 lb Fe)	Oxidation (lb/100 lb Fe)
Run 9	21.97	20.4	3.0	18.0	3.0	18.0	3.0	18.0	3.0	18.0	3.0	18.0	3.0
	26.4	20.4	3.0	18.0	3.0	18.0	3.0	18.0	3.0	18.0	3.0	18.0	3.0
	26.4	20.4	3.0	18.0	3.0	18.0	3.0	18.0	3.0	18.0	3.0	18.0	3.0
	26.4	20.4	3.0	18.0	3.0	18.0	3.0	18.0	3.0	18.0	3.0	18.0	3.0
	26.4	20.4	3.0	18.0	3.0	18.0	3.0	18.0	3.0	18.0	3.0	18.0	3.0
Run 10	21.97	20.4	3.0	18.0	3.0	18.0	3.0	18.0	3.0	18.0	3.0	18.0	3.0
	26.4	20.4	3.0	18.0	3.0	18.0	3.0	18.0	3.0	18.0	3.0	18.0	3.0
	26.4	20.4	3.0	18.0	3.0	18.0	3.0	18.0	3.0	18.0	3.0	18.0	3.0
	26.4	20.4	3.0	18.0	3.0	18.0	3.0	18.0	3.0	18.0	3.0	18.0	3.0
	26.4	20.4	3.0	18.0	3.0	18.0	3.0	18.0	3.0	18.0	3.0	18.0	3.0
Run 11	21.97	20.4	3.0	18.0	3.0	18.0	3.0	18.0	3.0	18.0	3.0	18.0	3.0
	26.4	20.4	3.0	18.0	3.0	18.0	3.0	18.0	3.0	18.0	3.0	18.0	3.0
	26.4	20.4	3.0	18.0	3.0	18.0	3.0	18.0	3.0	18.0	3.0	18.0	3.0
	26.4	20.4	3.0	18.0	3.0	18.0	3.0	18.0	3.0	18.0	3.0	18.0	3.0
	26.4	20.4	3.0	18.0	3.0	18.0	3.0	18.0	3.0	18.0	3.0	18.0	3.0
Run 12	21.97	20.4	3.0	18.0	3.0	18.0	3.0	18.0	3.0	18.0	3.0	18.0	3.0
	26.4	20.4	3.0	18.0	3.0	18.0	3.0	18.0	3.0	18.0	3.0	18.0	3.0
	26.4	20.4	3.0	18.0	3.0	18.0	3.0	18.0	3.0	18.0	3.0	18.0	3.0
	26.4	20.4	3.0	18.0	3.0	18.0	3.0	18.0	3.0	18.0	3.0	18.0	3.0
	26.4	20.4	3.0	18.0	3.0	18.0	3.0	18.0	3.0	18.0	3.0	18.0	3.0
Run 13	21.97	20.4	3.0	18.0	3.0	18.0	3.0	18.0	3.0	18.0	3.0	18.0	3.0
	26.4	20.4	3.0	18.0	3.0	18.0	3.0	18.0	3.0	18.0	3.0	18.0	3.0
	26.4	20.4	3.0	18.0	3.0	18.0	3.0	18.0	3.0	18.0	3.0	18.0	3.0
	26.4	20.4	3.0	18.0	3.0	18.0	3.0	18.0	3.0	18.0	3.0	18.0	3.0
	26.4	20.4	3.0	18.0	3.0	18.0	3.0	18.0	3.0	18.0	3.0	18.0	3.0

could not be evaluated. At 2500°F all failures were by a wearout mechanism, with coupons from the T0 and TC positions having thinner coatings, and, consequently, shorter lives than those from other positions. At 2700°F two coupons from the MC position failed by a coating defect mechanism. The earliest failure at any temperature was after 35 hours, and, except as mentioned, all other coupons failed through general wearout.

Coupons from Module 2 showed short lives at all temperatures as a consequence of the poor silicide coating formed using CrCl_3 as the activator. At 1800°F a normal distribution with a short life was encountered, and pack position and alloy analysis revealed no significant relationships. At 2500°F two early failures were found after the one hour inspection, which along with a third failure at 2-1/2 hours indicated a random early failure mechanism. In the Weibull analysis, both the pack position and alloy analyses breakouts indicated that a bimodal mechanism operated during oxidation of the coated B66 alloy specimens. The balance of the data displayed normal wearout for the other two alloys, but with short oxidation lives. At 2700°F most of the failures occurred after 2 hours exposure.

Module 3 specimens failed by a normal wearout mechanism at 1800°F, and two failure mechanisms operated at this temperature. Early failures were associated with Cb752 alloy rather than pack position. As a whole, failures at 2500°F displayed a normal distribution. However, pack position and alloy analyses showed a random failure mechanism for B66 alloy specimens, with no marked position dependence. At 2700°F random failures were observed. There was a specific wearout distribution for TC position, independent of the alloy. Coupons from this position were characterized as having a very light silicon coating on a normal Cr-Ti precoat, and the poor oxidation performance was a consequence of the poor silicon coating.

In Module 4 at 1800°F only one previously damaged specimen failed before testing was stopped after 200 hours, and the effects of pack position and alloy composition were not demonstrated. During the 2500°F tests a furnace over-shoot failure resulted in temperatures reaching 2900°F, and testing was terminated. Analysis of the data indicated a somewhat random wearout failure mode that showed no trend as to pack position or alloy. At 2700°F a wearout failure mode was displayed, and the oxidation performance appeared to be attributable to the slightly thinner coatings observed at the TC and T0 positions.

In general, the coatings from Module 5 performed poorly. At 1800°F, Weibull analysis of the failures indicated a mixed population distribution which was associated with an early failure mechanism exhibited by the Cb752 alloy. The B66 and C129Y alloys displayed

a random failure with some dependence on an early wearout failure due to the high Si/Cr-Ti coating ratio. At 2500°F the failures were by wearout following a nearly normal pattern. The Weibull analysis showed a mixed failure distribution which was a composite of a normal wearout pattern for Cb752 alloy specimens, with a fairly short life and steeper than normal failure distributions for the C129Y and B66 alloy specimens. No positional effect was noted.

Coatings from Module 6 also showed poor oxidation resistance at 1800°F as a consequence of a low-Cr-Ti/Si ratio. There appeared to be a mixed failure mechanism which was not clearly defined. All of the coupons coated at the TC pack position, and the B66 alloy specimens (independent of pack position) showed higher oxidation lives and a two-failure mechanism pattern, compared to a random failure mechanism for the remainder of the specimens. At 2500°F a reasonable oxidation life was displayed with a normal wearout pattern, while at 2700°F a good oxidation life was encountered with a slightly steeper than normal distribution.

Module 7 produced coatings which showed poor oxidation resistance. At 1800°F the failure distribution was of the same general pattern as that found for Module 6. The TC position and B66 alloy specimens both showed higher oxidation life and a bimodal failure pattern, compared to a general random failure distribution, but with a much shorter overall life than for Module Run 6. Consequently, the 2500 and 2700°F oxidation tests were curtailed and not analyzed.

The coatings produced from Modules 8 and 9 were not oxidation tested because the silicon weight gains achieved with SiF_4 activation were obviously insufficient to form a coating capable of providing long time protection.

Oxidation performance of coatings from Module 10 at 1800°F was characterized by random distribution, with early failures which were associated with the center pack positions, and with early random failures of the Cb752 alloy coupons. This poor low temperature life was anticipated since microscopic examination showed that silicon had diffused completely through the Laves phase. At 2500°F a normal wearout failure mechanism operated and showed no specific correlation with pack position or alloy. However, B66 alloy and the middle pack positions exhibited the best oxidation performance. At 2700°F a steep wearout distribution gave a 90% reliable life almost twice that of Module 1. No other dependence on pack position or alloy composition was found.

The coatings from Module 11 which were tested at 1800°F showed a random distribution based on six specimens that failed prior to the 200 hour test cutoff. These six early failures were either C129Y alloy or Cb752 alloy in the M0 and B0 pack positions. At 2500°F a wearout

failure mechanism operated, and analysis by pack position gave a narrow band of wearout curves with the TC specimens having the shortest life. Analysis by alloy composition showed steep parallel wearout curves with B66 alloy having the longest life. At 2700°F a near normal failure distribution with early wearout failures of the C129Y and B66 alloy specimens gave a 90% reliable oxidation life about half that of Module 1.

In Module 12, testing at 1800°F showed a random failure distribution with the same failure dependencies on pack position and alloy composition as Module 11, but with less than two thirds of the 90% reliable life. At 2500°F the occurrence of only one late failure indicated a long reliable life, but did not provide data on failure modes or correlations. At 2700°F a normal distribution was observed, with steep wearout failure mechanisms associated with B66 alloy and the center pack positions.

In Module 13, analysis at 1800°F revealed a less definite alloy failure mode identification, and a change that included the middle center (MC) pack position in the random failure occurrences, with the expected M0 and B0 correlation. At 2500°F the T0 and TC pack positions were found to contribute the early random-normal failures. The 2700°F oxidation tests showed parallel alloy distributions, with random early failures associated with the outer pack positions.

For the coupons coated in Module 14, a random failure distribution at 1800°F was associated with C129Y alloy and the outer pack positions. A bimodal failure distribution at 2500°F appeared to be associated with random failures in the T0 and MC pack positions, and a steep wearout distribution in the remaining pack positions. The random-normal distribution at 2700°F was revealed as influenced by early failures of C129Y and Cb752 specimens coated in the outer pack positions.

Coupons from Module 15 showed normal failure distributions at all three test temperatures, and the overall oxidation life was superior to those of the other four runs in this group. The only three failures after 200 hours exposure at 1800°F were C129Y and Cb752 alloy from the B0 and M0 positions, and these did not provide sufficient data for an analysis of the effects of alloy composition or pack position. Random failures at 2500°F were associated only with the center pack positions, while a steep wearout mechanism was displayed by the outer pack position specimens.

In general, coupons from Modules 10 through 15 exhibited the best uniformity in coating thickness, probably due to an improvement in pack temperature profile and temperature equalization

achieved by using hold steps at 2000°F during the Cr-Ti coating cycle, and 1600°F during the siliciding cycle, under a 100 to 150 torr helium pressure. The best oxidation performance was obtained with coupons from Modules 12 and 15 where CrCl_3 was used as the activator. These were followed by coupons from Modules 1 and 4 where NaF was used as the activator.

The oxidation performance of coupons at 2700°F was markedly influenced by the appearance of local regions of low density in the coating. This phenomenon, has been called 'wrinkling'. If in localized regions the Cr-Ti coating is not sufficiently thick, or it does not have the proper chemical composition, subsequent silicizing produces a coating which does not provide optimum protection above about 2500°F. The coating fails by the formation of localized protrusions, or 'wrinkles', at the defective regions. About 10 to 25% of the surface may be effected by this phenomenon.

Figure 15 shows that 'wrinkling' is observed on specimens which have been heated to 2700°F in a 1×10^{-5} torr vacuum, as well as on specimens exposed to cyclic oxidation in air at 1 atmosphere and 2700°F. Although Figure 15 shows the specimen appearance after 9 hours of cyclic oxidation testing, the 'wrinkling' appeared after one hour exposure, and the appearance of the coupon was not altered on continued exposure.

Figures 16 and 17 show sections through small and large 'wrinkles' in a vacuum treated B66 alloy coupon shown in Figure 15. The protruded region of the 'wrinkle' is formed at a region where there is no Cr-Ti enriched diffusion zone beneath the disilicide. Figure 18 shows a section through the oxidized B66 alloy coupon shown in Figure 15. Again, the presence of 'wrinkle' protrusions is associated with the absence of the Cr-Ti diffusion zone. The region of the 'wrinkle' appears to have melted. Since the phenomenon appeared in all three alloys, it is not dependent upon alloy composition. The areas of 'wrinkling' are apparently associated with localized chemistry differences, and the formation of relatively low melting eutectics. In the pseudo-binary system $\text{TiSi}_2\text{-CrSi}_2$, a eutectic at 95 mol percent TiSi_2 melts at 2372°F⁽⁷⁾. Also, in the binary Ti-Si system⁽⁸⁾ there are two eutectics melting below 2700°F; one at 8.5 weight percent silicon and the other at 78 weight percent silicon, both melting at 2426°F. The Cr-Si binary system⁽⁹⁾ exhibits two eutectics melting below 2700°F; one at 44.7 weight percent silicon melting at 2615°F, the other at 73 weight percent silicon melting at 2426°F.

A series of vacuum thermal treatments prior to exposure at 2700°F showed that the temperature for the onset of 'wrinkling'



B 66

C129Y

Cb 752

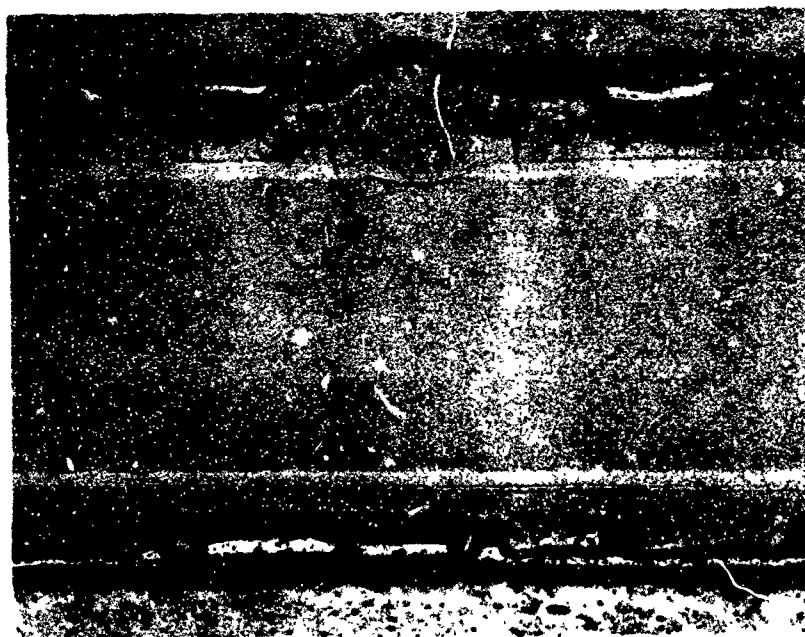
After Oxidation Exposure of 9 Hours at 2700°F



Cb 752

After 1 Hour at 1×10^{-5} Torr Vacuum and 2700°F

Figure 15. Wrinkling on Cr-Ti-Si Coated Columbium Alloys 3X



100X



250X

Figure 16. Section Through a Small "Wrinkle"
B-66 Alloy Heated 1 Hour in Vacuum at 2700°F



100X

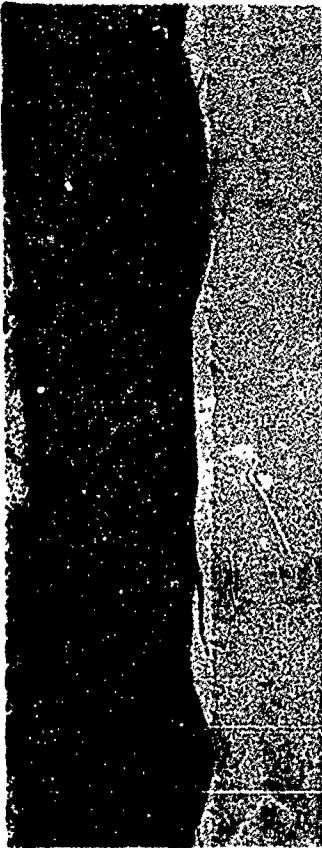


250X

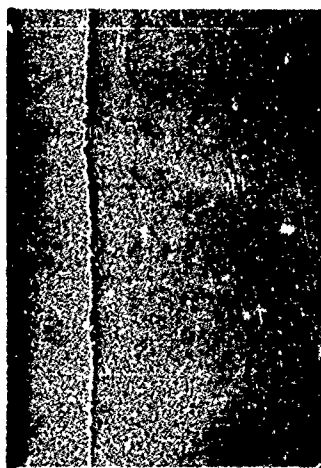
Figure 17. Section Through a Large "Wrinkle"
B-66 Alloy Heated 1 Hour in Vacuum at 2700°F



Cr-Ti-Si Coated



Cr-Ti-Si Coated



Cr-Ti Coated



Oxidized for
9 Hours at 2700°F

Figure 18. B-66 Alloy Specimen After 9 Hours at 2700°F - 250X

was $2630 \pm 20^\circ$, that an isothermal anneal at 2500 to 2600°F of approximately 1-1/2 hour prior to 2700°F testing prevented "wrinkling", or, a constant heating rate of slightly greater than 1°F per min between 2500 and 2700°F eliminated "wrinkling".

During the pre-treatment at 2500 to 2600°F, or slowly heating to 2700°F, sufficient lateral diffusion of chromium, titanium or silicon occurs to alter the local silicide chemistry and to form higher melting phases. It has also been noted that Cr-Ti coated specimens which have been over-silicided so that there was no retained Laves phase did not show this localized melting. Possibly sufficient columbium diffused into the intermediate regions so that no low melting silicide phase existed.

At 2700°F the oxidation performance of coupons coated in these module runs compared very favorably with the performance of other TRW Cr-Ti-Si coatings applied in the smaller coating furnaces. Figure 19 shows the 2700°F oxidation performance for Cr-Ti-Si coated B66 and D43 alloy coupons tested under a previous program⁽¹⁰⁾. The 90% reliable oxidation lives were 12, 15 and 20 hours, compared with module run values of 16, 18, 18, 38 and 26 hours. Extra specimens from Module 12, a run which gave a 90% reliable life of 8 hours in the initial oxidation tests and exhibited "wrinkling", were given a 2500°F - 5 hour post test anneal. Upon subsequent testing at 2700°F, the heat treated specimens did not "wrinkle" and exhibited the first failure at 34 hours. Therefore, the potential life of many of the coatings at 2700°F was greater than the results indicated.

The preceding discussion was based on a statistical analysis of the 90% reliable life using the cyclic oxidation test data. Additional understanding of the oxidation performance of the Cr-Ti-Si coating system can be gained from analysis of oxidation performance based upon coating morphology and coating thicknesses. For this purpose the module runs will be divided into two groups:

- 1) Module Runs 1 and 4 which were made utilizing NaF as the Cr-Ti cycle activator and,
- 2) Module Runs 3, and 10 through 15 which were made utilizing CrCl_3 as the Cr-Ti cycle activator.

The data previously represented in Table 3 are shown in Figures 20 and 21 where the hours to failure are plotted against the ratio of Cr-Ti weight gain ($\Delta\text{Cr-Ti}$) to silicon weight gain (ΔSi) for both 1800°F and 2500°F tests, respectively. The Cr-Ti weight gains fall in the range of 12 to 29 mg/cm² and the silicon weight gains fall in the range of 8-26 mg/cm². For optimum oxidation performance, the ratio of the Cr-Ti coating weight to the silicon weight is important in

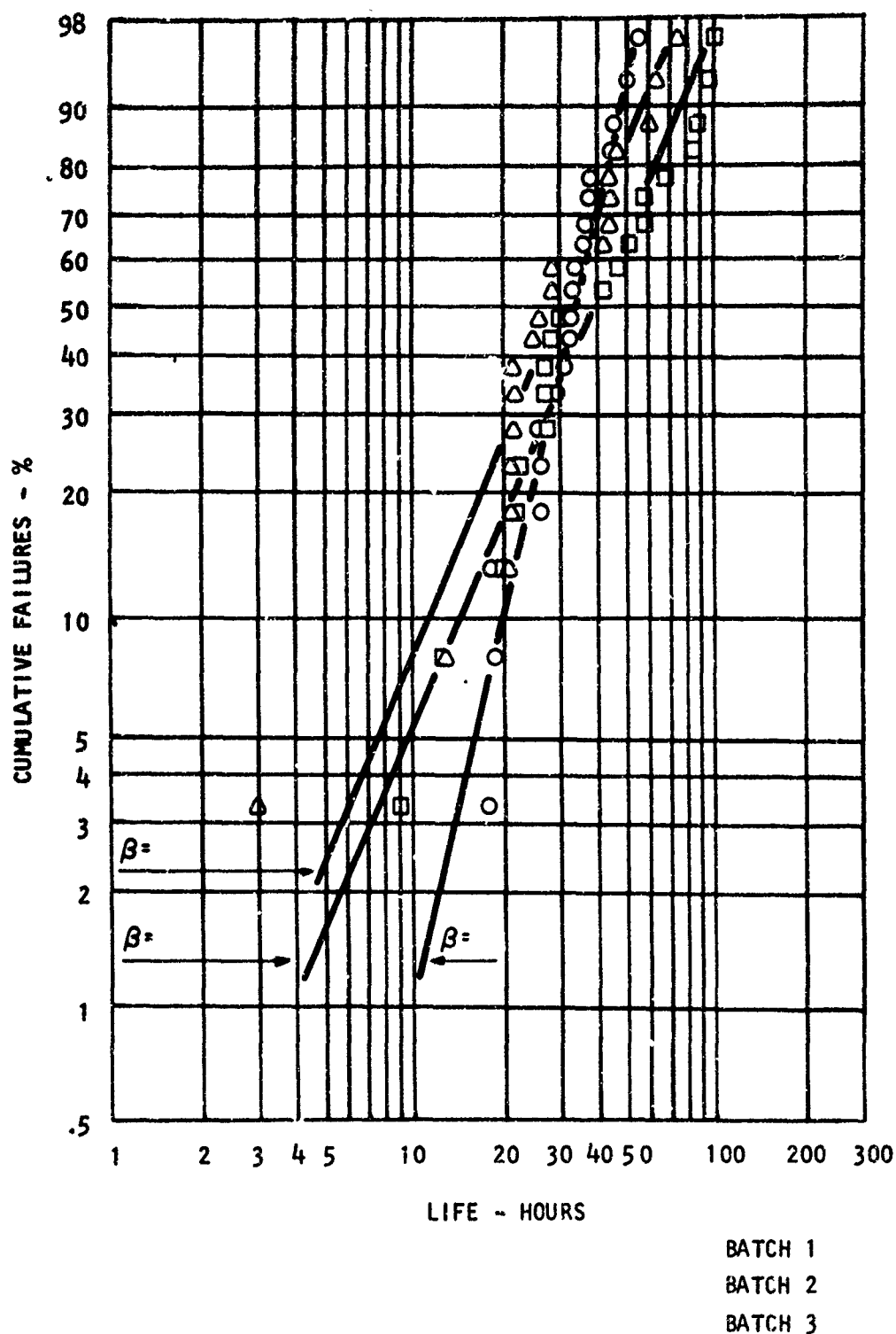


Figure 19 Percent Cumulative Failure Vs. Cyclic Oxidation Life at 2700°F for B66 and D43 Alloy Specimens (Ref. 4)

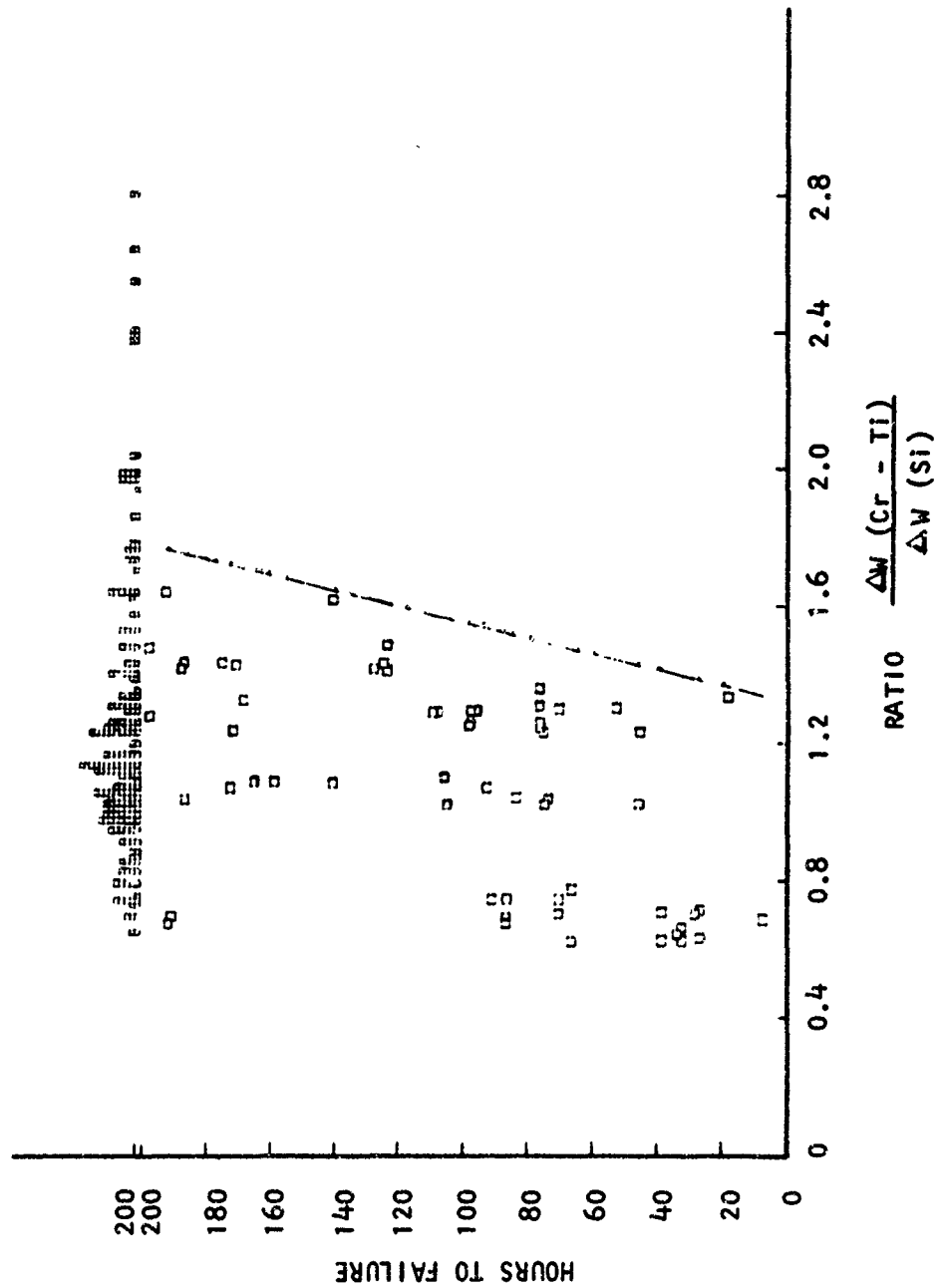


Figure 20 Hours to Failure Vs. Ratio $\Delta W_{Cr-Ti} / \Delta W_{Si}$ For Cr-Ti-Si Coated Cb Specimens Oxidation Tested at 1800°F

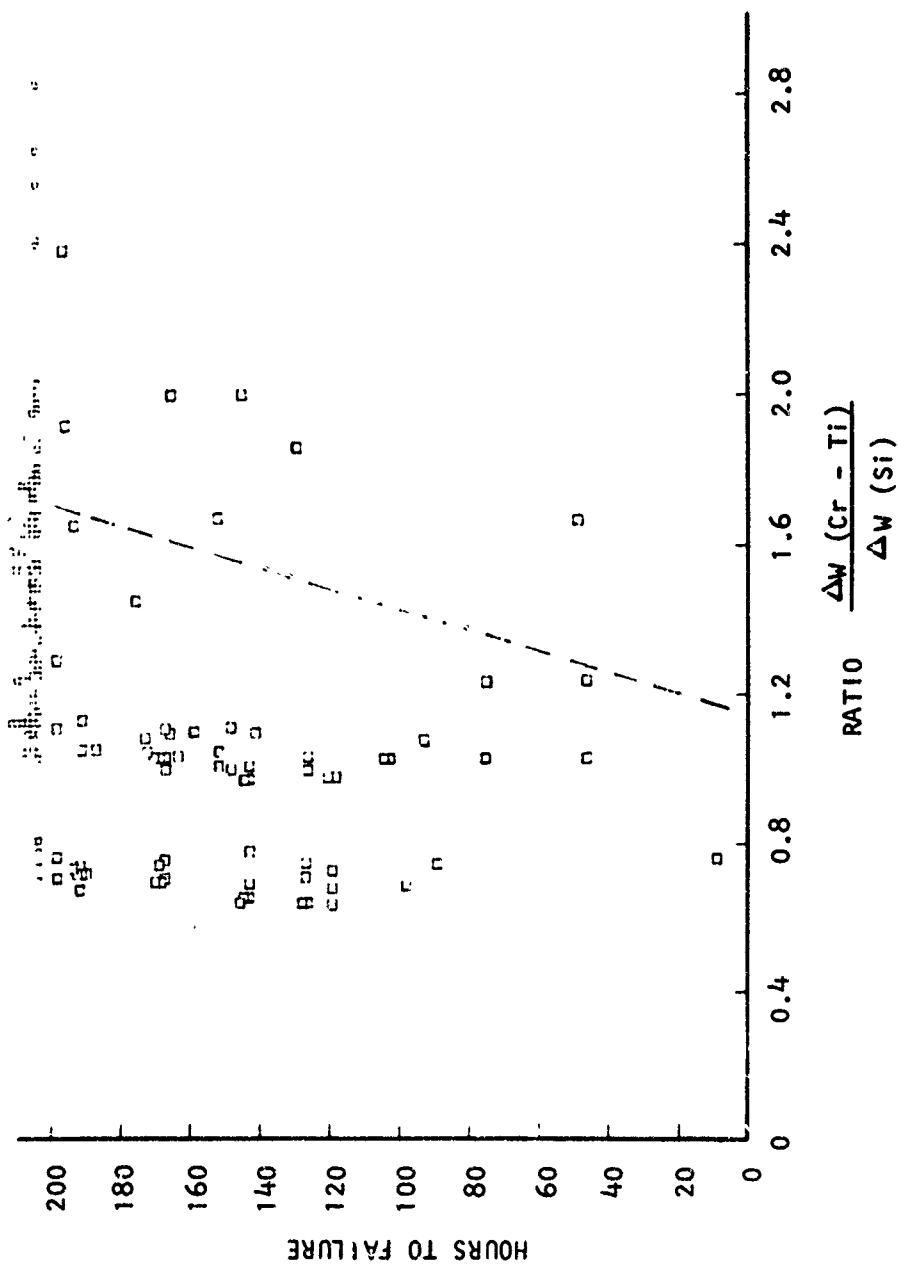


Figure 21 Hours to Failure Vs. Ratio $\Delta W_{Cr-Ti}/\Delta W_{Si}$ For Cr-Ti-Si Coated Cb Specimens Oxidation Tested at 2500°F

achieving maximum oxidation performance. The following oxidation performance can be achieved:

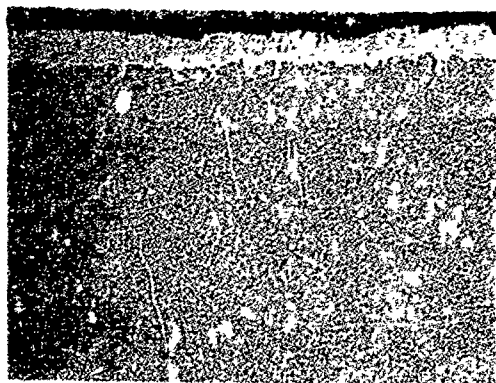
1) Life > 200 hours at 1800°F if the ratio of the Cr-Ti/Si coating weight gain is greater than approximately 1.6, a condition which ensures the presence of a continuous Laves phase between the silicide layer and the diffusion zone.

2) Life > 200 hours at 2500°F if the Cr-Ti/Si ratio of the coating element weight gain is greater than approximately 1.4.

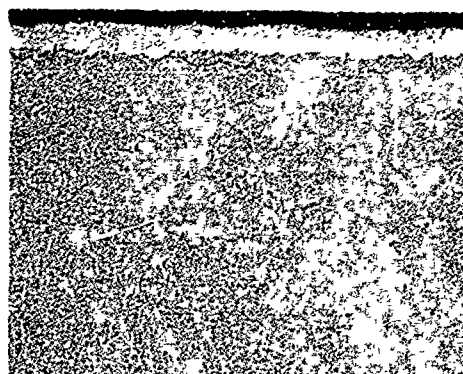
The scatter of the plotted points lying to the right of the dotted line in Figure 21 represents specimens which were all coated in Module 15. If these values were neglected, the ratio of the coating weight gain would be approximately 1.2 instead of 1.4 for life > 200 hours at 2500°F.

For Modules 1 and 4, in which NaF activator was used, there was a jagged interface separating the Laves phase overlay from the diffusion zone; and, massive Laves phase "spikes", as shown in Figures 22 and 23, penetrated into the diffusion zone. Figures 24 and 25 show that after siliciding these coatings, there was little retained Laves phase separating the silicide layer from the diffusion zone. These coupons showed oxidation lives of over 200 hours at 1800°F. The early failures (of the order of 50 hours) at 2500 and 2700°F were the consequence of low coating thickness; coupons which were in the desired weight gain range performed adequately at these temperatures.

Modules 3 and 10 through 15, utilizing CrCl_3 activator, produced coupons having random regions where the Laves phase overlay was thin or absent. There was generally a smooth interface between the Laves phase and the diffusion zone, and the "spikes" extending from the Laves phase into the diffusion zone were less massive and fewer than were observed in NaF activated coupons. As shown in Figure 26, the silicide layer on coupons from Module 10 completely penetrated the Laves phase, while for the other modules, as typified by Figure 27, there was a retained Laves phase layer between the silicide layer and the diffusion zone. The early failures at 1800°F are attributed to random areas where the silicon penetrated into the diffusion zone on coupons having a low Cr-Ti/Si weight gain ratio. This ordinarily occurred with coupons taken from the B0 and M0 pack positions. Figure 28 shows an example of random areas having a thin or absent Laves phase. These regions may have resulted from local inhomogenities either in the alloy substrate or in the pack. For example, the substrate may have been in contact with an inert particle, such as an oxidized Cr-Ti particle, or one which otherwise had a surface activity different from that of the bulk of the pack media. Areas of this type seemed more prevalent from runs conducted with CrCl_3 activator as opposed to NaF.



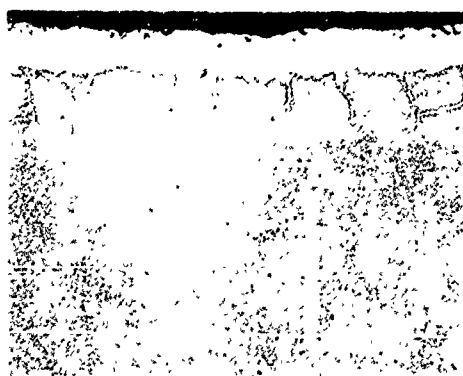
TO



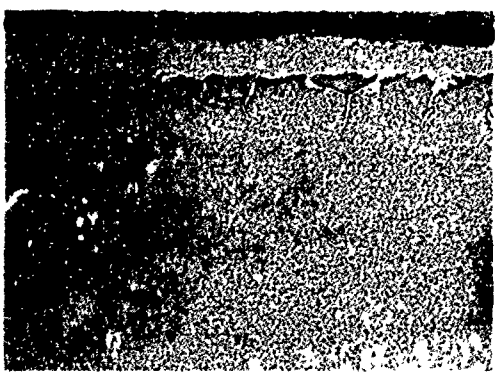
TC



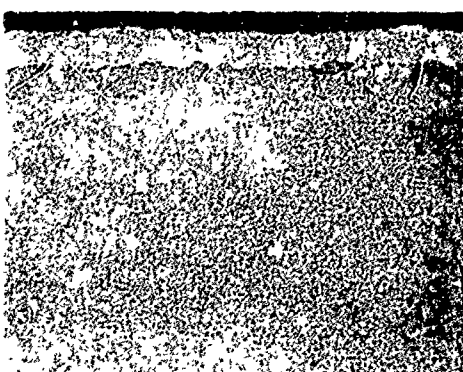
MO



MC



BO



BC

Figure 22. Cr-Ti Coated B-66 Alloy Specimens, Module Run 1 250X

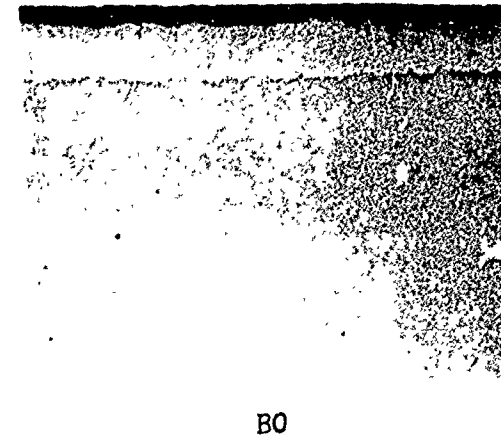
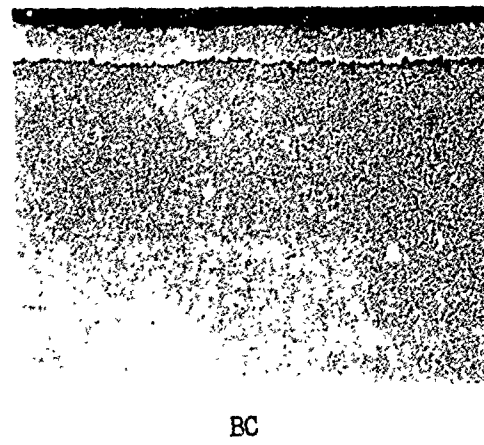
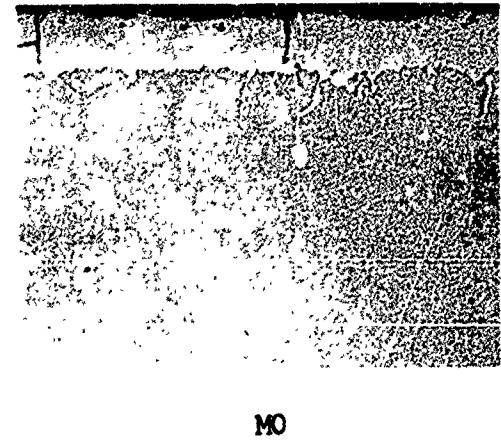
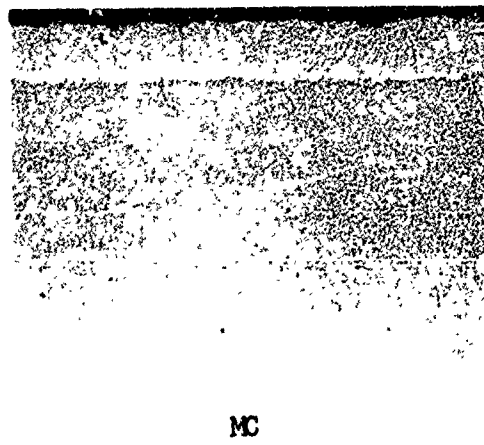
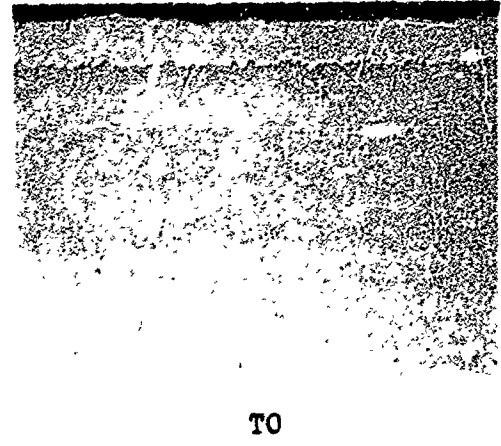
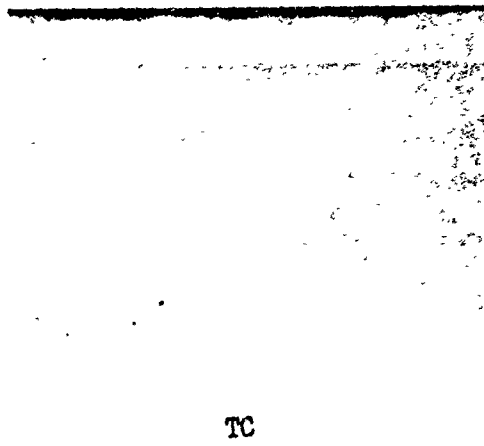
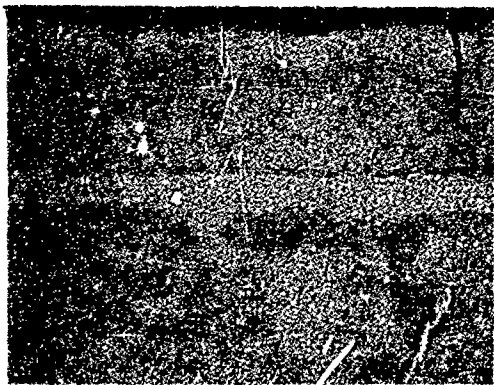


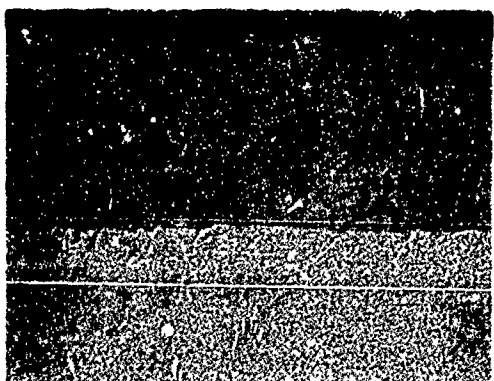
Figure 23. Cr-Ti Coated B-66 Alloy Specimens, Module Run 4



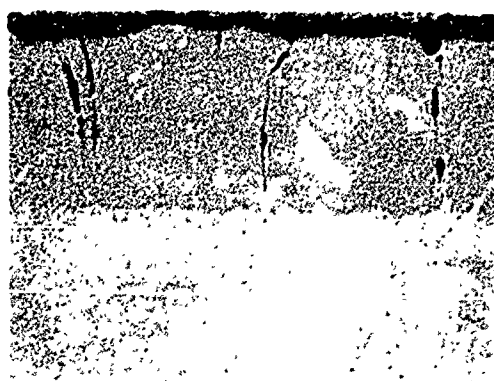
TO



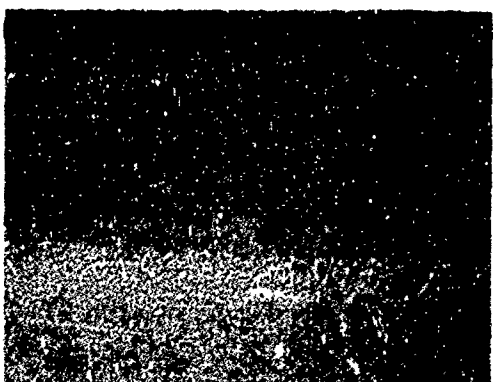
TC



MO



MC

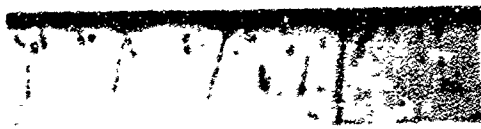


BO

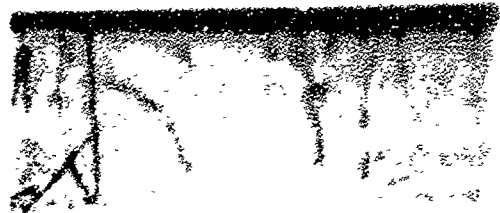


BC

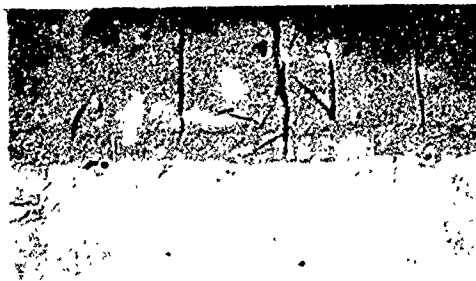
Figure 24. Cr-Ti-Si Coated B-66 Alloy Specimens, Module Run 1 250X



TC



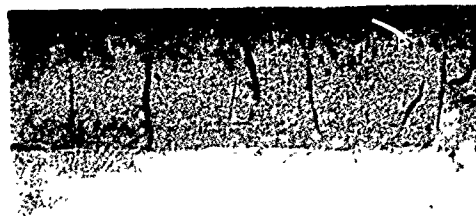
TO



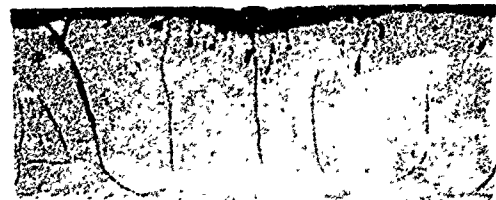
MC



MO



BC



BO

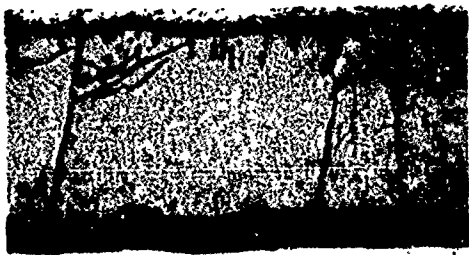
Figure 25. Cr-Ti-Si Coated B-66 Alloy Specimens, Module Run 4



TC



TO



MC



MO

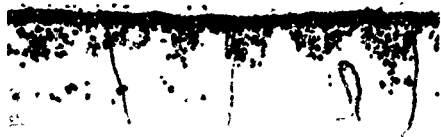


BC

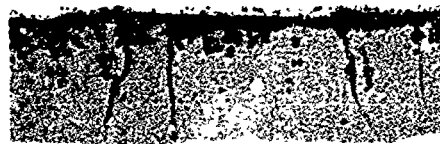


BO

Figure 26. Cr-Ti-Si Coated B-66 Alloy Specimens, Module Run 10 250X



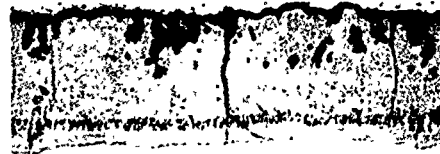
TC



TO



MC



MO

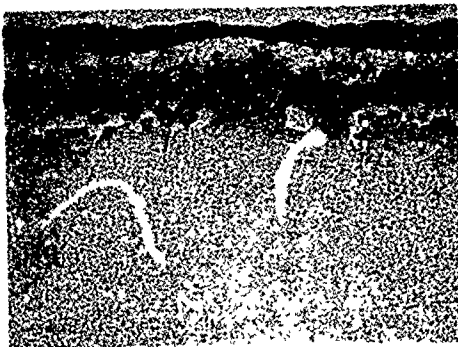


BC



BO

Figure 27. Cr-Ti-Si Coated B-66 Alloy Specimens, Module Run 15 250X



Mod 3



Mod 13

Figure 28. Photomicrograph of Cr-Ti Coated B-66 Alloy Specimens from Module Run 3 and Module Run 13 Showing the Random Thinning and Disappearances of the Cr-Ti Coating

250X

Conclusions were drawn from these module studies regarding the significant coating formation parameters; and, conditions for initial studies in the production scale furnace were selected.

4.2.4 Conclusions from the Pilot Scale Studies

4.2.4.1 Coating Powder Particle Size

All of the Cr-Ti and silicon coatings were deposited using -8 + 30 mesh powder. Previous work⁽⁵⁾ had shown that coating thickness was only slightly sensitive to particle size in the range -8 to + 200 mesh size. Finer powder particles were evaluated in the thermal diffusivity experiments and showed no significant improvement in thermal properties. Relatively coarse powder minimized sintering and sticking to the coupons, thereby facilitating removal of the coupons from the pack.

4.2.4.2 Powder Composition

Weight gain and metallographic evaluation of coupons coated in Module Runs 5, 6 and 7 showed that 70Cr-30Ti powder produced thinner coatings than 60Cr-40Ti powder. This was attributed to insufficient titanium transfer from the 70-30 alloy, an attendant low concentration of titanium in the coating, and, consequently, insufficient enhancement of chromium diffusion into the columbium surface.

Pure silicon powders were used in all siliconizing runs.

4.2.4.3 Temperature Pressure and Coating Time

In order to enhance heat transfer, thereby reducing the time required to reach the Cr-Ti coating temperature, the furnace was back-filled with a helium atmosphere of 100-150 torr during heat-up. There was also a one-hour temperature arrest at 2000°F, where the coating rate is negligible, to permit temperature equalization in the pack. Use of pressures of 1-10 torr during the isothermal segment of the cycle assisted coating deposition by facilitating temperature equalization and decreasing the rate of activator loss. All of the runs were made using a coating formation time of 8 hours.

Siliconizing was also performed using a heat-up in helium at a pressure of 100-150 torr. A temperature arrest of one hour at 1700°F, and a coating pressure of 1 torr held for 4 hours at 2000°F produced the best coatings.

4.2.4.4 Quantity and Type of Activator for the Cr-Ti Coating

For the formation of Cr-Ti coatings, the amount of activator required was not critical above a minimum amount of 50 grams (0.12w/o). Acceptable coatings were obtained with either NaF or CrCl_3 activator in amounts as low as 50 grams (0.12w/o), but more uniform coatings resulted from the use of 100 grams (0.25w/o) of activator. A plot of average Cr-Ti weight gain vs total amount of activator for runs utilizing 60Cr-40Ti powder packs is shown in Figure 29. The use of CrCl_3 as the Cr-Ti pack activator generally lead to heavier coatings, lower required activator levels, higher furnace equilibrium pressures and more uniform coating deposits with regard to pack position. From a processing viewpoint, CrCl_3 activation is preferred over NaF owing to the absence of free alkali metal (sodium) which deteriorates the alumina furnace hearth, platinum thermocouples, and protection tubes. However, microstructural analysis revealed that CrCl_3 activation generally produced insufficient titanium transfer from the 60Cr-40Ti alloy pack media; and, also contributed to a higher incidence of coating defects manifested as areas of locally thin or absent chromide overlay.

The use of CrCl_3 as an activator may be desirable based on the advantages cited above; however, to fully exploit the full oxidation performance potential indicated in this work, it is necessary to eliminate the random areas on the coated surface where the Laves phase has thinned or disappeared. A mixed CrCl_3 -NaF activator might combine the advantages of both, and limit the sodium contamination of the system. The quantity of NaF added to the CrCl_3 should be the minimum amount necessary to activate the Cr-Ti powder.

4.2.4.5 Quantity and Type of Activator for the Silicon Coating

The activators evaluated for the silicon coating were KF, CrCl_3 , and SiF_4 in amounts from 0.08 to 0.3 weight percent. The coating temperature for the silicon cycle varied from 1900 to 2100°F for times of 3 to 5 hours.

Neither CrCl_3 nor SiF_4 were effective as activators for silicon transfer. The best silicon coatings were deposited using KF activator.

4.2.4.6 Coating Parameters for use in the Production Scale Furnace

In order to achieve a good overall oxidation performance the proper coating morphology and chemistry is necessary. This is attained by forming a Cr-Ti coating in the weight range 20-25 mg/cm^2 , in conjunction with a silicide layer in the weight range 14-18 mg/cm^2 . For good low temperature performance (life > 200 hours at 1800°F), a continuous layer of the Laves phase must be present between the silicide layer and the diffusion zone. Therefore, the silicon should not completely diffuse through the Laves phase during the silicon coating cycle. However, for high temperature performance, the silicide layer must be sufficiently thick to provide an adequate supply of silicon.

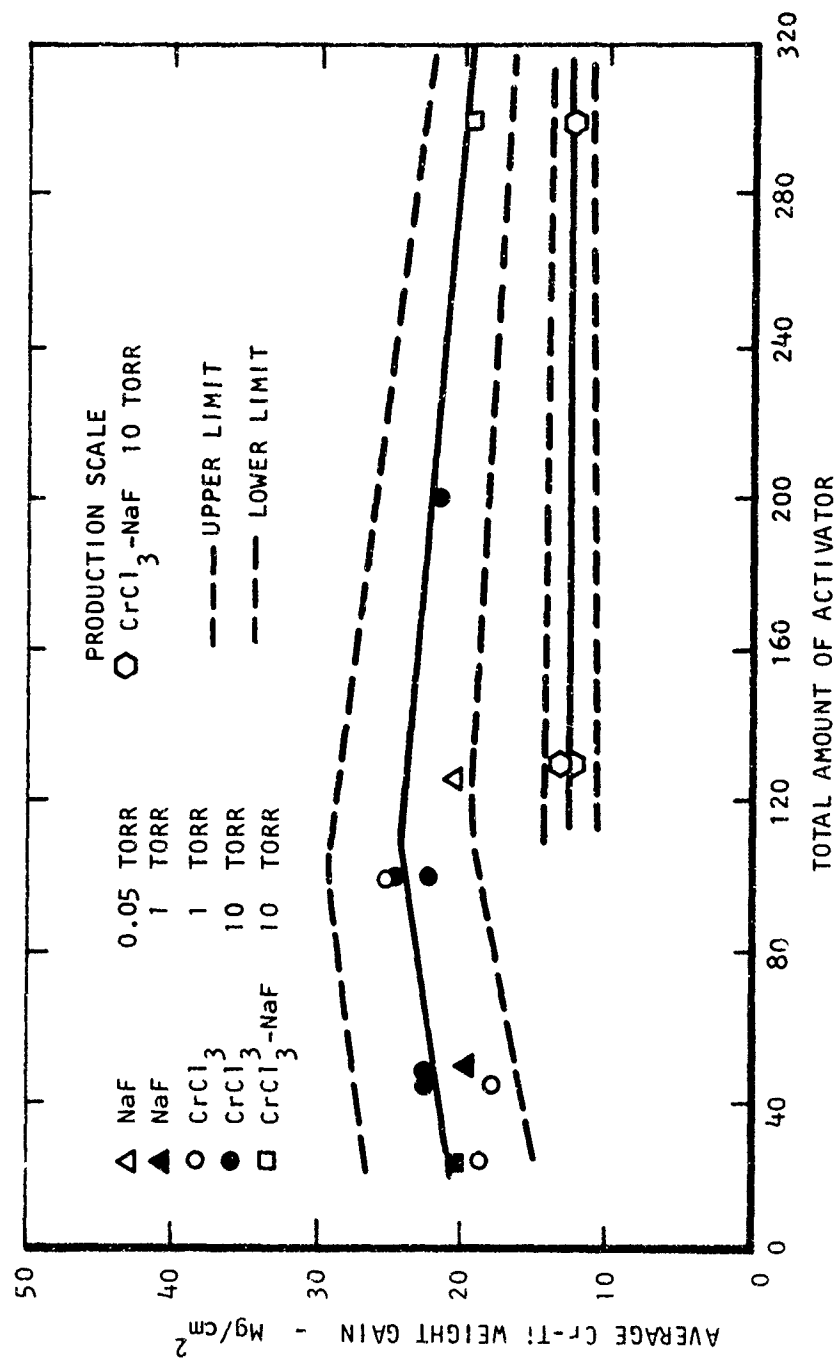


Figure 29 Average Cr-Ti Weight Gain Vs. Total Amount of Activator for All Coating Runs Using the Module Retort and 60 Cr-40 Ti Powder

Cr-Ti-Si coatings can be tailored to fit the desired application. The coating described above will provide good oxidation protection to about 2600°F. However, for use above this temperature, Cr-Ti-Si coating leaner in chromium and titanium would exhibit superior properties. Lives of approximately 70-80 hours at 2700°F can be achieved with the sacrifice of 1800°F life by decreasing the Cr-Ti to silicon weight ratio to 0.5-1.0. The selection of parameters for this program was based on forming Cr-Ti-Si coatings with good properties over the entire temperature spectrum.

Based on the Module Run experiments and the thermal diffusivity work, the following sets of process parameters were developed for use in the production-scale furnace experiments.

- 1) Cr-Ti cycle to give a weight pick up of 20-25 mg/cm²
 - a) 60Cr-40Ti powder of (-8 + 30 mesh) size
 - b) Temperature-pressure profile comprising a heat up at a pressure of 100-150 torr helium to a surface pack temperature of 2000°F, hold for one hour until the pack center temperature reaches 1800°F, then raise the surface temperature to 2300°F while reducing the system pressure to 10 torr. Maintain the 2300°F-10 torr condition for a coating time of 8 hours.
 - c) 0.75 weight percent CrCl₃-NaF mixed activator in a 2:1 ratio.
- 2) Si cycle
 - a) Silicon powder (-8 + 30 mesh) to give a weight pick up of 14-18 mg/cm²
 - b) Temperature-pressure profile comprising heating to a pack surface temperature of 1700°F at a pressure of 100-150 torr helium, holding 1 hour at 1700°F until the pack center temperature reaches 1500°F, then increasing the surface temperature to 1900°F while decreasing the system pressure to 1 torr and maintaining these conditions for a coating time of 4 hours.
 - c) 0.25 weight percent KF activator.

4.3 Coating Studies in the Production-Scale Furnace

The initial studies performed in the production scale facility were based upon the above process parameters. The coated specimens from each Cr-Ti-Si coating run were evaluated by metallographic examination, weight change evaluation and cyclic oxidation tests. In the following discussions the letters P and L after the module designation refer to the pilot-scale or the production-scale furnace respectively. The coating parameters utilized for the deposition studies performed in the production-scale furnace are compiled in Table 4. Coating weight gain and oxidation performance data are summarized in Table 5, and given in detail in Appendix V. The module retort (8" x 8" x 36") was used for runs 16L through 19L, however, only specimens from modules 16L and 17L were siliconized. Coating runs 20L and 22L were multiple experiments using two 7-1/2-inch diameter by 18-inch high retorts, and a 5" diameter by 10" high retort designed for a molten glass seal.

Runs 16L, 17L and 19L were made to determine base-line Cr-Ti and silicon weight gains for the module retort when used in the production-scale furnace. In all three runs the average Cr-Ti weight gain of 12.5 mg/cm² was considerably lower than had been obtained in the pilot-scale furnace. Run 18P was then made in order to evaluate the effect of mixed CrCl₃-NaF activator in the pilot-scale furnace, since only CrCl₃ or NaF alone had been used in previous runs in the pilot furnace. The average Cr-Ti weight gain from this run was 19.3 mg/cm², comparable to values observed in the earlier module runs using either CrCl₃ or NaF individually. This weight gain, along with microscopic evaluation, verified the premise that under similar processing conditions the use of mixed CrCl₃-NaF in a 2:1 ratio would produce Cr-Ti coatings generally equivalent in thickness and morphology to those obtained using either CrCl₃ or NaF individually.

A plot of the average Cr-Ti weight gain vs. the total amount of activator for these production-scale furnace runs, utilizing 60Cr-40Ti powder packs, was also shown in Figure 22. In this Figure the dashed lines, labeled "upper limit" and "lower limit", represent the highest and lowest coating weight gain to be expected based on the module runs. In the pilot-scale furnace the Cr-Ti weight gain increased from approximately 16 mg/cm² at 20 grams of activator to a value of approximately 24 mg/cm² at 100 grams of activator, and then decreased linearly to approximately 20 mg/cm² at 300 grams of activator. The Cr-Ti weight gain was independent of equilibrium pressure and type of activator, and only slightly dependent upon activator quantity in the 100 to 300 gram level. However, in the production-scale furnace, the Cr-Ti weight gain curve was displaced downward by approximately 9 to 11 mg/cm². As pointed out previously,

TABLE 4

PRODUCTION SCALE FURNACE PROCESS DEVELOPMENT PARAMETERS

Powder	Cr-Ti Cycle 2300°C-8 Hours		Coat Wt. mg/cm ²	Si-Cycle 4 Hours			Coat Wt. mg/cm ²	Remarks
	Activator (gms)	Pressure (torr)		Activator (gms)	Pressure (torr)	Temp. (°F)		
"10d 16L 60Cr-40Ti	CrCl ₃ (100) NaF (50)	10	12.9	KF (125)	1	1900	12.6	
"10d 17L 60Cr-40Ti	CrCl ₃ (200) NaF (100)	10	12.2	KF (125)	10	2000	16.2	
"10d 18P 60Cr-40Ti	CrCl ₃ (200) NaF (100)	10	19.3	-	-	-	-	
"10d 13L 60Cr-40Ti	CrCl ₃ (100) NaF (50)	10	12.6	-	-	-	-	
"10d 20L 60Cr-40Ti	CrCl ₃ (200) NaF (100)	10	14.1	-	-	-	-	(7-1/2" Dia. X 18" Retort)
60Cr-40Ti	CrCl ₃ (200) NaF (100)		14.1	-	-	-	-	(5" Dia X 10" Retort "glass seal")
60Cr-40Ti	CrCl ₃ (200) NaF (100)		26.1	-	-	-	-	(7-1/2" Dia. X 18" Retort)
"10d 24L 60Cr-40Ti	CrCl ₃ (200) NaF (100)	10	15.6	-	-	-	-	(5" dia. X 10" Retort-graphite enclosure)

TABLE 5

COMPILATION OF WEIGHT GAIN AND OXIDATION PERFORMANCE

Alloy	Average Coat Weight Cr-Ti, Si mg/cm ²	Surface Area cm ²	Life Hrs.	Coat Weight Cr-Ti, Si mg/cm ²	TC		TD		TC		TD		TC		TD		TC		TD		TC		TD		TC		TD	
					Coat Weight Cr-Ti, Si mg/cm ²	Life Hrs.	Coat Weight Cr-Ti, Si mg/cm ²	Life Hrs.	Coat Weight Cr-Ti, Si mg/cm ²	Life Hrs.	Coat Weight Cr-Ti, Si mg/cm ²	Life Hrs.	Coat Weight Cr-Ti, Si mg/cm ²	Life Hrs.	Coat Weight Cr-Ti, Si mg/cm ²	Life Hrs.	Coat Weight Cr-Ti, Si mg/cm ²	Life Hrs.	Coat Weight Cr-Ti, Si mg/cm ²	Life Hrs.	Coat Weight Cr-Ti, Si mg/cm ²	Life Hrs.	Coat Weight Cr-Ti, Si mg/cm ²	Life Hrs.	Coat Weight Cr-Ti, Si mg/cm ²	Life Hrs.	Coat Weight Cr-Ti, Si mg/cm ²	Life Hrs.
Mod 16L (12.6-12.6)	12.5	1800	190	11.3	9.9	200-200	12.1	10.8	75-122	200-200	12.5	12.8	12.5	12.8	12.5	12.8	12.5	12.8	12.5	12.8	12.5	12.8	12.5	12.8	12.5	12.8	12.5	12.8
			69	11.3	9.9	55-79	12.1	10.8	75-122	200-200	12.5	12.8	12.5	12.8	12.5	12.8	12.5	12.8	12.5	12.8	12.5	12.8	12.5	12.8	12.5	12.8	12.5	12.8
			34	11.3	9.9	34-34	12.1	10.8	75-122	200-200	12.5	12.8	12.5	12.8	12.5	12.8	12.5	12.8	12.5	12.8	12.5	12.8	12.5	12.8	12.5	12.8	12.5	12.8
			190	11.3	9.9	200-200	12.1	10.8	75-122	200-200	12.5	12.8	12.5	12.8	12.5	12.8	12.5	12.8	12.5	12.8	12.5	12.8	12.5	12.8	12.5	12.8	12.5	12.8
Mod 17L (12.2-16.2)	12.7	1800	190	11.3	9.9	200-200	12.1	10.8	75-122	200-200	12.5	12.8	12.5	12.8	12.5	12.8	12.5	12.8	12.5	12.8	12.5	12.8	12.5	12.8	12.5	12.8	12.5	12.8
			69	11.3	9.9	55-79	12.1	10.8	75-122	200-200	12.5	12.8	12.5	12.8	12.5	12.8	12.5	12.8	12.5	12.8	12.5	12.8	12.5	12.8	12.5	12.8	12.5	12.8
			34	11.3	9.9	34-34	12.1	10.8	75-122	200-200	12.5	12.8	12.5	12.8	12.5	12.8	12.5	12.8	12.5	12.8	12.5	12.8	12.5	12.8	12.5	12.8	12.5	12.8
			190	11.3	9.9	200-200	12.1	10.8	75-122	200-200	12.5	12.8	12.5	12.8	12.5	12.8	12.5	12.8	12.5	12.8	12.5	12.8	12.5	12.8	12.5	12.8	12.5	12.8

In the Cr-Ti cycle the transfer of an adequate amount of titanium from the powder pack to the surface being coated is necessary in order to transfer the chromium needed to achieve the desired coating morphology and weight gain. The Cr-Ti coating formed in the production scale furnace appeared metallographically to be deficient in titanium, as indicated by a thin chromide overlay and the absence of an underlying diffusion zone. This insufficient titanium transfer was related to a lower partial pressure of titanium-activated halide species in the vicinity of the work material, for the coating operation in the production furnace.

Runs 20L and 24L were made subsequently in an effort to increase the Cr-Ti weight gains to the desired 20-25 mg/cm² level. Coating run 20L contained the following three experimental retorts:

- 1) A small 5-inch diameter by 10-inch high columbium retort containing 60Cr-40Ti powder, and having a seal which was liquid at the coating temperature as an attempt to trap the activated halide species in the powder pack,

- 2) A 7-1/2-inch diameter by 18-inch high retort containing 60Cr-40Ti powder,

- 3) A 7-1/2-inch diameter by 18-inch high retort containing 50Cr-50Ti powder.

These latter two retorts did not have liquid seals.

In all of these packs the amount of activator was in the weight percent ratio equivalent to the 200 grams CrCl₃ and 100 grams NaF used for the module pack. These results showed that the liquid seal was not effective, i.e., both 60/40 packs gave identical coating weight gains of 14.1 mg/cm². The 50Cr-50Ti pack showed a weight gain of 26.1 mg/cm², about double the weight gain of the 60Cr-40Ti packs, indicating a gaseous atmosphere richer in titanium. However, the higher weight gain was accompanied by specimen to powder sintering, and pronounced localized titanium rich regions in the coating surface. Such areas are undesirable, since after siliconizing these areas are predominantly titanium disilicide which exhibits relatively poor high temperature oxidation resistance.

Another coating run, 24L, contained two experiments: a 5-inch diameter by 10-inch high retort containing 60Cr-40Ti powder and completely enclosed in a graphite container, and, a 4-inch diameter by 8-inch retort containing 60Cr-40Ti powder which was, in turn, embedded in 50Cr-50Ti powder contained in a 7-1/2-inch diameter by 18-inch high retort. For this run it was found that

the average weight gain for specimens in the 60Cr-40Ti powder pack, which was embedded in 50Cr-50Ti powder was 13.9 mg/cm², and the average weight gain for the graphite shielded pack was 15.6 mg/cm². The higher weight gains compared to runs 16L and 17L suggest more efficient trapping of the halide species in the retort.

The results from the entire series of Cr-Ti coating runs made in the production-scale furnace are summarized below. The initial Cr-Ti coating runs performed in the module retort gave an average coating weight gain of 12-13 mg/cm², appreciably thinner than the desired 20-25 mg/cm² achieved in the pilot-scale facility. The average coating weight gain was independent of total activator quantity in the range 100 to 300 grams, used with approximately 200 pounds of 60Cr-40Ti powder. Mixed CrCl₃-NaF activator in the ratio of 2:1 yielded coating thicknesses generally equivalent to either CrCl₃, or NaF alone. Higher Cr-Ti weight gains in coating run 24L indicated better retention of the activator, thus a greater partial pressure of Ti halides in the retort. The smaller spread in the Cr-Ti coating weight gains in the production furnace, as shown in Figure 22, indicated better temperature control and coating uniformity in the production-scale furnace.

The Cr-Ti coating weight gain of 12 to 13 mg/cm² and the silicon weight gain of 11-16 mg/cm² observed for module runs 16L and 17 L in the production-scale furnace were lower than the desired values of 20 to 25 mg/cm² and 17-20 mg/cm² for the Cr-Ti and silicon weight gains, respectively. However, since the oxidation performance (Table 5) of these coatings met the program performance goals, it was decided to proceed with the coating reproducibility studies.

4.4 Coating Process Reproducibility Studies

In order to determine the reproducibility of the vacuum pack coating process, three Cr-Ti and three silicon coating runs were made using the production-scale furnace. In each run the coatings were formed on thirty-six Cb752 alloy coupons approximately 0.75-inch long x 0.5-inch wide x 0.030-inch thick. Separate retorts were used for the Cr-Ti and silicon coating cycles. The coating deposition parameters used for these runs were based upon the results of module studies conducted in the pilot and production scale furnaces, and are summarized in Table 6. The coating time and temperature chosen for the silicon coating cycle depended upon the Cr-Ti overlay thickness, and varied only slightly from run to run. Since the previous module studies indicated that for balanced oxidation performance the desired ratio of Cr-Ti weight gain to Si weight gain should be about unity, the silicon coating parameters were chosen to provide this weight gain ratio.

TABLE 6

PARAMETERS USED FOR THE VACUUM PACK REPRODUCIBILITY RUNS

Run	Pack Powder	Cr-Ti Cycle				Si Cycle			
		Activator (gms)	Pressure (torr)	Temp. (°F)	Time (Hrs)	Activator (gms)	Pressure (torr)	Temp (°F)	Time (Hrs)
A	60Cr-40Ti	CrCl ₃ (200)(1) NaF (100)	10	2300	8	KF 100(3)	1	1900	3.5
B	60Cr-40Ti	CrCl ₃ (200) NaF (100)	10	2300	8	KF 100	1	1900	4.0
C	60Cr-40Ti	CrCl ₃ (200) NaF (100)	10	2300	8	KF 100	1	1900	3.5

(1) Corresponds to 0.75 weight percent of the pack powder.

(2) Corresponds to 0.25 weight percent of the pack powder.

(3) Heat up under 100-150 torr He to 2000°F - hold at 2000°F for 1 hour - increase temperature to 2300°F then decrease pressure to equilibrium pressure.

(4) Heat up under 100-150 torr He to 1500°F - hold at 1500°F for 1 hour - increase temperature to coating temperature then decrease pressure to equilibrium pressure - pump down to 150 torr starting one-half hour prior to end of coating cycle.

The principal criteria for evaluating process reproducibility was the oxidation performance of the coated coupons. The target oxidation performance conditions were a 90% reliable life greater than 125 hours at 1800°F, a 90% reliable life greater than 50 hours at 2600°F, a deviation from the average life of not more than ± 10 hours, and the occurrence of failure by a wearout mechanism, as indicated by value of the Weibull shape factor (β) greater than unity. In addition to these reproducibility criteria, the coupons were also evaluated for coating microstructure and coating element weight gain.

The results of cyclic oxidation testing at 1800 and 2600°F are summarized in Table 7, and Weibull plots for the individual tests are given in Appendix VI. The Cr-Ti weight gain to silicon weight gain ratios varied from 0.97 to 0.86 for these runs. These variations in both individual coating weight gains and in the coating weight gain ratios did not significantly effect the 1800 and 2600°F oxidation performance. The 90% reliable lives and the shape factor values for all three runs at 1800 and 2600°F exceeded the minimum requirements of the process reproducibility criteria.

Figures 30 to 32 show microstructures of the coatings from each of these runs. The morphology of the coatings from runs A and B cannot be considered as optimum, since there was no evidence of Laves phase in the diffusion zone, and the Cr-Ti layer was completely consumed by the silicide coating. However, the oxidation performance of these coatings did meet the reproducibility performance criteria. The coating from run C showed evidence of chromide "spikes" in the diffusion zone and the original Cr-Ti coating was not completely consumed by the silicide coating. The morphology of this coating resembles the ideal morphology proposed for the Cr-Ti-Si coating. The 1800°F life of coating C was superior to that of the coatings from runs A and B due to the increased low temperature protection offered by the Cr-Ti rich region which had not been silicided.

For the investigations conducted to this point, the same 60Cr-40Ti alloy powder had been used for all Cr-Ti coating runs, as well as for other Cr-Ti-Si coating work on other programs. During the experiments for this program no chemical analysis of the pack was made. Therefore, before conducting the preliminary proof, it was decided to chemically analyze the pack powder. The bulk composition of the powder was found to be substantially reduced in titanium, apparently as a result of progressive removal or oxidation of the titanium during continued use of the pack. Figure 33 shows photomicrographs of Cr-Ti coatings formed on Cb752 alloy utilizing both relatively unused 60Cr-40Ti alloy powder, and pack material which had experienced extensive use. These coatings were formed in a laboratory furnace. Both microstructures show the continuous Laves band, while only the coating formed from the

TABLE 7

COMPILATION OF RESULTS FOR THE VACUUM PACK REPRODUCIBILITY COATING RUNS

Run	Test Temperature (°F)	Reproducibility Tests				Major Milestone Goal	
		Coating Weight Cr-Ti (mg/cm ²)	Weight Gain Si (mg/cm ²)	Cr-Ti/Si Ratio	90% Reliable Life (Hrs)	90% Reliable Life (Hrs)	β
A	1800	12.7	13.1	0.97	168	125	1
	2600				54	50	1
B	1800	15.0	15.5	0.97	142	125	1
	2600				33	50	1
C	1800	12.0	14.0	0.86	290	125	1
	2600				50	50	1



TO



TC



MO



MC

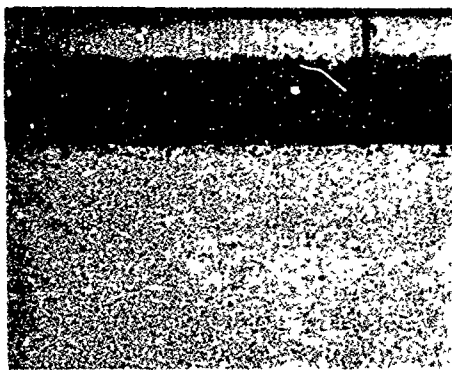


BO

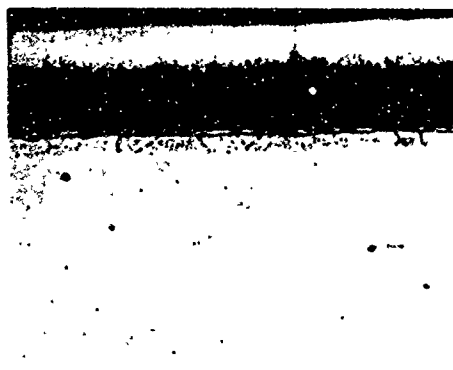


BC

Figure 30. Cr-Ti-Si Coated Cb-752 Alloy Specimens
from Vacuum Pack Reproducibility Run A Unetched 250X



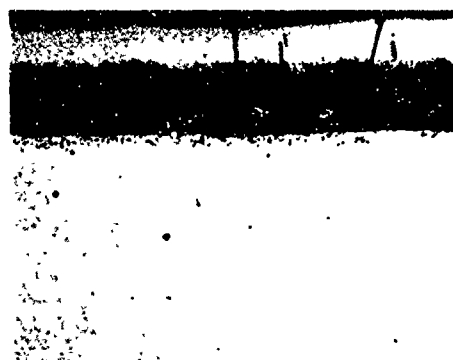
TO



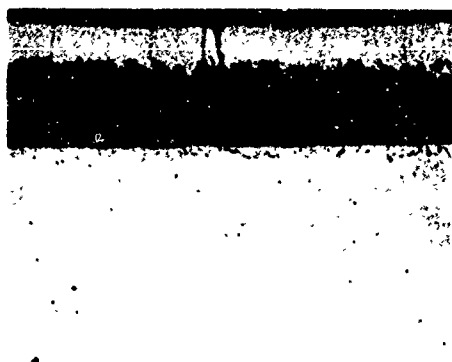
TC



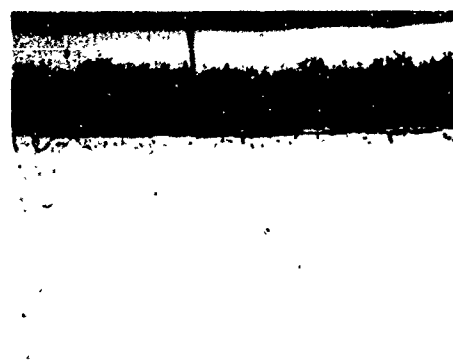
MO



MC



BO



BC

Figure 31. Cr-Ti-Si Coated Cb-752 Alloy Specimens
from Vacuum Pack Reproducibility Run B Etched 250X



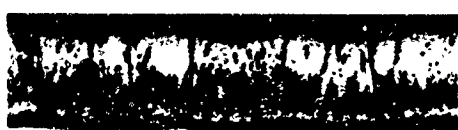
TO



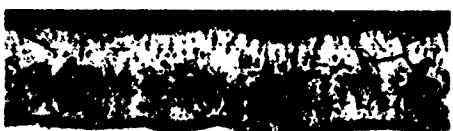
TC



MO



MC



BO



BC

Figure 32. Cr-Ti-Si Coated Cb-752 Alloy Specimens
from Vacuum Pack Reproducibility Run C Etched 250X

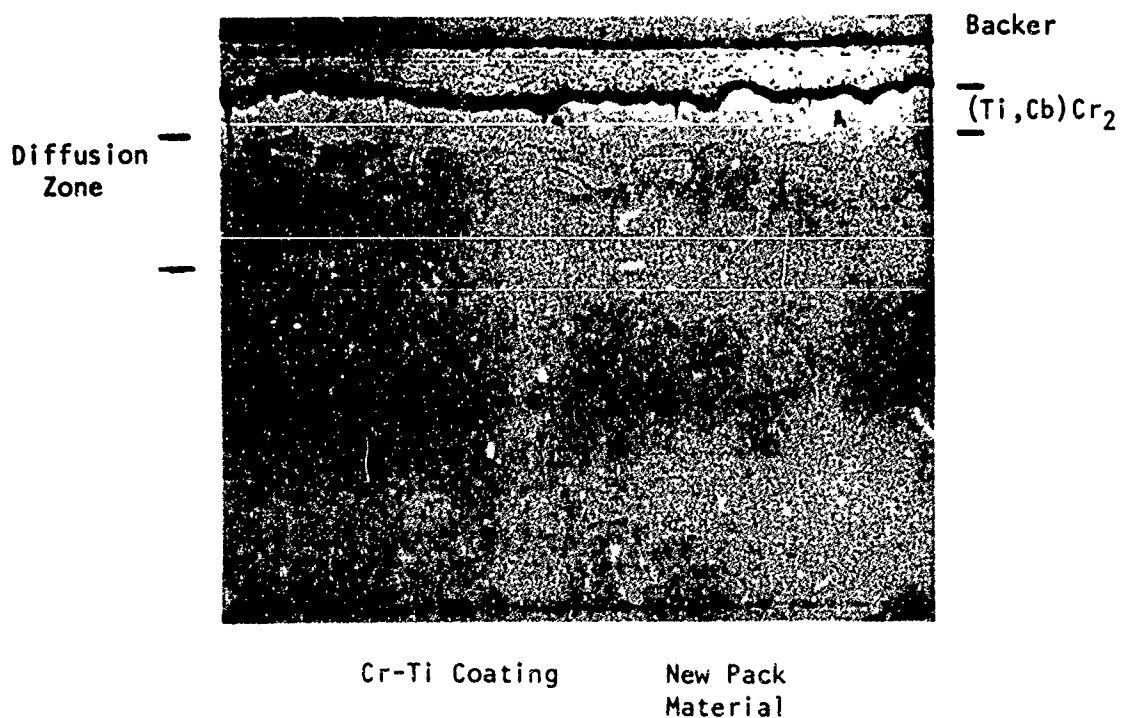
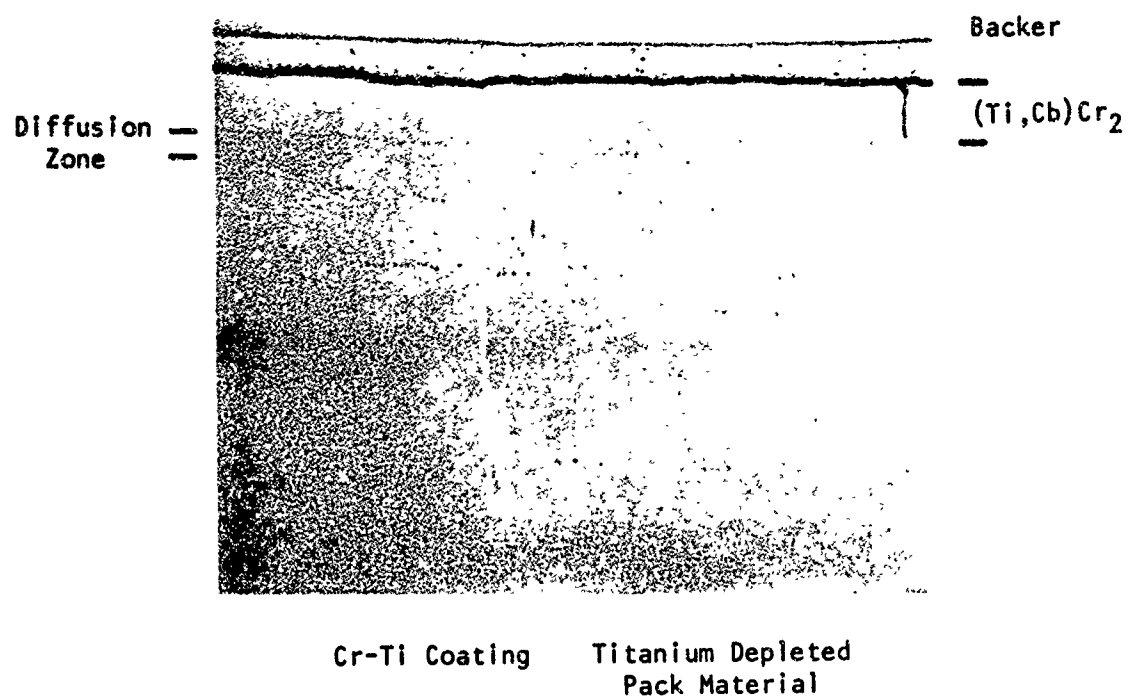


Figure 33. Cr-Ti Coatings on Cb-752 Columbian Alloy Formed from Used (Depleted) and New 60Cr-40Ti Alloy Pack Material 250X

unused pack exhibits a pronounced diffusion zone. This latter microstructure represents a nearly optimum Cr-Ti precoat for formation of the Cr-Ti-Si coating. Chromium diffuses relatively slowly in unalloyed columbium, and combines with columbium to form the intermetallic compound CbCr_2 . Introduction of titanium into the columbium lattice enhances the diffusion of chromium, possibly by lowering the required activation energy or by expanding the lattice. Thus, during the co-deposition of chromium and titanium, sufficient titanium is required in the pack vapor phase to adequately promote chromium diffusion. Since TiCr_2 and CbCr_2 are isomorphous compounds, the titanium serves both to support the intermetallic growth, and to enhance dissolution of coating elements in the host lattice. With the unused 60Cr-40Ti alloy pack media the Ti/Cr balance in the pack vapor phase sustained the desired diffusion process, while the extensively used Cr-Ti material provided an inadequate supply of titanium species.

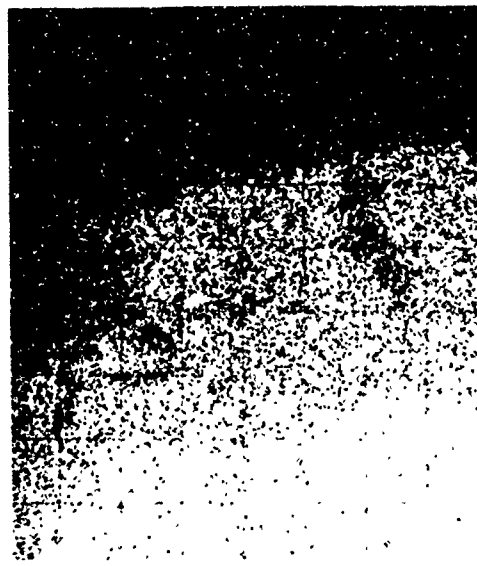
The degree of substrate alloying accomplished in the Cr-Ti cycle is illustrated more clearly in the electron microprobe X-ray traces shown in Figures 34 and 35. Figure 34 shows current and X-ray images for a Cr-Ti coating formed on Cb752 alloy using a new, unused 60Cr-40Ti alloy powder. The outer Laves phase $(\text{Cb},\text{Ti})\text{Cr}_2$ is observed to be very rich in chromium and titanium, with negligible columbium near the outer surface. The intermediate "spikes" are the result of preferred coating element diffusion down the substrate grain boundaries. The diffusion zone beneath the chromide layer exhibits high concentrations of chromium and titanium dissolved in the columbium matrix.

Figure 35 shows analogous EMP traces for a Cr-Ti coating formed from a 60Cr-40Ti alloy pack media which had experienced 1-2 years of prior use. The Laves phase "spikes" which are indicative of enhanced chromium diffusion are absent; the chromide phase appears richer in columbium; and little coating element dissolution in the substrate is evident beneath the chromide layer. This latter Cr-Ti precoat produces a Cr-Ti-Si coating which is too rich in columbium, and does not have the underlying Cb-Cr-Ti solid solution region.

Both chemical and microstructural analyses were made of the used 60Cr-40Ti alloy pack material. The surface chemistry of the powder is most critical, since only the powder surface contributes directly to the composition of the pack vapor phase. However, wet chemical analyses were performed on the alloy to assess any changes in the bulk chemistry. The results were as follows:



Current Image



Cb X-Rays

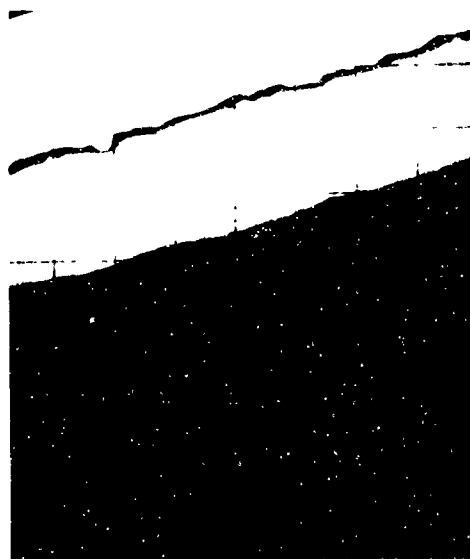


Ti X-Rays

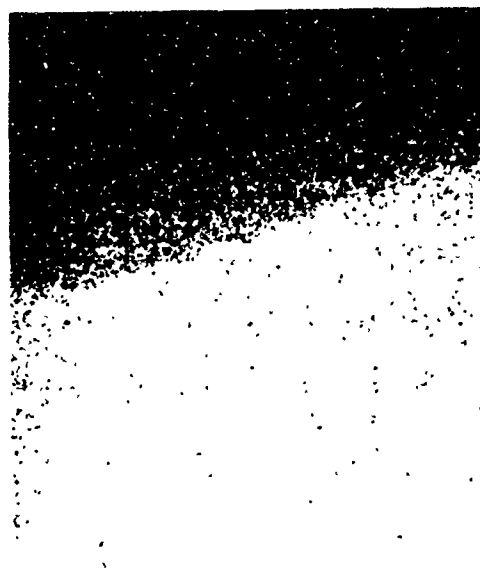


Cr X-Rays

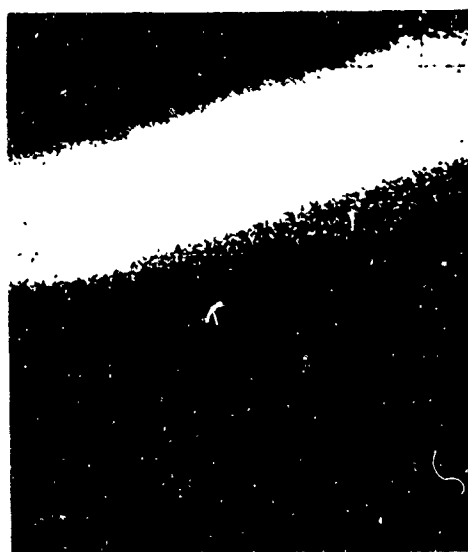
Figure 34. EMP Images of Cr-Ti Coating on Cb-752 Columbium Alloy Formed from New 60Cr-40Ti Alloy Pack Media



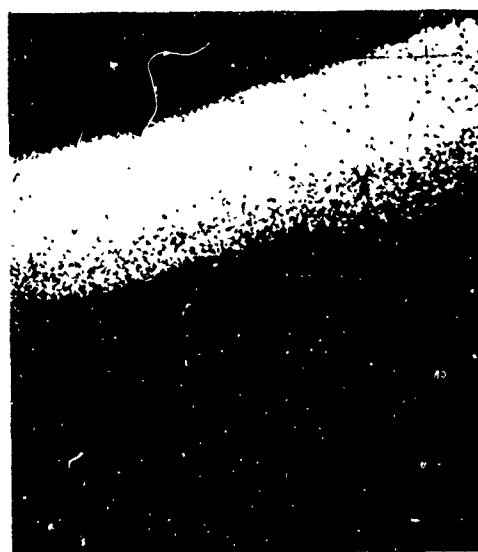
Current Image



Cb X-Rays



Cr X-Rays



Ti X-Rays

800X

Figure 35. EMP Images of Cr-Ti Coating on Cb-752 Columbian Alloy Formed from Used (Depleted) 60Cr-40Ti Alloy Pack Media

Element	Weight Percent		
	Original	Lot 1	Lot 2
Cr	57	57.8	57.4
Ti	42	26.5	33.3
Residuals	1	15.7	9.3

Although the bulk chromium content remained relatively unchanged, a substantial decrease in titanium content is observed, along with the formation of significant quantities of an insoluble residual phase of undetermined composition, possibly titanium oxide.

Figure 36 is a photomicrograph showing a cross section through a 60Cr-40Ti alloy particle from the used pack. The secondary phase in the $TiCr_2$ matrix is β titanium. A titanium depleted zone at the particle surface is quite apparent, and this reduction in titanium concentration is shown more clearly by the accompanying EMP X-ray traces. At the very surface of the particle the concentration of titanium in the chromide phase is extremely low, and for some distance from the surface there is generally an absence of the β titanium phase. The titanium rich band parallel to the particle surface appears to be β titanium; however, it may be titanium oxide on the surface of an open void intersected by the plane of the metallographic cross section.

Depletion of titanium from the 60Cr-40Ti pack material may occur by both oxidation and reaction with the halide additive. Residual oxygen in the vacuum furnace is gettered by the titanium, which serves to protect the columbium hardware from interstitial contamination. Both chromium and titanium react with the halide in the transfer process, and chromium is also transferred by direct metallic vaporization. It is unlikely that elements are removed from the alloy particles at rates equivalent to 60Cr-40Ti. Thus, changes in the alloy microstructure and chemistry are to be expected.

The three reproducibility runs were completed before it had been determined that titanium depleted Cr-Ti powder was used to form the coatings. The absence of Laves phase formation in the diffusion zone of these coatings was a consequence of the lower titanium transfer from the depleted powder. However, the reproducibility of coating weight gains was not considered to have been influenced by the use of the depleted pack media. Subsequent work on the preliminary proof of the diffusion pack coating process was therefore done with a new lot of 60Cr-40Ti powder.

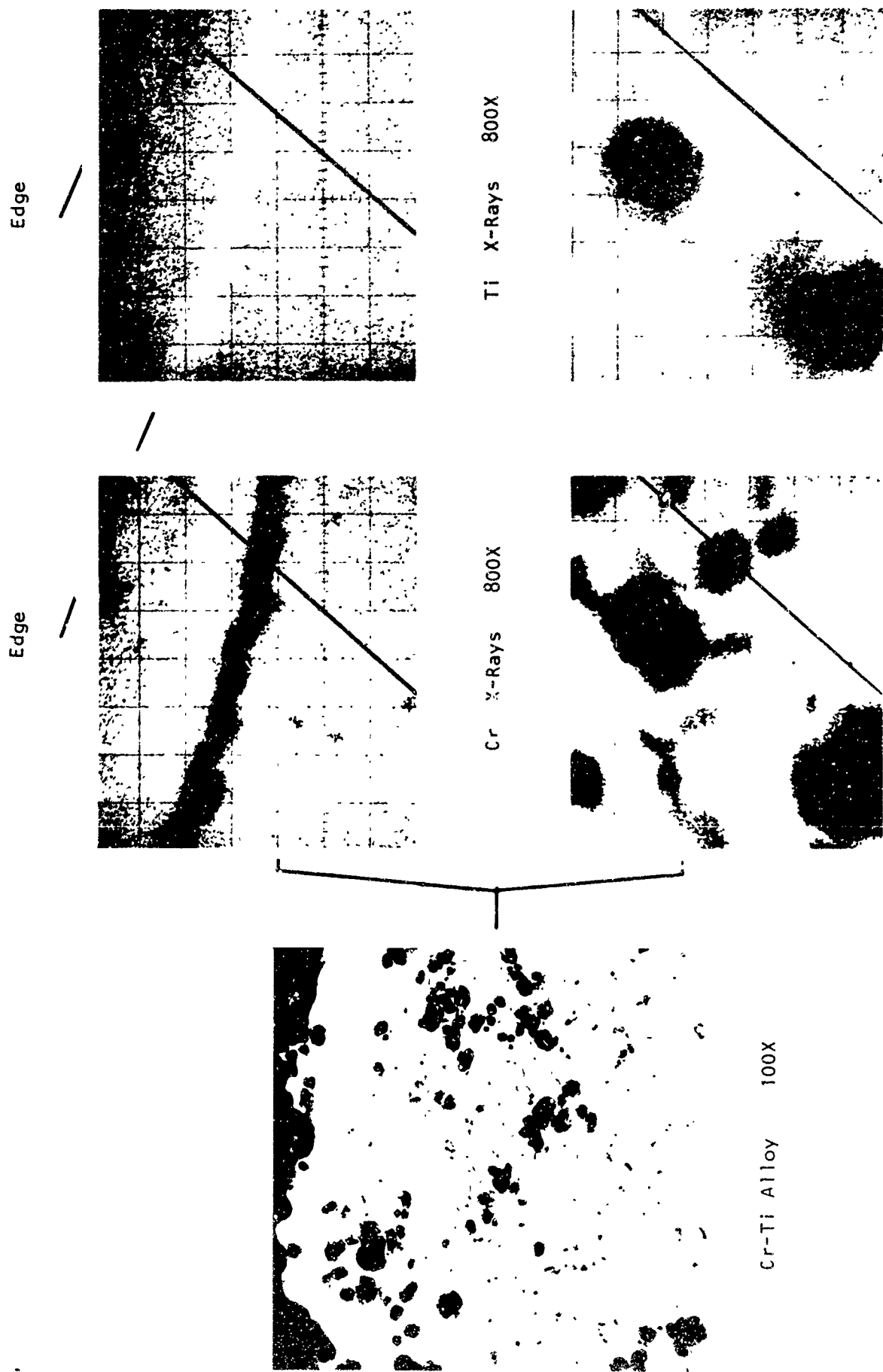


Figure 36. Photomicrograph and EMP X-Ray Images from Cross Section of Used (Depleted) Nominal 60Cr-40Ti Alloy Pack Particle

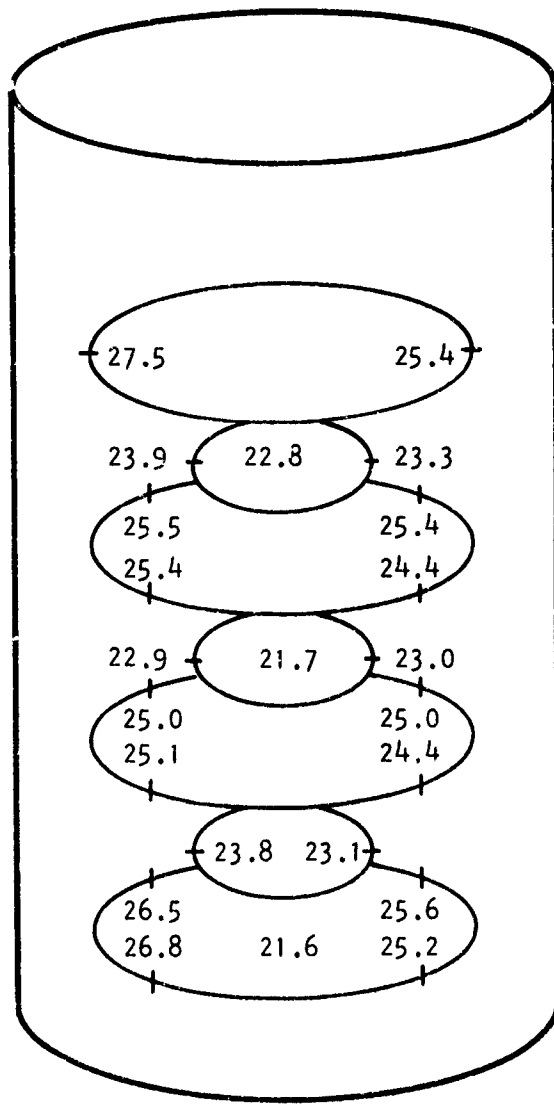
4.5 Preliminary Production Proof

Before conducting the preliminary production proof experiments a Cr-Ti coating run was made in the production furnace in order to evaluate the coating characteristics of the new lot of 60Cr-40Ti powder which was to be used for this work. This was done by positioning Cb752 alloy coupons in a 12" diameter Cr-Ti coating retort at various locations in the pack, as shown schematically in Figure 37. This figure also shows the specimen weight gains observed after depositing the coating in a 8 hour run at 2300°F under a pressure of 10 torr helium. The average weight gain was 24.6 mg/cm². The variations in coating weight gains at the different positions are an indication of the temperature gradients which were present in the pack during the coating process, the higher coating weight gains being indicative of a higher temperature for a longer period of time. The variation of ± 10 percent from the average weight gain indicates good temperature uniformity in the pack.

The coating deposition properties of the silicon powder were also checked before coating the hardware configurations. The Cr-Ti coated coupons just discussed were placed into the siliconizing retort in the same manner as before. Siliconizing was accomplished at 2000°F for 4 hours at 10 torr, as in the reproducibility runs. The silicon weight gains observed at various pack positions are shown in Figure 38. The average silicon weight gain was 19.1 mg/cm² with about a ± 10 percent variation with pack position. This variation was the same as that observed in the prior Cr-Ti coating runs.

Although the coating weight gains for the Cr-Ti and silicon coating cycles were in the desired range, microscopic examination of representative coupons from the Cr-Ti coating cycle showed evidence of excessive titanium in the coating. As discussed previously, excessive titanium is manifested as : 1) a broad titanium rich diffusion zone, 2) extensive chromide precipitation in this region, and 3) a discontinuous chromide overlay. Siliciding of this type of microstructure produces a titanium rich disilicide which exhibits protective properties quite inferior to the optimum Cr-Ti-Si chemistry.

Since the parameters employed in performing this latter run were identical to those utilized in the reproducibility runs, failure to produce the proper Cr-Ti coating chemistry and morphology in this run rendered these parameters potentially inadequate. Previous investigations of the Cr-Ti-Si coating process had, however, defined a relatively sensitive relationship between the ambient pressure in the furnace system and the composition of the pack vapor phase. Higher system pressures tend to suppress activator loss from the retort thereby increasing the concentration and residence time of



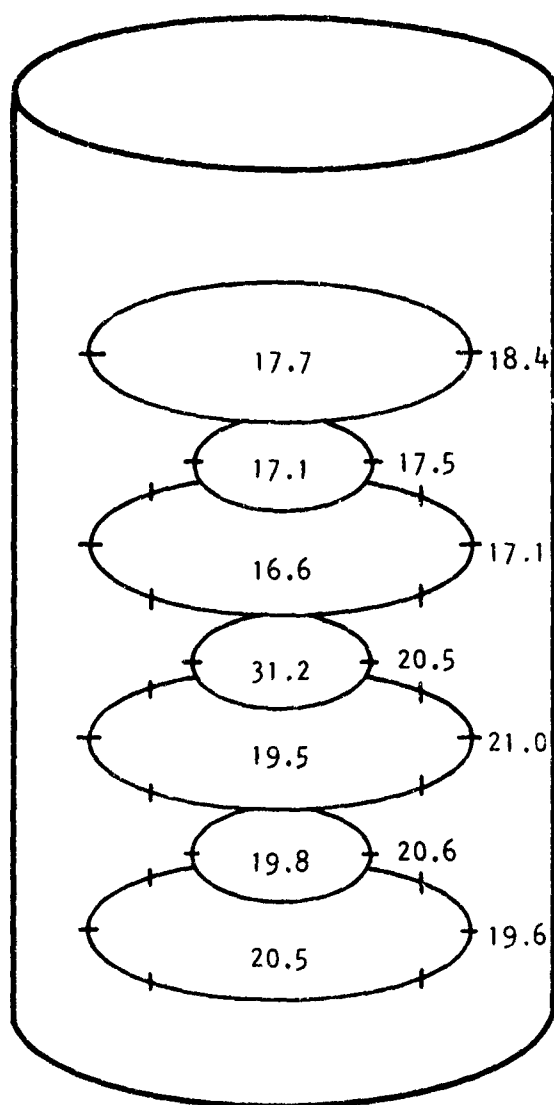
LARGE CIRCLES ARE 8-INCH DIAMETER

SMALL CIRCLES ARE 4-INCH DIAMETER

LOWEST LEVEL OF COUPONS 2-INCH ABOVE BOTTOM OF RETORT, WITH SUCCESSIVE LEVEL 2-INCH ABOVE EACH OTHER.

NUMBERS INDICATE COATING WEIGHT GAIN ON COUPONS AT THAT POSITION.

Figure 37 Cr-Ti Coating Weight Gain at Various Positions in the 12-inch Diameter Retort



LARGE CIRCLES ARE 8-INCH DIAMETER

SMALL CIRCLES ARE 4-INCH DIAMETER

LOWEST LEVEL OF COUPONS 2-INCH ABOVE BOTTOM OF RETORT, WITH SUCCESSIVE LEVEL 2-INCH ABOVE EACH OTHER.

NUMBERS INDICATE COATING WEIGHT GAIN ON COUPONS AT THAT POSITION.

Figure 38 Silicon Coating Weight Gain at Various Positions in the 12-inch Diameter Retort

titanium halides in pack. On the other hand, dynamic conditions produced by continuous furnace evacuation significantly reduce the transport of titanium, particularly in the later stages of the coating cycle; and, in fact, enhance the transport of chromium by promoting direct metal vaporization. In the module and reproducibility coating trials conducted in this program, titanium depleted 60Cr-40Ti alloy pack material was employed. The 10 torr pressure condition proved optimum for these experiments owing to the necessity of encouraging titanium transfer. With the new 60Cr-40Ti media the greater activity of titanium at the particle surface eliminated this need for activator retention, thus continuous evacuation of the furnace during the isothermal portion of the coating cycle would be more appropriate. This latter thermal-pressure condition is consistent with the parameters employed for Cr-Ti coating in the laboratory facilities. Based on this thesis, the decision was made to use continuous furnace evacuation (10^{-2} torr) for the preliminary production proof run. Sodium fluoride activator was used, rather than the CrCl_3 -NaF mixture, owing to three factors: 1) there were no conclusive benefits defined for use of the CrCl_3 activator, 2) the substantially greater cost of CrCl_3 as compared to NaF, and 3) the lower vapor pressure of NaF.

In the preliminary production proof experiment the approach was to coat a configuration large enough to represent an aerospace structure, and yet small enough to be tested in the available laboratory facilities. This was accomplished by using a segmented structure. The center portion of this structure consisted of two elliptical right cylinder. Adjacent to these cylinders were four panel configurations, two box panels and two corrugated panels. The individual configurations were fabricated from 0.018 inch thick Cb752 alloy sheet using different joining techniques. Each of the elliptical right cylinders was 2-3/4 inch high, with a 3-inch major axis and a 2-3/8 inch minor axis and having a TIG butt-welded seam. The corrugated panels were 6-3/4 x 3-3/4 x 1-1/4 inch, with the corrugation spot welded to the skin panel. Molybdenum electrodes were used to avoid the contamination which generally occurs with copper electrodes. The box panels were 7 x 3 x 3/8 inch, and were fabricated using TIG and electron beam welding techniques. These structures are shown (after coating) in Figure 39. The mottled appearance of the parts is characteristic of the diffusion-pack deposited Cr-Ti-Si coating, and is the result of varying degree of contact between the surface of the part and the pack material.

These structural configurations, together with tensile test specimens metallography specimens and oxidation test coupons, were

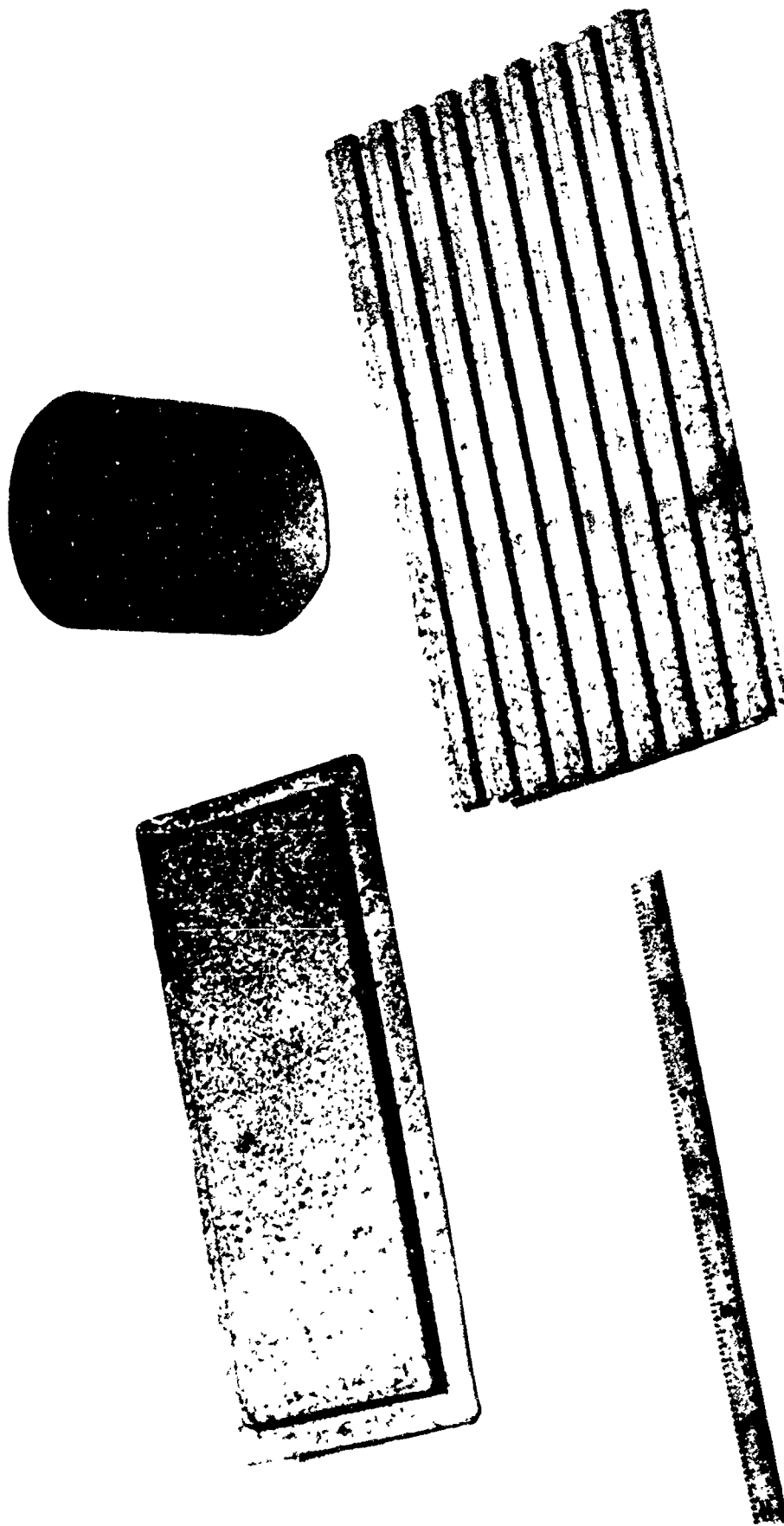


Figure 39. Diffusion Pack Cr-Ti-Si Coated Cb-752 Alloy Segmented Structures

coated in the 12-inch diameter retorts. Also coated with these parts were six 3 x 6 x 0.030 inch sheet panels; 2 each of Cb-752, B66 and C129Y alloys. The Cr-Ti coating was formed using the following parameters:

Pack media	60Cr-40Ti
Activator	0.75w/o NaF
Temperature	2300°F
Time	10 hours
System Pressure	10 ⁻² torr

The time-temperature heat-up profile was similar to that developed in the module studies, and used in the reproducibility runs. The average Cr-Ti coating weight gain as measured on control coupons was 21 mg/cm², and the average silicon weight gain was 15 mg/cm². A representative microstructure is shown in Figure 40. The photomicrograph shows Laves phase formation in the diffusion zone, and the silicon coating had not completely consumed the prior Cr-Ti coating. This coating morphology and chemistry has been shown to produce a coating with good high-and low-temperature oxidation resistant properties. Table 8 summarizes the oxidation test results obtained with control coupons coated with the fabricated structures:

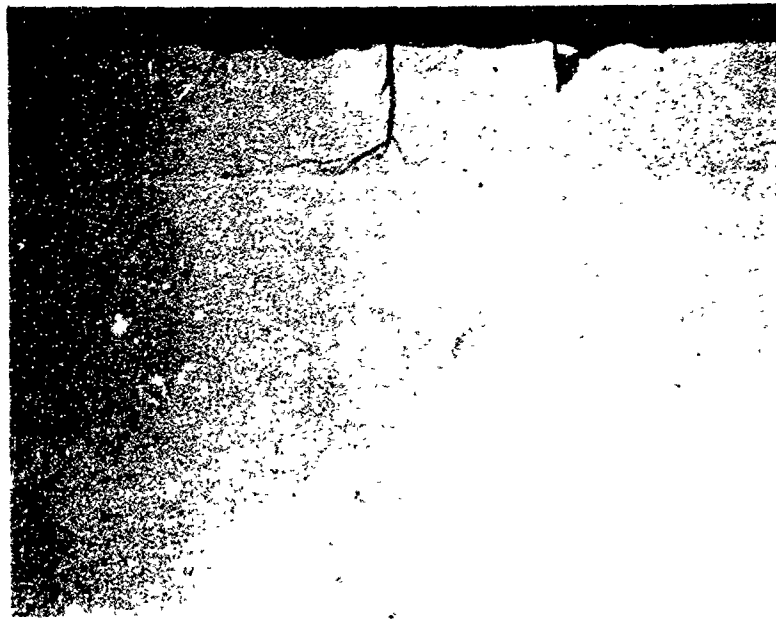
TABLE 8

OXIDATION TEST RESULTS-PRELIMINARY PRODUCTION PROOF COUPONS

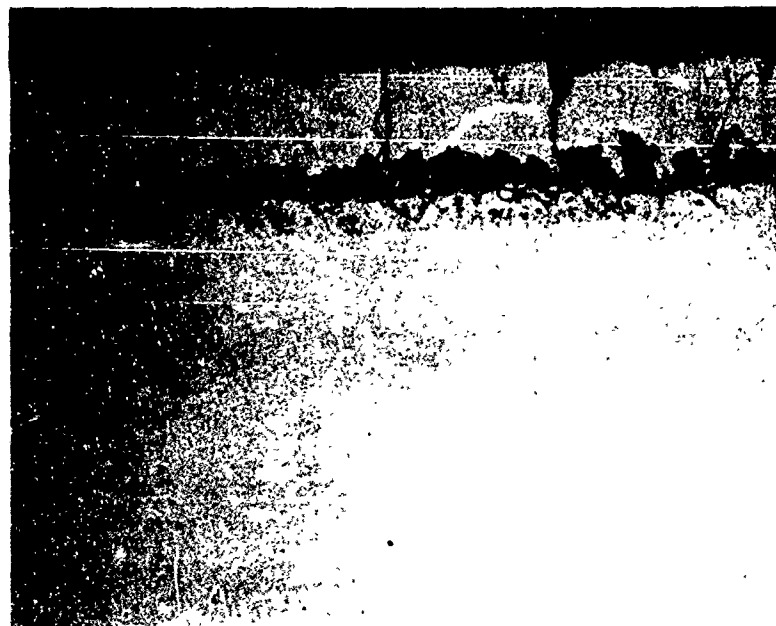
<u>Test °F</u> <u>Temp.</u>	<u>90% Reliable</u> <u>Oxidation Life</u>	<u>8</u>	<u>Time to Failure, Hours*</u>
1800	690	-	>690(12) Test terminated no failures
2200	320	0.7	134(1), 514(2), 538(1), > 569(7)
	500	10	Test terminated
2600	110	-	>109(6), 120(2), 133(1), 144(1), >156(2)
	60**	3.5	Test terminated
2800	20	-	20(1), >33(13) Test terminated

* Numbers in () are the number of coupons associated with the indicated time. A total of 12 coupons were tested at each temperature.

** Extrapolated value.



250X Unetched



250X Etched

Figure 40 Photomicrographs of the Cr-Ti-Si Coating on a Control Coupon from the Diffusion-Pack Preliminary Production Proof.

At 1800°F, the target criterion of an oxidation life of 125 hours was exceeded. Since there were no failures during the test period, it was not possible to determine a value for β , the Weibull slope. Although at 2600°F bimodal distributions were observed, the target criteria of a 90% reliable life of 50 hours and a Weibull slope, $\beta > 1.0$ were attained or exceeded.

4.5.1 Oxidation Testing of Cr-Ti-Si Coated Segmented Structures

One each of the segmented structures and sheet panels were oxidation tested using a simulated flight-temperature profile, and the others were life tested at 2600°F using the cyclic procedures employed with the control coupons.

The simulated flight-temperature tests were made by placing a structure or panel onto quartz pads, inside an open-ended refractory brick box with a loose fitting lid. This box was then placed into a resistance heated furnace and the time-temperature profiles at the center of a longitudinal edge, and also along this edge at a point half-way between the center and the transverse edge of the panel, were determined using an optical pyrometer. The center temperature on the box above the test specimen was simultaneously measured using a Pt vs. Pt 10Rh thermocouple. For the box panel and the corrugated panel, the temperature profile on cooling was measured at three places along the longest dimension of the panel, at the center, half way between the center and end, and at the end. These temperature profiles were also obtained using an optical pyrometer. The complete temperature profile is shown in Figure 41. The rate of cooling and heating was a maximum at the ends, and decreased toward the center of the panels. The refractory box also introduced transverse temperature gradients in the test panels. Measurements using the thermocouple showed that when the transverse center temperature was 2600°F, the corresponding temperature at the hardware edge, near the wall of box, was 2550°F. Since this edge was facing the unheated furnace door, the somewhat lower temperature was to be expected. The cylinder was placed horizontally in a separate refractory brick box and the temperature rise profiles, which were essentially the same as for the panels, were separately determined at the ends and center of the cylinder.

The oxidation performance observed using the simulated flight-temperature profile tests and the life tests are given in Table 9.

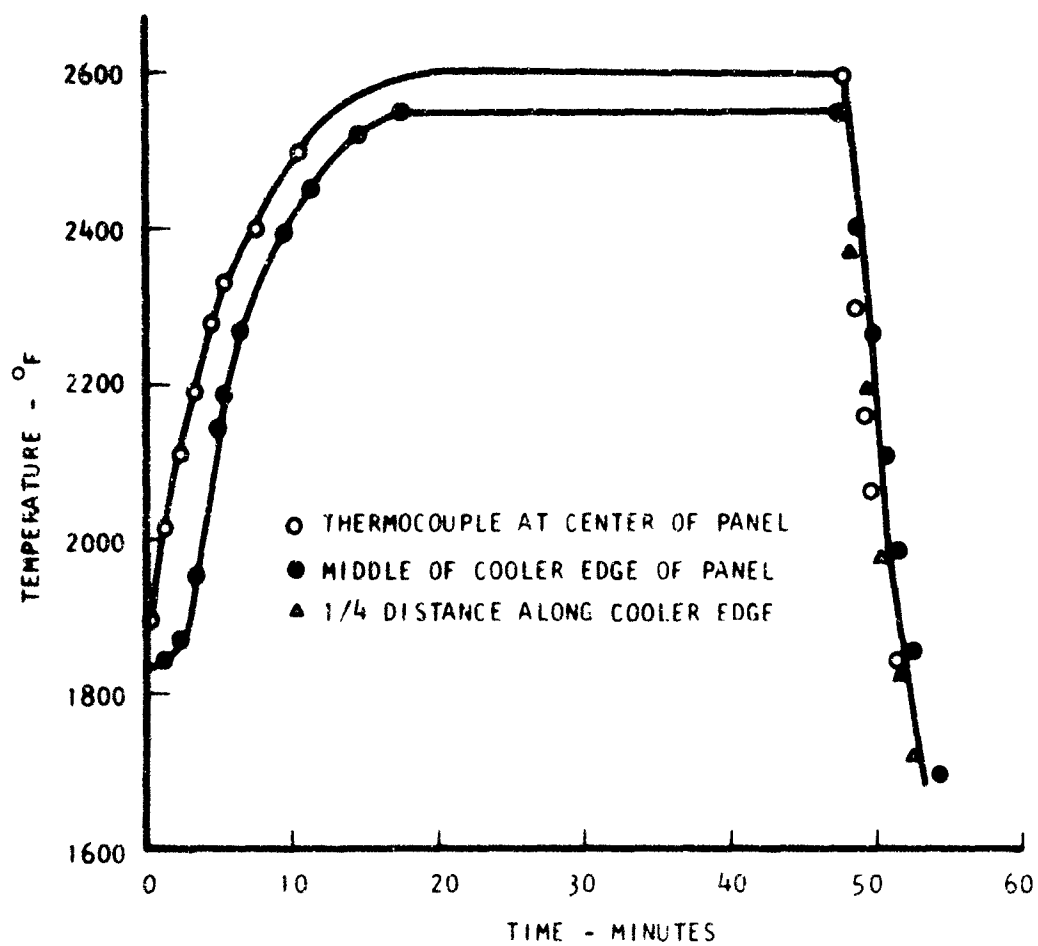


Figure 41 Simulated Flight Temperature Profile Used For Cyclic Oxidation Testing Coated Structures

TABLE 9

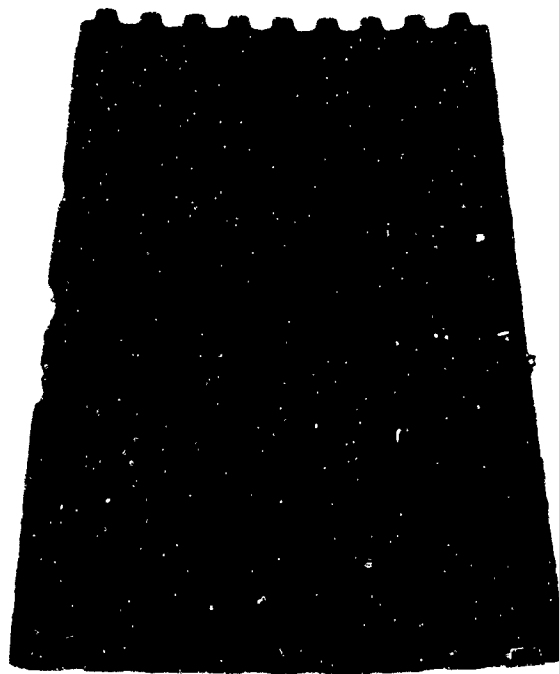
VACUUM-PACK Cr-Ti-Si COATED HARDWARE-OXIDATION TEST RESULTS

<u>Configuration</u>	<u>2600°F Profile Test No. of Cycles to Failure</u>	<u>2600°F Life Test Hours Exposure to Failure</u>
Cb752 Corrugated Panel	Not tested	3
Cb752 Box Panel	6	12
Cb752 Cylinder	9	>97 no failure
Cb752 3 x 7 x 0.018 inch sheet	6	59
B66 3 x 7 x 0.030 inch sheet	>10	88
C129Y 3 x 7 x 0.060 inch sheet	>10	>122 no failure

The appearance of these panels and cylinders after testing is shown in Figures 42 to 47. Figure 42 shows the corrugated panel after 3 hours exposure to air at 2600°F in a box furnace. Failures occurred at the faying surfaces on the longitudinal joints where there was poor contact. On transverse faying surfaces, where spot welding produced better contact between the surfaces, there were no failures up to the 3 hour test time. Figure 43 shows the closed box panels after testing. After 9 simulated flight-temperature cycles the box panel showed localized failures on the panel surface and at the corners and edges. The failures on the panel surfaces occurred at regions which had an excess of titanium in the coating, as evidenced by a shiny appearance of these areas on the as-formed coating. The failures at the edges and the corners occurred on the weld material. This was caused by the inadvertent use of unalloyed columbium as weld filler, rather than Cb752 alloy, and the Cr-Ti-Si coating as formed by the parameters used in this work was not optimum for protecting unalloyed columbium. The cylinders after oxidation testing are shown in Figure 44. One of the cylinders was exposed to 2600°F air for 97 hours without failure, at which time testing was terminated. The cylinder which was tested under the simulated flight temperature cycle survived 9 cycles before failing along one edge, as well as at an area on the cylinder where a titanium rich spot was detected during pre-test examination.

Figures 45 to 47 show the three different alloy sheet panels after oxidation testing. The Cb752 alloy panel survived 59 hours exposure to 2600°F air before failure occurred at a small spot on the surface. Testing of the Cb752 panel using the simulated flight-temperature cycle was stopped after 6 cycles. The panel was dropped on one edge during the examination after the fifth cycle. This chipped the coating and failure occurred at the chipped area during the next cycle.

The protective capability of the coating was further assessed by testing B66 and C129Y alloy sheet panels. Figures 46 and 47 show

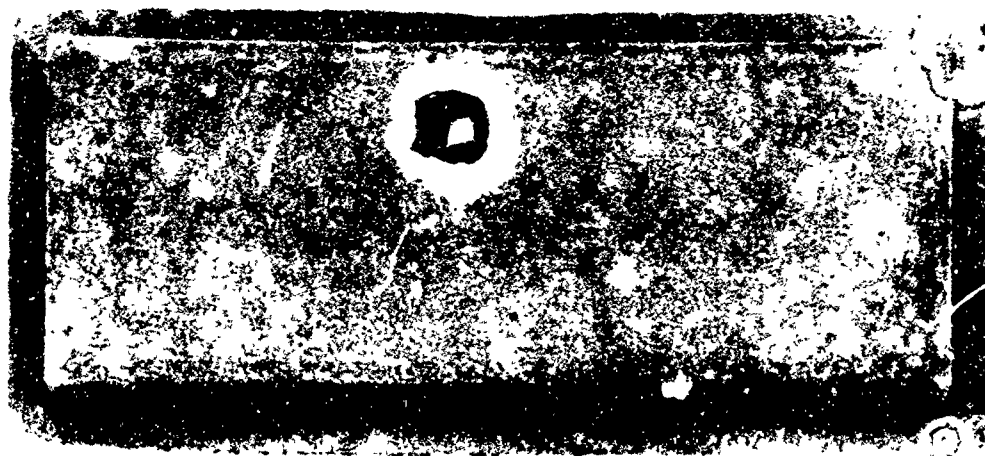


After 3 Hours at 2600°F



After 3 Simulated Flight-Temperature Cycles

Figure 42. Diffusion Pack Cr-Ti-Si Coated Cb-752 Alloy
Corrugated Panel After Oxidation Testing

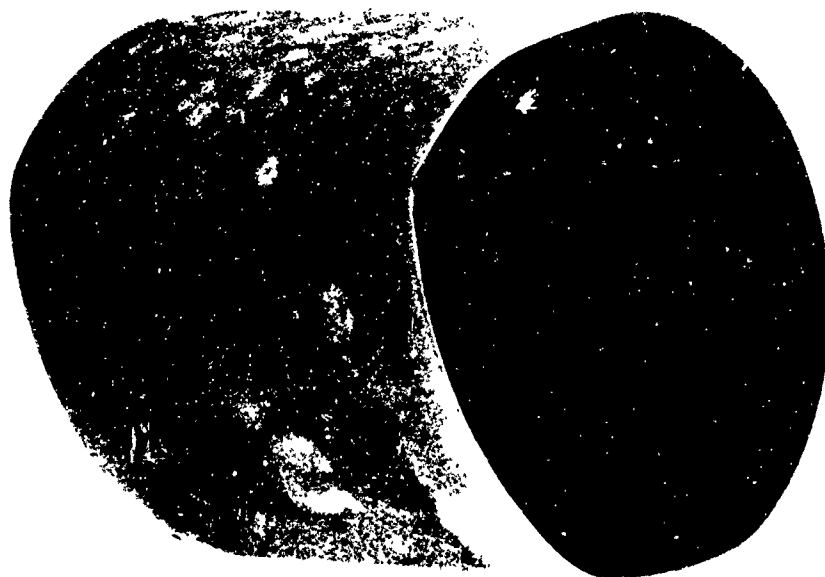


After 12 Hours at 2600°F



After 9 Simulated Flight-Temperature Cycles

Figure 43. Diffusion Pack Cr-Ti-Si Coated Cb-752 Alloy Box Panels After Oxidation Testing

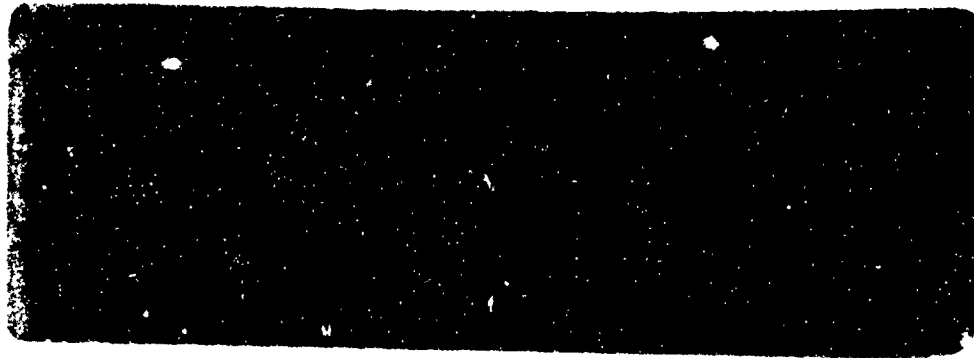


After 97 Hours at 2600°F



After 9 Simulated Flight-Temperature Cycles

Figure 44. Diffusion Pack Cr-Ti-Si Coated Cb-752 Alloy Cylinders After Oxidation Testing

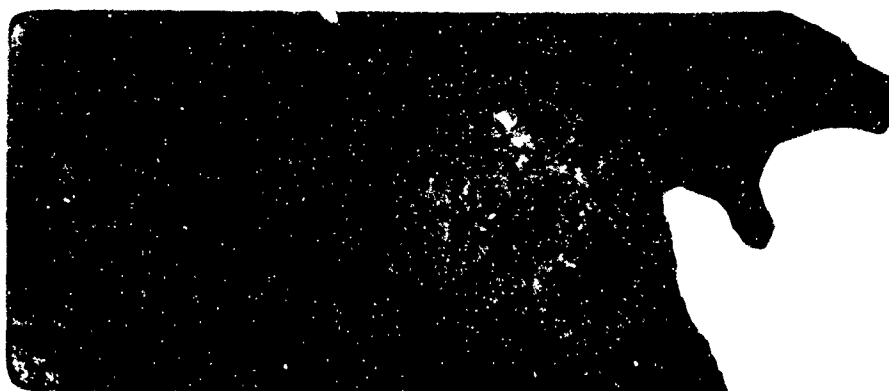


After 59 Hours at 2600°F



After 6 Simulated Flight-Temperature Cycles

Figure 45. Diffusion Pack Cr-Ti-Si Coated Cb-752 Alloy Sheet Panels After Oxidation Testing

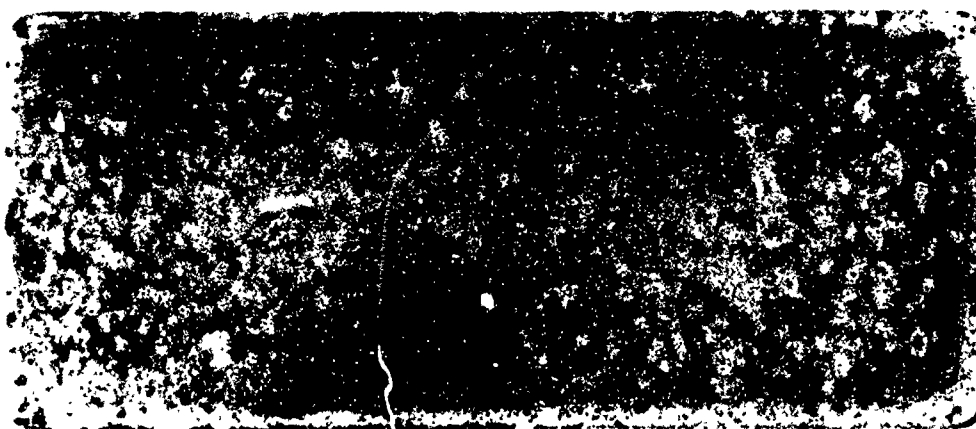


After 88 Hours at 2600°F

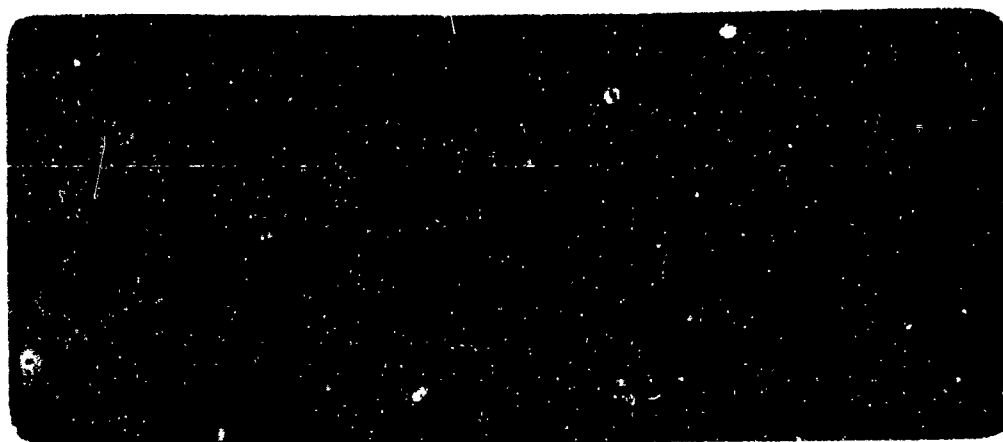


After 10 Simulated Flight-Temperature Cycles No Failure

Figure 46. Diffusion Pack Cr-Ti-Si Coated B-6f Alloy
Sheet Panels After Oxidation Testing



After 122 Hours Exposure at 2600°F



After 10 Simulated Flight-Temperature Cycles

Figure 47. Diffusion Pack Cr-Ti-Si Coated C129Y Alloy Sheet Panels After Oxidation Testing

these panels after oxidation testing. Under simulated flight-temperature testing, the performance of both alloys exceeded the target criterion of 10 cycles without failure. On life test, the B66 alloy sheet showed evidence of coating deterioration, i.e., the formation of a light brown region, after 84 hours exposure to 2600°F air, and complete failure was observed at the next inspection after 88 hours exposure. The C129Y panel survived 122 hours exposure to 2600°F air without failure, at which time testing was stopped.

The reproducibility runs have shown that the Cr-Ti-Si coating, as formed by the vacuum-pack process, was not capable of providing long-term protection to hardware with faying surfaces. However, when applied to relatively large parts without faying surfaces, the coating provided oxidation protection for times well beyond the goals of 125 hours of protection at 1800°F and 50 hours at 2600°F. Under simulated flight-temperature testing, sheet panels which were free of fabrication defects survived the 10 cycle test goal without failure. Failures which occurred at shorter times in the segmented structures were traceable to causes which were not associated with the coating chemistry, but, rather, with specific defects introduced during fabrication. Within these limitations the overall results of the coupon tests, life tests and simulated flight-temperature tests on sheet panels and segmented structures indicated that the vacuum-pack process was capable of forming a coating which will protect properly fabricated columbium alloy structures against air oxidation for times greater than 125 hours at 1800°F and 50 hours at 2600°F.

5 SLURRY-DIFFUSION PROCESS DEVELOPMENT

The slurry-diffusion process for the application of the Cr-Ti-Si coating to columbium alloy parts is a two-step process. In the first step the parts to be coated are encased in a 0.020 to 0.030-inch thick bisque composed of fine Cr-Ti alloy powder, a small amount of activator, and a low residue binder. The bisque is air dried, and the material is placed into a retort which is subsequently heated in a vacuum furnace to effect transfer of Cr- and Ti from the bisque to the surface being coated. After firing, the spent bisque is removed from the coated surface by peeling and/or brushing. In the second step, the Cr-Ti coated part is silicided in an analogous manner using a bisque consisting of silicon powder, activator, and binder. The slurry-diffusion process is simply an offshoot of the vacuum-pack process, with the particulate bisque serving as a thin pack.

5.1 Laboratory Investigation

The purpose of these laboratory experiments was to consider the effects of the bisque thickness, slurry application techniques, gettering technique and support methods on the basic slurry-diffusion coating process. In addition, the following process parameters were briefly examined to aid in choosing the variable levels for a more detailed investigation into the relationships among the parameters and the properties of the coatings:

1. Slurry composition variables:
 - a. metal powder composition (w/o): 60Cr-40Ti and 50Cr-50Ti for the Cr-Ti coating cycle and 100 Si for the silicon cycle;
 - b. powder size: + 80 mesh to -325 mesh;
 - c. activator: NaF, CrCl_3 + NaF and KF in the Cr-Ti coating cycle and KF in the Si cycle;
 - d. binder: Vistanex and F525;
 - e. slurry vehicle: toluol.
2. Diffusion temperature: 2300°F (Cr-Ti) and 2100°F (Si).
3. Coating time: 4-10 hours.
4. System pressure: 0.01, 10 and 100 torr.
5. Substrate: Cb752, B66, C129Y columbium alloys.

Experimental coating runs were conducted in a cold-wall, resistance-heated, laboratory-scale furnace similar in design to both the pilot-scale and production-scale furnaces. The ratio of coating retort volume to hot volume of the laboratory furnace was approximately equivalent to the same volume ratio for the production retort and furnace.

5.1.1 Bisque Thickness

The effect of bisque thickness on the properties of the coatings was not investigated. It had been previously reported (4) that for a bisque thickness greater than 0.020-inch, the Cr-Ti-Si coating weight gain did not depend on bisque thickness. This was observed for 60Cr-40Ti, 50Cr-50Ti and silicon powders over a wide range of particle sizes. For the Cr-Ti powders the bisque weight (mg/cm^2) was numerically equivalent to approximately 6 times the bisque thickness measured in mils; and for the silicon bisque weight 3.5 times the thickness. These numbers were independent of particle size, activator, type of binder and other slurry variables.

5.1.2 Slurry Application Technique

Slurries were applied to the parts to be coated by dipping, brushing and spraying. An experimental determination of the effect of bisque coating method was made using specimens on which the same slurry was applied by the three different methods. All specimens were processed simultaneously in the same coating run. There was little or no effect on Cr-Ti coating thickness among brush, dip, or spray applied bisques. Based on the comparison of the data outlined in Table 10, the spray technique was selected as the application method for use in developing the slurry-diffusion technique. As an illustration of the appearance of a spray-coated part, a coupon sprayed with a silicon bisque is shown in Figure 48.

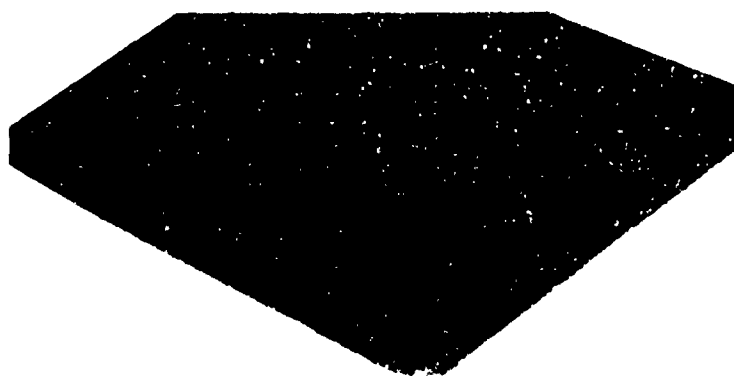
5.1.3 Gettering Technique

In order to minimize the chance of substrate contamination and subsequent embrittlement of the base alloy, it was considered that some form of active gettering be used to prevent the gaseous impurities, which may be present in the coating furnace atmosphere, from coming into contact with the parts being coated. The gettering methods evaluated using a columbium retort were:

TABLE 10

OBSERVATIONS REGARDING SLURRY APPLICATION METHODS

	<u>Spray</u>	<u>Dip</u>	<u>Brush</u>
Bisque Thickness	Wide range available	Total thickness limited by flow characteristics	Thickness inherently non-uniform
Solvent Content of Slurry	Not critical, easily adjustable	Critical, low level required	Critical, workability effected
Powder Size	-170 mesh	-200 mesh Viscosity control critical	Minimum determined by "float" and settling characteristics
Binder Content of Slurry	Medium level easily adjustable	Thixotropic control requires low level binder	Resolution and "float" require high binder content
Contact Marks	Negligible	Require brush repair	Self process repair
Process Controls	Air pressure Operator skill	Viscosity, Withdrawal rate	Viscosity Operator skill
Remarks	Overspray wasted	Large slurry volumes. Slurry stability critical. Thick edges Drain points	Non-uniform thickness



4X

Figure 48. Slurry Coated Specimen Showing Bisque Finish and Edge Coverage.

- 1) a layer of coarse Cr-Ti coating material in the bottom of the retort,
- 2) titanium alloy sheet material lining the inside of the retort, and
- 3) a powder seal filled with the Cr-Ti coating powder.

Of the three techniques tested, the powder seal getter technique was the most effective, as well as being more applicable for use in the coating of large parts in the production-scale furnace. A schematic sketch of the coating retort is pictured in Figure 49. Any gasses passing into or out of the retort must pass through the getter powder, in which case oxygen or hydrogen reacts with the powder and is removed from the retort atmosphere. In the present study, both fine 50Cr-50Ti and 60Cr-40Ti powder were effective in isolating the parts to be coated from the general furnace atmosphere. The getter seal was also effective in retarding activator loss from the bisque to the furnace environment.

5.1.4 Support Method

The parts to be coated must be physically supported in the retort. Three means of specimen support were investigated:

- 1) titanium metal configurations to hold the parts,
- 2) coarse "bubbled" and fused alumina packed around the parts, and
- 3) various columbium metal support configurations.

The titanium supports locally sintered to the part being coated and were therefore unsuitable. Both coarse "bubbled" alumina and fused alumina proved unsatisfactory for use as support material. Either a reaction occurred between the halide activator and the surface of the alumina, or there was sorption of the activator on the alumina. In any event, significantly thinner coatings were formed when the sprayed coupons were supported on alumina.

The use of both uncoated and precoated columbium support configurations were investigated. Coated columbium supports were preferred to uncoated supports. There appeared to be transfer of Cr-Ti or silicon from the bisque to the uncoated supports, which reduced element transfer to the object being coated. The support configurations studied were grids, screens, spirals and corrugated shapes. The type of configuration was not critical, and any convenient configuration could be used. These supports have the advantages of being light, easy to handle and reusable. Because these

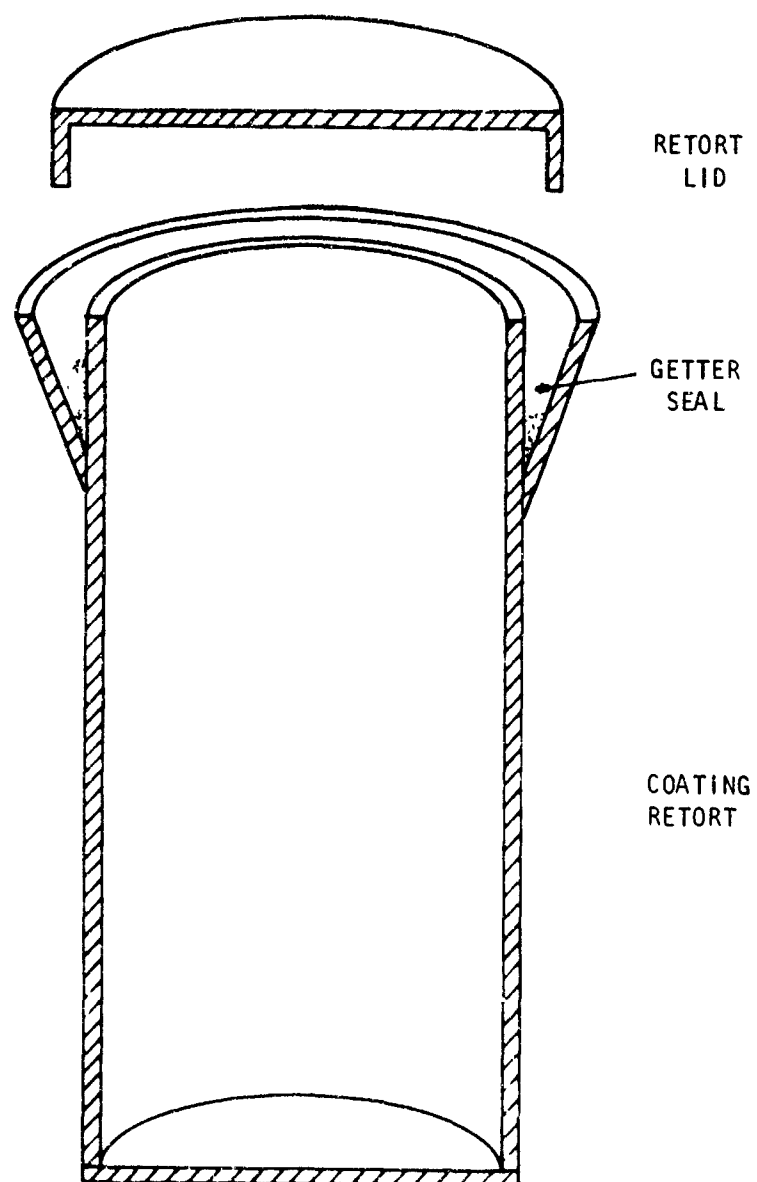


Figure 49 Schematic Sketch of the Columbium Coating Retort Showing the Cr-Ti Getter Seal

metal supports have relatively low mass and are a good conductor of heat, they do not reduce the time required to bring the hardware or specimens to the coating temperature.

5.1.5 Effect of Slurry Variables on Cr-Ti Coating Characteristics

Two binders, a 13 percent solution of Vistanex* in toluene and F525* were evaluated for use with Cr-Ti and silicon slurries. No significant differences in coating morphology or oxidation performance could be attributed to the use of either binder.

The use of three activator compositions, CrCl_3 -NaF in a 2:1 ratio, NaF and KF, each at levels to 5-weight percent, were evaluated for the Cr-Ti cycle. Under identical processing conditions, using NaF and CrCl_3 -NaF activators resulted in coatings which were nearly equivalent in thickness, whereas KF activation produced thinner Cr-Ti coatings. In general, NaF produced more uniform coatings.

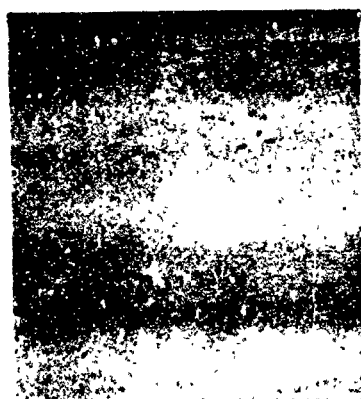
The effect of varying the system pressure from 10^{-2} to 100 torr, for 50Cr-50Ti and 60Cr-40Ti powder bisques, on coating microstructure is shown in Figure 50. There appears to be little or no variation in the coating overlay thickness as a function of pressure, although the diffusion zone beneath the Laves phase overlay increased as pressure increased. The results of an earlier study (10) on the slurry-diffusion application of Cr-Ti coatings are summarized in Figure 51, where the typical microstructures of Cr-Ti coated B66 and D43 alloy specimens are reviewed. The effects of both the Cr-Ti powder composition and the system pressure are shown. The diffusion time and temperature are the same for both system pressures. The higher system pressure (150 torr argon) yielded a thicker coating with a more pronounced diffusion zone, indicating enhanced Ti transfer at the higher pressure. This latter observation is attributed to the increased retention of the activator in the bisque at the higher system pressure, and as discussed previously, this influence of system pressure on coating composition is observed with the vacuum-pack method as well.

5.1.6 Evaluation of Coating Process Parameters

The preliminary tests previously discussed were used to determine the levels at which the process variables would be evaluated in detail. For the detailed study, coatings were again formed using a laboratory-scale furnace. Two complete sets of coating retort and support hardware were constructed. One set was Cr-Ti coated and used for application of the Cr-Ti coating, and the other was Cr-Ti-Si coated for use in siliconizing. Based upon the preliminary work previously discussed, and prior experience with the Cr-Ti-Si coating system,

* Enjay Company trade name for polyisobutylene.

** Harshaw Chemical Company binder composed of an acrylic polymer in petroleum ether.



60 Cr-40 Ti Slurry

100 torr Ar



50 Cr-50 Ti Slurry

100 torr Ar



60 Cr-40 Ti Slurry

10 torr Ar



50 Cr-50 Ti Slurry

10 torr Ar



60 Cr-40 Ti Slurry

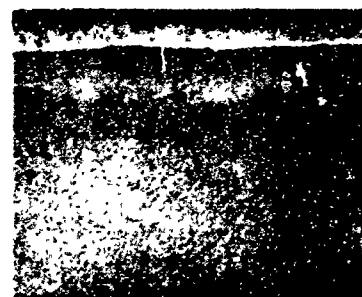
10^{-2} torr

Figure 50. Cr-Ti Coated Cb-752 Alloy Specimens Showing the Effect of Varying the System Pressure

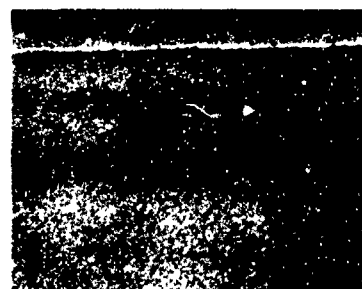
250X



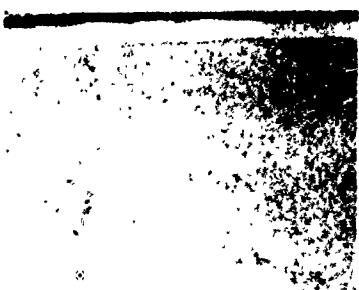
50 Cr-50 Ti Slurry
0.5 w/o NaF
150 torr Ar



60 Cr-40 Ti Slurry
0.5 w/o NaF
150 torr Ar



50 Cr-50 Ti Slurry
2.0 w/o NaF
10⁻² torr



60 Cr-40 Ti Slurry
2.0 w/o NaF
10⁻² torr



Figure 51. Summary of Cr-Ti Coatings on S-66 and D-43 Alloys
by the Slip Pack Technique (Reference 10)

the variables listed below were selected for the parametric study.
In this listing the value (+) represents the higher value for the individual variables.

1) Cr-Ti coating cycle

Coating temperature	+ 2350°F - 2250°F
System pressure	+ 100 torr - 10 torr
Coating time	+ 10 hours - 6 hours
Activator	+ NaF - Mixed NaF (1part)- CrCl ₃ (2 parts)
Activator quantity	+ 6 w/o - 2 w/o
Particle size	S ₁ - 170 + 250 mesh S ₂ - 250 + 325 mesh
Powder composition	C ₁ 50Cr-50Ti C ₂ 60Cr-40Ti

2) Silicon coating cycle

Coating temperature	+ 2100°F - 2000°F
System pressure	+ 100 torr - 10 torr
Coating time	+ 8 hours - 4 hours
Activator	KF
Activator quantity	+ 6 w/o - 2 w/o
Particle size	S ₁ - 170 + 250 mesh S ₂ - 250 + 325 mesh

These variables were the subject of a statistically designed experiment to evaluate the effect of varying processing conditions on the oxidation performance of the Cr-Ti-Si coatings. Twelve process variables were evaluated in each coating cycle. For this discussion the variables were divided into "powder variables" and "furnace variables" as follows:

<u>Furnace Variables:</u>	<u>Cr-Ti Cycle</u>	<u>Si Cycle</u>
Activator Composition	x	
Quantity of Activator	x	x
Deposition Time	x	x
Deposition Temperature	x	x
Deposition Pressure	x	x
 <u>Powder Variables:</u>		
Powder Composition	x	
Powder Size	x	x

Each variable was restricted to two levels or values. In statistical work, such controlled variables are called the factors in the experiment and each factor is said to be at two levels.

For the nine "furnace variables", tests at two different levels necessarily involved the production of test specimens in two separate furnace runs, even if all else were unchanged. Because of this requirement, and because of the time, expense, and difficulty in performing each furnace run, these "furnace variables" were considered separately in deriving the experimental design. Specimens with all possible combinations of the powder variables were produced in every furnace run of the design.

The design established for the furnace variables was a 2^{9-5} (read "two to the nine-minus-five") fractional factorial. This means there were nine factors, each at two levels, but that only 2^{9-5} (i.e. 2^4 or 16) distinct combinations of levels were used in the experiment. For this design sixteen furnace runs suffice, each run comprising two coating cycles, a Cr-Ti and a silicon cycle. The name of this design further expresses that it is a $1/2^5$ ($1/32$) fraction of the full factorial, which would employ all 2^9 or 512 possible combinations of the factor levels. A full factorial experiment would furnish sufficient data to estimate statistically all main and interaction effects of the nine furnace variables, but it would of course, be excessively time consuming. The fractional factorial experiment represented a compromise which would still provide enough information to calculate statistical estimates of the main effects of all nine furnace variables upon the physical characteristics measured

after processing through both coating cycles. These main effects were not confounded with the first order interaction effects; this fact contributes to the accuracy of the analysis of results.

The design for the powder variables is a 2^3 or 8 full factorial embedded in each of the 16 furnace runs. All main and interaction effects among the three powder variables could therefore be estimated independently; furthermore, the interaction of any furnace variable with any of these effects could also be estimated.

The 2^{9-5} fractional factorial design was randomized for the purpose of avoiding possible systematic bias due to sequencing of runs and regularity in the allocation of physical variables and levels. The randomized fractional factorial design is given in Table 11. Each treatment (i.e., combination of levels of the furnace variables) contains the eight design points or combinations of levels of the powder variables.

In the analysis, advantage was taken of the fact that there is a smaller design that results if all factors relating to the silicon cycle are removed from consideration. The smaller design can be used only for estimating effects of the Cr-Ti variables on physical characteristics that are measured prior to conducting the silicon cycle. It consists of a 2^{5-1} fractional factorial for the Cr-Ti cycle furnace variables, with an imbedded 2^2 full factorial design for the Cr-Ti cycle powder variables. The advantage gained here is that many of the interaction effects among the furnace variables can be estimated, together with further interactions between furnace variables and powder variables.

An analysis of variance was applied to the data from the Cr-Ti coating cycles. A total of 64 effects, comprising main effects, first, second and third order interactions, were calculated from the data summarized in Appendix VII. Appendix VII contains all of the coating weight gain and oxidation test data for the entire statistical experiment. The significance of these effects was evaluated using the "student" t-ratio. The calculated values for the effects and interactions are summarized in Table 12 along with calculated values for the t-ratio.

For each main or interaction effect the t-ratio, which is the ratio of the absolute value of the effect to the standard error of the effect, is used in the determination of the statistical significance of the effect. It also serves as a guide to interpretation of the physical significance of the effects. When t is very large the effect is very significant, and when t is close to zero the effect is insignificant. A statistical t-test can be made by comparing the t-ratio to a constant, 2.807 for 960 degrees of freedom and

TABLE II
RANDOMIZED FRACTIONAL FACTORIAL EXPERIMENT

Run No.	Cr-Ti Coating Cycle					Si Coating Cycle			
	T	P	t	A	a	T	P	t	a
	Temperature (°F)	Pressure (torr)	Time (Hrs.)	Activator	Activator Quantity (%)	Temperature (°F)	Pressure (torr)	Time (Hrs.)	Activator Quantity (%)
A	+	+	+	+	-	+	-	+	-
B	-	-	-	-	-	-	+	+	-
C	-	-	+	-	+	-	-	-	-
D	-	-	+	+	-	+	+	+	+
E	+	-	-	+	-	-	+	-	-
F	+	-	+	-	-	+	+	-	+
G	-	-	-	+	+	+	-	-	+
H	+	+	-	-	-	-	-	+	+
I	-	+	+	-	-	+	-	-	-
J	+	+	-	+	+	+	+	-	-
K	+	-	-	-	+	+	-	+	+
L	-	+	-	+	-	-	-	-	+
M	-	+	+	+	+	-	+	+	+
N	+	+	+	-	+	-	+	-	+
O	-	+	-	-	+	+	+	+	-
P	+	-	+	+	+	-	-	+	-

+ High Value (N₂)
- Low Value (N₁)

For Activator

+ NaF A₁
- NaF-CrCl₃ A₂
(Ratio 1/2)

Cr-Ti Cycle

T - + 2350°F
- 2250°F
P - + 100 torr
- 10 torr
t - + 10 hours
- 6 hours
A - + NaF
- NaF-CrCl₃
(Ratio 1/2)
a - + 6 w/o
- 2 w/o

Si Cycle

T - + 2100°F
- 2000°F
P - + 100 torr
- 10 torr
t - + 8 hours
- 4 hours
a - + 6 w/o
- 2 w/o

TABLE 12

COMPILATION OF MAIN EFFECTS AND INTERACTIONS CALCULABLE FOR THE
Cr-Ti COATING CYCLE BY THE ANALYSIS OF VARIANCE METHOD.

	Effect (mg/cm ²)	t-ratio		Effect (mg/cm ²)	t-ratio
I	11.04		P	7.163	16.280
T	6.509	147.931	PT	0.221	5.023
t	2.429	55.204	Pt	-0.064	1.454
tT	1.294	29.409	PC	-0.178	4.045
C	-1.385	31.477	PCT	-0.180	4.098
CT	-0.790	17.954	Pct	-0.053	1.200
Ct	-0.184	4.182	Pa	-0.551	12.523
CtT	-0.028	0.636	PaC	0.446	10.136
a	-0.829	18.241	PA	-0.601	13.659
aT	-0.535	12.159	PAC	-0.052	1.186
at	0.511	11.614	S	0.125	2.841
aC	0.477	10.159	ST	0.018	0.418
aCT	0.313	7.114	St	0.108	2.455
aCt	0.103	2.341	StT	-0.173	4.045
A	-0.204	4.636	SC	-0.045	1.023
AT	0.291	6.614	SCT	-0.030	0.068
At	-0.650	14.773	SCt	0.039	0.886
AC	0.467	10.614	SCtT	0.090	2.039
ACT	0.041	0.930	Sa	0.016	0.361
Act	-0.123	2.795	SaT	0.178	4.046
Aa	0.134	3.045	Sat	0.055	1.257
AaC	0.088	2.000	SaC	-0.055	1.243

TABLE 12 (Continued)

	<u>Effect</u> <u>(mg/cm²)</u>	<u>t-ratio</u>		<u>Effect</u> <u>(mg/cm²)</u>	<u>t-ratio</u>
SaCT	-0.303	6.886	SP	-0.142	3.227
SaCt	-0.241	5.477	SPT	-0.015	0.348
SA	-0.275	6.250	SPt	-0.139	3.159
SAT	-0.184	4.182	SPC	0.161	3.659
Sat	-0.100	2.273	SPCT	0.035	0.802
SAC	0.201	4.568	SPCt	0.215	4.886
SACT	0.044	1.002	SPa	0.033	0.759
SACt	0.067	1.514	SPaC	0.008	0.177
SAa	0.225	5.114	SPA	-0.182	4.136
SAaC	-0.142	3.227	SPAC	0.140	3.182

l - overall average
 t - time, hours
 T - temperature, °F
 C - powder composition
 A - activator
 a - activator quantity
 S - particle size

$|t| \geq 2.807$ is significant at the 0.005 level, i.e., if no real effect existed, then chance alone would produce a $|t| \geq 2.807$ about 0.5% of the time.

No. of data items 1024
 No. of effects 64
 No. of degrees of freedom 960

at the 0.005 significance level. If $t > 2.807$, the corresponding effect is statistically significant at the 0.005 significance level. This means that there is only a 0.005 (or 1/2 percent) probability that the result could be due to chance alone.

In the present analysis the values for the t-ratio are calculated in the following manner:

1) $s^2 = 0.5048 \text{ mg/cm}^2$, pooled variance (unbiased population estimate) of individual measurements of weight gain for all specimens.

2) $s = 0.7105 \text{ mg/cm}^2$, pooled standard error of individual measurements.

3) $s^2_{\text{effect}} = \frac{s^2}{\sqrt{512}} + \frac{s}{16} = 0.04441 \text{ mg/cm}^2$, the standard error for each effect.

4) $t_{\text{effect}} = \frac{\text{Effect}}{s_{\text{effect}}} \quad (960 \text{ degrees of freedom})$

The results of the analysis of variance were as follows:

1) The overall average of the Cr-Ti coating weight gain was 11.04 mg/cm^2 .

2) The main effects of the variables studied were all statistically significant, with the particle size being least significant and type of activator next to the least significant.

3) Deposition temperature, coating time, powder composition, activator quantity and system pressure were most significant.

4) The negative sign associated with the value of the effect for the concentration (C) can be explained on the basis that 60Cr-40Ti powder was chosen initially to represent the "high" value for C, whereas the use of 50Cr-50Ti ("low" value of C) gave heavier coatings.

5) The negative sign associated with the variable A, the type of activator, signifies that a mixture of 1 NaF-2CrCl₃ (lower level), was more effective as an activator than "pure" NaF (higher level).

6) The negative sign associated with a , the quantity of activator, signifies that larger coating weight gains were found at the lower activator level, which was an unexpected result. A possible explanation, drawing an analogy to the vacuum-pack process, might be as follows:

It is postulated that the NaF or other activator remains as a passive element in the coating process until volatilization of the halide occurs. The gaseous halide reacts with the Cr-Ti powder to form lower valent halides of both Cr and Ti. These halides exhibit lower vapor pressures than $TiCl_4$ and $CrCl_3$. The rate of volatilization of the halide activator is such that complete reaction to Ti and Cr halides does not occur, and the excess activator can "sweep" the Ti and Cr halides out of the coating retort. In the vacuum-pack technique the effect of increasing activator quantity upon Cr-Ti weight gain has been to first increase the total coating deposition, reach a maximum value, and then to decrease the total quantity deposited.

7) Of the 63 effects calculated 42 were statistically significant. The results of this analysis of variance were subsequently used to establish the coating parameters for the process reproducibility runs.

The analysis of variance was not carried out on the oxidation life data because it was recognized that main effects alone would not adequately describe the dependence of life upon the process variables. The analysis of the Cr-Ti weight gain data had demonstrated that there must surely be a number of significant second order (and even third order) interaction effects. In the analysis of variance the main effects would be confounded with these interactions in spite of the feature of the design that prevents such confounding with first order interactions: i.e., the calculated estimate of any main effects would be subject to possibly large error, since it would actually be a statistical estimate of an inseparable linear combination of several effects together, namely, the main effect and certain interaction effects not intended to be measured by the experiment. The oxidation data were therefore treated by regression analysis.

A stepwise multiple regression analysis was run on the IBM 360 (Model 50) computer for each of two cases. These are the cases treating $\log(1800^\circ\text{F oxidation life})$ and $\log(2600^\circ\text{F oxidation life})$ as functions of the Cr-Ti weight gain and Si weight gain only.

The equations reached by this stepwise procedure for the two analyzed cases were:

$$\begin{aligned} \log (1800^{\circ}\text{F life}) = & 3.98 - 30.1 \left(\frac{1}{\Delta W_1} \right) + 152. \left(\frac{1}{\Delta W_2} \right) \\ & + 0.025 \frac{(\Delta W_2)^2}{\Delta W_1} - 106 \frac{\Delta W_1}{(\Delta W_2)^2} + 5.1 \frac{\Delta W_1}{\Delta W_2}. \end{aligned} \quad (1)$$

$$\begin{aligned} \log (2600^{\circ}\text{F life}) = & 23.22 + 5490. \left(\frac{1}{\Delta W_2} \right)^2 - 292. \left(\frac{1}{\Delta W_1} \right) \\ & - 703 \frac{\Delta W_1}{(\Delta W_2)^2} - 0.032 (\Delta W_2)^2 + 11.1 \frac{\Delta W_2}{\Delta W_1} \\ & + 20.5 \left(\frac{\Delta W_1}{\Delta W_2} \right)^2 + 0.00213 (\Delta W_1) (\Delta W_2)^2 \\ & - 0.00164 (\Delta W_1)^2 (\Delta W_2) - 0.40 (\Delta W_2). \end{aligned} \quad (2)$$

In these equations ΔW_1 represents the Cr-Ti weight gain and ΔW_2 the silicon weight gain in mg/cm^2 .

The results of cyclic oxidation testing at 1800 and 2600°F presented in Appendix VII indicated that the hours to failure for each individual specimen could be qualitatively related to the respective value for the ratio of Cr-Ti coating weight to Si coating weight. The hours to failure appeared to have maximum values at ratios between approximately 0.6 to 0.8. Below a ratio value of 0.6 the specimen life dropped sharply, and above approximately 0.8 the life also decreased. For this series of coatings the Cr-Ti weight gains for the specimens exhibiting good lives were 12-20 mg/cm^2 range. The reason for the optimum Cr-Ti/Si being less than unity, while the optimum ratio for the pack applied coatings is greater than unity, was not ascertained.

Specimens from these sixteen statistically designed Cr-Ti-Si coating runs were also evaluated microscopically.

The results of microscopic examination of the coatings from these factorial coating runs are summarized as follows:

i) The Cr-Ti coating thickness in most cases was not optimum. Only in runs A and H did the chromide overlay begin to approach the desired thickness of about 0.001 inch, corresponding to a weight gain of about 20 mg/cm^2 .

2) The Cr-Ti coatings, except for run H (50Cr-50Ti), can be characterized as thin coatings without Laves "spikes" penetrating into the diffusion zone. The thin coatings and the absence of Laves "spikes" indicate inadequate Ti transfer during the coating cycle.

3) The morphology of the Cr-Ti coatings formed using 50Cr-50Ti powders for the slurry-diffusion technique differed markedly from the comparable coatings applied using 50Cr-50Ti in the vacuum-pack process. The vacuum-pack Cr-Ti coatings showed discontinuous blocky islands of Laves phase in a Ti-rich matrix, as compared with a continuous $(\text{Cb,Ti})\text{Cr}_2$ overlay formed using the slurry-diffusion technique.

4) The general coating morphology of the Cr-Ti-Si coating, except for runs A and H, was characterized by the complete penetration of the silicide layer through both the Cr-Ti layer and the underlying diffusion zone. In factorial run B this was evidenced by the almost complete separation of the silicide layer from the substrate, and in extreme cases, spalling of the coating.

5) Based upon pack-coating studies, the silicon coating thickness in all of the slurry coatings was much greater than was considered optimum for any particular Cr-Ti overlay.

5.2 Coating Process Reproducibility Studies

Calculations using equations (1) and (2) showed that a Cr-Ti weight gain in the range 13-17 mg/cm², and a silicon weight gain of at least 18 mg/cm², were required to produce a Cr-Ti-Si coating which would have an oxidation life in excess of 50 hours at 2600°F and 125 hours at 1800°F.

Three reproducibility runs were made using 0.030 inch thick coupons of three columbium alloys: C129Y, B66, and Cb752. The coupons were cleaned in an $\text{HNO}_3\text{-H}_2\text{SO}_4\text{-H}_2\text{O}$ etching solution, dried and spray coated with a bisque composed of the coating powders and activator suspended in a solution of "Vistanex" and toluene. The coupons were placed into a 12 inch diameter x 36 inch high retort previously described (Figure 49). As for the pack coating process, separate retorts were used to perform the Cr-Ti and the silicon coating cycles.

The retort was placed into the production scale furnace and evacuated to a pressure of approximately 0.01 torr. The retort temperature was raised slowly in order to eliminate the binder and out-gas the system. When the temperature reached about 800°F the polyisobutylene binder volatilized, and the temperature was slightly

reduced in order to keep the pressure below 0.01 torr. . As the pressure decreased, the temperature was increased until 1000°F was reached. Depending upon the rate of vapor evolution, the time required to reach 1000°F varied from 30 to 45 minutes. At the low temperature, this time variation had no effect on the coating deposition process.

The retort was then held at this temperature for one-half hour under continuous evacuation. During this time the pressure steadily dropped to about 0.025 torr. The furnace and retort were then back-filled with argon to a pressure of 100 torr, and the retort temperature was raised as rapidly as possible to the required coating temperature, while maintaining a pressure of 90 to 110 torr. The reproducibility of the time vs. retort temperature cycles, after the half-hour hold period at 1000°F, for three Cr-Ti reproducibility runs is shown in Figure 52, and for the silicon runs in Figure 53. The parameters for the Cr-Ti and silicon coating runs are given in Table 13.

TABLE 13

COATING PARAMETERS FOR SLURRY-DIFFUSION REPRODUCIBILITY RUNS

Powder Composition (w/o)	50Cr-50Ti	100Si
Particle Size (mesh)	-250 + 325	-250 + 325
Activator NaF (w/o)	2	
KF (w/o)		2
Bisque Weight (gm/cm ²)	0.2	0.2
Coating Temperature (°F)	2350	2000
Coating Time (hrs)	10	2
System Pressure (argon, torr)	100	100

The values for these parameters were based upon the results of the significant interactions among the process variables as presented in Table 11. The time for silicon coating deposition was reduced from the previously used 4 hours to 2 hours after it was determined during preliminary runs that reducing the time lowered the silicon weight gain by only 5 percent.

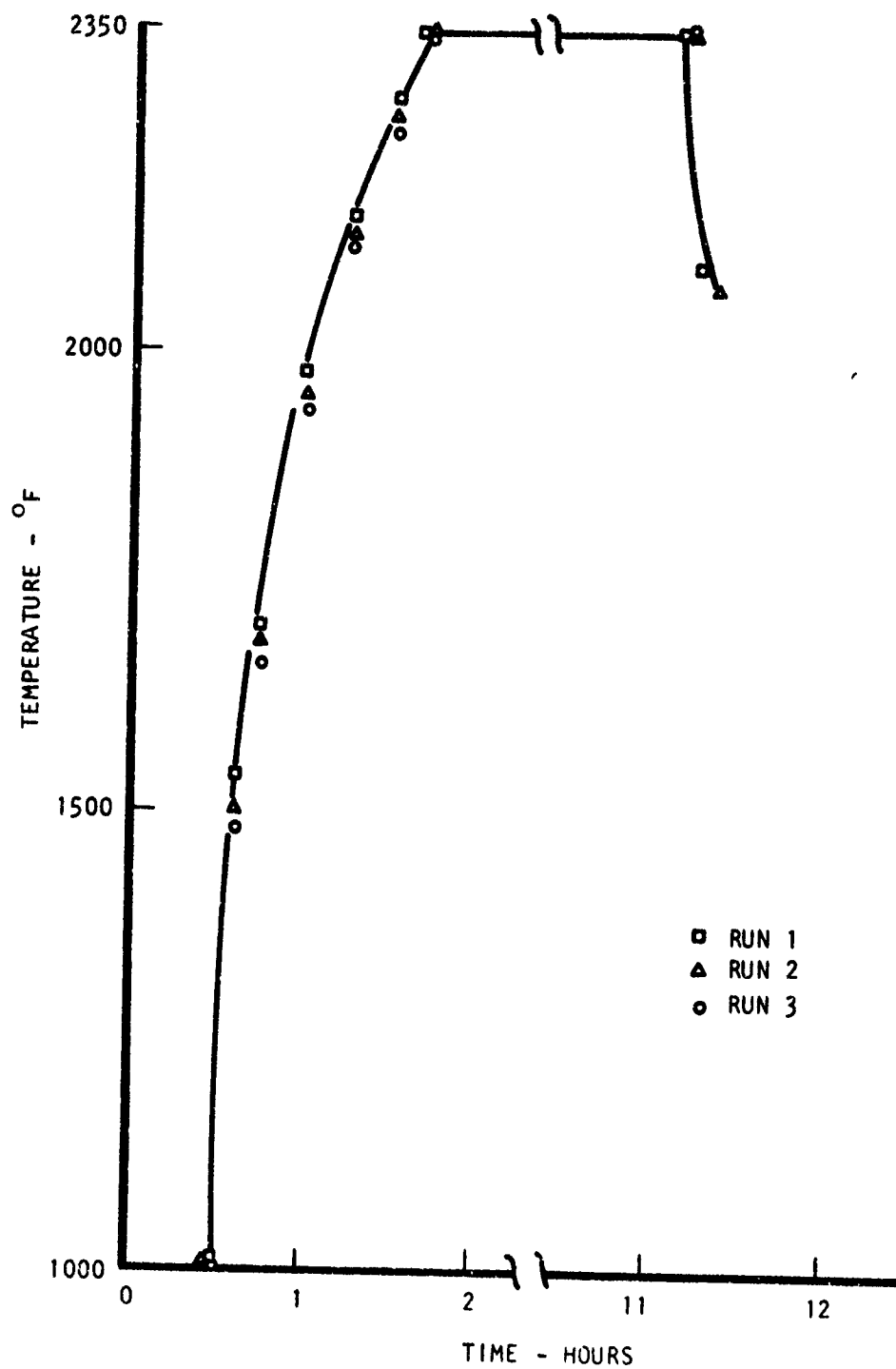


Figure 52 Cr-Ti Coating Cycle

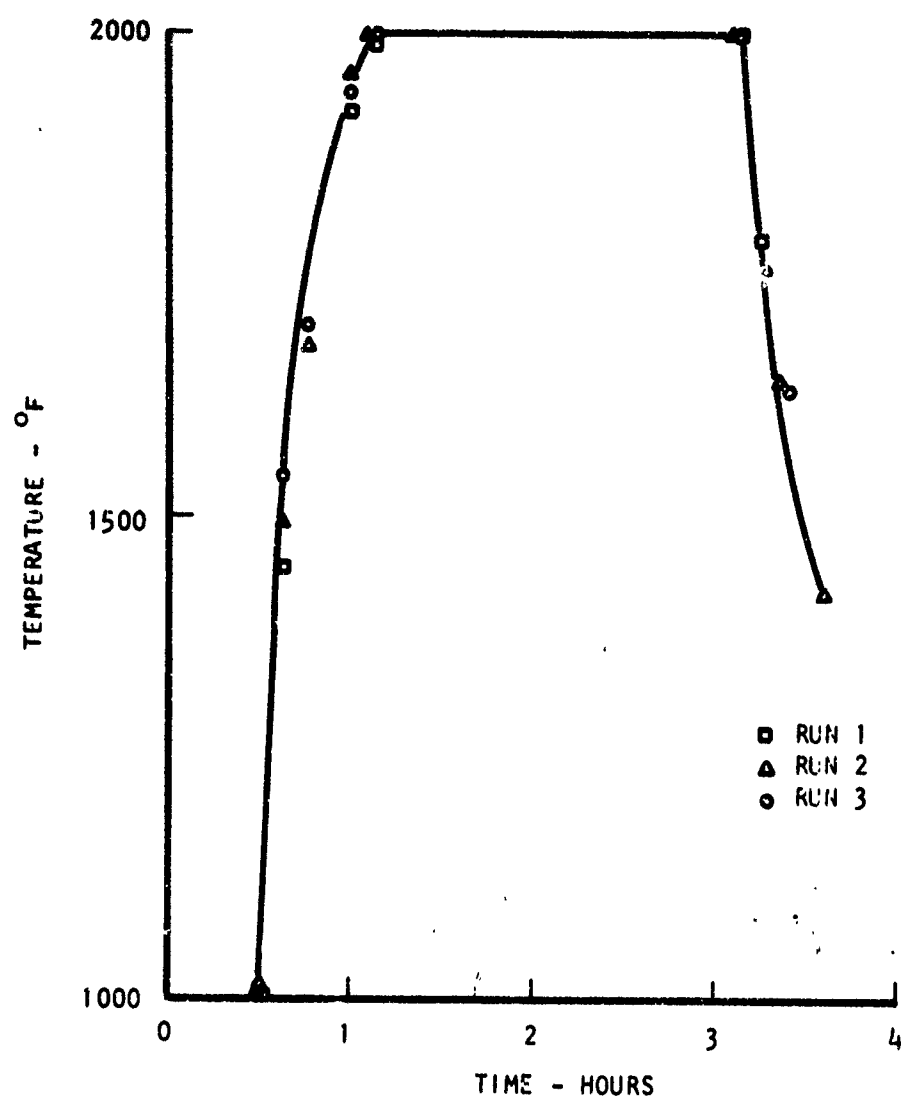


Figure 53 Silicon Coating Cycle

Coating weight gains, and the results of cyclic oxidation testing at 1800 and 2600°F for these reproducibility runs, are summarized in Table 14. Fourteen coupons of each alloy were tested at each temperature. These results show that the coatings formed in the reproducibility runs had 90 percent reliable lives well in excess of the target values of 50 hours at 2600°F and 125 hours at 1800°F. Values of the shape factor (β) for Weibull plots of the data were all greater than the target value of unity, indicating that a wearout mechanism was operating. The microstructure of the Cr-Ti-Si coating from each of these runs is shown in Figures 54 to 56. None of these coatings displayed what would be called an optimum microstructure for the Cr-Ti-Si coating; there were no dichromide "spikes" in the diffusion zones, and depending upon the run, the silicon layer either completely (Run A) or nearly completely (Runs B,C) consumed the prior Cr-Ti coating. However, the oxidation performance of these coatings did exceed the target oxidation protection lives. Based on the previous analyses with the vacuum-pack applied Cr-Ti-Si coatings, retention of a portion of the Laves phase after siliciding would not be expected for the Cr-Ti/Si weight ratios obtained in these runs (0.7-0.8). On the other hand, the good performance of these "through silicided" coatings at the lower temperature (1800°F) was not anticipated. However, based on this performance, the decision was made to proceed with the preliminary production proof experiment.

5.3 Preliminary Production Proof

Before undertaking the preliminary production proof of the slurry-diffusion process, a run was made to evaluate the effects of increasing the area of the coated surface on the Cr-Ti coating formation. It was anticipated that increasing the substrate surface area, and consequently the total quantity of bisque and activator in the system, might significantly influence the relative concentrations of coating-elements (Ti/Cr) in the bisque vapor phase. Several 3-inch x 7 inch x 0.030-0.060 inch sheet panels of Cb752, B66 and C129Y alloys were acid etched and spray coated with the halide activated 50Cr-50Ti slurry. The total exposed area of these panels was approximately the same as that of the hardware which would be used in the preliminary production proof. These sheet panels were placed into the 12-inch diameter retort, and heated in the production furnace according to the time-temperature cycle which had been previously developed in the process reproducibility work. Figure 57 shows a typical panel after completing the Cr-Ti coating cycle. The coating was very non-uniform, and was characterized by large regions which were either bright and shiny or grey matted. Figure 58 shows photomicrographs of each of these regions. The microstructures of both areas are characterized by gross titanium diffusion into the substrate, which was accompanied by chromium penetration into the titanium enriched region

TABLE 14

COMPIATION OF RESULTS FROM THE SLURRY-DIFFUSION REPRODUCIBILITY COATING RUN

Run	Alloy	Average Coating Weight Gain mg/cm ²		90% Reliable Life Hours		Shape Factor g		Failure History Hours of Test Temperature (1)	
		Cr-Ti	Si	2600°F	1800°F	2600°F	1800°F		
A	C129Y	15.7	19.9	123	674	3.5	NA	123(2), 156(2), 252(10)	
	B66	16.6	19.2	123	674		NA	>674(14) 123(14)	
	Cb752	16.5	19.2	120	674		NA	>674(14) 123(9), 252(5)	
							NA	>674(14)	
B	C129Y	13.1	20.9	80		5		93(4), 110(5), 131(1), 141(1), 142(1), 157(1), 165(1)	
	B66	13.1	19.3	85	380	5	10	364(1), 419(5), 443(4), 467(2), 508(1), 561(1)	
	Cb 752	14.1	19.8	80	604	4.5	NA	93(3), 110(6), 126(1), 141(3), 181(1) >604(14)	
								88(1), 90(2), 93(3), 126(4), 157(1), 188(1), Lost (2)	
C	C129Y	14.6	20.2	88	340		10	337(2), 337(3), 419(6), 443(1), 467(2)	
						4	NA	93(1), 94(1), 99(1), 110(2), 126(2), 142(2)	
	B66	15.6	18.8	90	400		10	157(2), 180(1), 183(1) 387(1), 443(1), 461(1), 467(4), 568(2), 516(1), 539(2), 604(2)	
	Cb 752	14.4	19.5	88	604	4	NA	90(3), 93(3), 110(4), 113(2), 176(1), Lost(1) 601(1), >604(13)	
								90(2), 93(3), 99(1), 110(3), 126(1), 180(2), Lost (2)	
					380		10	387(2), 419(6), 437(1), 443(1), 467(4)	

(1) Numbers in () indicate the number of coupons which failed at the indicated time.

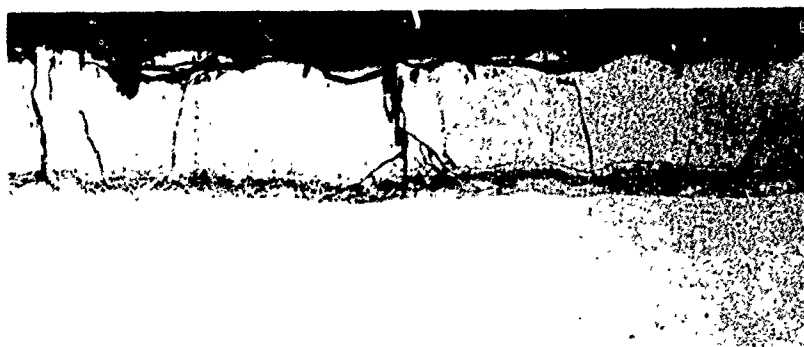
NA Not available since no specimens failed up to exposure times equal to the indicated 90% reliability life.



B66



C129Y

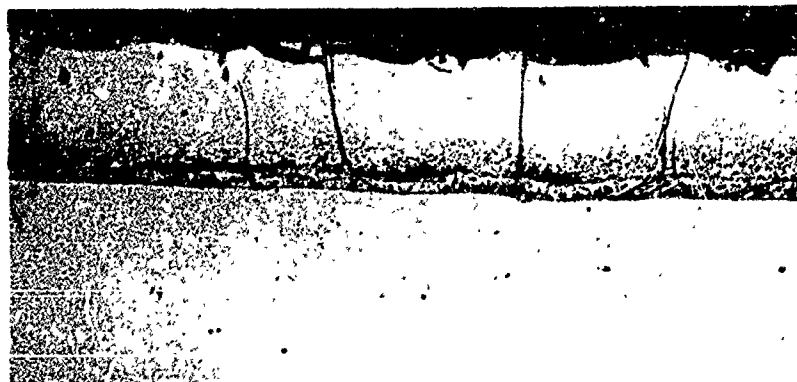


Cb752

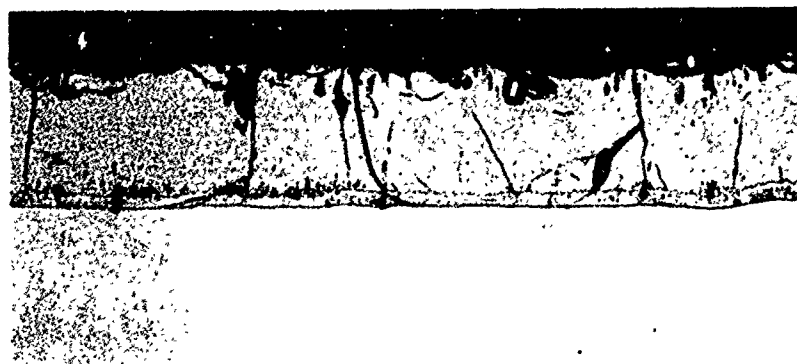
Figure 54 Cr-Ti-Si Coated Columbian Alloy Specimens from
Slurry-Diffusion Process Reproducibility Run A.
Etched 250X



B66



C129Y



Cb752

Figure 55 Cr-Ti-Si Coated Columbian Alloy Specimens from
Slurry-Diffusion Process Reproducibility Run B.
Etched 250X



B66



C129Y



Cb752

Figure 56 Cr-Ti-Si Coated Columbian Alloy Specimens from
Slurry-Diffusion Process Reproducibility Run C.
Etched 250X

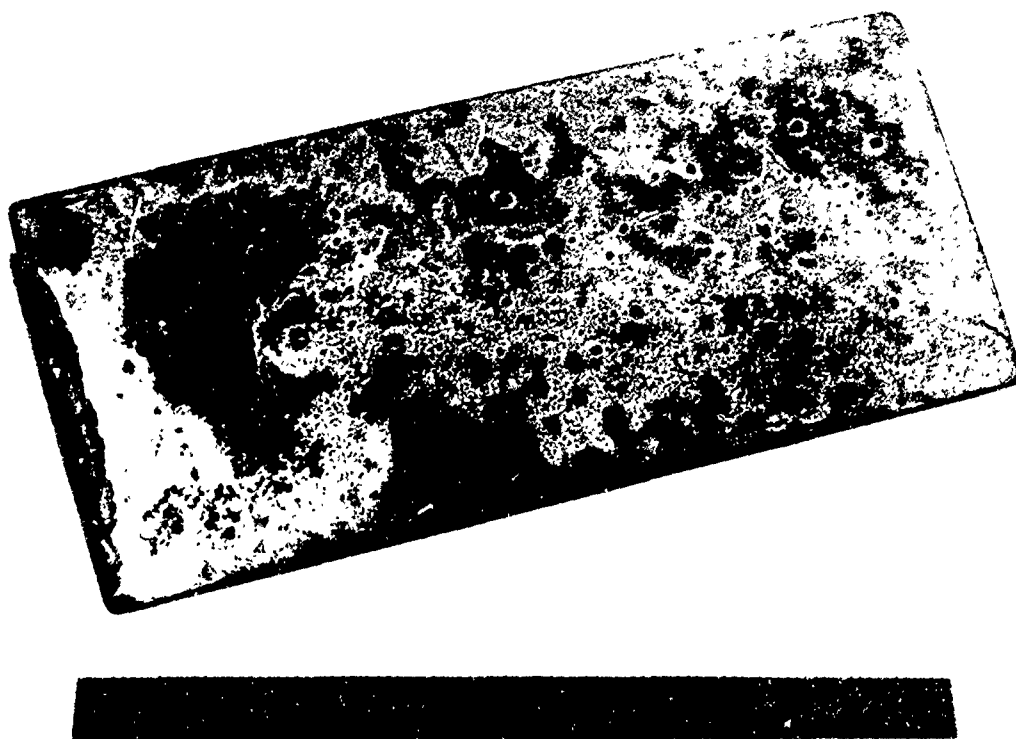
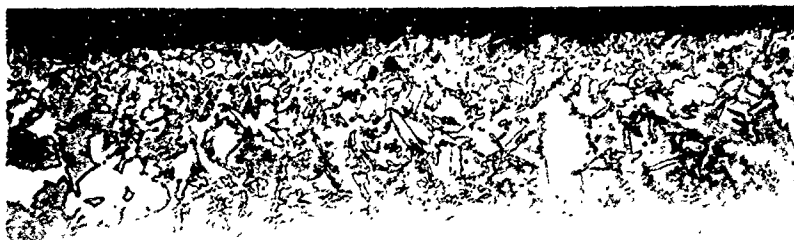
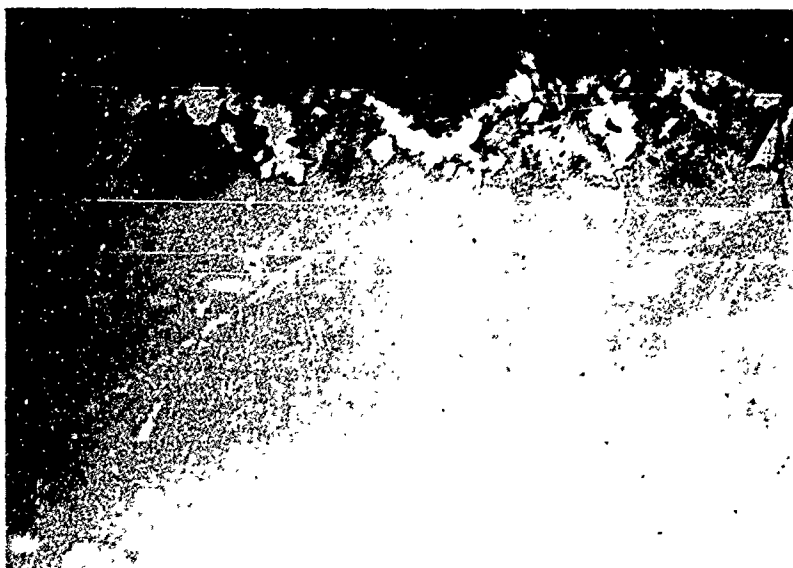


Figure 57. Non-Uniform Cr-Ti Coating on B-66 Alloy Sheet Panel



A. Grey Region on B66 Alloy Sheet



B. Shiny Region on B66 Alloy

Figure 58 Photomicrographs of Cr-Ti Coating on B66 Alloy Sheet Panel. Etched 250X

rather than the formation of a continuous chromide surface layer. As discussed in previous sections of this report, high titanium concentrations at the Cr-Ti coating surface produce a non-protective, titanium rich disilicide.

The coating weight gain was 41 mg/cm^2 , or about twice the anticipated amount. The reason for this large coating element transfer and the imbalance in chromium and titanium concentrations in the coating is again the interaction between system pressure, activator efficiency and coating powder composition. The slurry-diffusion processing parameters were first optimized on the basis of coating small groups of coupons in the large retort and furnace, and 50Cr-50Ti alloy proved most satisfactory. Increasing the total surface area to be coated correspondingly increased the total quantity of bisque and activator in the system, which significantly increased the residence time of the activator in the bisque; as well as increasing the efficiency of both the Cr-Ti powder and activator as it is used in the growth process. Since the activator reacts preferentially with the titanium in the powder, this condition shifted the vapor-diffusion process in favor of excessive titanium transfer. The result was a too high Ti/Cr concentration ratio in the coating, and an improper Cr-Ti coating morphology.

As a result of these observations, it was decided to use 60Cr-40Ti powder for the preliminary production proof, rather than 50Cr-50Ti powder. The preliminary production proof was conducted using 12-inch diameter retorts. The segmented structure specimen dimensions and configurations were the same as those used for the vacuum-pack preliminary proof experiments; 2 cylinders, 2 box panels and 2 corrugated panels. In addition, oxidation test coupons, tensile test coupons and two 3 x 7 inch sheet panels from two columbium alloys (Cb752 and C129Y) were also coated. With the exception of Cr-Ti powder composition, the previous parameters for the preliminary production run were the same as those used previously in the reproducibility runs and summarized in Table 12. The Cr-Ti coating formation parameters were: 2 weight percent NaF activator, and a 10 hour isothermal cycle at a temperature of 2300°F , under a 100 torr argon atmosphere. The Cr-Ti coating weight gain was 22 mg/cm^2 . This coating was silicided for two hours at 2000°F and 100 torr argon. The resulting silicon weight gain was 16 mg/cm^2 .

Figure 59 shows a photomicrograph of the Cr-Ti-Si coating from this run. The silicide coating did not completely consume the prior Cr-Ti coating Laves phase, and there were "spikes" from the Cr-Ti coating into the underlying diffusion zone. A coating having this morphology has been shown to provide good high-and low-temperature oxidation protection for columbium. This is further demonstrated by the following data, Table 15, obtained from oxi-

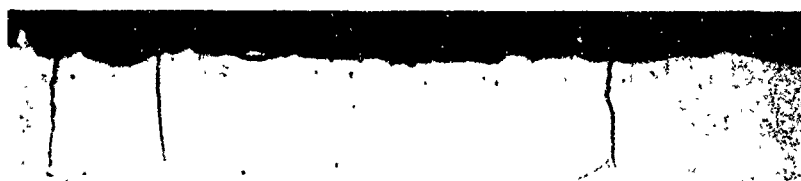


Figure 59 Cr-Ti-Si Coating on Cb752 Coupon from Slurry-Diffusion Preliminary Proof Run.
Unetched 250X

ation testing of coupons coated in the preliminary production proof run:

TABLE 15

SLURRY-DIFFUSION COATED COUPON OXIDATION TEST RESULTS

<u>Test Temp°F</u>	<u>90% Reliable Life</u>	<u>β</u>	<u>Time to Failure, Hours*</u>
1800	509	-	> 509(14) Test terminated, no failures
2200	400	-	> 400(14) Test terminated, no failures
2600	160	8.5	166(2), 190(3), 198(2), 203(2), 229(1), 234(2)
2800	22	3	24(5), 32(2) > 32(5) Test terminated

* Numbers in () are the number of coupons associated with the indicated time.

The performance exhibited by the coating on these coupons exceeded the target values of 90% reliable life > 125 hours at 1800°F, a 90% reliable life > 50 hours at 2600°F and $\beta > 1$ at both temperatures. This coating was also more oxidation resistant than the coatings formed in the process reproducibility runs. This is a consequence of two factors; (1) the overall coating thickness (as measured by total weight gain) is greater, thus providing a greater reservoir of coating elements, and (2) since the Cr-Ti layer was not completely silicided, the Cr-Ti-Si coating displayed better overall protective properties.

5.3.1 Oxidation Testing of Slurry-Diffusion Cr-Ti-Si Coated Segmented Structures

Figures 60 and 61 show parts of the segmented structure and the sheet panels after Cr-Ti-Si coating. Since there were no large particles in the bisque to produce "bridging", the coating on these parts was very uniform in appearance as compared to the mottled surface produced in the diffusion pack. The structures and sheet panels were oxidation tested using the simulated flight temperature cycle and 2600°F life tests employed previously for the diffusion-pack. Performance criteria were protection for 10 flight temperature cycles, or 50 hours life at 2600°F. The results of these tests are summarized in Table 16.

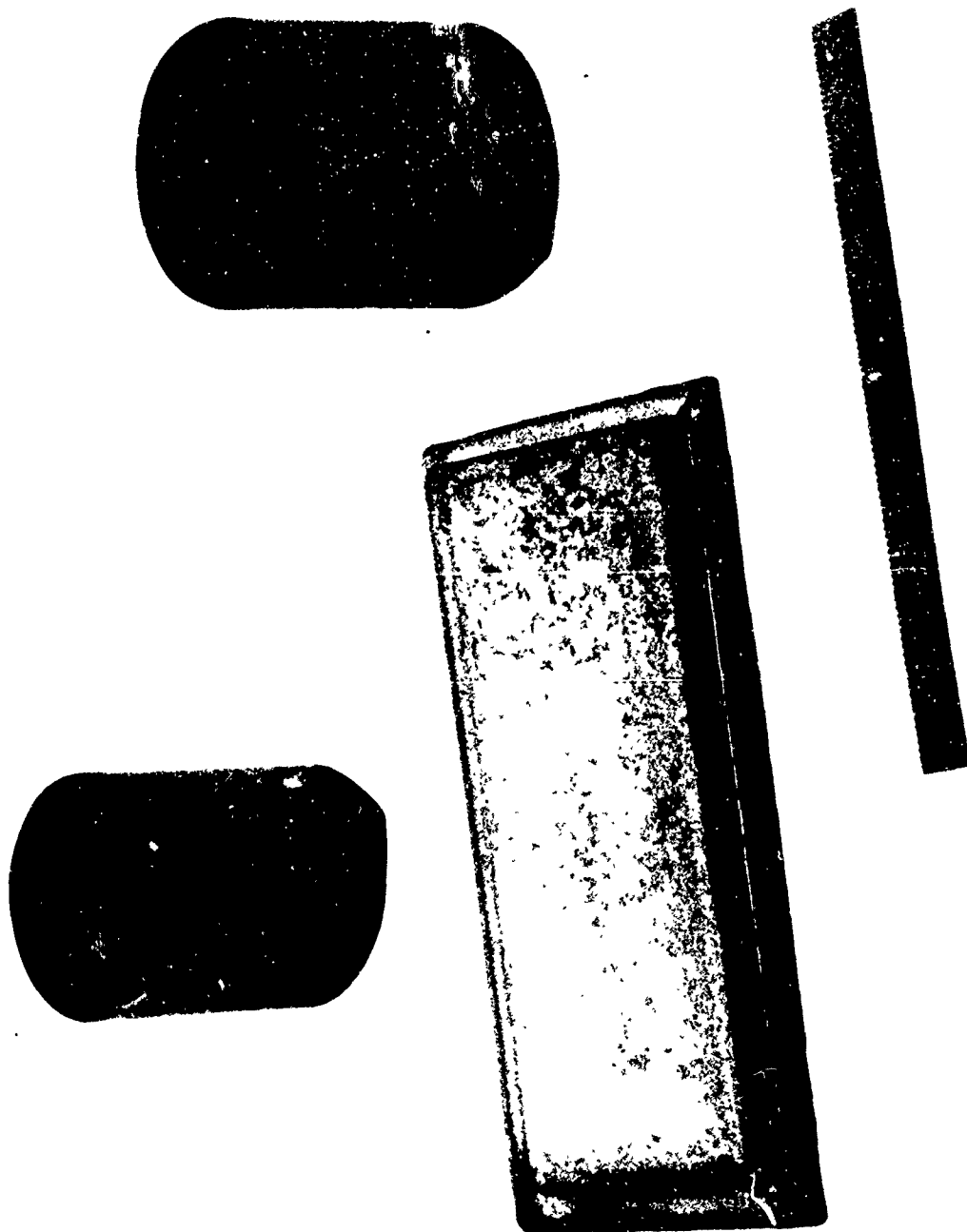


Figure 60. Segmented Structure Parts Cr-Ti-Si Coated
Using the Slurry Diffusion Process -
Preliminary Production Proof Run

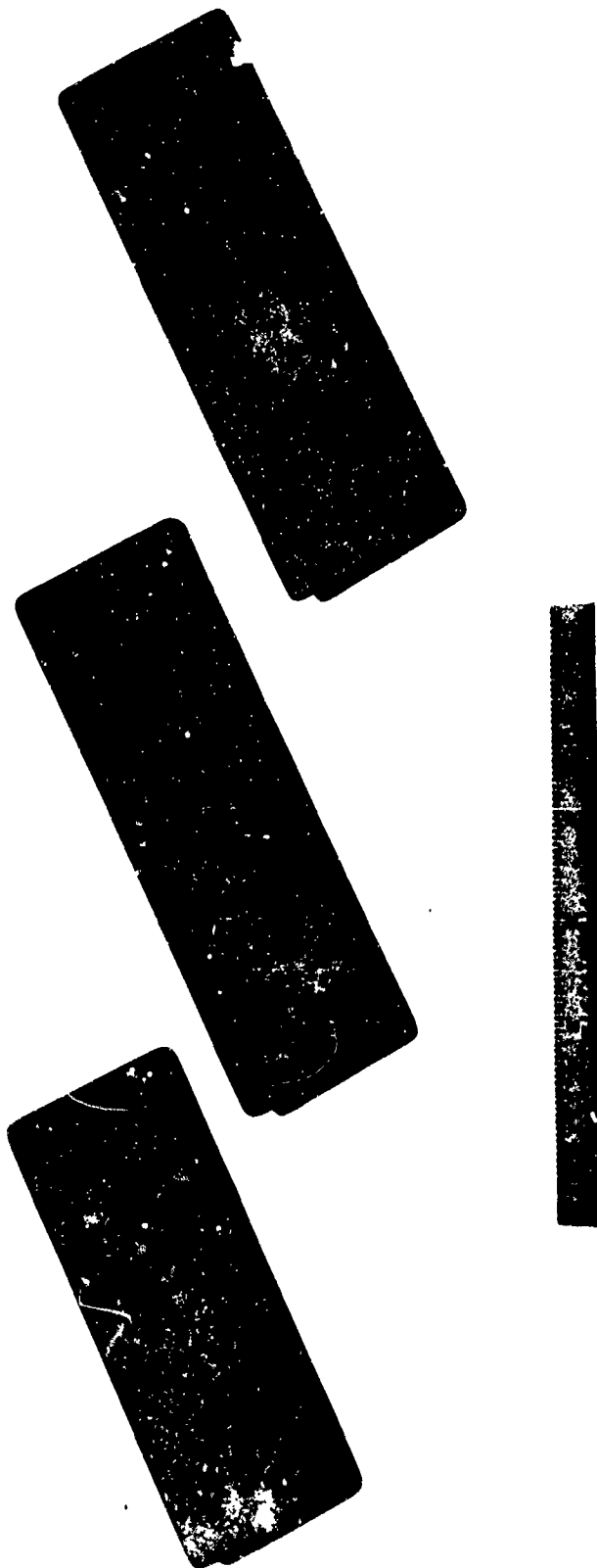


Figure 61. Columbian Alloy Sheet Panels Cr-Ti-Si Coated
Using the Slurry Diffusion Process -
Preliminary Production Proof Run

TABLE 16

SLURRY-DIFFUSION Cr-Ti-Si COATED HARDWARE-OXIDATION TEST RESULTS

	<u>2600°F Profile Test</u> <u>No. of Cycles to Failure</u>	<u>2600°F Life Test</u> <u>Hours Exposure to Failure</u>
Cb-752 Corrugated Panel	Not tested	2
Cb-752 Box Panel	6	50
Cb-752 Cylinder	10	>90 Test terminated
Cb-752 3 x 7 x 0.018 inch sheet	10	>50 Test terminated
Cl29Y 3 x 7 x 0.060 inch sheet	10	>64 Test terminated

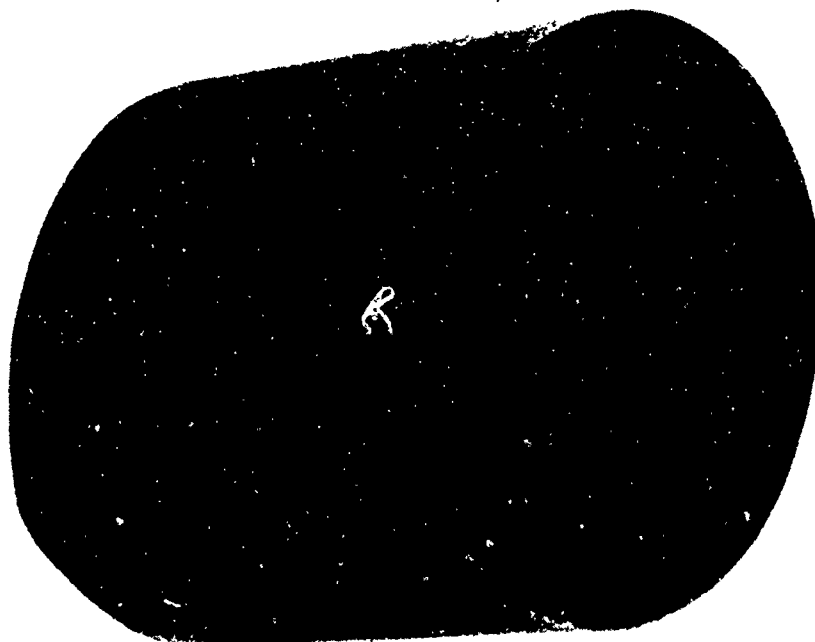
The appearance of the parts after testing is shown in Figures 62 to 66. Figure 62 shows the corrugated panel after 2 hours exposure at 2600°F. The slurry-diffusion coating did not protect the faying surfaces. Consequently, the corrugated panel was not tested under simulated flight-temperature conditions. Figure 63 shows the cylindrical structures after 90 hours exposure to 2600°F air, and 10 simulated flight-temperature cycles, at which times testing was stopped. Both pieces survived the tests without failure, and met or exceeded the 10 cycle and 50 hour protective life goals. Figure 64 shows box panels after 50 hours at 2600°F and 10 simulated flight-temperature cycles. The panel which was flight-profile tested failed at weld regions, again as a consequence of using unalloyed columbium weld material on this panel. Figures 65 and 66 show the alloy sheets after testing under the cyclic conditions. One Cb752 panel was cyclic oxidation tested for 83 hours at 2600°F without failure. The other Cb752 panel was exposed to 12 simulated flight-temperature cycles before failures occurred in many local regions on the surface and edges. The performance of both of these Cb752 alloy panels exceeded the goals of 50 hour life and 10 cycles without failure. The Cl29Y alloy panels survived 64 hours exposure to air at 2600°F and 10 simulated flight temperature cycles without failure, and also met or exceeded the performance goals.

These oxidation tests have shown that the segmented structures formed from Cb752 alloy were well protected by the Cr-Ti-Si coating formed in the production furnace by the slurry-diffusion process. It has been further shown that other alloys, e.g., Cl29Y can also be reliably protected by this coating. The coatings formed in the production furnace by the slurry-diffusion process generally displayed better properties than those formed using the diffusion pack technique. The relative merits of the two processes will be discussed in further detail in the following section.

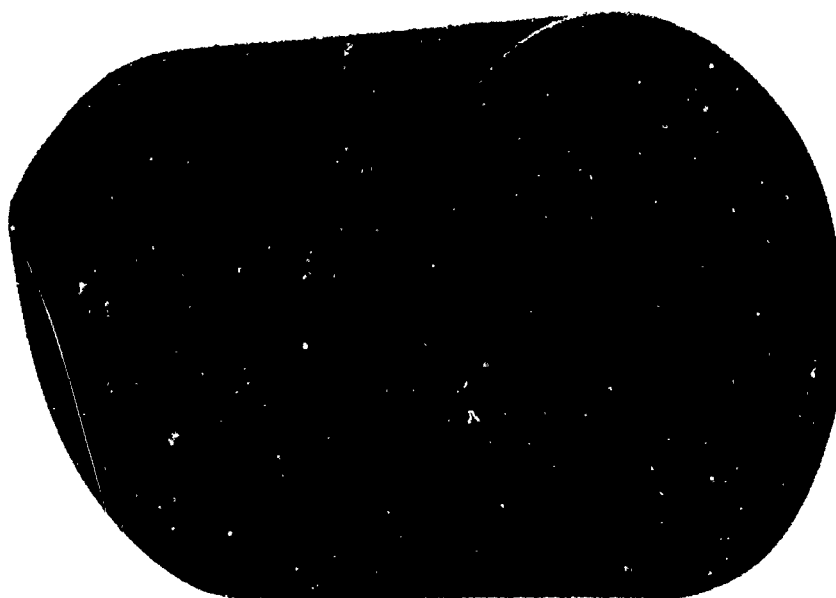


After 2 Hours at 2600°F

Figure 62. Slurry Diffusion Cr-Ti-Si Coated Corrugated Panel After Oxidation Testing

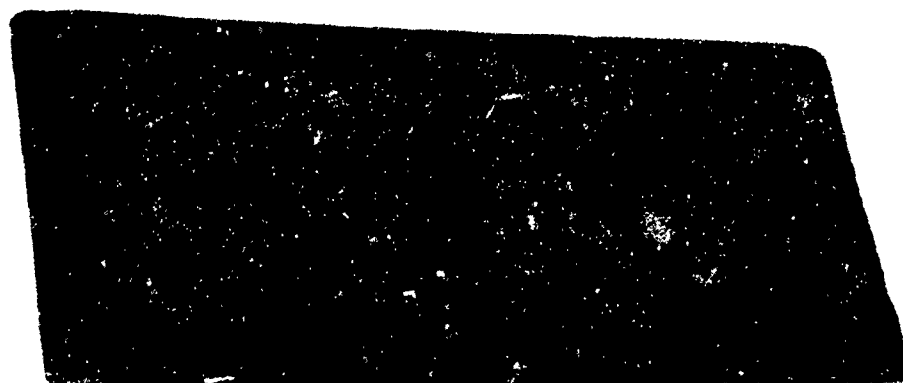


After 90 Hours at 2600°F

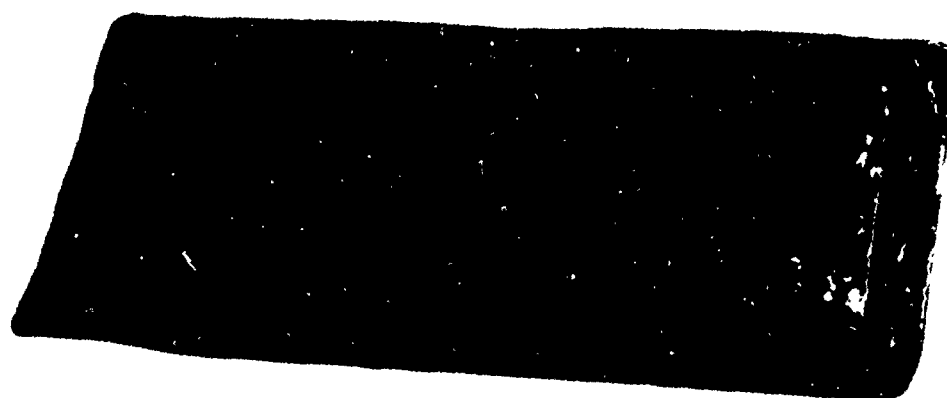


After 10 Simulated Flight-Temperature Cycles

Figure 63. Slurry Diffusion Cr-Ti-Si Coated Cylinders After Oxidation Testing

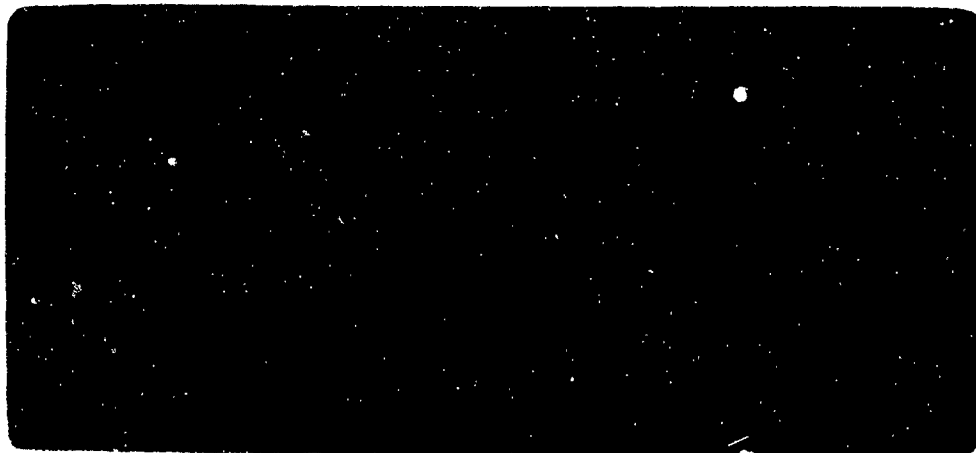


After 50 Hours at 2600°F



After 10 Simulated Flight-Temperature Cycles

Figure 64. Slurry Diffusion Cr-Ti-Si Coated Box Panels After Oxidation Testing



After 83 Hours at 2600°F - No Failure

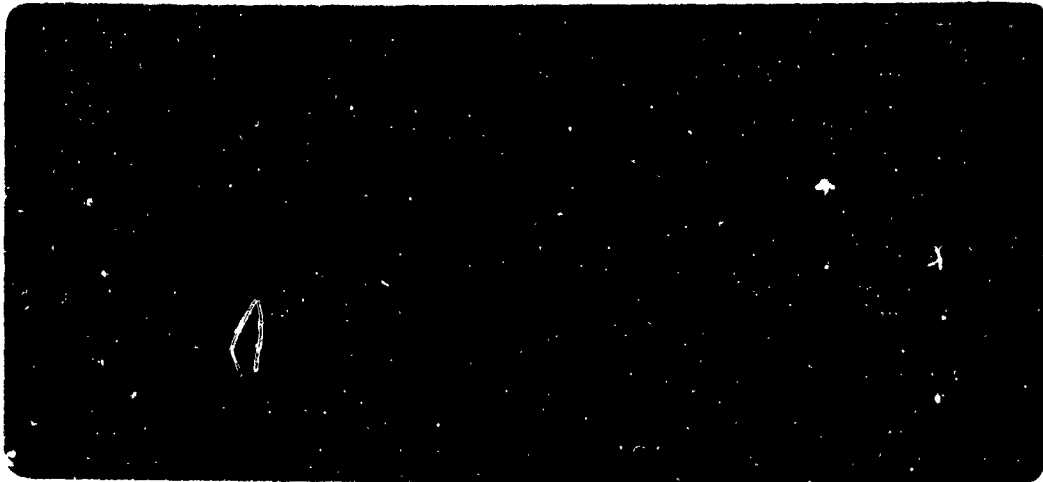


After 12 Simulated Flight-Temperature Cycles - Spot Failures

Figure 65. Slurry Diffusion Coated Cb-752 Alloy Sheet
Panels After Oxidation Testing



After 64 Hours at 2600°F - No Failure



After 10 Simulated Flight Temperature Cycles - No Failure

Figure 66. Slurry Diffusion Coated C129Y Alloy
Sheet Panels After Oxidation Testing

6 PRODUCTION PROOF

As a proof of its utility as a production-scale coating process, the Cr-Ti-Si coating was applied, in three Cr-Ti-Si coating runs, to full-scale aerospace components. The slurry-diffusion process was selected based upon coating microstructure and oxidation performance of the parts coated in the two preliminary production proof tests. Secondary considerations, and a comparison of the vacuum-pack and slurry-diffusion coating processes are summarized in Table 17.

Two Cb752 columbium alloy configurations were coated in this production proof. One was a portion of a nose cone assembly, the other an equipment support ring, acquired from McDonnell-Douglas Corporation under contract AF 04(694)-674. The nose cone had been previously LB-2 coated, oxidation tested and subsequently stripped by McDonnell-Douglas Aircraft Corporation before being sent to TRW. As received, the nose cone, Figure 67, had a longitudinal crack extending upward from the base of the cone. The cone material was brittle, and in order to obtain a coatable section, the cracked portion was cut off about 6 inches above the base of the cone. The ring, in the as-received condition, is shown in Figure 68. In order to provide hardware pieces for the second and third coating runs, the ring was cut along a diameter into two parts. These two parts and the coatable portion of the nose cone are shown in Figure 69. The parts were prepared for coating by rounding all sharp corners with a file, deburring the holes and saw cut regions, and then etching in a solution composed of 8HNO_3 - 15HF - $15\text{H}_2\text{SO}_4$ - $62\text{H}_2\text{O}$ (parts by volume).

In each coating run one of the hardware parts was placed in the 12 inch diameter retort along with control oxidation test and metallography coupons from a different lot of Cb752 alloy. Oxidation test and metallography coupons cut from either the ring or the cone, and one Cb752 3 inch x 6 inch sheet panel were also coated with each large part. For each coating cycle, parts to be coated were sprayed with a slurry bisque 0.020 to 0.030 inch thick. The coating formation parameters for each of the runs are given in Table 18,

TABLE 17

COMPARISON BETWEEN VACUUM-PACK AND SLURRY-DIFFUSION COATING PROCESSES

<u>Vacuum Pack</u>	<u>Slurry-Diffusion</u>
<p>Prone to forming mottled, heterogeneous coatings as a result of bridging between large powder particles and irregular powder contact with the surface to be coated.</p> <p>Temperature gradient in the pack may result in a coating thickness gradient across the coated hardware surface.</p> <p>Longer coating times are required in order to obtain uniform temperatures throughout the pack.</p> <p>Requires retort to hold powder, thereby limiting the maximum size of parts which may be coated.</p> <p>Pack provides support for parts in the retort.</p> <p>Pack particles adhere lightly to part after completion of coating process but are readily removed.</p> <p>Large amounts of coating powder are required, and the media is reusable but not indefinitely.</p> <p>Retorts can be bulky and difficult to handle.</p> <p>Pack generally requires outgassing before starting coating cycle.</p>	<p>Fine particles form a more homogeneous and uniform coating.</p> <p>Temperature gradients are minimized, thus a uniform temperature and more uniform coating thickness are attainable.</p> <p>Uniform temperatures are attainable in shorter times, since only the work must be brought to the coating temperature.</p> <p>Parts may be supported in a furnace without using a retort so that furnace dimensions limit the size of the coated part.</p> <p>Fixturing may be required to support part during coating.</p> <p>Coating bisque very easily removed after completion of coating cycle.</p> <p>Relatively small amount of powder is required in the bisque, and the bisque is not reusable.</p> <p>Only parts to be coated and in some cases relatively light supports require handling.</p> <p>Binder must be volatilized before starting coating cycle.</p>



Figure 67. As Received Cb-752 Alloy Nose Cone



Figure 68. As Received Cb-752 Alloy Equipment Support Ring

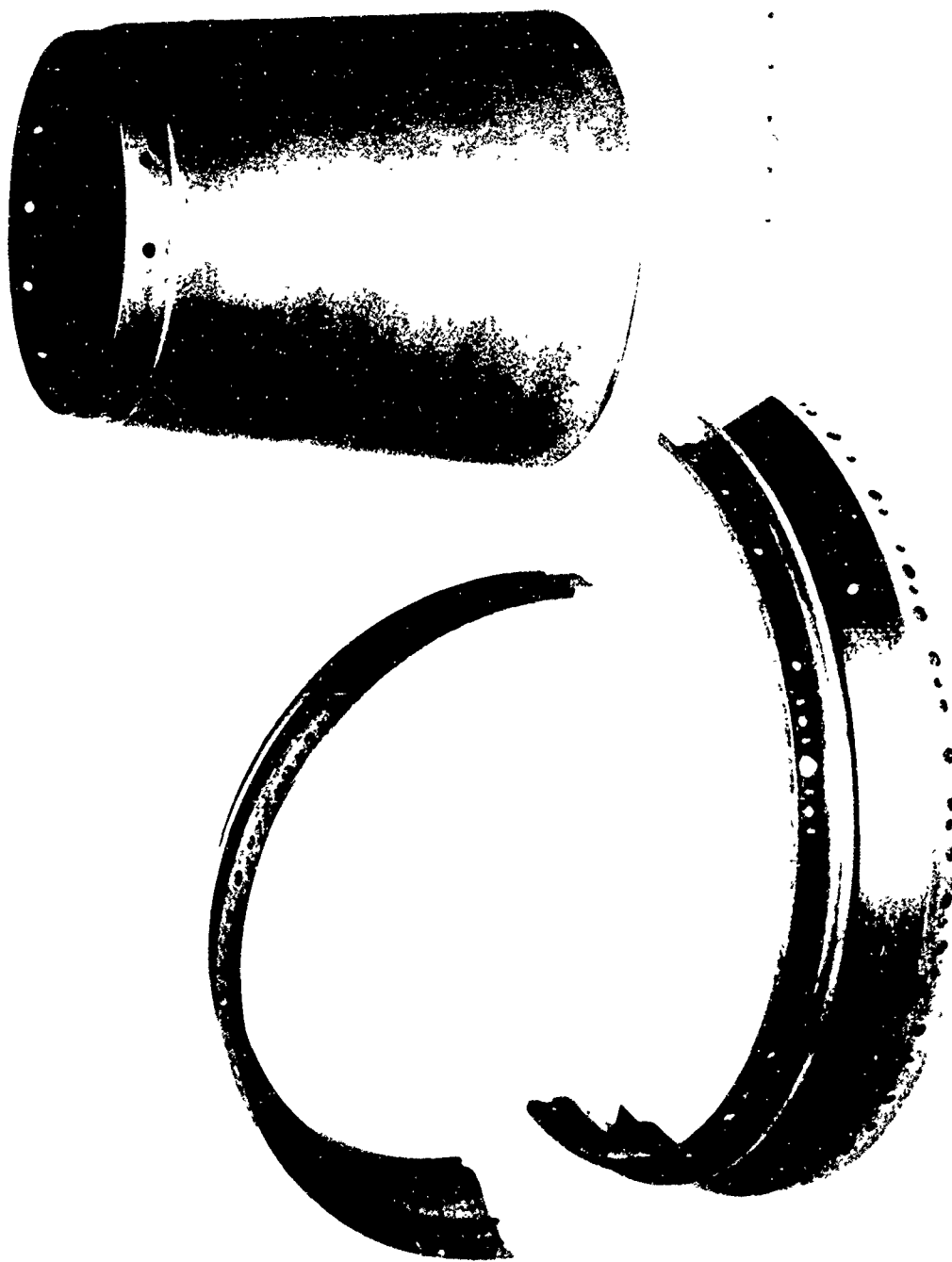


Figure 69. Cb-752 Alloy Ring and Cone Sections Before Cr-Ti-Si Coating

TABLE 18

SLURRY-DIFFUSION COATING PARAMETERS FOR PRODUCTION PROOF

	<u>Cr-Ti Coating</u>	<u>Silicon Coating</u>
Powder Composition (w/o)	60Cr-40Ti	100 Si
Particle Size (mesh)	-250 +325	-250 + 325
Activator NaF (w/o)	2	
KF (w/o)		2
Bisque Weight (gm/cm ²)	0.2	0.2
Coating Temperature (°F)	2350	2000
Coating Time (Hours)	10	2
System Pressure (Argon, torr)	100	100

The sprayed and dried bisque was somewhat fragile, and it was necessary to minimize handling of the sprayed parts. This was done by placing the nose cone onto a columbium alloy plate which was previously covered with either a Cr-Ti or a silicon bisque, depending upon which coating was to be applied. Figure 70 shows the silicon bisque adhering to the nose cone and support plate after completing the siliconizing thermal cycle. Figure 71 then shows the ease with which the silicon bisque was removed. The Cr-Ti bisque was removed with equivalent ease. Figures 72 and 73 show the appearance of the silicon bisque on the rings after completing the silicon coating cycle. The light area on each of these rings is the region where the rings were supported in a tray of silicon powder during the coating cycle. The ease with which the bisque was removed from the rings is illustrated in Figure 74. The appearance of all three pieces after completion of the Cr-Ti and the silicon coating cycles is shown in Figure 75. The average coating weight gains, as determined from control coupons included with each part, are given in Table 19.

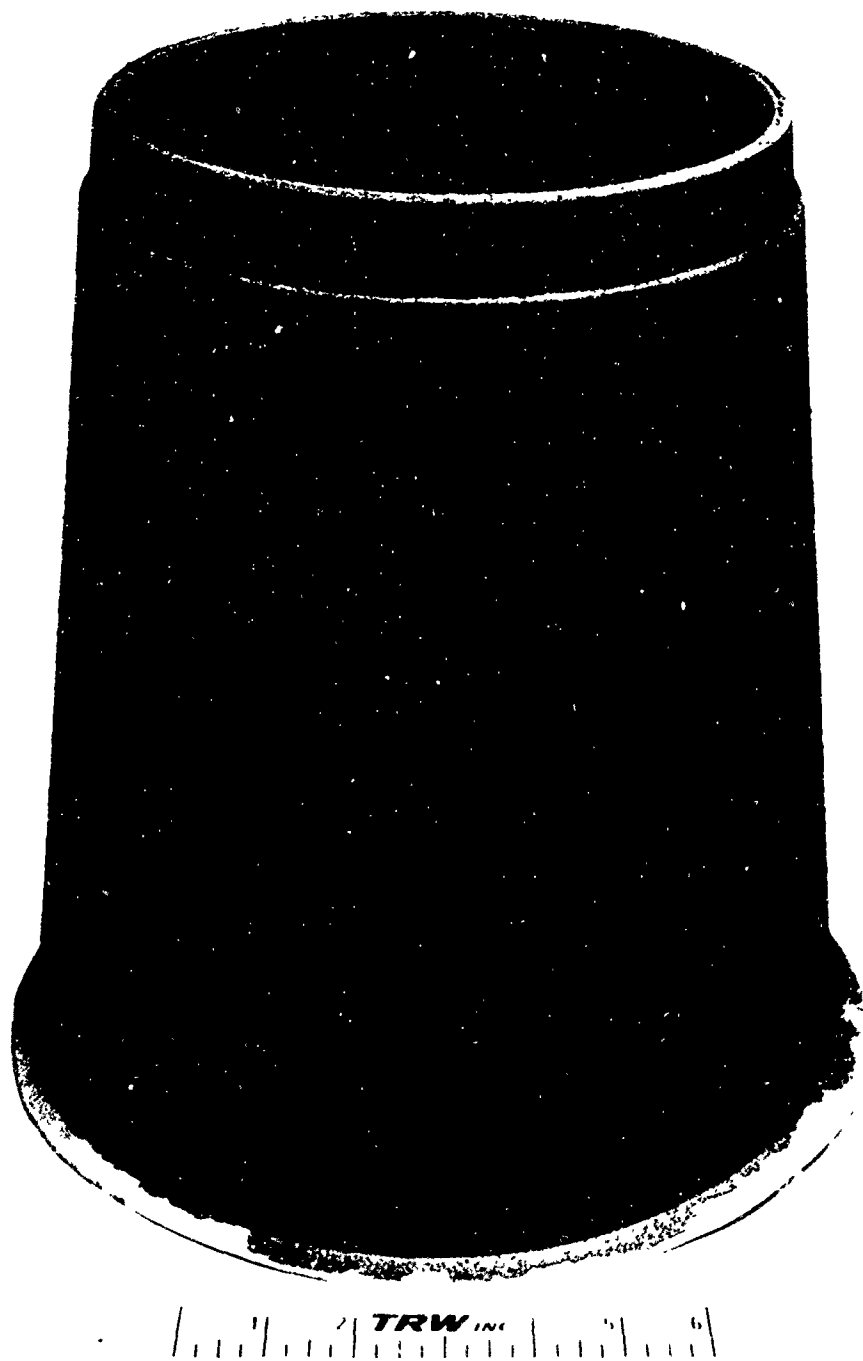


Figure 70. Silicon Bisque on Nose Cone After Silicon Coating Cycle



Figure 71. Nose Cone and Silicon Bisque After Bisque Removal



Figure 72. Ring Section 1 with Silicon Bisque After Coating

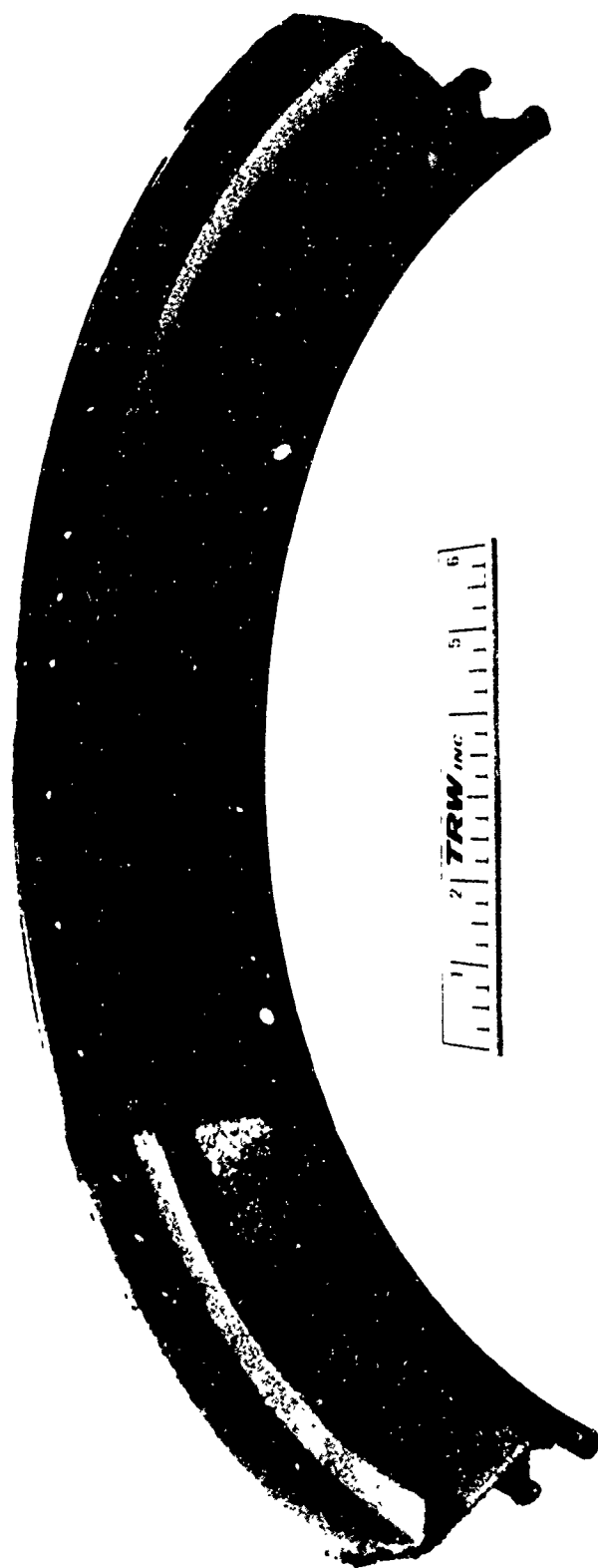


Figure 73. Ring Section 2 with Silicon Bisque After Coating

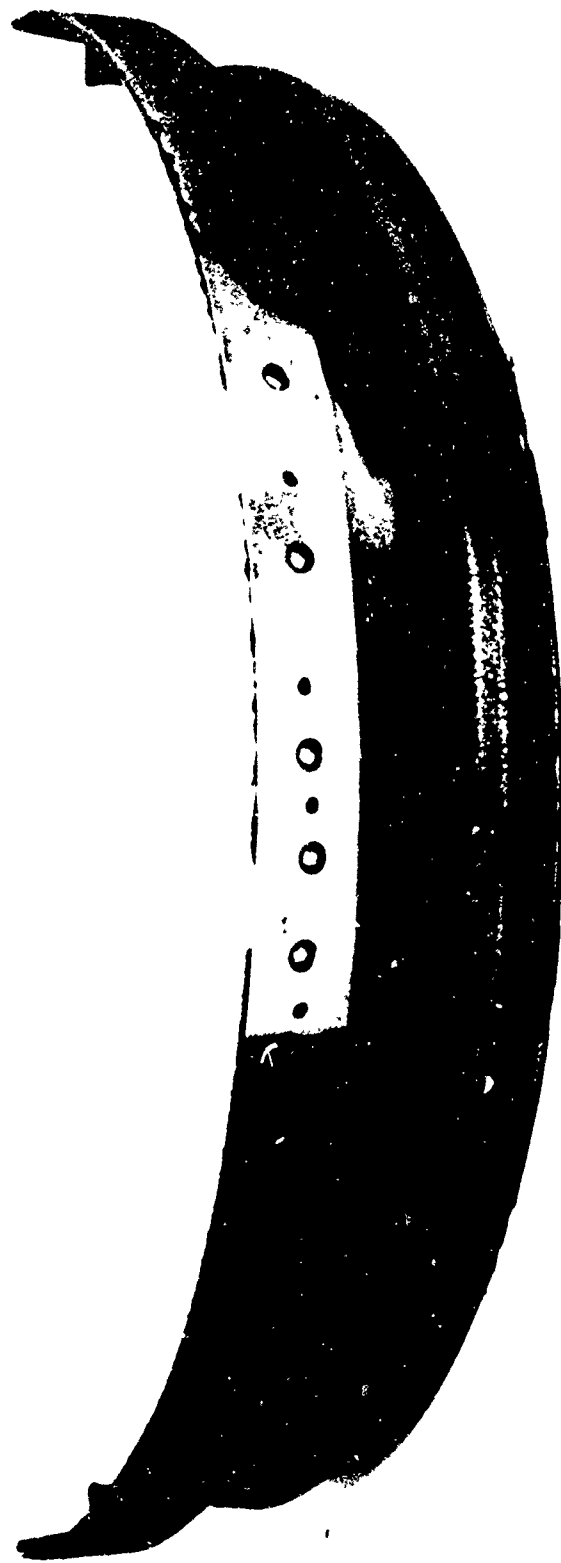


Figure 74. Ring Section 2 with a Portion of the Silicon Bisque
Removed After Completion of the Coating Cycle

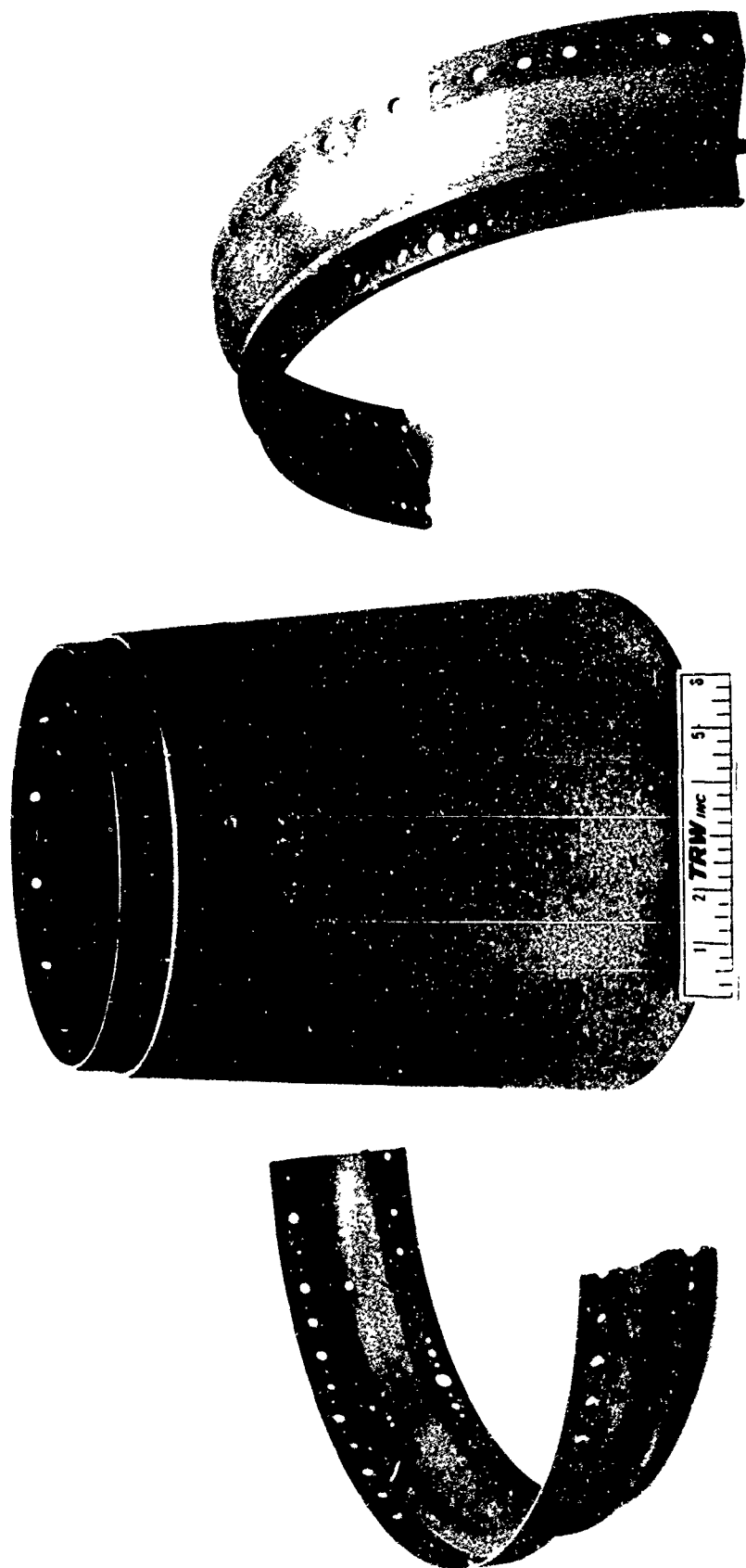


Figure 75. Cr-Ti-Si Coated Nose Cone and Ring Sections

TABLE 19

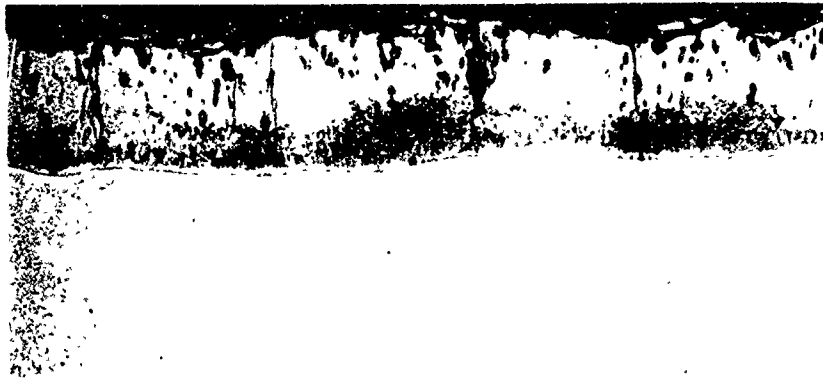
PRODUCTION PROOF COATING WEIGHT GAINS-CONTROL COUPONS

<u>Coating Run</u>	<u>Cr-Ti, mg/cm²</u>	<u>Silicon, mg/cm²</u>
Cone	19.0	14.6
Ring 1	18.4	15.1
Ring 2	19.0	14.4

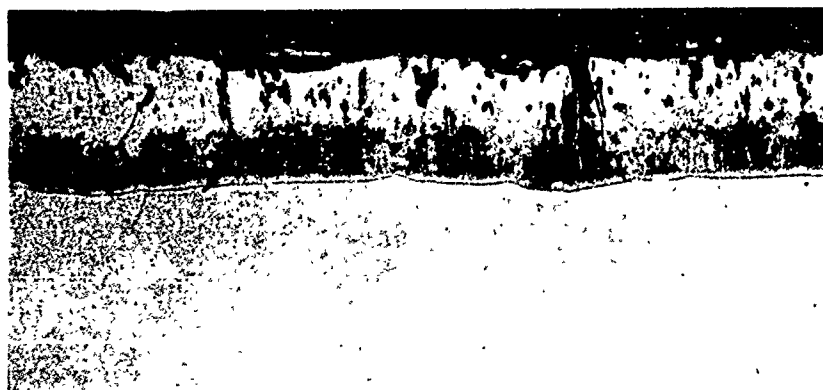
The reproducibility of both the Cr-Ti and the silicon weight gain was excellent. The weight gains were somewhat lower than were obtained during the preliminary proof, i.e., 22 mg/cm² Cr-Ti and 16 mg/cm² silicon. However, the differences between the weight gains obtained in this production proof and the weight gains obtained in the preliminary proof are within the run-to-run variability observed during the reproducibility study and subsequent slurry-diffusion runs.

Figure 76 shows the microstructures of Cr-Ti-Si coatings on control coupons which were cut from the as-received production proof parts. The coatings on all three pieces were characterized by regions in which the Cr-Ti coating was completely silicided, and regions in which siliciding did not completely consume the prior Cr-Ti coating. There was evidence of dichromide spikes in the diffusion zone of each coating. Although local regions showed through siliciding of the chromide overlay, the presence of a substantial Cr-Ti enriched diffusion zone beneath the entire silicide layer is representative of a good quality Cr-Ti-Si coating.

Coated control coupons and coupons representative of each production proof piece were cyclic oxidation-life tested at 1800 and 2600°F. Twelve control coupons and six coupons from the production proof pieces were tested at each temperature. At 1800°F there were no failures to 200 hours of testing, at which time the tests were terminated. At 2600°F there were four coating failures in the group of thirty-six control coupons which were tested for 125 hours, as shown below in Table 20.



Ring 1



Ring 2



Nose Cone

Figure 76 Microstructures of the Cr-Ti-Si Coating on Production
Proof Test Control Specimens-Cb752 Alloy.
250X Etched

TABLE 20

OXIDATION PERFORMANCE OF CONTROL COUPONS FROM THE PRODUCTION PROOF

<u>Cr-Ti-Si Coating Runs</u>	<u>Times to Failure at 2600°F, Hours</u>
Ring 1	22(1), 118(1), > 125(10)
Ring 2	22(1), >125(11)
Nose Cone	46(1), >125(11)

In this table the number in () indicates the number of coupons associated with the indicated time, and the symbol > is used to indicate that failure had not occurred after 125 hours. After 125 hours of testing at 2600°F, there were no failures associated with any of the coupons cut from the production-proof pieces. Each of the sheet panels was tested using the simulated flight-temperature cycle. The panels coated with Ring 1 and the Nose Cone survived 10 cycles without failure, while the panel coated with Ring 2 failed after 8 cycles. These panels are shown in Figure 77. From these oxidation tests it is concluded that the coating formed in the production proof is equivalent in properties to that formed during the preliminary production proof experiments. No test were conducted on large pieces coated in these runs. These pieces have been submitted to the Air Force.



Figure 77. Columbian Alloy Sheet Panels After Ten Simulated Flight Temperature Cycles

7 EDGE EFFECT AND COATING DEFECT REPAIR STUDIES

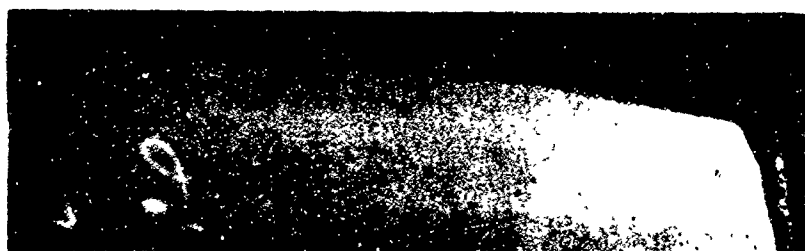
The anomalous oxidation behavior of edges and corners on test coupons and other parts has been well documented in oxidation and corrosion literature. It is known that coatings may undergo premature failures at these locations, and that edge and corner failures become less pronounced when the corner and edges are rounded. For this reason oxidation testing of coatings is frequently done on specimens having a minimum thickness of 0.030 inch, and the edges are abrasive tumbled so as to produce a large edge radius.

The work in this portion of the program was undertaken to evaluate the effect of sheet thickness and edge radius on the oxidation performance of the Cr-Ti-Si coating, and to develop suitable repair techniques for coating defects which may occur on edges, corners or flat portions of coated parts. The effects of substrate thickness and sheet preparation were considered with regard to protection provided by the Cr-Ti-Si coatings as formed by either the diffusion-pack or the slurry-diffusion processes. The majority of this coating work was performed in the production furnace.

7.1 Edge Effect Studies

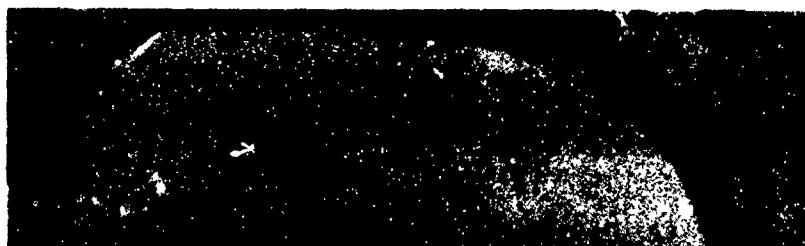
A number of specimens of 0.030 inch Cb752 were edge-finished by various methods to determine the radius of curvature to be expected from various finishing techniques, and possible effects of average edge radii in relation to edge coverage. Figure 78 illustrates the different edge curvatures which were obtained by grit blasting, abrasive tumbling or by hand honing using a rubberized abrasive stone. The thickness of the sheet in the range 0.015 to 0.030 inch was not a factor in the appearance of the edges as prepared by either method. It was found that when care was used, hand-finished sheet edges were more uniform and of larger radius than the tumbled finish, which had a radius of curvature considered adequate to minimize edge failures.

Material from a single heat of Cb752 alloy was rolled into 0.030, 0.020 and 0.015 inch thick sheet. In addition, some of the 0.030 inch sheet was etched to a thickness of 0.015 inch using an aqueous $\text{HF-HNO}_3\text{-H}_2\text{SO}_4$ mixture. Coupons were sheared from these sheets and one-half of each of the four lots was tumbled. The remaining half-lots were finished to about 0.002 inch edge radius by abrasion with a rubberized stone. This radius of curvature was chosen to determine the edge effects at a radius intermediate between the as-sheared and as-tumbled conditions. These coupons were Cr-Ti-Si coated using both the diffusion-pack process and the slurry-diffusion process.



As Sheared

Min. Rad. 0.002 to 0.0013 inch



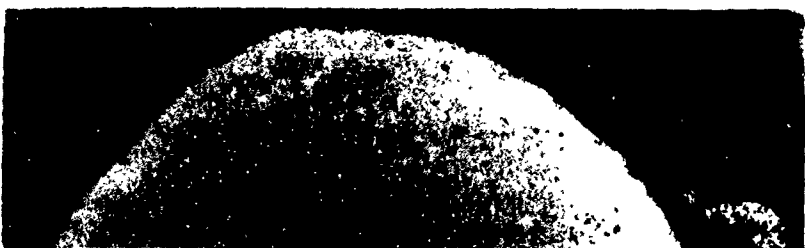
As Tumbled

Min. Rad. 0.0047 to 0.0086 inch



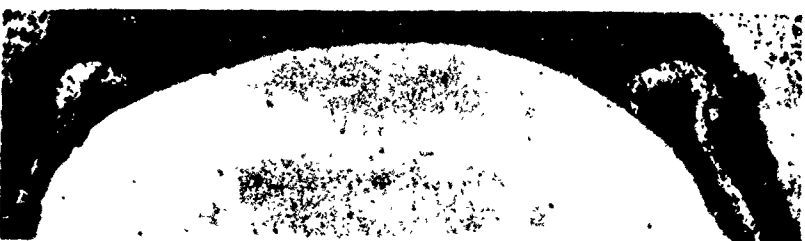
Hand Finished

Min. Rad. 0.010 to 0.013 inch



Zirconia Blast Finished

Min. Rad. 0.008 to 0.011 inch



Rough Blast Plus Hand Finished

Min. Rad. 0.008 to 0.010 inch

Figure 78. Typical Edge Finishes on 0.030 inch Thick Cb-752 Alloy Coupons

7.1.1 Edge Effect with Diffusion Pack Coated Coupons

Two compositions, both nominally 60Cr-40Ti, were used to coat the coupons. One of these packs inadvertently contained material in which the titanium content was partially depleted through extensive use. Consequently, the coating process was repeated with previously unused powder and another set of coupons. Both of these Cr-Ti coatings and the silicon coatings were formed using the conditions which were developed for this process and discussed earlier in Section 4.3 of this report. Typical photomicrographs of the coated edges are given in Figure 70.

The 1800°F and 2600°F oxidation lives of coupons which were Cr-Ti coated with titanium depleted powder, Tables 21 and 22, were not satisfactory. As shown in Figure 79A, there were no chromide spikes in the diffusion zone of the coating formed using titanium depleted powder, thus indicating little chromium and/or titanium in solution in the columbium matrix.

The 1800°F cyclic oxidation resistance of coupons coated using the new Cr-Ti powder was significantly better. Each one of the eight edge preparations were tested using six coupons. After 667 hours of exposure none of the forty-eight coupons had failed. The fact the coating weight gains were higher also contributed to the improved oxidation performance.

After oxidation testing for 14 hours at 2600°F abrasive tumbled (type 3TP-Table 23) coupons failed catastrophically, and it was not possible to determine whether failure was initiated at the edge or at the flat portion of the coupon. Testing at 2600°F was considered too severe to permit reliable location of failure origins. The coupons were replaced with others similarly prepared, and testing was resumed at 2500°F. Therefore, the 2500°F failure times, except as noted in Table 23, include 14 hours prior exposure at 2600°F. As shown in the Table several coupons failed in more than one manner. The early failure of the type 3TP coupons was unusual; these coupons were the thickest and had the largest edge radius, and previous experience indicated that these coupons should have had the longest oxidation lives. As a group, coupons coated using new 60Cr-40Ti powder showed better oxidation resistance than did the coupons which were Cr-Ti coated with titanium depleted powder. Although testing at a lower temperature undoubtedly had some effect, the improved performance is largely a consequence of a thicker coating which had the proper morphology and chemistry.

The manner of failure for coupons which survived 394 hours at 2500°F was different from that of coupons which failed after shorter exposure times at 2500 and 2600°F. Earlier failures were isolated in

TABLE 21

COMPILATION OF HOURS TO FAILURE AND FAILURE MODE OF EDGE STUDY
COUPONS PACK COATED WITH TITANIUM DEPLETED 60Cr-40Ti AND
SILICON-OXIDATION TESTED AT 1800°F

Coupon Specimen Preparation (1)	Thickness (mils)	Edge Radius (mils)	Weight Gain mg/cm ²		Ratio Cr-Ti/Si	Total Hours to Failure (2)
			Cr-Ti	Si		
CHP	15	2-3	11.8	14.3	0.83	4E, 8E, 11F, 29E, 48F, 82F, 90F, 145E, 179E
1HP	15	3-4	14.0	9.3	1.51	8FC, 13EF, 43E, 49F, 51E, 75F, 174E, 328E
2HP	20	1-2	13.4	9.8	1.37	29F, 43E, 59F, 110E, 155F, 174E, 192E, 204E, 253E
3HP	30	2-3	13.0	10.8	1.20	6E, 10F, 14E, 34F, 34F, 38E, 43F, 62E, 122E, 204C
CTP	15	5-6	10.9	10.9	1.00	6F, 6E, 6E, 7FE, 8E, 10F, 20E, 21F, 48E, 57F, 59F, 60F
1TP	15	5-6	11.7	11.5	1.02	29E, 54C, 57E, 102F, 130F, 145E, 209E, 247C
2TP	20	8-9	12.2	9.5	1.28	49C, 82F, 82E, 122F, 145F, 101E, 192E
3TP	30	8-9	12.9	14.8	0.87	15F, 20F, 21F, 23F, 48F, 49F, 54F, 109F, 135E, 212C, 216E

(1) C - Chem-milled to 15 mil thickness.
HP - Rubberized stone edge preparation.
TP - Abrasive tumble edge preparation.

(2) C Denotes corner failure
E Denotes edge failure
F Denotes defect failure on flat surface.

TABLE 22
 COMPILATION OF HOURS TO FAILURE AND FAILURE MODE OF EDGE STUDY
 COUPONS PACK COATED WITH TITANIUM DEPLETED 60Cr-40Ti AND
 SILICON-OXIDATION TESTED AT 2600°F

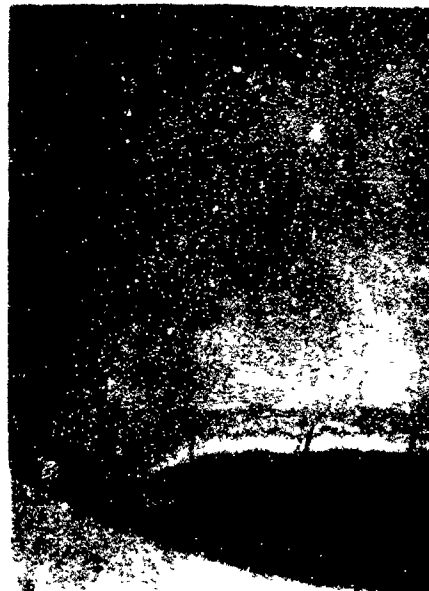
Coupon Specimen Preparation (1)	Thickness (mils)	Edge Radius (mils)	Weight Gain mg/cm ²		Ratio Cr-Ti/Si	Total Hours to Failure (2)
			Cr-Ti	Si		
CHP	15	2-3	11.8	14.3	0.8	27E, 61F, 61F, 69EF, 70F, 78C, 90E, 111EF, 121E
1HP	15	3-4	14.0	9.3	1.51	40C, 62CF, 62E, 64C, 71C, 82C, 111F, 129F, 189CF
2HP	20	1-2	13.4	9.8	1.37	21E, 65E, 71C, 71CE, 74E, 74C, 89E, 94E
3HP	30	2-3	13.0	10.8	1.20	27F, 58F, 62E, 65E, 65C, 69C, 71C, 71CF, 74CF, 74E,
CTP	15	5-6	10.9	10.9	1.00	64E, 70E, 78E, 86E, 90E, 149F, 165C, 170C
1TP	15	5-6	11.7	11.5	1.02	25C, 61C, 74C, 74CE, 85C, 102E, 117E, 178C, 189CF
2TP	20	8-3	12.2	9.5	1.28	61E, 72F, 74E, 88E, 102C, 117F, 146E
3TP	30	8-9	12.9	14.8	0.87	62E, 64E, 70E, 77C, 78E, 86F, 121E, 153F

(1) C Chem-milled to 15 mil thickness.
 HP - Rubberized stone edge preparation.
 TP - Abrasive tumble edge preparation.

(2) C Denoted corner failure
 E Denotes edge failure
 F Denotes defect failure on flat face surface.



Abrasive Tumbled
0.008" to 0.009" Edge Radius



Hand Honed
0.001" to 0.002" Edge Radius

A. Coated with Titanium Depleted 60 Cr-40 Ti Powder



Abrasive Tumbled
0.006" to 0.009" Edge Radius



Hand Honed
0.001" to 0.002" Edge Radius

B. Coated with Previously New 60 Cr-40 Ti Powder

Figure 79. Cr-Ti-Si Coated 0.020 Inch Thick Edge Effect Coupons

100X

TABLE 23

COMPILATION OF HOURS TO FAILURE AND FAILURE MODE OF EDGE STUDY COUPONS
PACK COATED WITH 60Cr-40Ti ALLOY AND SILICON
OXIDATION TESTED AT 2500°F.

<u>Coupon(1)</u>	<u>Thickness</u> (mils)	<u>Edge Radius</u> (mils)	<u>Weight Gain</u> mg/cm ²		<u>Ratio</u> Cr-Ti/Si	<u>Total Hours To Failure (2)</u>
			<u>Cr-Ti</u>	<u>Si</u>		
CHP	15	2-3	24.7	15.3	1.61	<u>14EC, 14EC, 14EC, 66F, 142F, 148EF</u>
1HP	15	3-4	25.4	16.0	1.58	<u>192E, 192F, 192F, 192F, 394F, 394F</u>
2HP	20	1-2	26.7	11.6	2.30	<u>138C, 138F, 138F, 138EF, 142F, 142C</u>
3HP	30	2-3	25.5	16.4	1.55	<u>11EF, 142F, 192F, 192F, 192EF, 394F</u>
CTP	15	5-6	24.8	15.6	1.59	<u>14F, 14F, 142F, 394F, 394F, 394F</u>
1TP	15	5-6	23.8	16.5	1.44	<u>14E, 14EF, 394F, 394F, 394F, 394F</u>
2TP	20	8-9	23.4	11.9	1.97	<u>138CE, 138F, 142F, 148F, 148F, 148F</u>
3TP	30	8-9	25.3	12.5	2.02	<u>(3) 26C, 26C, 26C, 39 C, 394C, 394F, 394F</u> <u>14E, 14EF, 14EF, 14F, 14F, 14F</u>

(1) C - Chem-milled to 15 mil thickness
 HP - Rubberized stone edge preparation
 TP - Abrasive tumble edge preparation

(2) C - Denotes corner failure
 E - Denotes edge failure
 F - Denotes defect failure on flat surface
 Underlined hours to failure are at 2600°F,
 Times included 14 hours exposure at 2600°F.

(3) These coupons were exposed at 2500°F only

local defect regions at edges, corners or on the flat surface of the coupon, while long-time failures were a general uniform degradation or wear out of the coating. Typical examples of these different types of failures are shown in Figure 80. The localized failures likely occurred at isolated regions of random thinning of the Cr-Ti coating or at isolated regions which were deficient in chromium (11). The long-time failure is believed to be due to a uniform degradation of the coating by the inward diffusion of oxygen and outward diffusion of metallic constituents into the silicide coating.

The results of the edge effect tests using diffusion pack coated coupons may be summarized by stating, that for the conditions investigated, failure did not depend upon coupon preparation method, coupon radius, coating weight or Cr-Ti weight gain to silicon weight gain ratio. Also, the preparation methods employed generally represent those utilized in preparing hardware edges prior to coating.

7.1.2 Edge Effect with Slurry Diffusion Coated Coupons.

Coupons identical to those used in the diffusion pack work were Cr-Ti-Si coated using the Cr-Ti and silicon coating parameters used for the slurry pack process reproducibility runs discussed in Section 5.2. The microstructures of the coatings were similar to those observed for the reproducibility runs, Figures 54 to 56.

Four coupons of each edge preparation, a total of 32 coupons, were Cr-Ti-Si coated and oxidation life tested at 1800°F for 802 hours without the occurrence of coating failures. The results of oxidation life testing at 2600°F are given in Table 24. There was no correlation between the times to failure and coupon edge preparation or radius. However, the oxidation tests at both temperatures showed that, at least under these particular coating formation and test conditions, the slurry diffusion applied coating was more protective than the coating applied by the diffusion pack.

7.2 Coating Defect Repair Studies

The coating repair portion of this work considered ways to repair two types of coating defects. The first comprised damage to an unoxidized coating, resulting from dents, nicks, or scratches, such as might result from handling of coated hardware. The second type was a localized coating failure, either at an edge, corner or a flat portion of a surface, observed after exposure to an elevated temperature, oxidizing environment. For both applications, a successful repair coating should satisfy the following requirements:



Edge and Defect Failure
148 Hours at 2500°F



Corners and Edge Failure
26 Hours at 2500°F



Uniform Degradation
394 Hours at 2500°F

Figure 80 Failure Modes on Cr-Ti-Si Coated Cb752 Alloy Coupons.
3X

TABLE 24
COMPILATION OF HOURS TO FAILURE AND FAILURE MODE OF EDGE STUDY COUPONS
DIFFUSION-PAK COATED WITH 50CF-50TF ALLOY AND SILICON
OXIDATION TESTED AT 2600°F

Coupon (1)	Thickness (mils)	Edge Radius (mils)	Coating Weight Gain mg/cm ²		Ratio Cr-Ti/Si	Total Hours to Failure (2)
			Cr-Ti	Si		
CHP	15	2-3	11.4	18.4	0.62	137EF, 150C, 150CF, 150F
1HP	15	3-4	12.6	19.5	0.65	79EC, 140EC, 140CF, 150F
2HP	20	1-2	12.7	19.8	0.64	137CF, 146F, 150F, 150F
3HP	30	2-3	12.4	19.4	0.64	79C, 140CEF, 146EF, 146EC
CTP	15	5-6	11.8	19.0	0.62	140F, 146EF, 146EC, 150EC
1TP	15	5-6	12.2	18.3	0.67	146F, 146F, 150EF, 150F
2TP	20	8-9	12.2	19.7	0.62	146CF, 146C, 150EF, 150F
3TP	30	8-9	12.2	18.5	0.66	146EF, 150F, 150F, 150F

(1) C - Chem-milled to 15 mil thickness.

HP - Rubberized stone edge preparation

TP - Abrasive tumble edge preparation.

(2) C - Denotes corner failure

E - Denotes edge failure

F - Denotes defect failure in flat surface

1. It must be compatible with the original Cr-Ti-Si coating and/or the metal substrate as to:

- (a) thermal shock properties,
- (b) thermal expansion match,
- (c) formation of a chemical or diffusion bond,

2. Should exhibit self healing characteristics,

3. Must provide oxidation resistance at all contemplated use temperatures.

The repair coating may also be usable as a means of providing additional oxidation resistance at edges and corners, by the local buildup of coating thickness in these areas. It would also be desirable to locally apply the repair coating to the damaged area of the part without having to subject the entire part to a thermal treatment. For easy application to the defect region, the coating should be deposited from a slurry, and should be capable of being formed in a relatively short time.

7.2.1 Repair of Defects in Unoxidized Coatings

Intentional defects were introduced into Cr-Ti-Si coatings on Cb752 alloy coupons by bending the coupons, thereby producing cracks which extended both longitudinally and transversely along the crease direction; and by filing, or grinding away the coating to expose the metal substrate at a corner, along an entire edge, or at a spot having an area of about 1/32 of a square inch on the flat surface.

The repair slurries were brushed onto the defect area and air dried. The coupons were then treated in one of three different ways:

- 1) immediately cyclic oxidation tested at 1800 or 2600°F,
- 2) heated in air using an oxy-acetylene torch, and then oxidation tested, or
- 3) heated in vacuum prior to oxidation testing.

Table 25 summarizes the results of various slurry compositions which either produced unsatisfactory repairs or only moderately successful repairs, and were not investigated further. Mixed oxide slurries, MgO-SiO and MgO-Al₂O₃, produced porous coatings at 1800°F and reacted with the silicide coating at 2600°F. Slurries containing carbides were not protective at either temperature. Repair slurries consisting of MoSi₂

TABLE 25

SUMMARY OF RESULTS FOR EDGE DEFECT STUDY

Slurry Composition (Weight Percent)	Cyclic Oxidation		Thermal Mismatch	Failure Mode	
	Temperature (°F)	Cycles (1)		Reaction with Coating	No Bonding of Powder
MgO-50SiO ₂	1800	1			X
	2600	1		X	
MgO-50Al ₂ O ₃	1800	1			X
	2600	1		X	
TiC-50Si	1800	1			X
	2600	1		X	
Al-50MoSi ₂	1800	1		X	
	2600	1		X	
MoSi ₂ 20 7740 glass	1800	1-2	X	X	
	2600	1	X	X	
MoSi ₂	1800	1-2	X		
	2600	1	X		
TiSi ₂	1800	1			X
	2600	1			X
Cr-33Si-33TiSi ₂	1800	1-2		X	
	2600	1-2		X	
Cr-33Si-33MoSi ₂	1800	1-2		X	
	2600	1-2		X	
Cr-33Si-33TiAl	1800	4-8	X		
	2600	2-4	X		
W-20Si-20V-20Cr	1800	5-8	X		
	2600	6-8	X		
Al-30(Cr-40Ti-20Si)	1800	6-8	X		
	2600	4-5	X		
Sn-80(Cr-40Ti-20Si)	1800	6-9	X		
	2600	4-8	X		
Ag-80(Cr-40Ti-20Si)	1800	6-9	X		
	2600	4-8	X		
Sn-90(Cr-40Ti-20Si)	1800	6-12	X		
	2600	6-10	X		

(1) Test specimens cycled to room temperature every hour.

and Corning glass 7740 were applied to defected areas and fused in an oxy-acetylene flame. Only short-time protection was afforded.

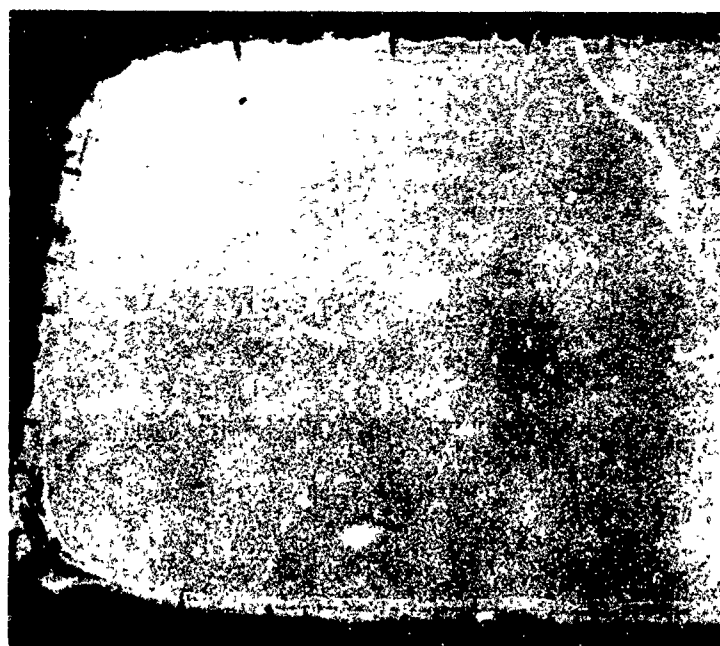
Systems containing different combinations of chromium, silicon or titanium and one of either silver, copper, tin or aluminum were protective for 5-10 hours at both temperatures. Tungsten and vanadium, in combination with chromium and silicon, also formed a slurry that provided short-time protection. However, on cycling to room temperature, differences between the thermal expansion properties of the coating and the substrate appeared to have resulted in exfoliation of the coating and subsequent oxidation failure.

Slurries containing chromium, TiSi_2 and either silver, aluminum or tin showed promise as repair materials. Figure 81 shows the cross-section of a Cr-Ti-Si coated Cb752 alloy coupon through both an unrepaired and repaired edge using a slurry composed of 1 part aluminum, 1 part chromium and 1 part TiSi_2 by weight, and annealed at 2350°F for 8 hours in vacuum. The slurry reacted with the Cr-Ti-Si coating to form a continuous layer approximately three times the thickness of the original Cr-Ti-Si coating. This figure shows the repaired area after exposure to air at 2600°F .

The most successful repairs were made using two fused slurry silicide compositions; Si-20Fe-20Cr and Si-20Fe-20Cr-10VSi₂(12). Each of these slurries, in a cellulose nitrate base, was painted over flat-surface (ground holes) and edge defects in coupons. The repaired coupons were then heated at 2600°F for one hour either in air at atmospheric pressure or in argon at a pressure of 100 torr. After heating in air both slurries formed adherent, fused deposits over the defect area. After heating in argon, the specimens were covered with a powdery residue which was easily brushed off, leaving a metallic appearing coating over the defect. The argon treatment was preferred, since the fused silicide flowed more readily in the cleaner environment, and there was little or no build-up from the repair slurry.

Figure 82 shows typical flat surface and edge repairs made with these two slurries after firing at 2600 for 1 hour in argon. The surface of the original Cr-Ti-Si coating has a crazed appearance, while the regions on the surface and edge are relatively smooth. The slurries wet the Cr-Ti-Si coating and prevented crazing in the wetted regions. This crazing was not detrimental to the oxidation resistance.

Figure 83 shows a section through an edge repaired with the Si-20Fe-20Cr-10VSi₂ slurry, and further illustrates the compatibility between the repair slurry and the original coatings. At the defected edge, the original Cr-Ti-Si coating had been completely removed, and



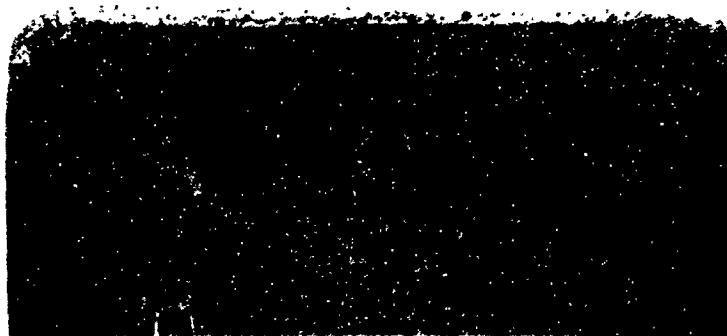
Unrepaired 100X



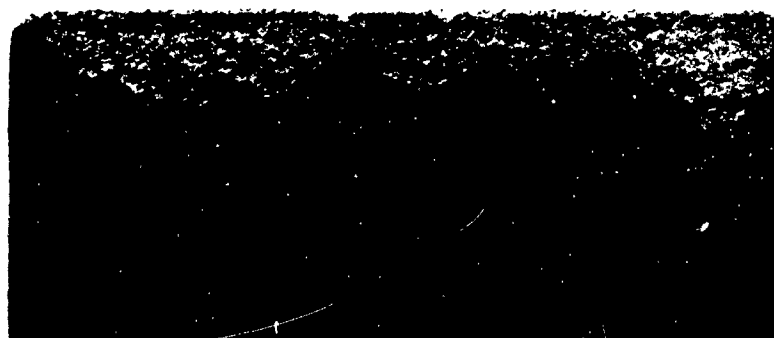
Repaired - 1 Hour @ 2350°F in Vacuo 100X

Al-33 Cr-33 Ti Si₂ Slurry

Figure 81. Cb-752 Coupon Edges After Air Oxidation for One Hour at 2600°F



Si-20Cr-20Fe-10VSi₂ Slurry



Si-20Cr-20Fe Slurry



Si-20Cr-20Fe-10VSi₂ Slurry

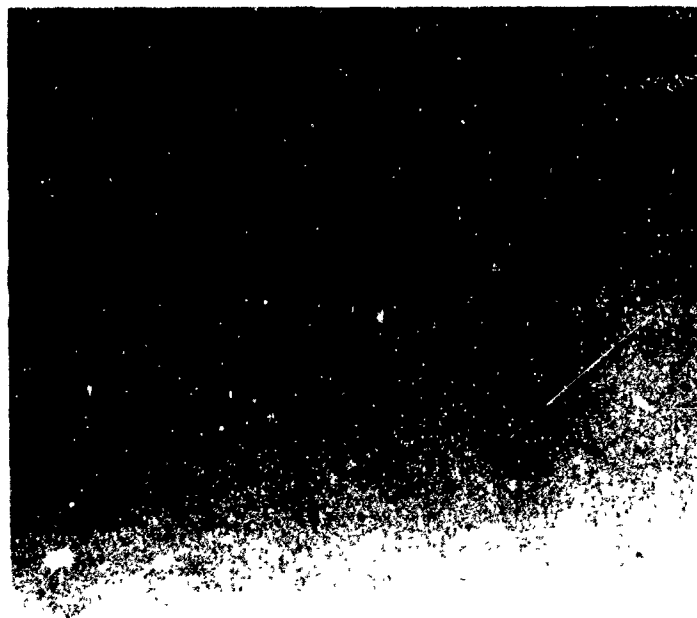


Si-20Cr-20Fe Slurry

Figure 82 Edge and Surface Defect Repairs on Cb752 Alloy Using Fused Slurry Silicides - Argon - 2600°F - 1 Hour. 8X



Unetched 100X



Unetched 250X

Figure 83 Edge Repair on Cb752 Alloy Coupon Made With Fused Si-20Cr-20Fe-10VSi₂ Slurry.

the Cb752 alloy substrate was covered by the repair slurry. The repair slurry coating overlapped the undamaged original coating. It was not possible to determine a zone of demarcation between the two silicide coatings. The arrows on the photographs indicate the boundary of the edge defect. The outer region, which appears to have pulled away from the adherent coating, is a metallic backer which was added before mounting and polishing the specimen for metallographic examination.

Figure 84 shows the external appearance of repaired surface defects after oxidation testing. Each coupon had a defect ground into it near the center, and these defects were repaired with either the Si-20Cr-20Fe or Si-20Cr-20Fe-10VSi₂ slurries fired in argon before oxidation testing. The good compatibility between the original coating and the repair coating is retained after oxidation testing at 1800 and 2600°F. Figures 85 and 86 show sections through these repaired defect areas after testing at 1800 and 2600°F. These photomicrographs were taken of regions near the edge of the defect, and show a gradual thickening of the coating as the periphery of the defect region is approached. The good compatibility between the repair slurry and the original coating was retained throughout the oxidation test.

Table 26 summarizes the results of cyclic oxidation testing at 1800 and 2600°F. At 1800°F both air fired and argon-fired slurries appeared to provide long time protection at defects ground in the flat surface of the coupons. At 2600°F air-fired slurries provided adequate protection at flat surface defects. However, when applied to defects formed by grinding away the original Cr-Ti-Si coating along an edge of the coupons, the air fired slurries were not protective. After one-hour exposure the edge repairs spalled violently. On the other hand, the argon-fired slurries were protective when applied to both flat surface and edge defects. The better degree of protection provided by the argon-fired slurries, and the observation that there is an excessive build-up of slurry at the air-fired repair region, indicate that the use of argon-fired slurries is preferred for both types of repairs. Slurry build-up on the air-fired specimens suggests incomplete fusion and wetting as a result of minor oxidation. It is extremely encouraging, however, that the repairs applied in air provide reliable short term protection, thus providing an excellent means of field repairing coating defects. Both slurry compositions provided essentially equivalent repairs.

7.2.2 Repairs of Defects in Oxidized Coatings

When subjected to air oxidation, the Cr-Ti-Si coating on parts or test coupons may fail in one of three ways: (1) general, uniform



Si-20Cr-20Fe-10VSi₂
44 Hour Exposure

Si-20Cr-20Fe
44 Hour Exposure

Oxidation Tested at 2600°F

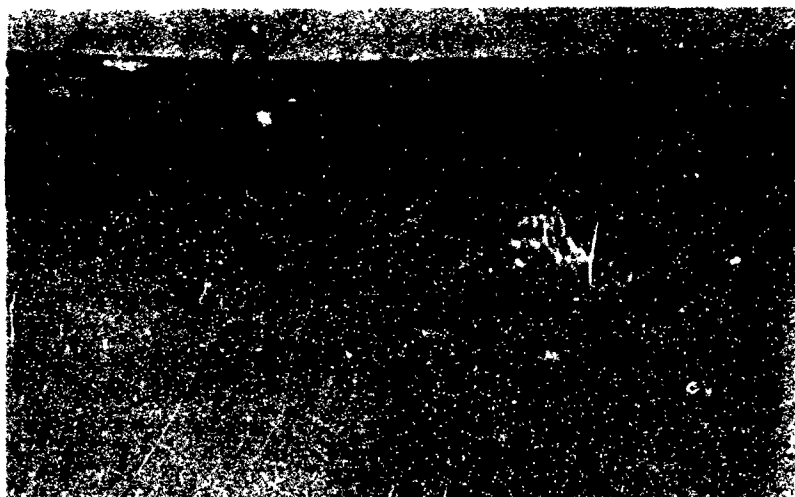


Si-20Cr-20Fe-10VSi₂
377 Hour Exposure

Si-20Cr-20Fe
794 Hour Exposure

Oxidation Tested at 1800°F

Figure 84 Repaired Surface Defects on Cr-Ti-Si Coated
Cb752 Alloy - After Oxidation Testing. 3X



Coupon 28
Si-20Cr-20Fe-10VSi₂
377 Hour Air Exposure

Backer and Foil

Slurry and Original
Cr-Ti-Si
Original Cr-Ti-Si
Coating

Substrate



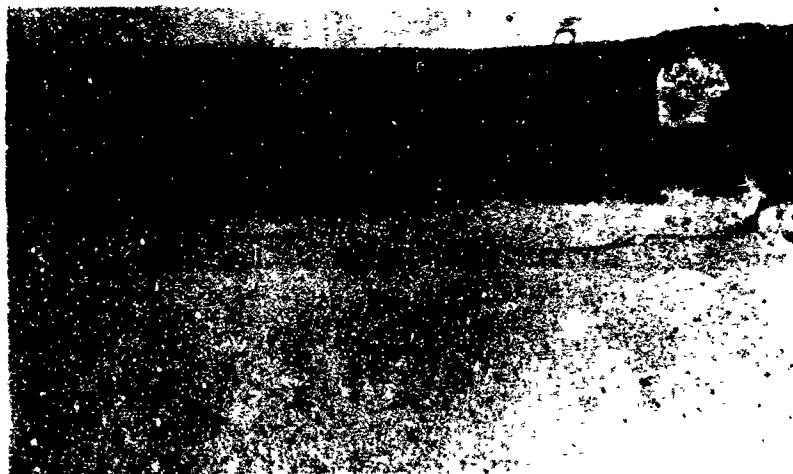
Coupon 11
Si-20Cr-20Fe
794 Hour Air Exposure

Backer and Foil

Slurry and Original
Cr-Ti-Si
Original Cr-Ti-Si
Coating

Substrate

Figure 85 Repaired Surface Defects in Cr-Ti-Si Coated Cb752
Alloy - After Oxidation Testing at 1800°F.
Unetched 250X



Coupon 34
 Si-20Cr-20Fe-10VSi₂
 44 Hour Air Exposure

Backer and Foil

Slurry and Original
 Cr-Ti-Si

Original Cr-Ti-Si
 Coating

Substrate



Coupon 20
 Si-20Cr-20Fe
 44 Hour Air Exposure

Backer and Foil

Slurry and Original
 Cr-Ti-Si

Original Cr-Ti-Si
 Coating

Substrate

Figure 86 Repaired Surface Defects in Cr-Ti-Si Coated Cb752
 Alloy - After Oxidation Testing at 2600°F.
 Unetched 250X

TABLE 26

OXIDATION PERFORMANCE OF REPAIRS TO DEFECTS IN
Cr-Ti-Si COATED Cb-752 COUPONS

Slurry Composition	Slurry Application	Oxidation Temp. °F	Hours to Repair		Undefected Control (4)
			Surface Defect	Failure (3) Edge Defect	
Si-20Cr-20Fe	Air (1)	1800	36, >55, >55	not tested	
		2600	50, 50, 50	1, 1, 1, 1, 1	
	Argon (2)	1800	794, 794, 794	not tested	4, 8, 98, 98, 152, 152
		2600	>44, >44, >44, >44	>4, 69, 122, 128, 152	
Si-20Cr-20Fe-10%Si ₂	Air (1)	1800	>22, >102, >102	not tested	
		2600	50, 50, >106	1, 1, 1, 1, 1	
	Argon (2)	1800	>84, >227, >377	not tested	4, 8, 98, 98, 152, 152
		2600	>44, >44, >44, >44	>1, 69, 122, 152, 178	

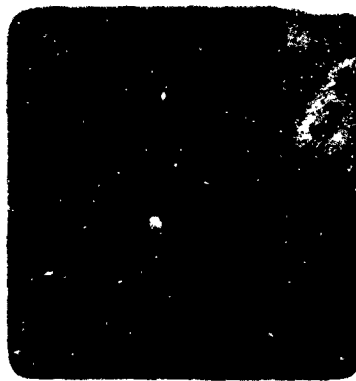
- (1) Coating was applied by heating in air for one hour at 2600°F.
 (2) Coating was applied by heating in 100 torr argon for one hour at 2600°F.
 (3) Times indicate defect failure of individual coupons. When indicated with > failure was at an unrepaired region and coupon was removed from test.
 (4) Failures through 98 hours testing were edge or corner failures; remaining failures were by uniform degradation of the coating or flat surfaces.

degradation of the coating, (2) failure along an edge or at a corner or (3) local failure at a defect on planar surface. For this portion of the coating defect repair work, coupons were selected which showed the latter two types of failure after oxidation exposure at 1800 and 2600°F. These coupons were taken from failures collected during the fractional factorial experiments performed during the slurry-diffusion development work.

Typical defect failures of the type used in this work are shown in Figure 87A and 88A. The area around each defect was cleaned by removing all of the oxidized alloy substrate by grinding with an abrasive wheel followed by abrasive blasting. A portion of the undamaged, oxidized coating surrounding the defect was also removed so as to expose a region of unoxidized coating. This newly exposed coating had a metallic luster similar to the coated coupons before oxidation exposure and had a crazed appearance which was not evident on the oxidized surface. Before applying the repair coating, the defect regions on some of the coupons were etched with $\text{HF-HNO}_3\text{-H}_2\text{SO}_4$ to evaluate whether this improved the compatibility between the oxidized coating and the repair slurry.

The cleaned regions were then coated with either Si-20Fe-20Cr-10VSi₂ or Si-20Fe-20Cr slurry and fired for one hour at 2600°F in an argon atmosphere at a pressure of 150 torr. The appearance of these coupons after firing is shown in Figures 87B and 88B. Heating to 2600°F produced a lightening of the color of the oxidized part of the coupon, probably as a result of partial volatilization of the oxidized coating. The entire coupon now assumed the crazed surface as was previously observed at regions where the surface oxide had been removed. On some coupons, such as A-15, in Figure 88, the repair slurry flowed over the entire coupons.

After coating the defect regions, the coupons were again subjected to the respective oxidation test conditions. Figure 87C and 88C show the appearance of the coupons after various additional exposure times. These coupons did not fail at the repaired areas, but at unrepaired regions where failures may have occurred if the original oxidation test had been continued. With only two exceptions, testing was terminated because the coupon was destroyed as a consequence of failure at an unrepaired region. This is indicated in the summary of oxidation test results given in Table 27, showing the repair lives as being greater than the indicated exposure times. Since unrepaired regions of the coupons rather than the repairs failed, it was not possible to differentiate between the relative effectiveness of the slurry compositions or the treatment to the defect region; neither was it possible to more definitely state the ultimate life of the repair coating. However, this work has demonstrated that it is feasible to repair edge, corner and flat



17 Hours Oxidation
A. Cleaned Defects in Preoxidized Coupons

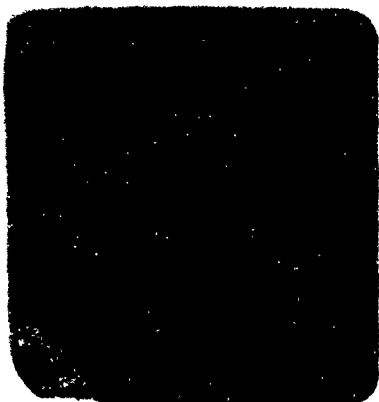


Si-20Cr-20Fe-10VSi₂
B. Slurry Coated Repaired Defects



74 Hours Additional Oxidation
C. After Additional Oxidation Testing of Repair

Figure 87 Repaired and 1800°F Oxidation Tested Defects in
Preoxidized Coupons. 3X



49 Hours Oxidation



33 Hours Oxidation

A. Cleaned Defects in Preoxidized Coupons

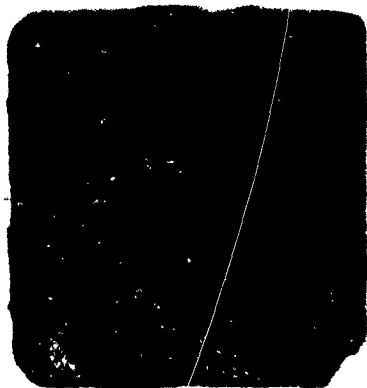
No Photograph



Si-20Cr-20Fe

Si-20Cr-20Fe-10VSi₂

B. Slurry Coated Repaired Defects



C. After Additional Oxidation Testing of Repair.

Figure 83 Repaired and 1800°F Oxidation Tested Defects in Preoxidized Coupons. 3X

TABLE 27

OXIDATION PERFORMANCE OF REPAIRS TO DEFECTS IN PREOXIDIZED
Cr-Ti-Si COATED C6752- COUPONS

Repair Slurry	Coupon No.	Oxidation Temp. °F	Original Coating Weight Gain		Hours Life at Indicated Temperature		
			Cr-Ti	Si Ratio	Original	Repair Life	
Si-20Cr-20Fe	I-42	1800	8.8	18.2	0.48	6	> 24
	I-44		9.6	18.2	0.53	6	> 37
	I-86		9.6	18.2	0.53	12	> 37
	I-22		9.4	18.4	0.51	17	> 12
	K-23		9.5	24.4	0.39	20	4
	A-53	2600	19.9	17.1	1.16	41	> 38
	I-27		9.2	18.4	0.50	63	> 20
	I-84		9.8	17.8	0.55	58	> 30
	A-38		17.2	15.3	1.12	37	> 30
	I-45		9.5	18.8	0.50	49	> 14
Si-20Cr-20Fe-10VSi ₂	K-24	1800	9.2	24.5	0.37	20	> 37
	K-44		9.4	25.0	0.38	17	> 4
	I-67		8.3	17.1	0.48	15	> 4
	I-31		10.3	18.3	0.56	10	> 15
	K-78		12.0	23.9	0.50	10	> 37
	I-25	2600	9.1	18.9	0.49	55	> 16
	I-46		9.1	18.5	0.49	55	> 18
	I-82		9.7	18.4	0.53	49	> 18
	A-15		20.8	13.4	1.55	33	> 38
	I-63		8.1	18.7	0.43	44	> 14

Acid Etched
Acid Etched

Acid Etched
Acid Etched

Acid Etched
Acid Etched

Acid Etched
Acid Etched

surface defects in Cr-Ti-Si coatings by using either of the two fused slurry silicides, and that these repairs provide significant, long-term oxidation protection for columbium at 1800 and 2600°F.

Although in this work, repairs to oxidized and unoxidized coatings were made by heating a small coupon, the techniques should be applicable to forming local repairs on large surfaces. Such repairs could be made either by using large furnaces which could accommodate the entire part, or by local heating using a small portable furnace or torch.

8 TENSILE PROPERTIES OF Cr-Ti-Si COATED Cb752 ALLOY SHEET

The effect of the Cr-Ti-Si coating on the tensile properties of Cb752 alloy was evaluated by coating tensile test specimens in each of the preliminary production proof runs. These tensile test specimens, sketched on Table 28, were cut from the 0.018 inch sheet used in the fabrication of the segmented structures for the preliminary production proof experiments. The rolling direction of the sheet was in the longitudinal direction of the test specimens.

In order to evaluate the effect of coating temperature alone on the sheet, tensile specimens were annealed under a 1×10^{-5} torr vacuum in a Brew vacuum furnace for 10 hours at 2350°F, approximating the conditions used in both the vacuum-pack and slurry-diffusion preliminary proofs. The tensile testing procedure was presented previously in Section 3.

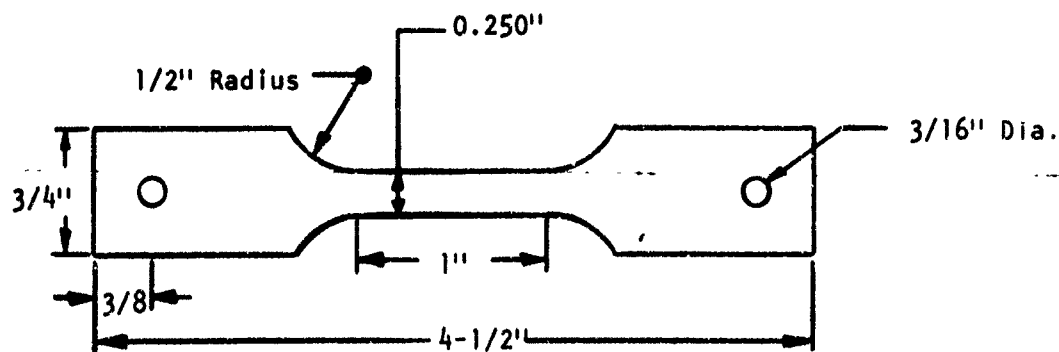
Table 28 presents the results of tensile tests on the uncoated and coated 0.018 inch sheet used in this work. The uncoated sheet was not tested at 2200°F due to equipment problems. The room temperature tensile properties of the uncoated sheet were essentially in agreement with the range of values for several different heats of Cb752 alloy reported by Schmidt and Ogden (13) and summarized in Table 29. As indicated in Table 28, the tensile ductility (percent elongation) of both diffusion-pack and slurry-diffusion Cr-Ti-Si coated Cb752 alloy was markedly less than that of the uncoated alloy. Low room temperature ductility of Cr-Ti-Si coated Cb752 alloy has also been observed by Allen and Bartlett (14) who attributed this to an increased ductile-to-brittle transition temperature caused by the coating or coating process. Since the simulated coating heat treatment did not embrittle the alloy, it is quite apparent that the notch effect produced by the brittle silicide coating was a significant factor contributing to the reduction in ductility.

Although uncoated Cb752 was not tested at 2200°F, comparison between the tensile properties of the alloys in Table 29 and uncoated alloys in Table 28, indicates that at 2200°F in air, the U.T.S. was essentially unaffected by the coating or coating process. The tensile ductility at 2200°F, as measured by percent elongation, was not significantly affected by the presence of the coating or coating process. On the other hand, data presented by Allen and Bartlett (14), comparing the reduction in area of uncoated Cb752 alloy tension tested in vacuum with values obtained from tension testing Cr-Ti-Si coated Cb752 alloy in air, show that the coating or the coating process reduced the ductility. However, the significance of a comparison between these apparently conflicting results is not clear, particularly since the areas used in the work

TABLE 28

**TENSILE PROPERTIES OF AS RECEIVED AND Cr-Ti-SI
COATED 0.018-INCH .C6752 SHEET**

<u>Coated condition</u>	<u>Tensile Test Temperature °F</u>	<u>U.T.S. 1000PSI</u>	<u>0.2% offset Y.S. 1000PSI</u>	<u>% Elong.</u>
As received	Room	83.1	61.9	24.2
		84.8	54.2	27.2
Annealed	Room	79.8	58.4	31.4
		80.2	59.9	29.2
Vacuum-Pack Coated	Room	72.9	61.5	2.2
		70.6	57.9	1.4
Slurry-Diffusion Coated		75.2	64.9	1.6
		74.7	60.1	1.5
Vacuum Pack Coated	2200	27.4	17.2	27.4
		25.5	15.0	20
Slurry Pack Coated		28.0	16.6	14.1
		26.2	16.4	56.3



TENSILE TEST SPECIMEN

TABLE 29

TENSILE PROPERTIES OF Cb752 SHEET (13)

<u>Sheet Thickness</u>	<u>Sheet Condition</u>	<u>Tensile Test Temperature°F</u>	<u>U.T.S. 1000PSI</u>	<u>0.2% Offset Y.S. 1000 PSI</u>	<u>% Elong (1)</u>
0.012	As-received	Room	74-79	57-66	15-23
0.018	As-received		73-80	53-63	25-27
0.030	As-received		80-84	63-70	24-26
0.030	Annealed 1 hr 2300°F		80-84	65-68	22-26
		2200			
0.030	As received		29-36	23-26	22-33
0.030	Annealed 1 hr 2200°F		26-34	17-28	27-42

(1) One inch gage length.

of Allen and Bartlett were calculated using estimated substrate dimensions, including the diffusion zone but excluding Laves or silicide phases; whereas, original substrate areas were used in this work, and a quantitative relationship between elongation and reduction in area has not been established. The cause of the relatively large variation in elongation at 2200°F was not determined.

9 CONCLUSIONS

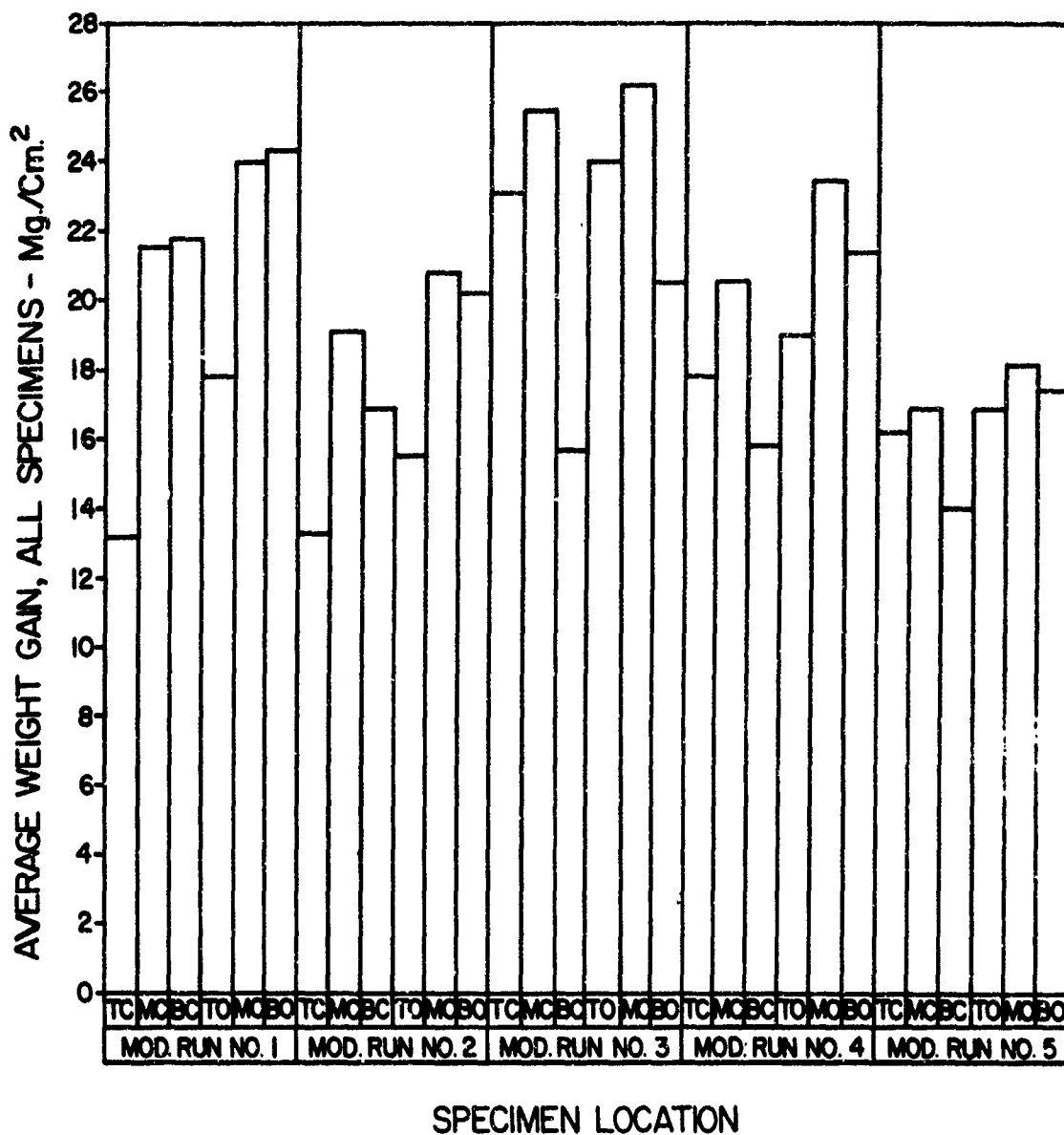
1. The thermal diffusivities of granular 60Cr-40Ti alloy and pure silicon metal packs can be increased by a factor of 3 to 7 by the introduction of a 150 torr helium gas pressure into the evacuated (10^{-2} torr) furnace.
2. Helium is approximately 2 to 3 times as effective as argon in increasing the thermal diffusivity of these granular media.
3. The time lag for temperature equilibrium in the granular pack can be markedly reduced by backfilling the evacuated furnace with an inert gas.
4. A manufacturing-scale vacuum furnace with hearth size 42 inches diameter x 48 inches high was constructed and successfully adapted to application of the Cr-Ti-Si coating to large columbium alloy hardware.
5. Operating parameters for this furnace were developed for producing the Cr-Ti-Si coating on columbium alloys by both the vacuum pack and slurry diffusion processes.
6. Cr-Ti-Si coatings formed by both of these processes, using the production-scale furnace, exhibited 90% reliable oxidation protective lives of at least 125 hours at 1800°F and 50 hours at 2600°F on several columbium alloys.
7. The slurry-diffusion method was considered superior to the vacuum pack for applying the Cr-Ti-Si coating to large scale hardware in the production furnace.
8. Reliably protective Cr-Ti-Si coatings were applied to Cb752 alloy aerospace hardware by the slurry-diffusion process using the production facility. Processing this hardware, a nose cone section 10.5 inches diameter x 12 inches high and two halves of a 16 inch diameter support ring, constituted the Production Proof for the program.
9. The prealloyed Cr-Ti pack media becomes depleted in titanium with continued use, thereby limiting reuse of the material. Scheduled monitoring of the pack composition must be maintained.
10. In the sheet thickness range 0.015 to 0.030 inches, and edge radius range 0.002 to 0.009 inches, no preferential oxidation attack at 1800 and 2600°F was observed on edges or corners of specimens Cr-Ti-Si coated by either the vacuum pack or slurry diffusion methods.

11. Two fused slurry silicides, Si-20Cr-20Fe and Si-20Cr-20Fe-10VSi₂ were equally effective in repairing defects in unoxidized and oxidized Cr-Ti-Si coatings. On unoxidized coatings, repair lives were greater than 794 hours at 1800°F, and 150 to 180 hours at 2600°F. On oxidized coatings the repair lives at both of these temperatures were greater than 38 hours. Firing of the repair coatings can be accomplished in air or argon with the latter producing more reliable coatings.
12. The ultimate strength of 18 mil thick Cb752 alloy at room temperature and 2200°F was not altered by application of the Cr-Ti-Si coating.
13. The room temperature tensile ductility of Cb752 alloy was significantly reduced by the presence of the Cr-Ti-Si coating, while the ductility at 2200°F was unaffected.

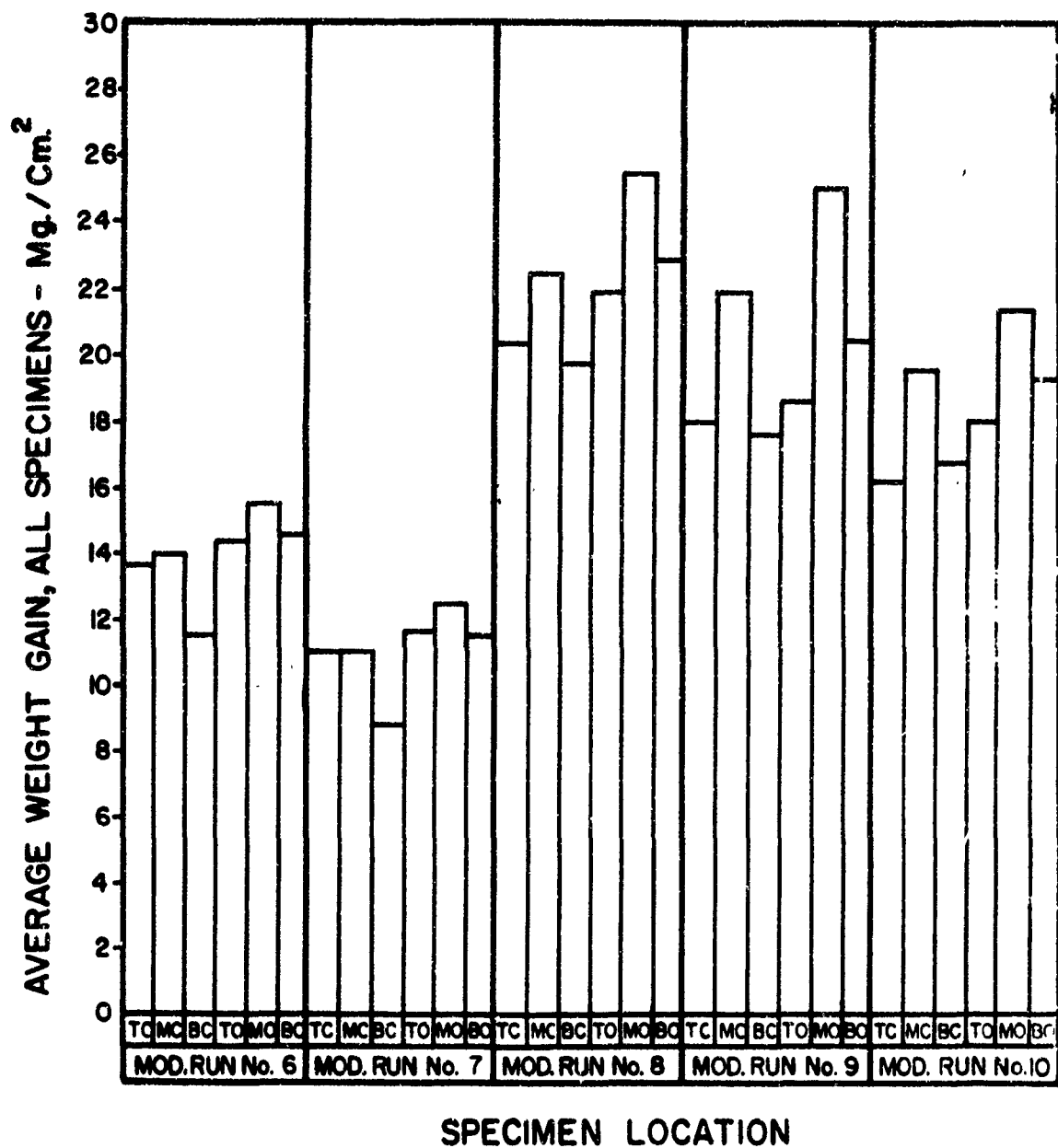
10 BIBLIOGRAPHY

1. "Procedures for Evaluating Coated Refractory Metal Sheet", Division of Engineering and Industrial Research, National Academy of Sciences-National Research Council, Report MAB-201-M, August 3, 1964.
2. J. D. Wurst, "The Evaluation of High Temperature Materials", Report ML-TDR-64-62, AFML,RTD. March, 1964 .
3. Lloyd S. Nelson, "Weibull Probability Paper", Evaluation Engineering, p. 24-25, May/June 1967.
4. J. D. Gadd, " Advancement of Protective Coating Systems for Columbium and Tantalum Alloys", Report AFML-TR-65-203, April 1965.
5. Max Jakob, "Heat Transfer, Vol. 1", p. 130, John Wiley and Sons, New York, 1949.
6. Ibid, p. 265
7. A. S. Bereznoi, "Silicon and Its Binary Systems", p. 187, Consultants Bureau, New York, 1960.
8. Ibid, p. 145
9. Ibid, p. 163-64
10. R. A. Jefferys and J. D. Gadd, "Development and Evaluation of High Temperature Protective Coatings for Columbium Alloys", Report ASD-TR-61-66 Pt 1, May 1961.
11. R. C. Stinebring and R. Cannon, "Development of Nondestructive Methods for Evaluating Diffusion-Formed Coatings on Metallic Substrates", Technical Report AFML-TR-67-178, June 1967.
12. S. Priceman and L. Sama, "Development of Fused Slurry Silicide Coatings for Elevated-Temperature Oxidation Protection of Columbium and Tantalum Alloys", Reports STR 66-5501, 7 March 1966, and STR 66-5501.10 June 1966, prepared under Contract AF 33(615)-3272.
13. F. F. Schmidt and H. R. Udden, "The Engineering Properties of Columbium and Columbium Alloys", DMIC Report 188, September 1963.
14. B. C. Allen and E. S. Bartlett, "Elevated-Temperature Tensile Ductility Minimum in Silicide Coated Cb-10W and Cb-10W-2.5Zr", Trans. ASM 60, 3, 295-304, September 1967.

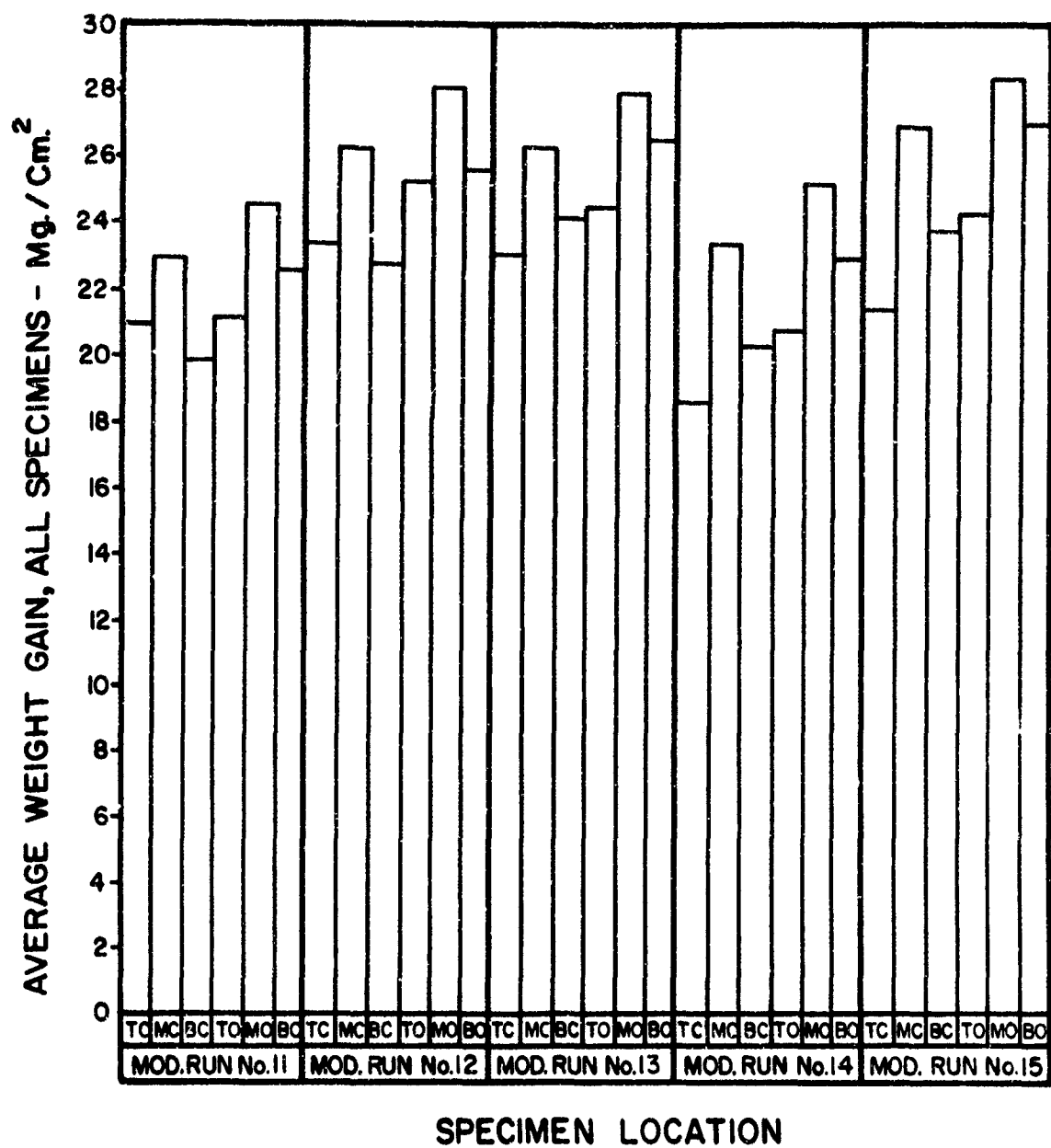
APPENDIX I Cr-Ti AND SILICON WEIGHT GAINS ON COLUMBIUM
ALLOY COUPONS COATED IN MODULE RUNS 1-15 AS A FUNCTION OF PACK POSITION



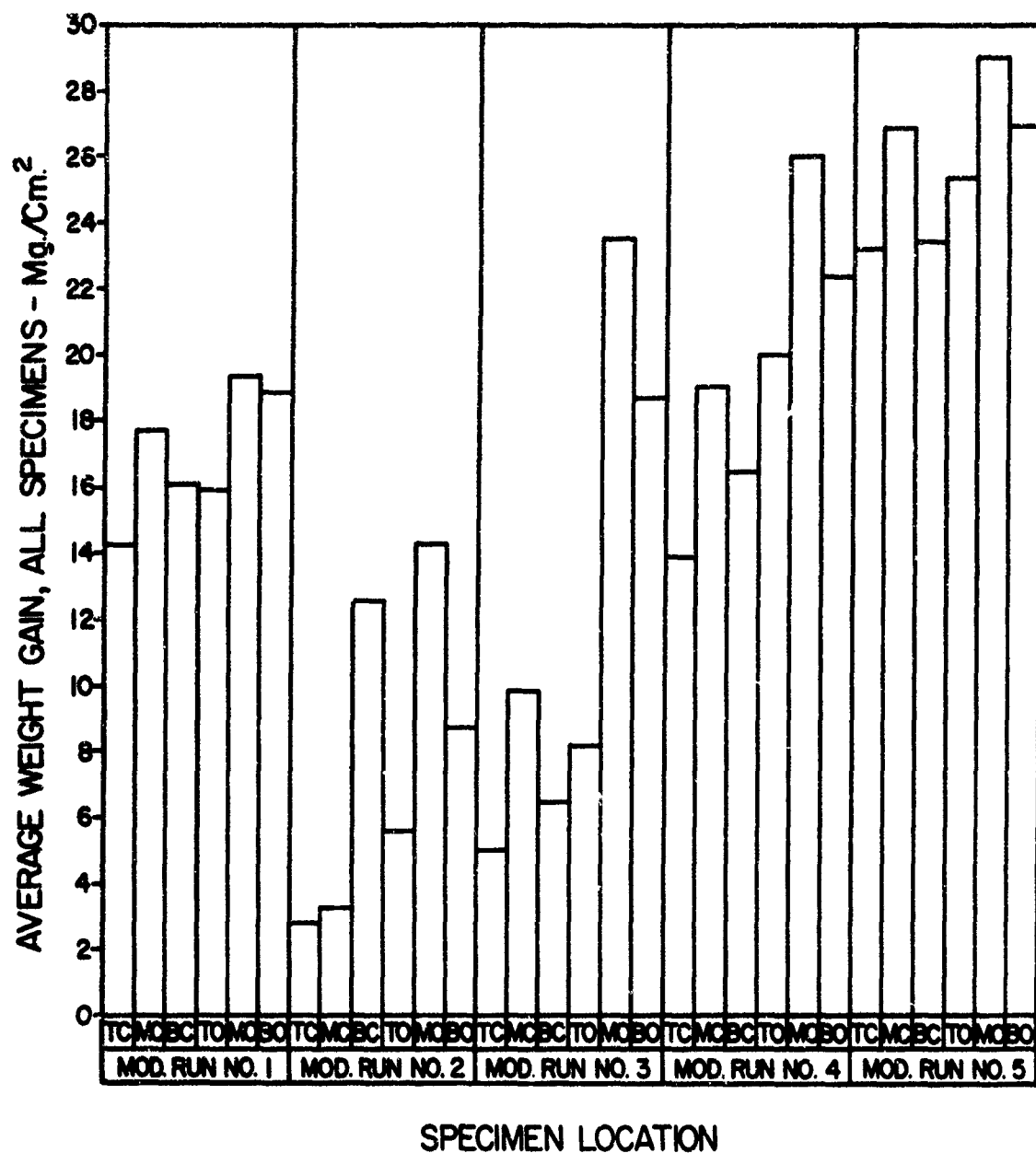
Average Weight Gains Resulting from Cr-Ti Coating Cb Alloy Specimens - Module Runs #1 - #5.



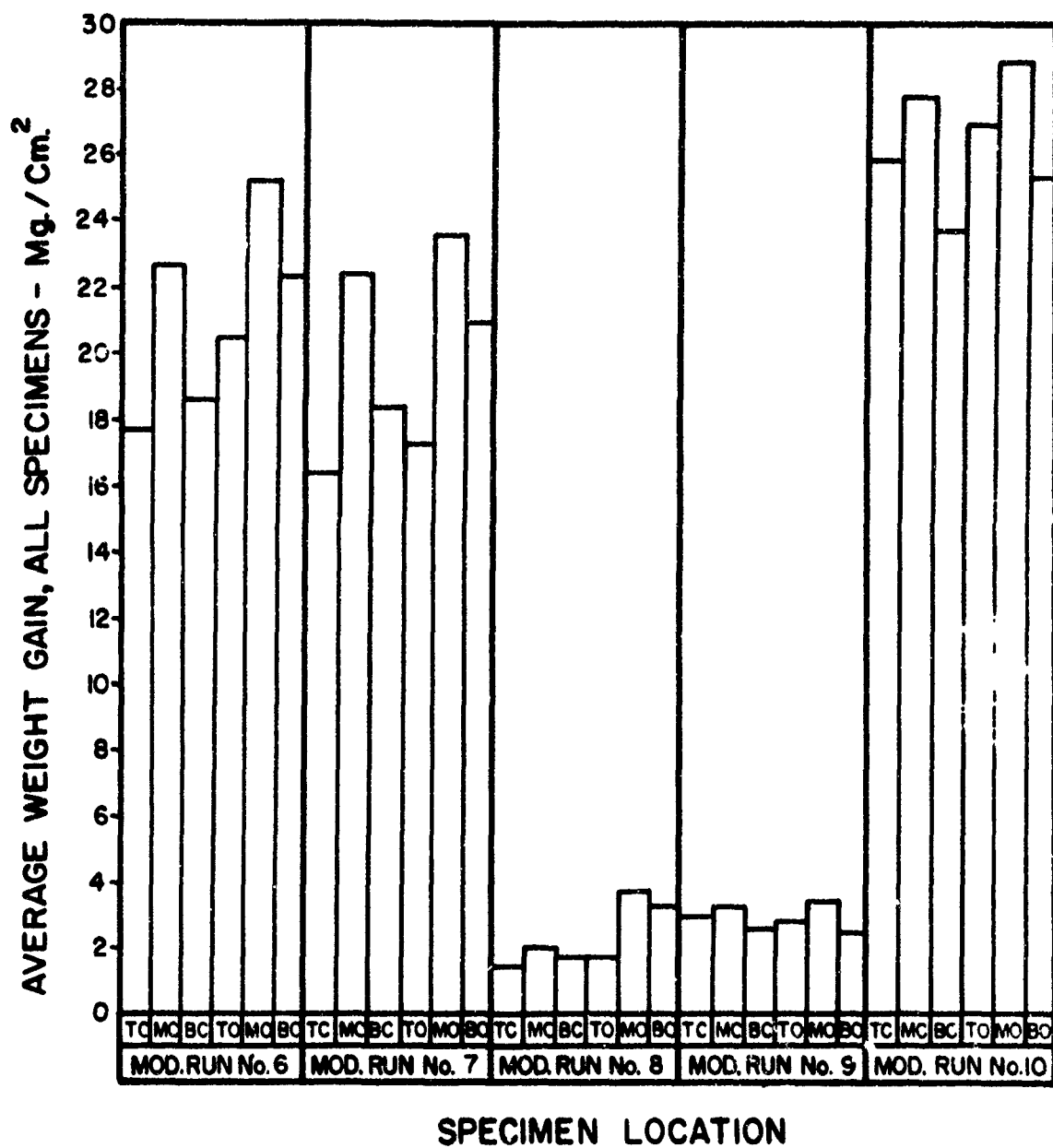
Average Weight Gains Resulting from Cr-Ti Coating Ob Alloy
Specimens - Module Runs #6 - #10.



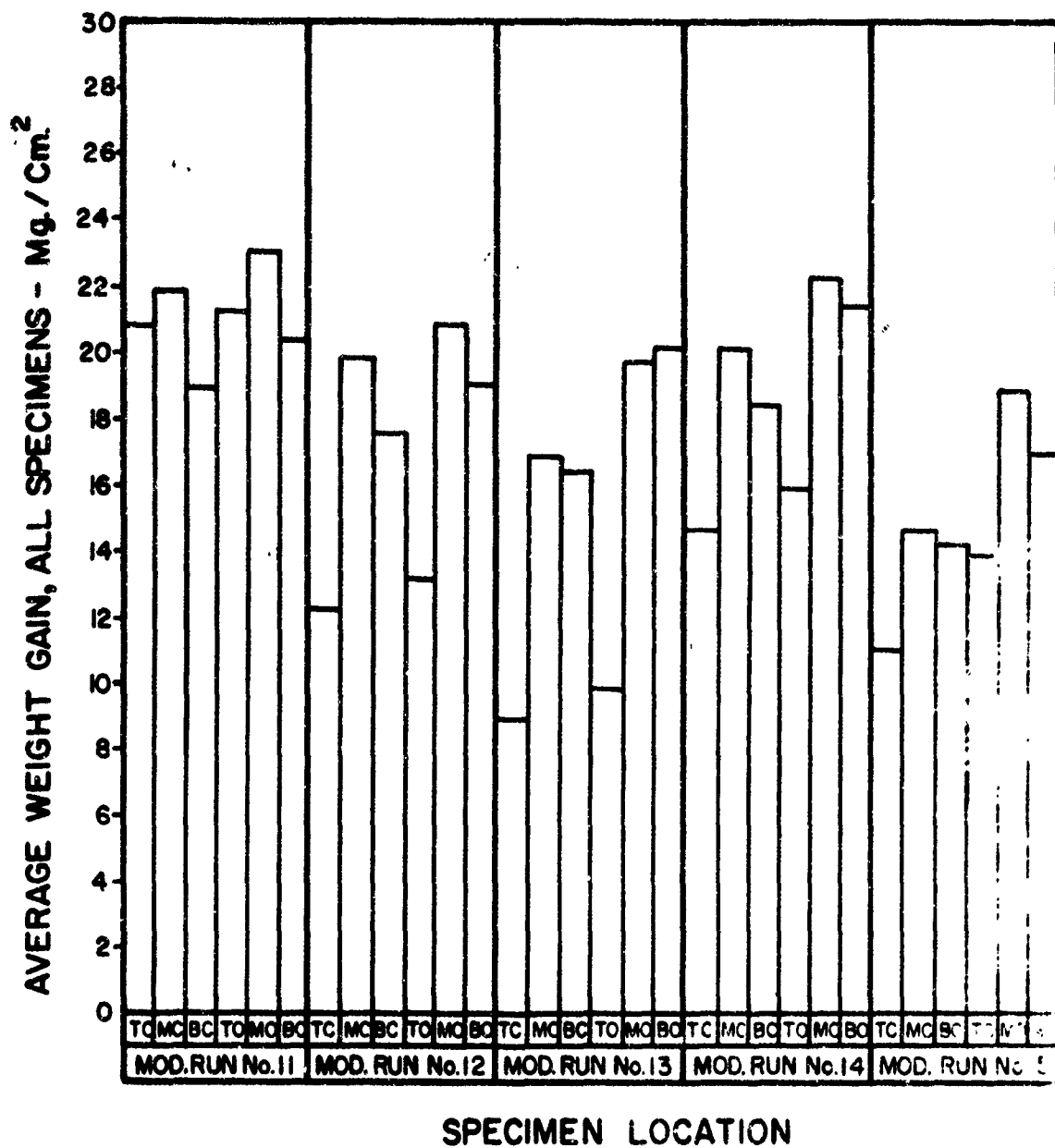
Average Weight Gains Resulting From Cr-Ti Coating Co Alloy
Specimens - Module Runs #11 - #15



Average Weight Gains Resulting from Silicon Coating Cr-Ti Coated Cb Alloy Specimens - Module Runs - #1 - #5.



Average Weight Gains Resulting from Silicon Coating Cr-Ti Coated Cb Alloy Specimens - Module Runs #6 - #10.



Average Weight Gains Resulting From Silicon Coating
Cr-Ti Coated Cb Alloy Specimens - Module Runs #11 - #15

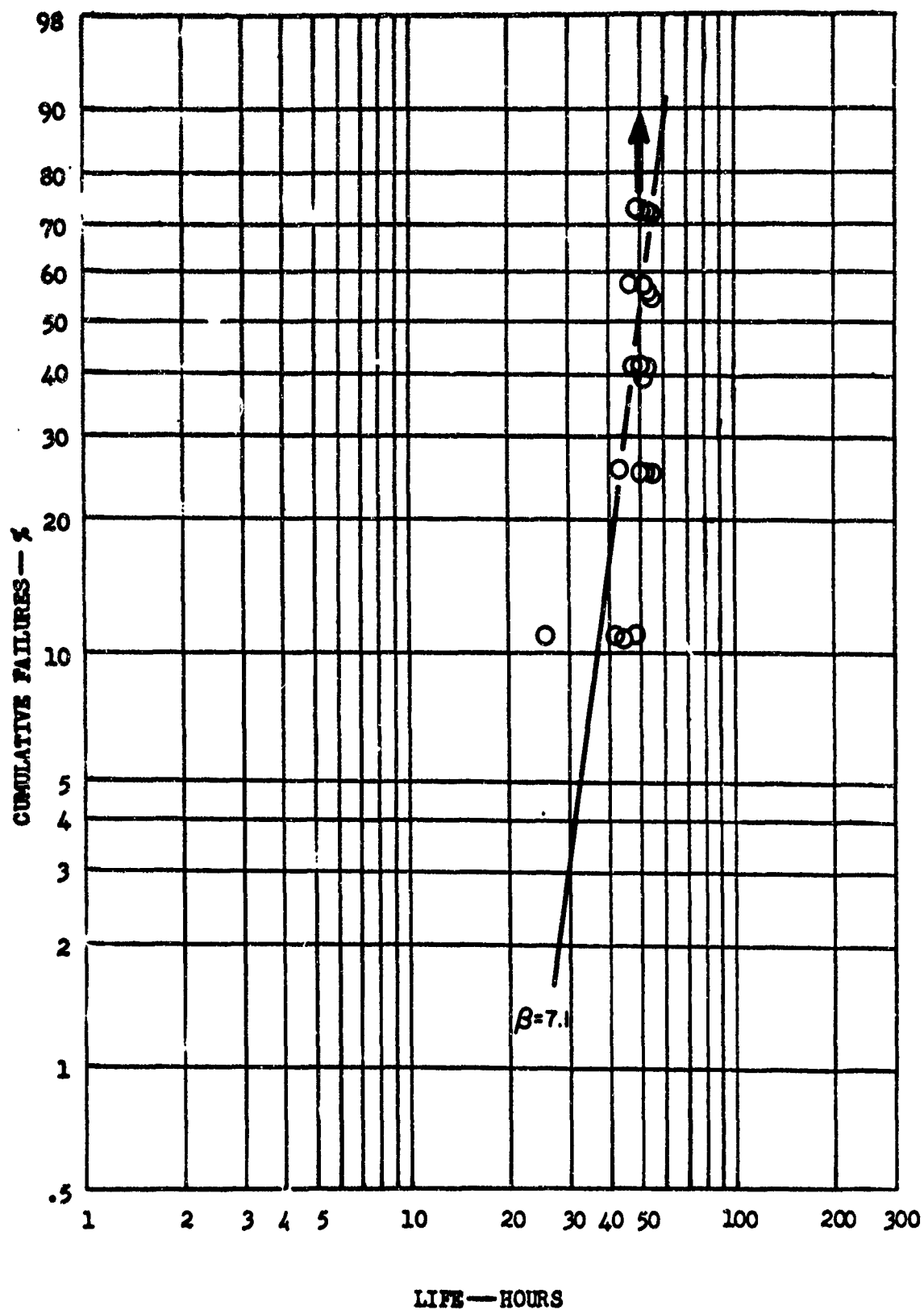
APPENDIX II OXIDATION LIVES OF MODULE VACUUM PACK COATED COUPONS
AS A FUNCTION OF PACK POSITION

Performance data for the following modules was not included because the number of coupons which failed at each temperature was not sufficient to permit a meaningful analysis:

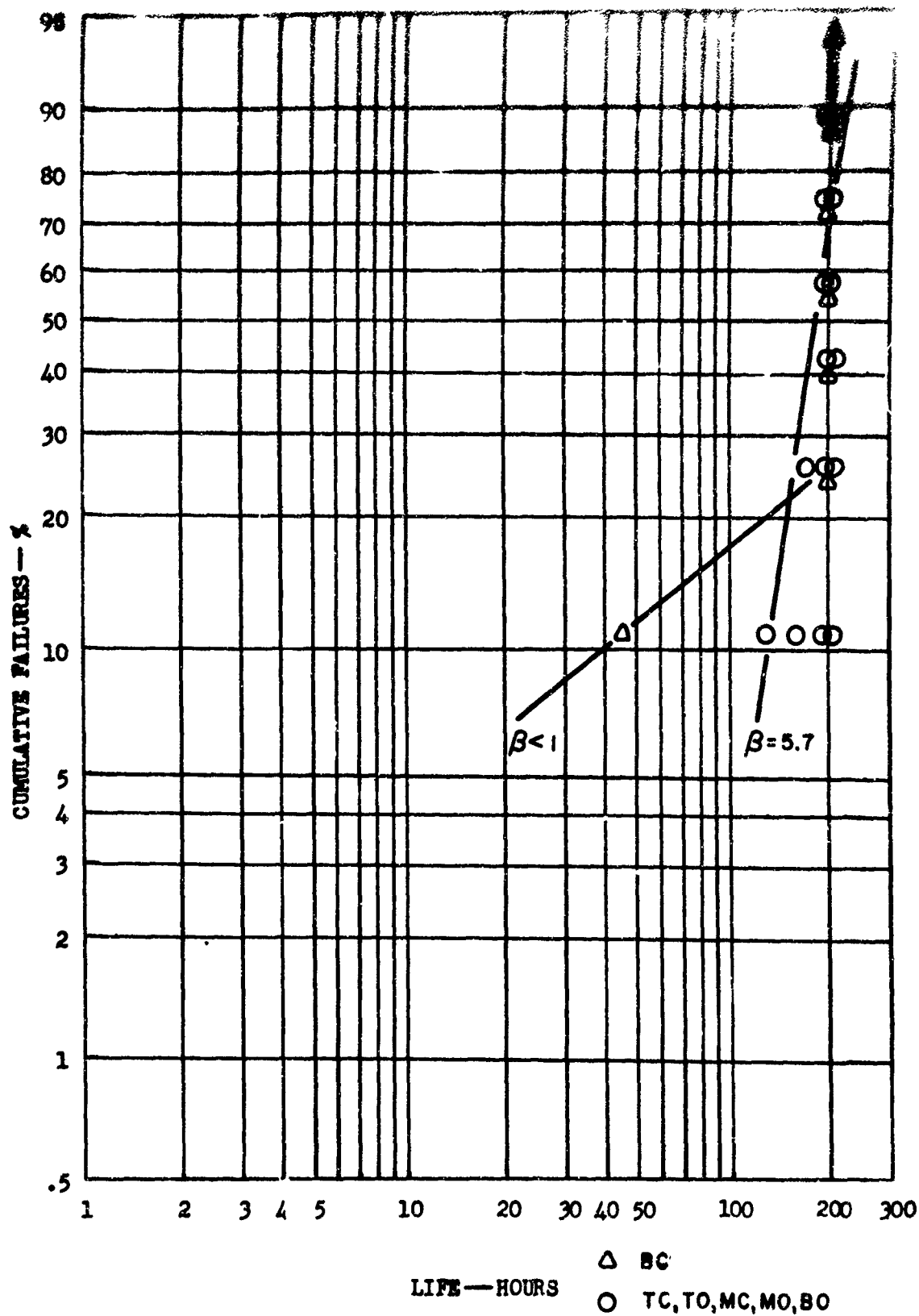
1800°F Modules 1,4,8,9,15

2500°F Modules 4,6,7,8,9,12

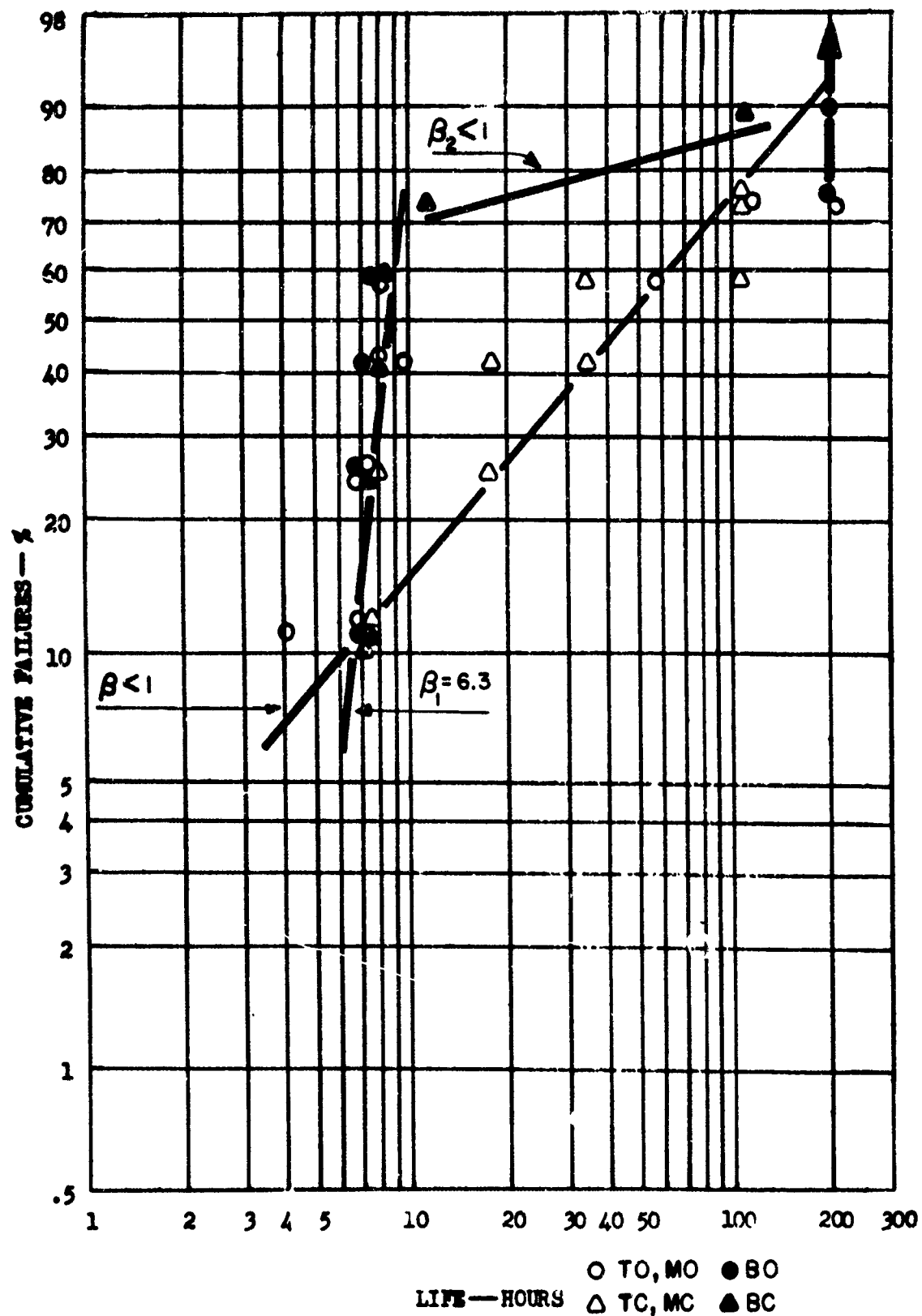
2700°F Modules 2,6,7,8,9



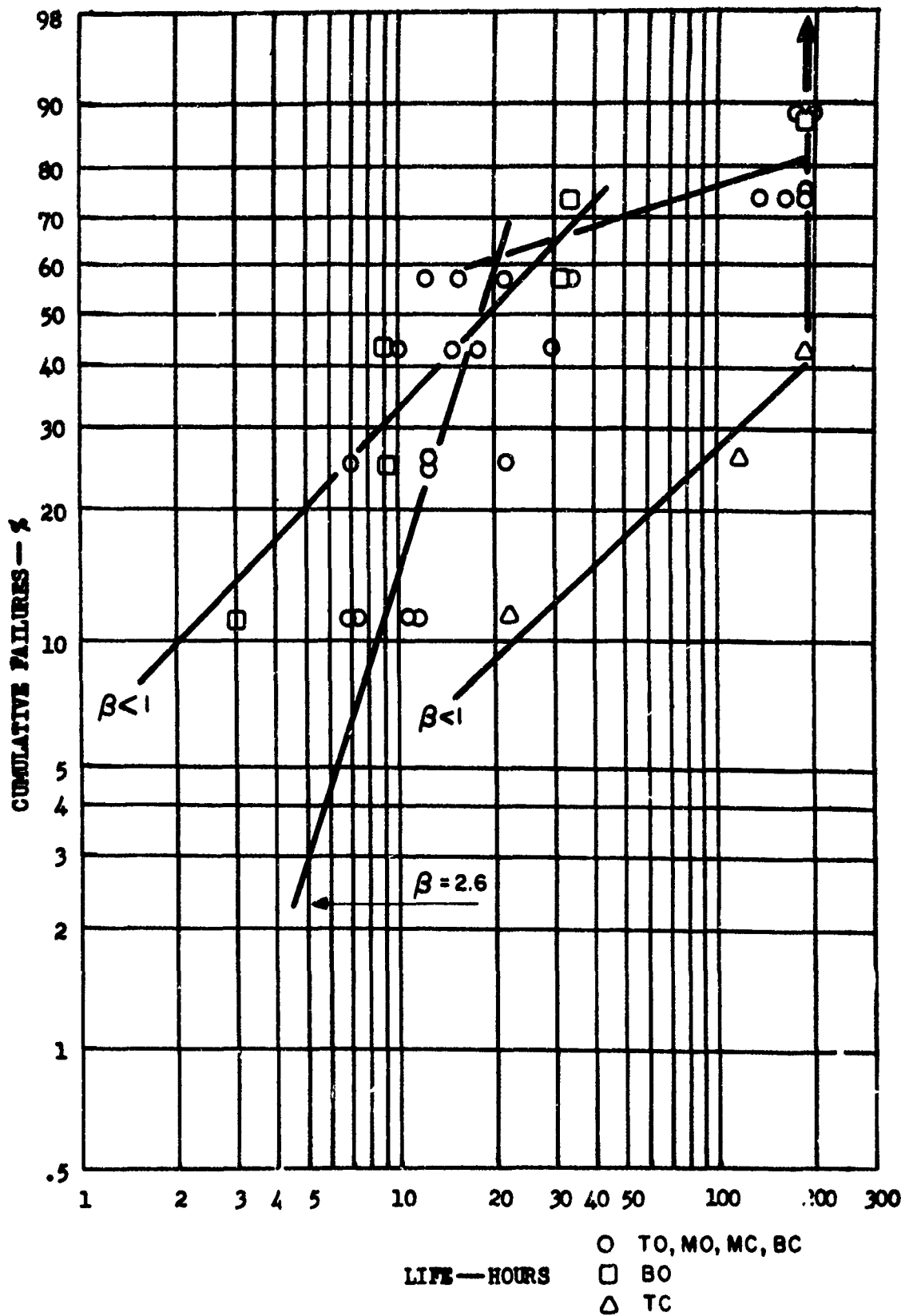
Percent Cumulative Failure vs. Cyclic Oxidation Life at 1800°F
for Specimens Coated in Module Run #2
Pack Position Breakout



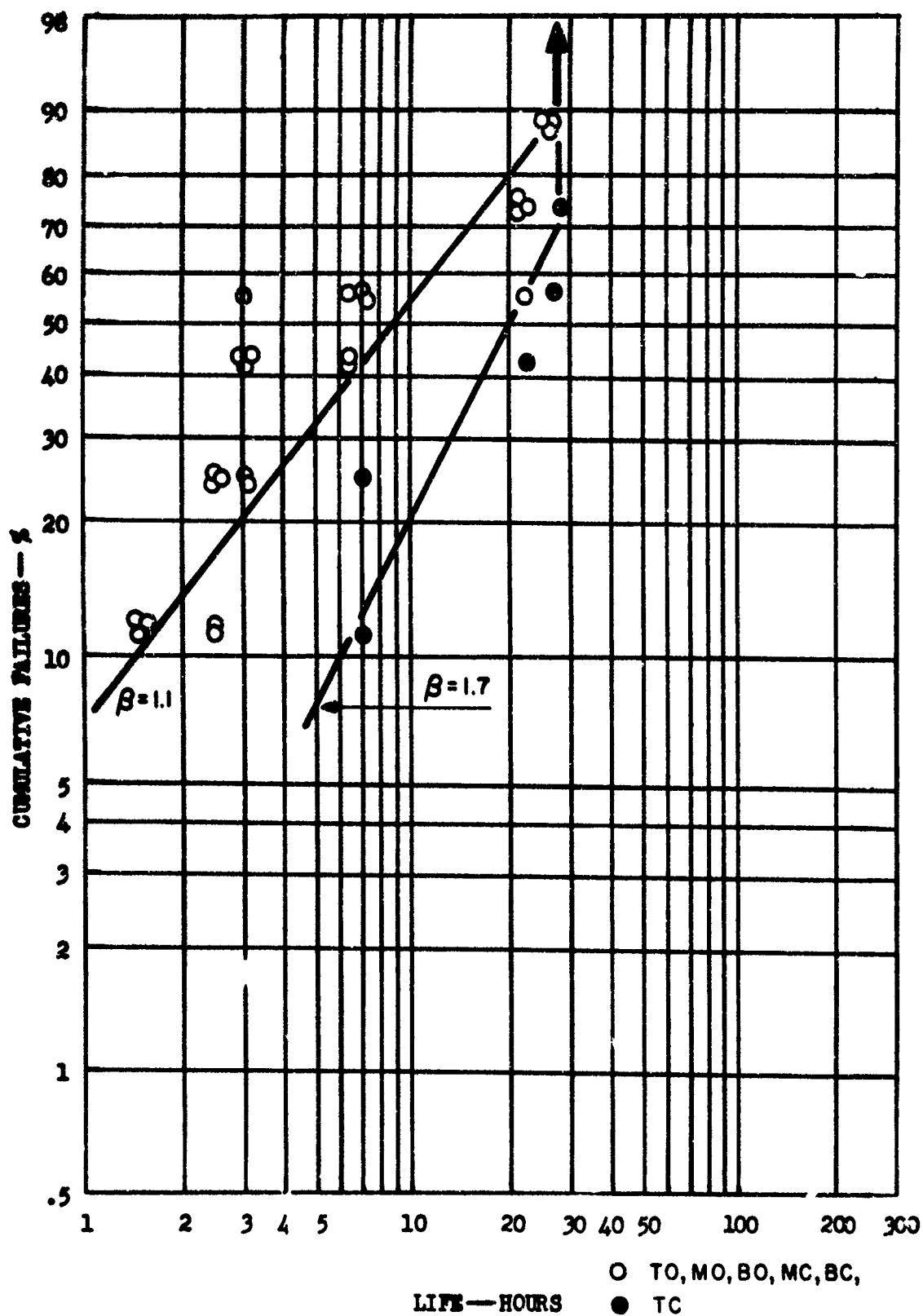
Percent Cumulative Failure vs. Cyclic Oxidation Life at 1800°F
for Specimens Coated in Module Run #3
Pack Position Breakout



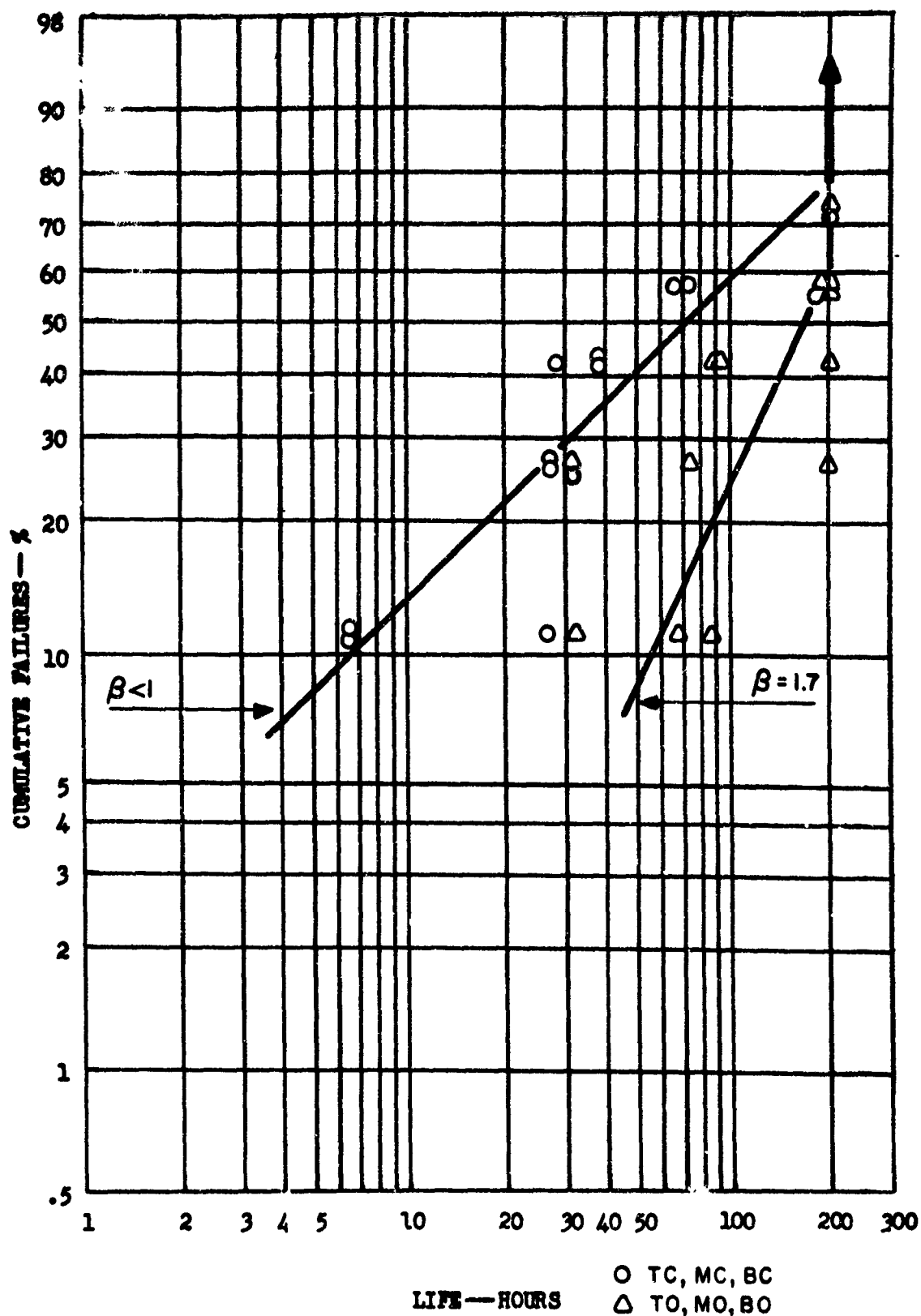
Percent Cumulative Failure Versus Cyclic Oxidation Life at 1800°F for Specimens Coated in Module Run #5, Pack Position Breakout.



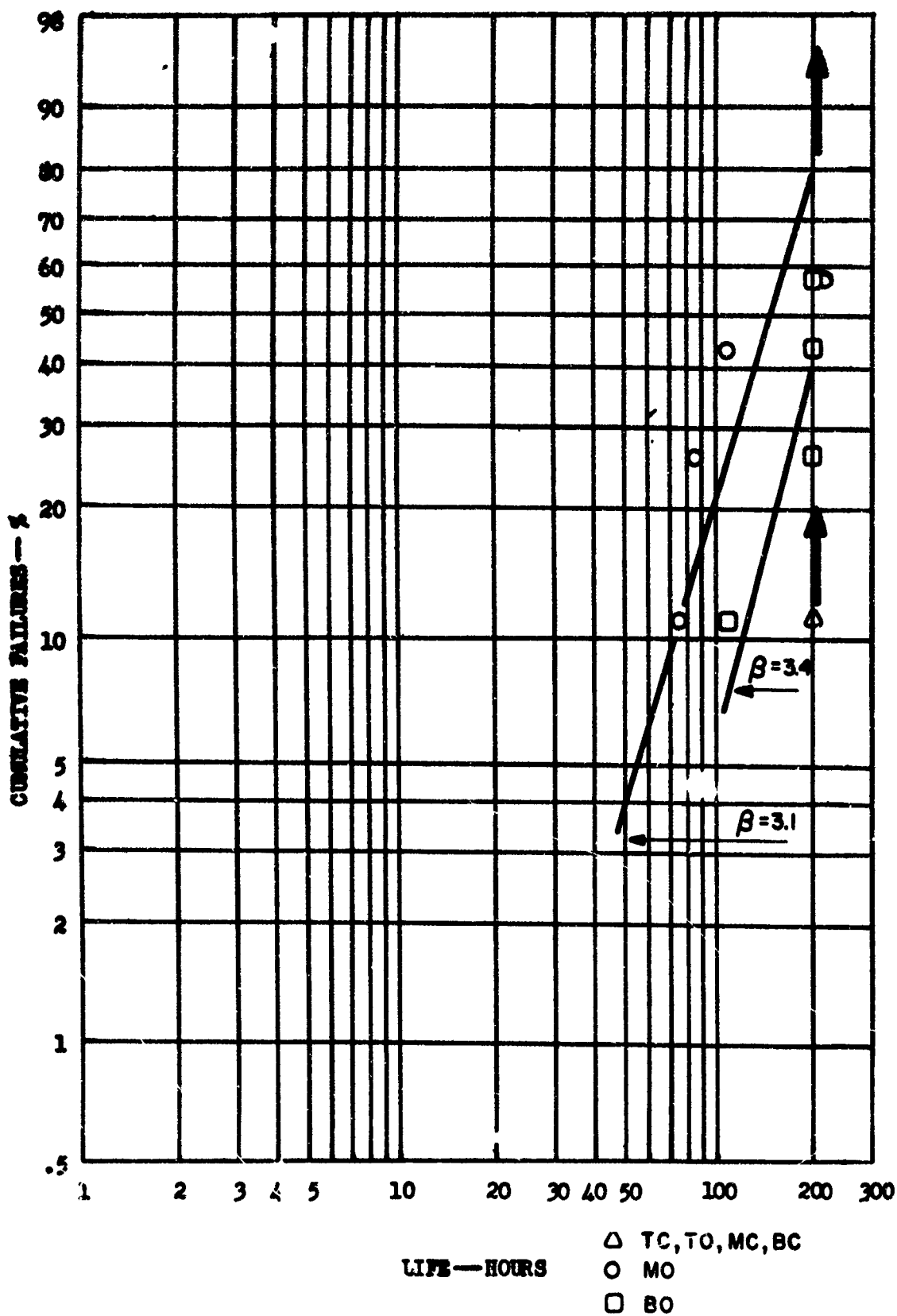
Percent Cumulative Failure Versus Cyclic Oxidation Life at 1800°F for Specimens Coated in Module Run #6, Pack Position Breakout.



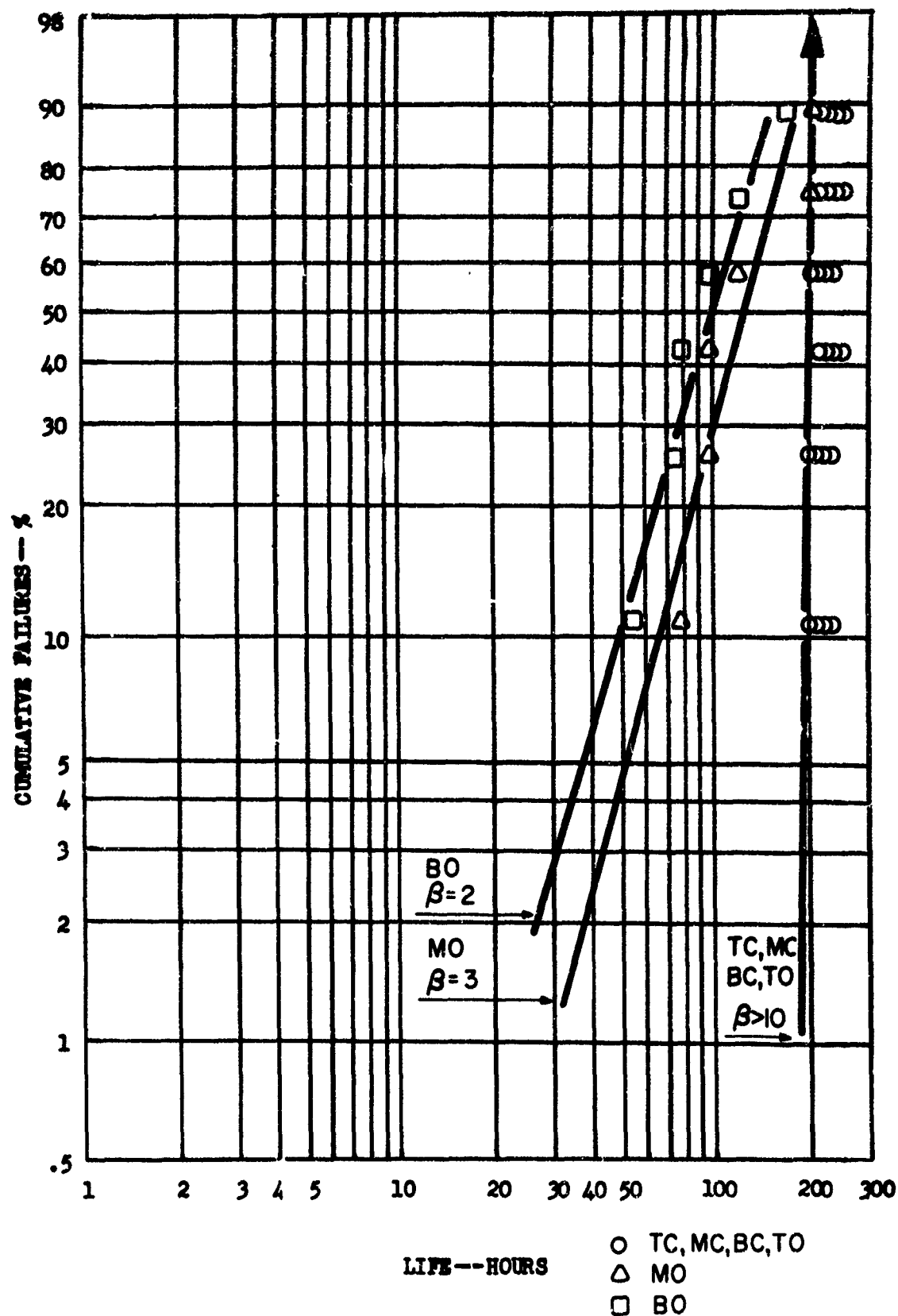
Percent Cumulative Failure Versus Cyclic Oxidation Life at 1800°F for Specimens Coated in Module Run #7, Pack Position Breakout.



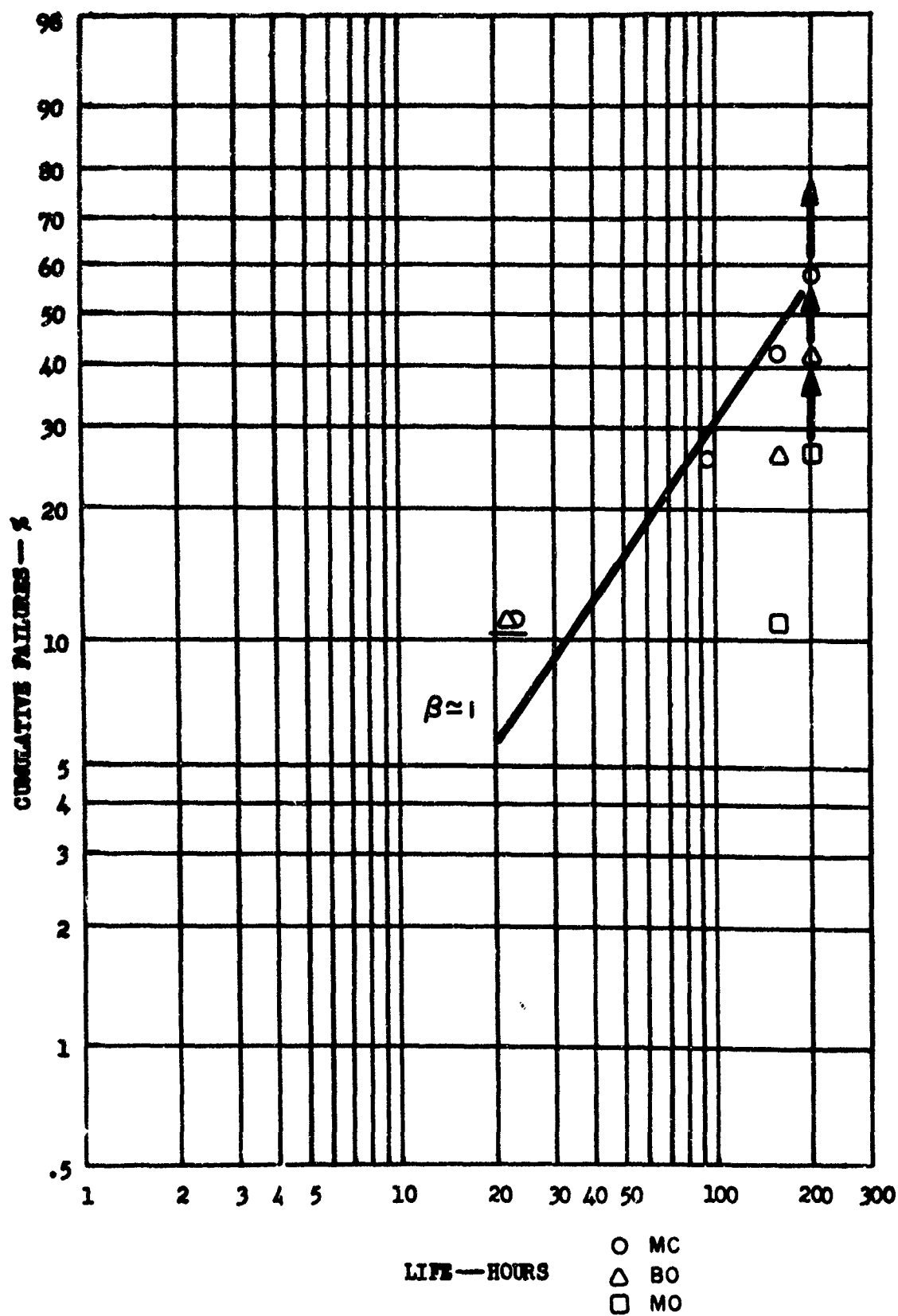
Percent Cumulative Failure Versus Cyclic Oxidation Life at 1800°F for Specimens Coated in Module Run #10, Pack Position Breakout.



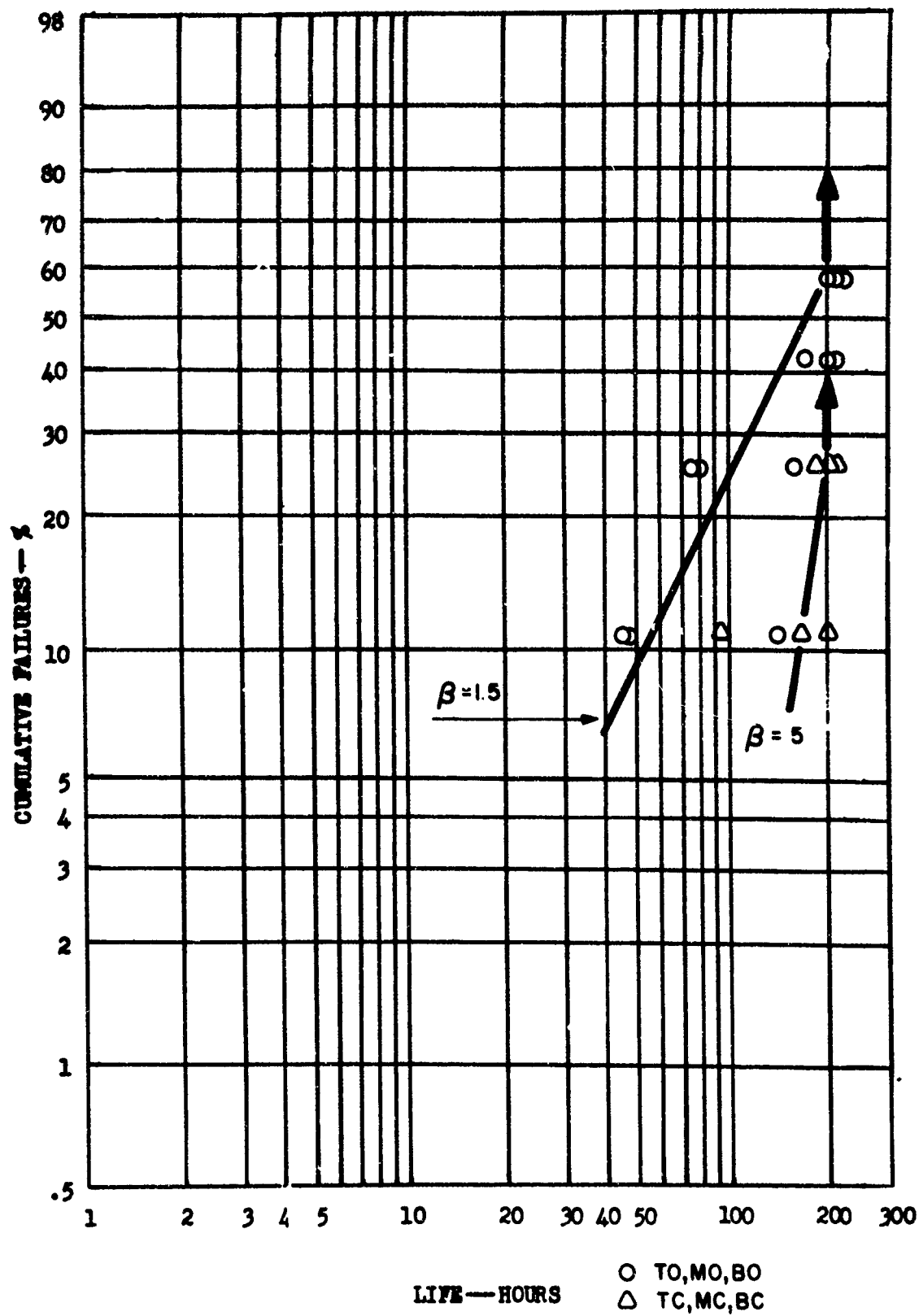
Percent Cumulative Failure Versus Cyclic Oxidation Life at 1800°F for Specimens Coated in Module Run #11, Pack Position Breakout.



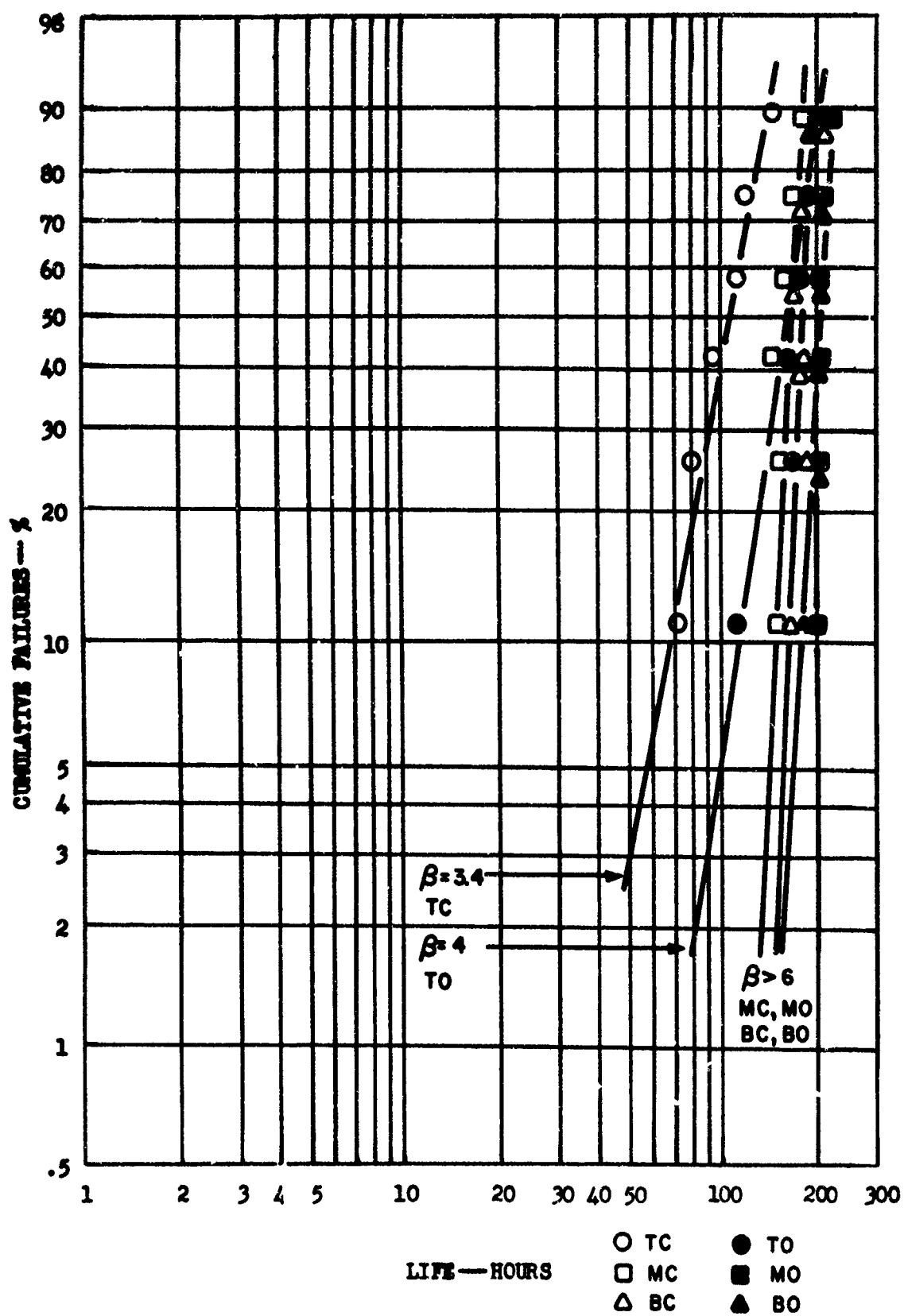
Percent Cumulative Failure vs. Cyclic Oxidation Life
At 1800°F For Specimens Coated In Module Run #12-
Pack Position Breakout



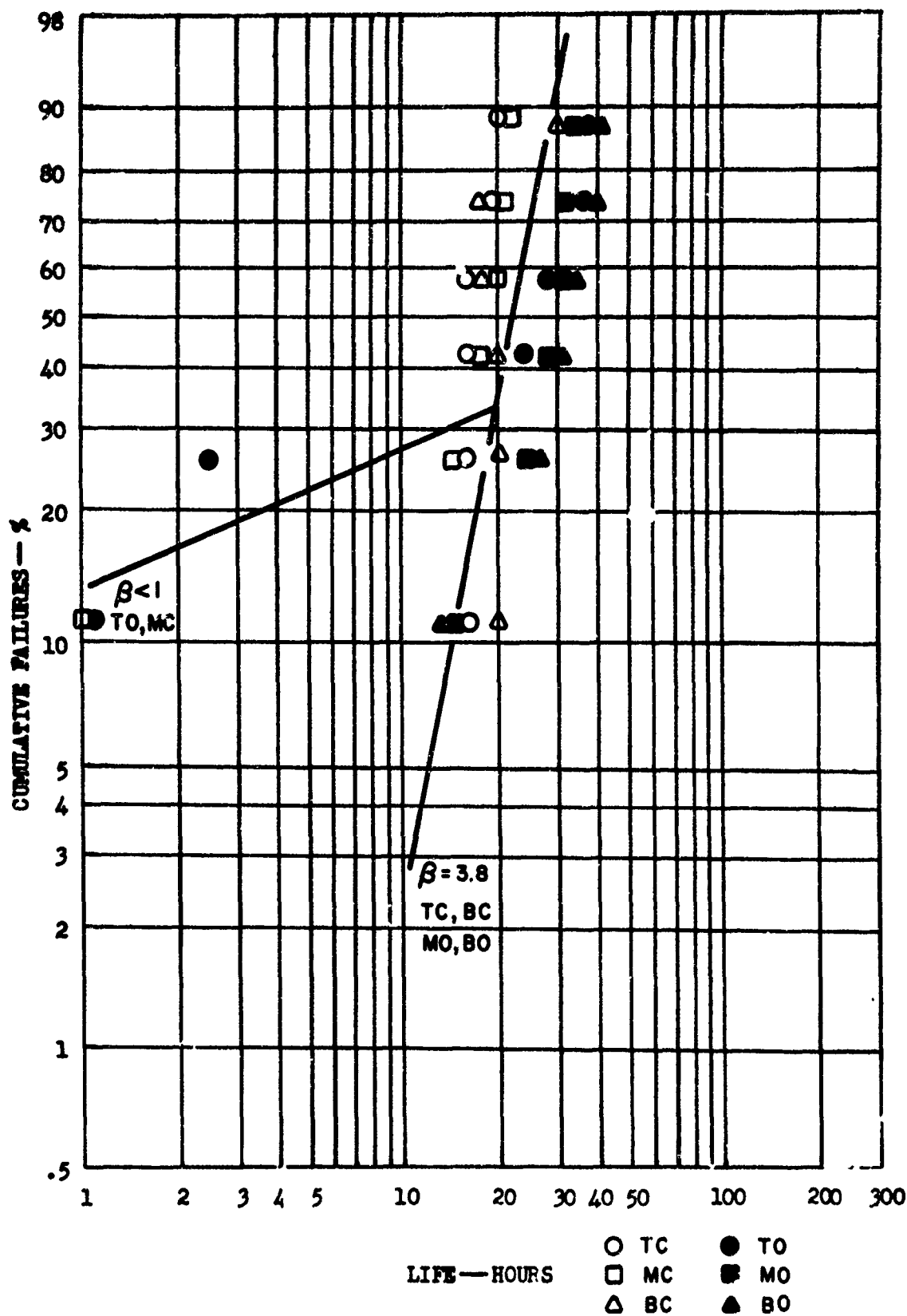
Percent Cumulative Failure vs. Cyclic Oxidation Life
 At 1800°F for Specimens Coated in Module Run #13-
 Pack Position Breakout



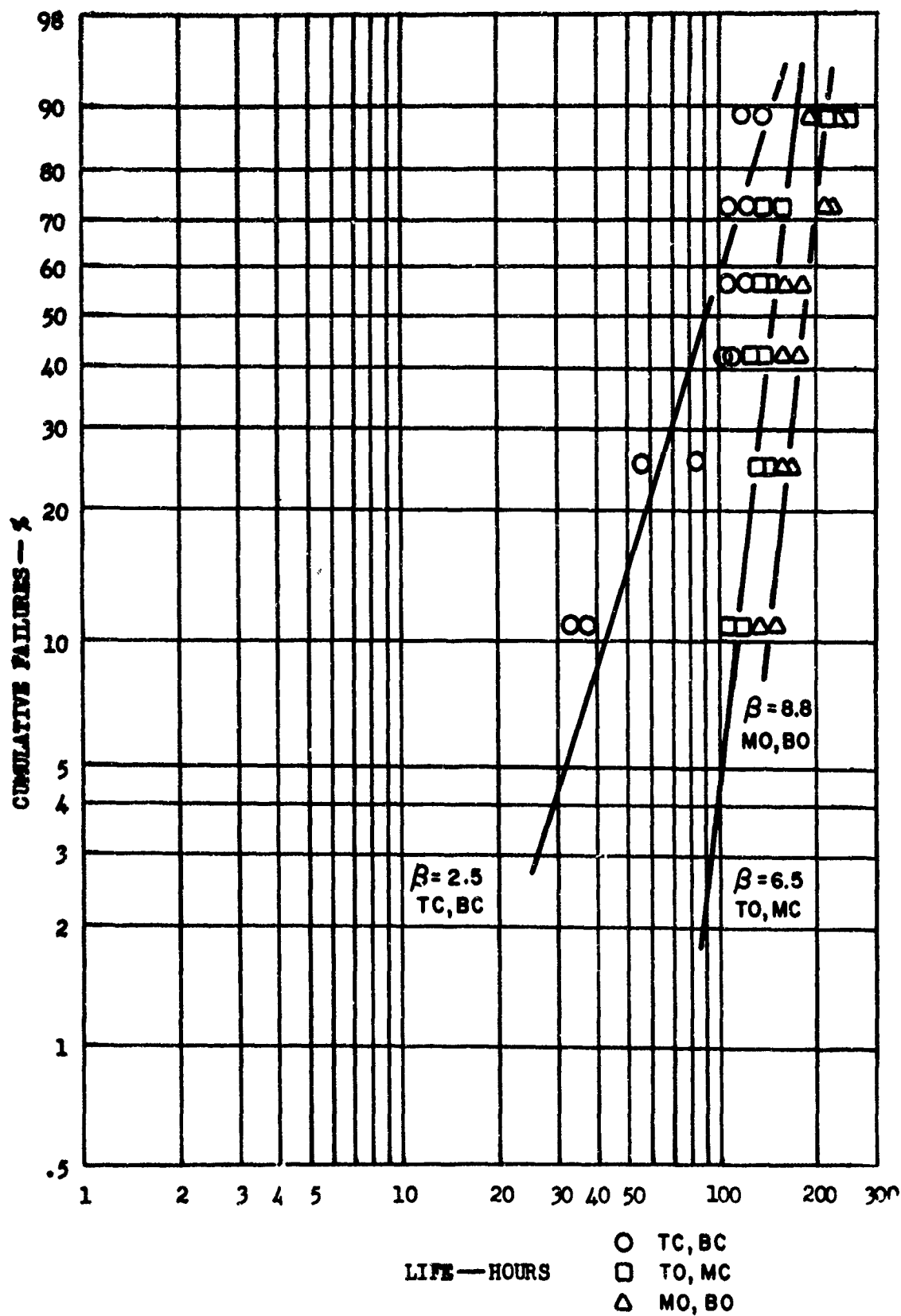
Percent Cumulative Failure vs. Cyclic Oxidation
Life At 1800°F For Samples Coated In Module Run #11
Pack Position Breakout



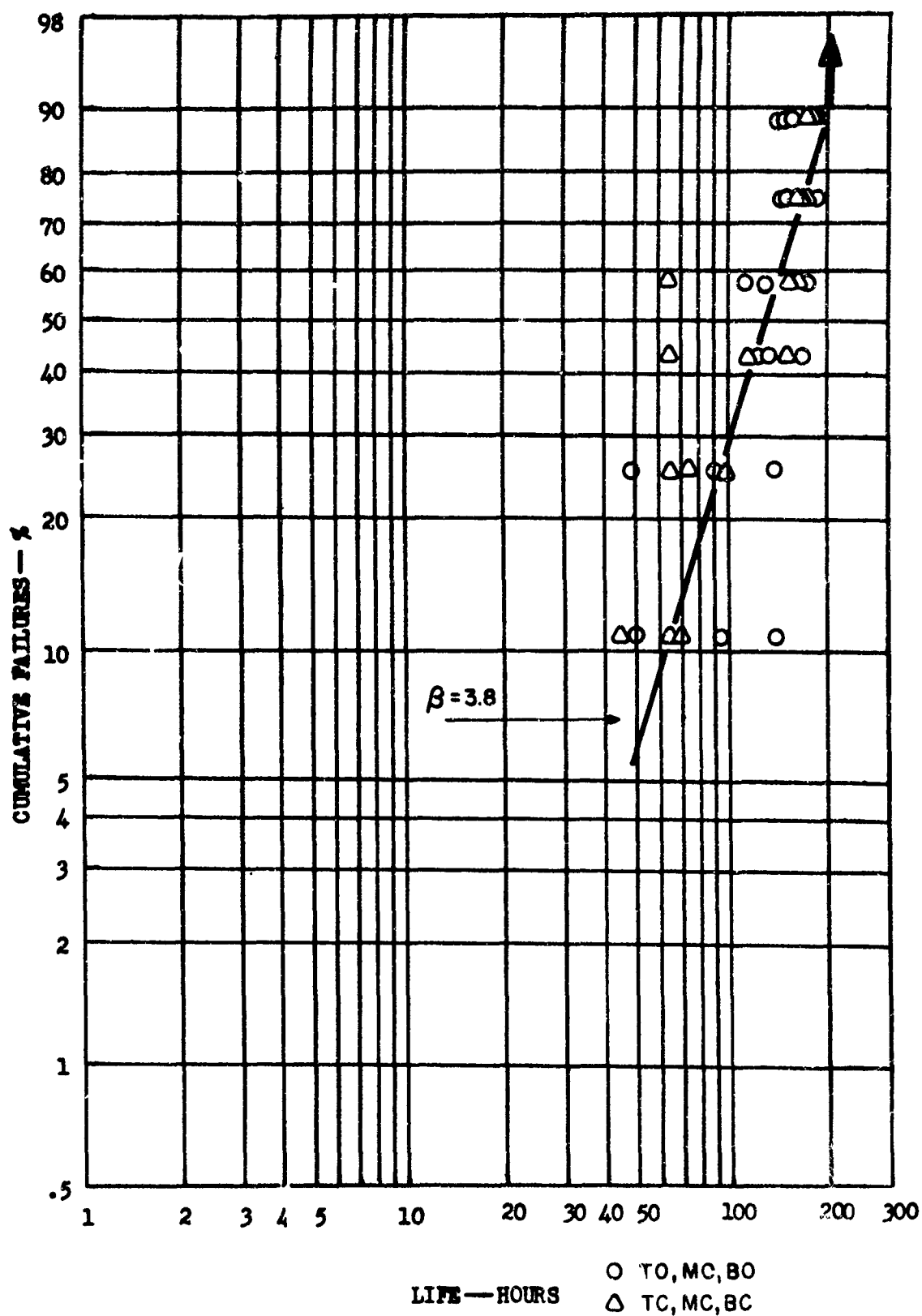
Percent Cumulative Failure vs. Cyclic Oxidation Life at 2500°F
for Specimens Coated in Module Run #1
Pack Position Breakout



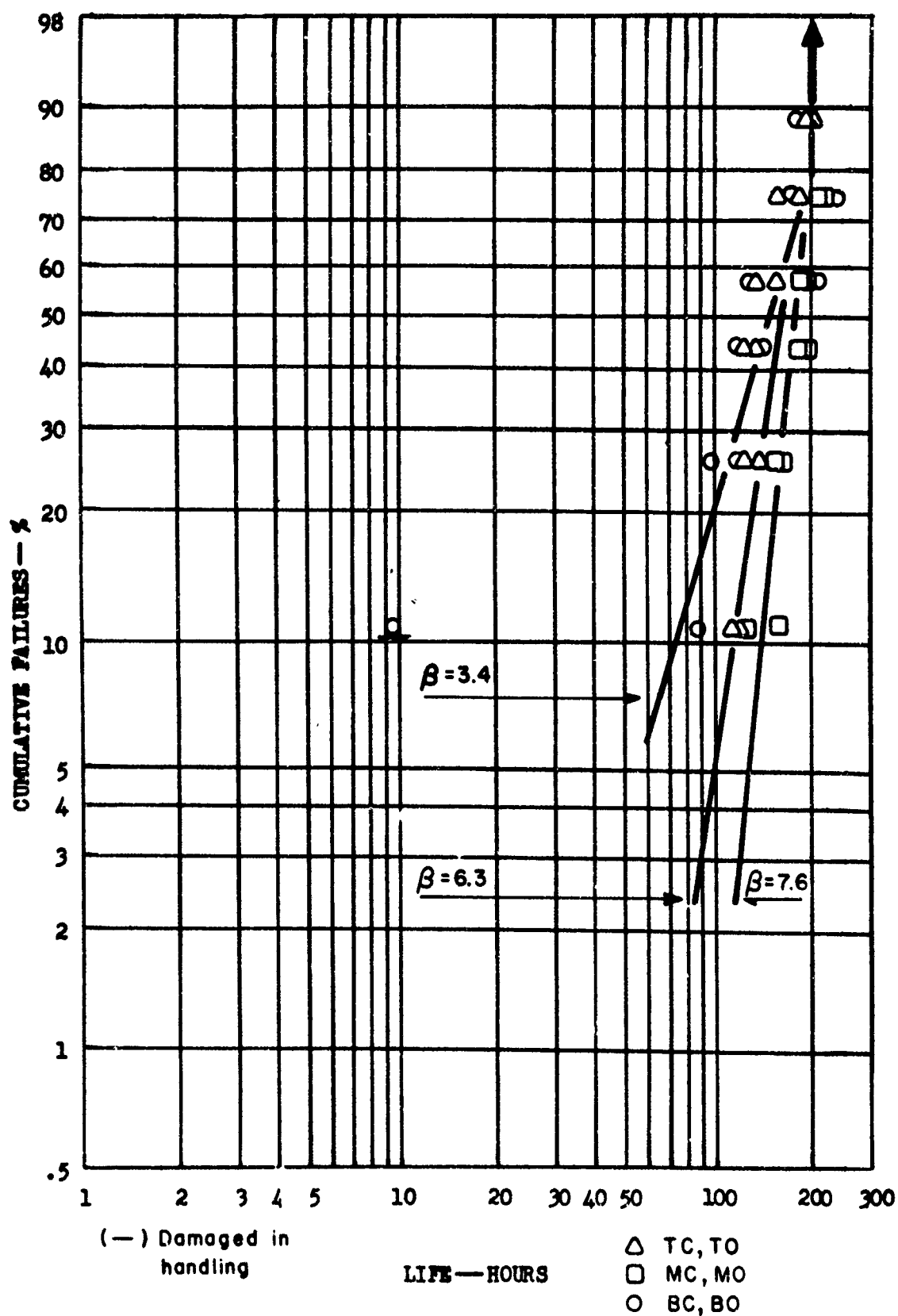
Percent Cumulative Failure vs. Cyclic Oxidation Life at 750°F
for Specimens Coated in Module #2
Pack Position Breakout



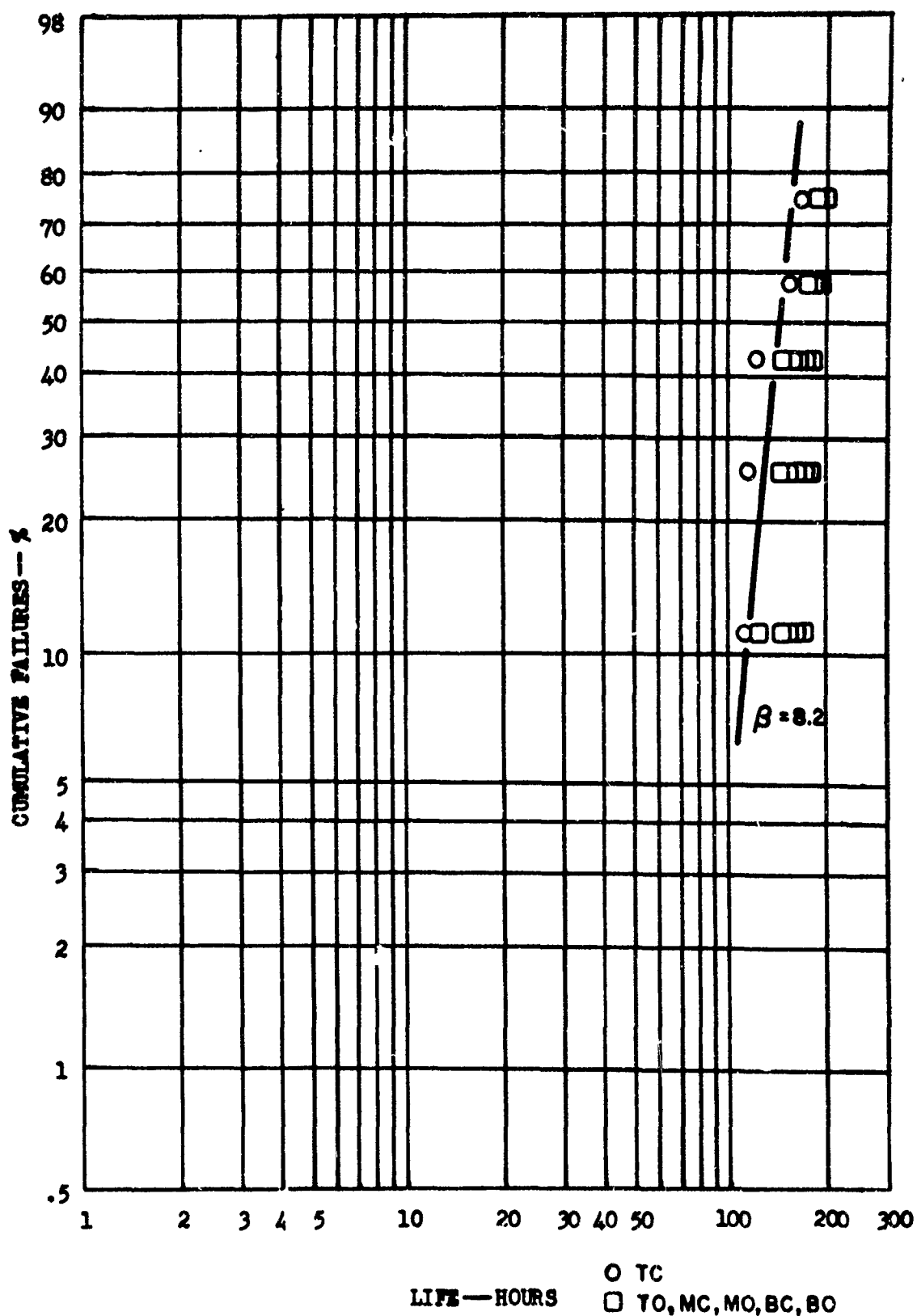
Percent Cumulative Failure vs. Cyclic Oxidation Life at 2500°F
for Specimens Coated in Module Run "3"
Pack Position Breakout



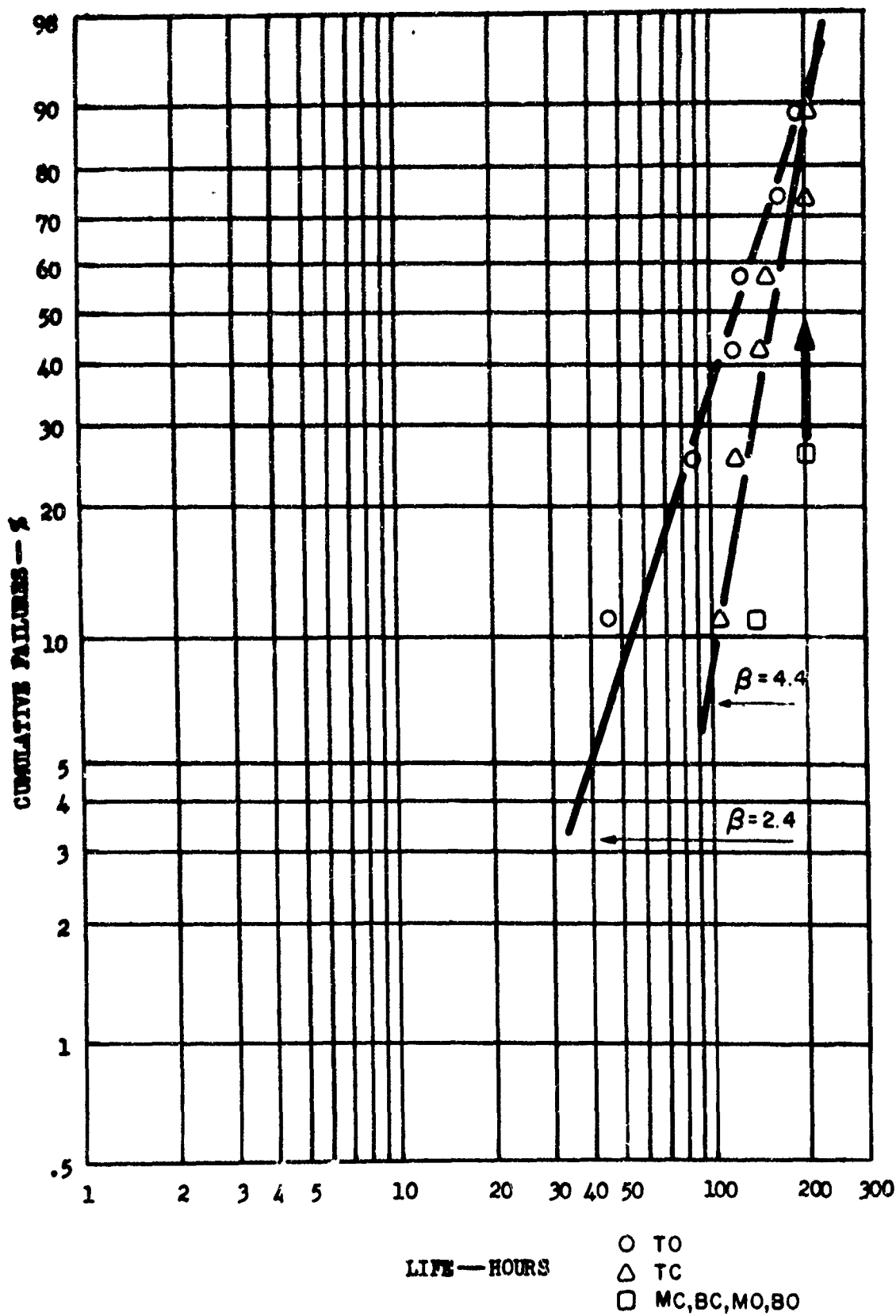
Percent Cumulative Failure Versus Cyclic Oxidation Life at 2500°F for Specimens Coated in Module Run #5. Pack Position Breakout.



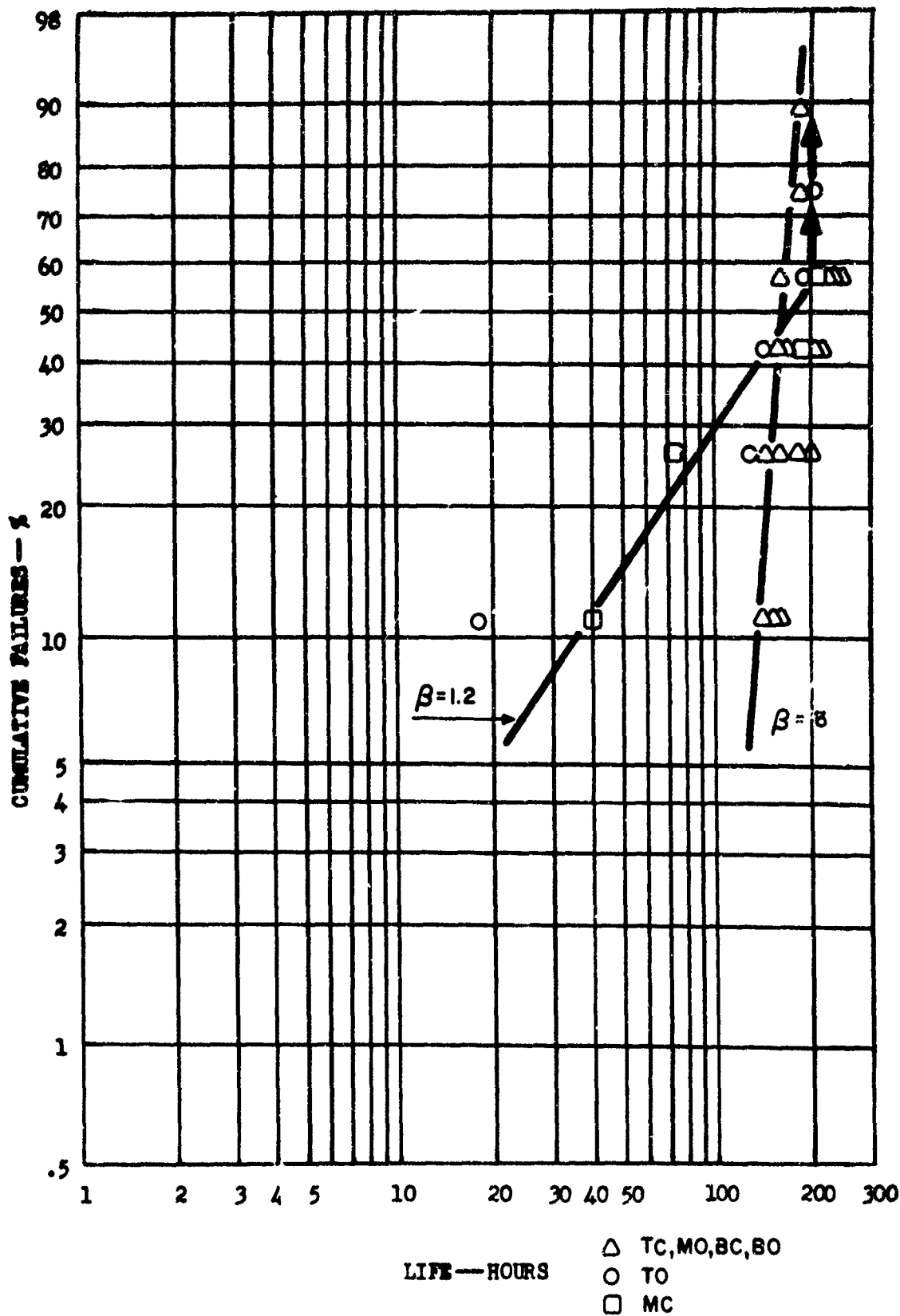
Percent Cumulative Failure Versus Cyclic Oxidation Life at 2500°F for Specimens Coated in Module Run #10, Pack Position Breakout.



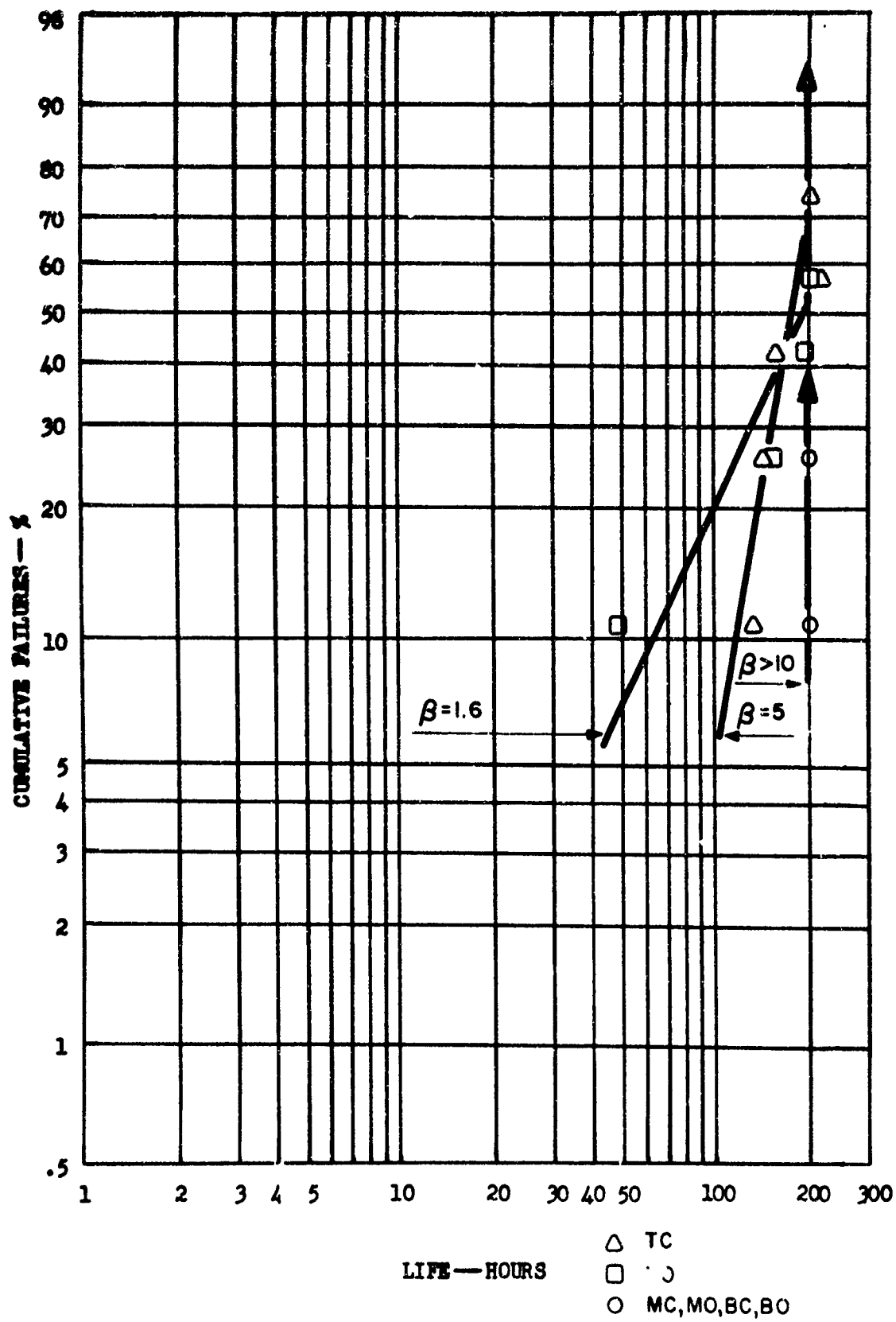
Percent Cumulative Failure Versus Cyclic Oxidation Life at 2500°F for Specimens Coated in Module Run #11, Pack Position Breakout.



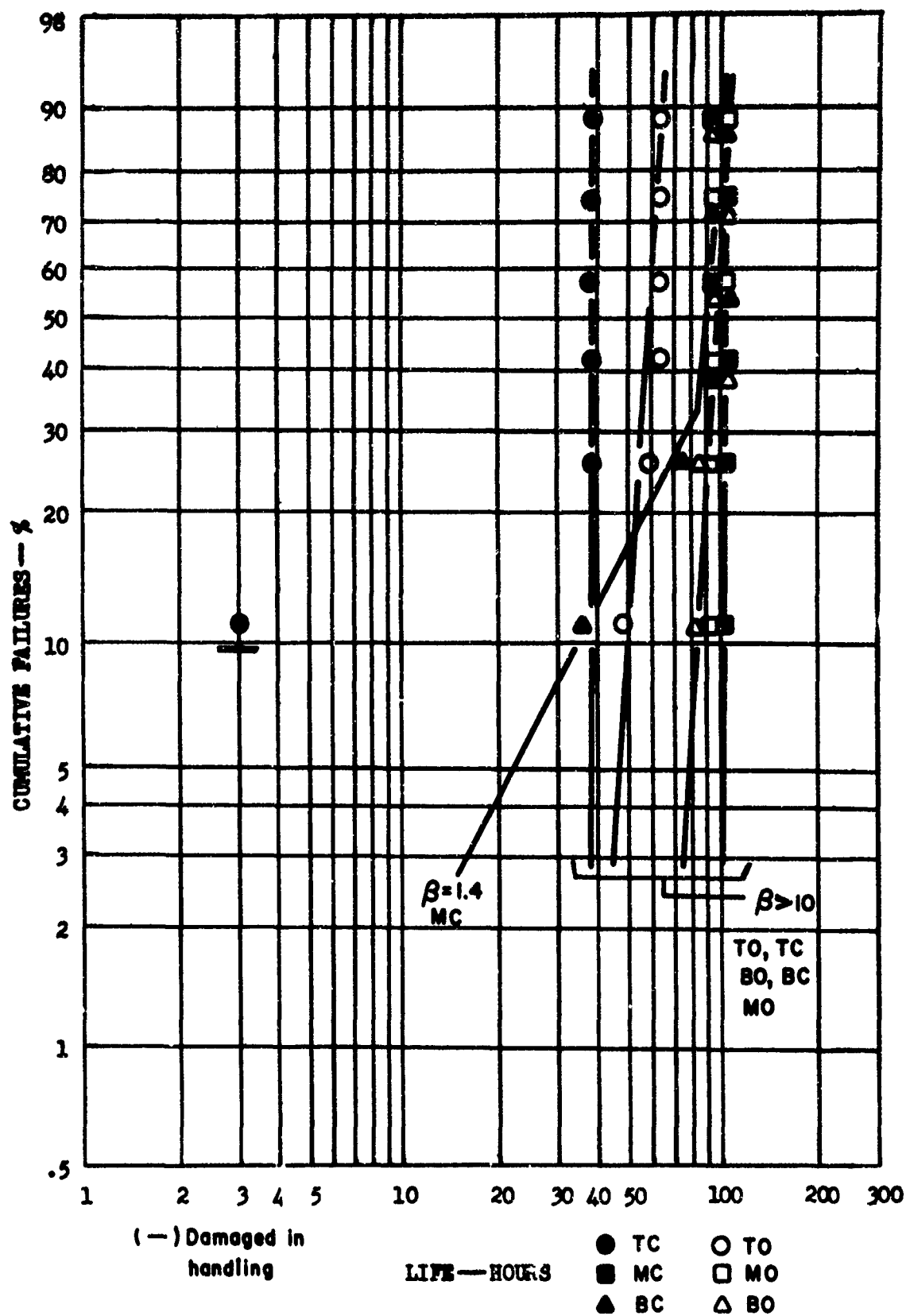
Percent Cumulative Failure vs. Cyclic Oxidation Life
 at 2500°F for Specimens Coated in Module Run #13-
 Pack Position Breakout



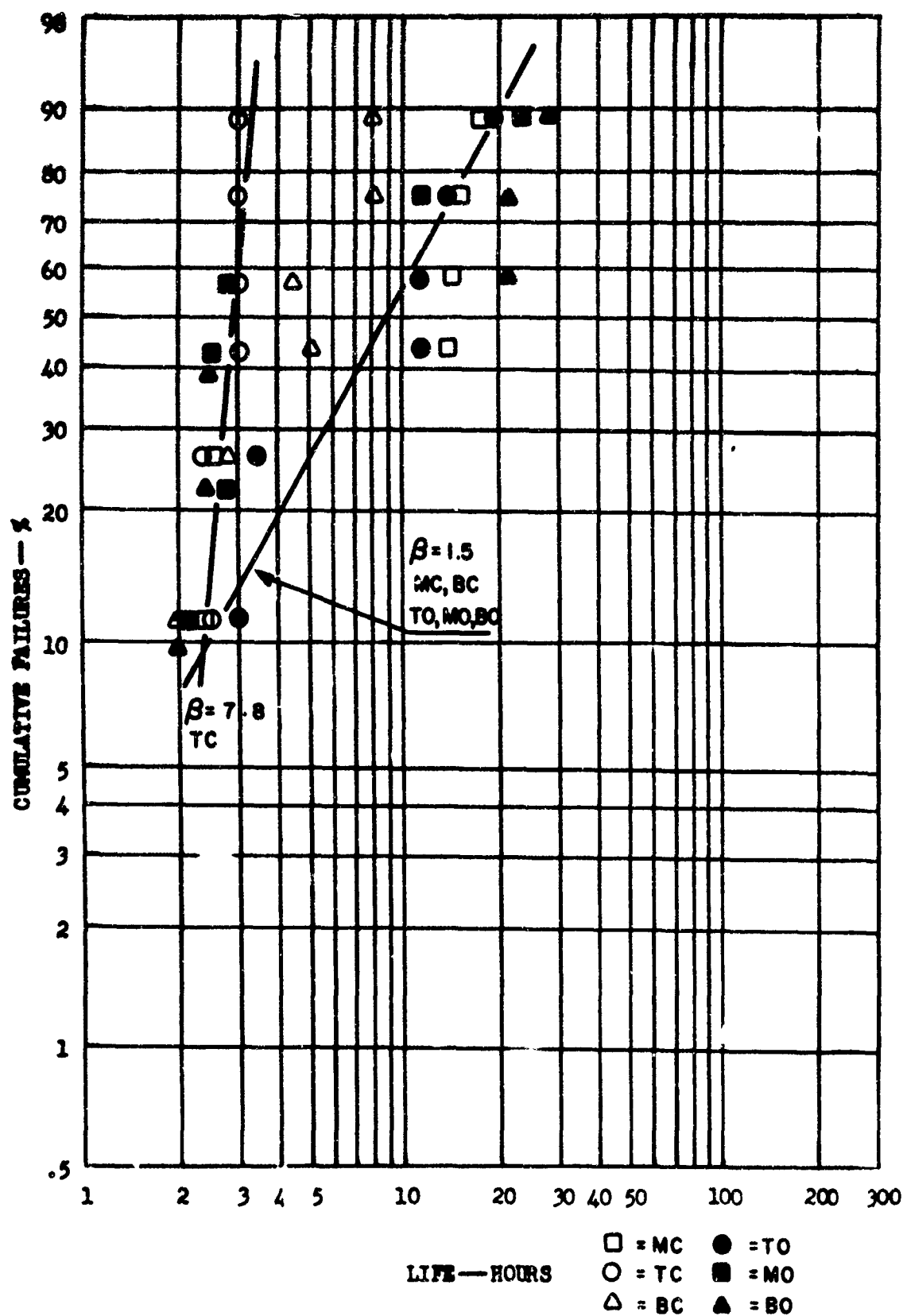
Percent Cumulative Failure vs. Cyclic Oxidation Life
At 2500°F For Specimens Coated In Module Run #14-
Pack Position Breakout



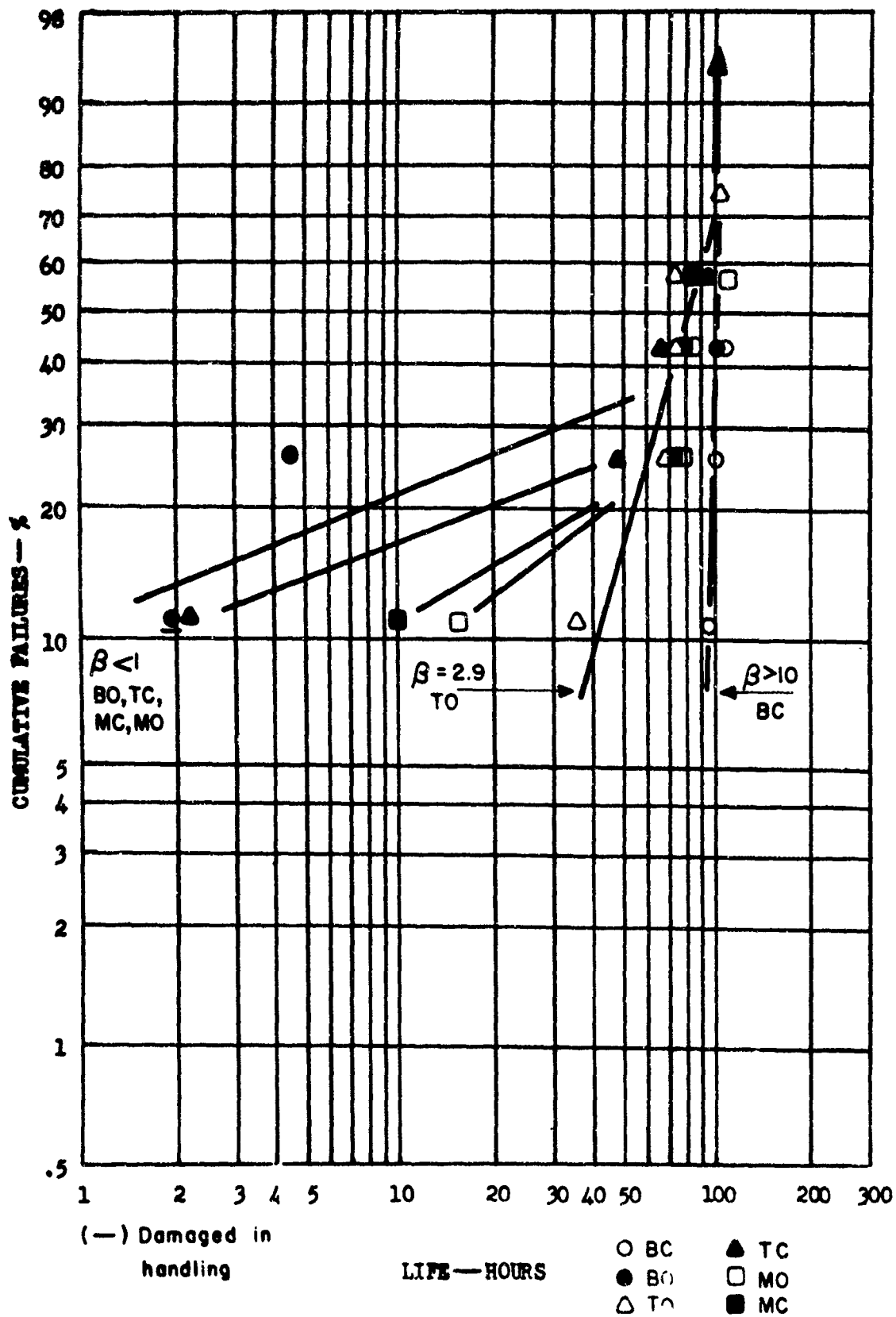
Percent Cumulative Failure vs. Cyclic Oxidation Life
 At 2500°F For Specimens Coated In Module Run #15-
 Pack Position Breakout



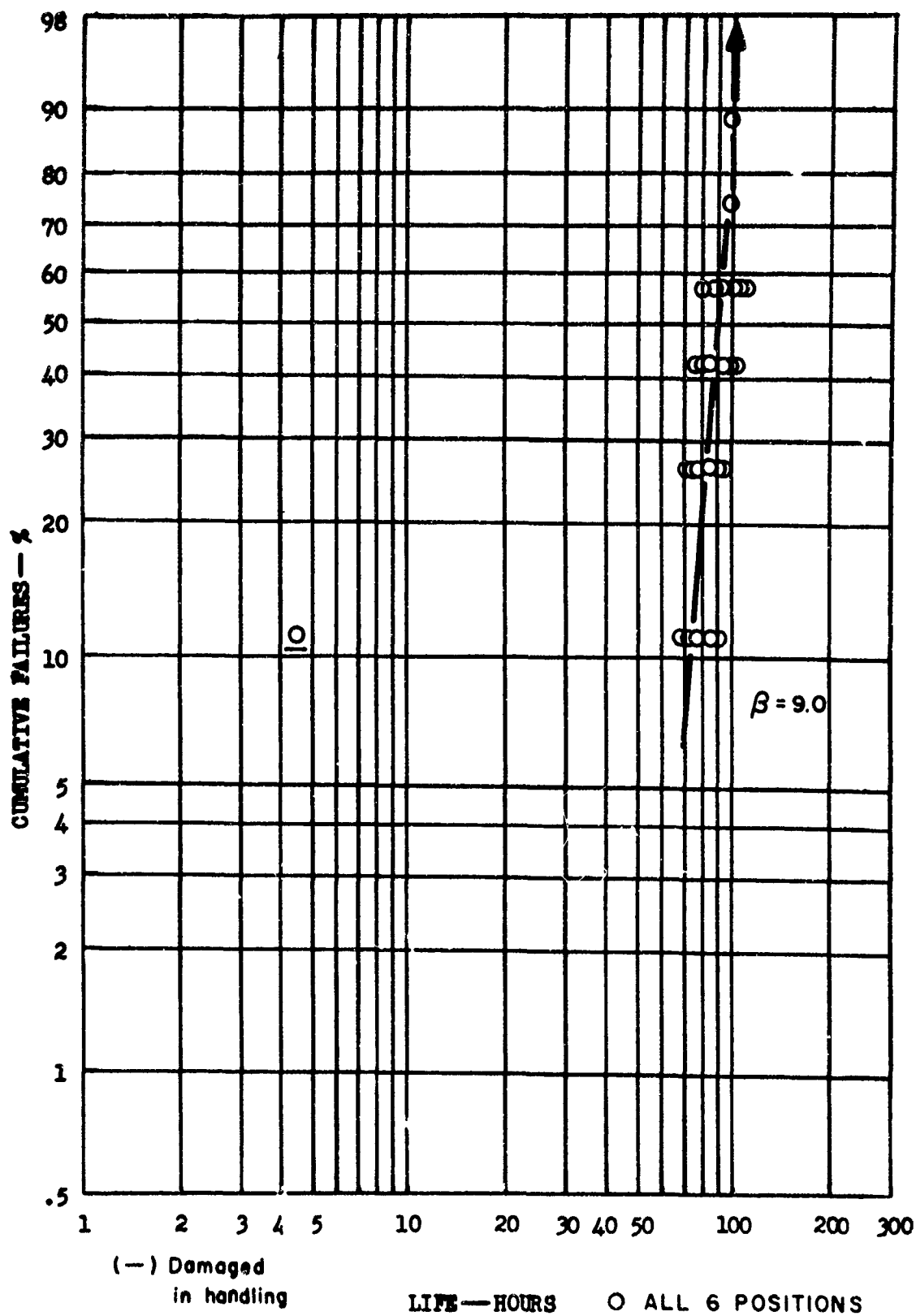
Percent Cumulative Failure vs. Cyclic Oxidation Life at 2700° F
for Specimens Coated in Module Run #1
Pack Position Breakout



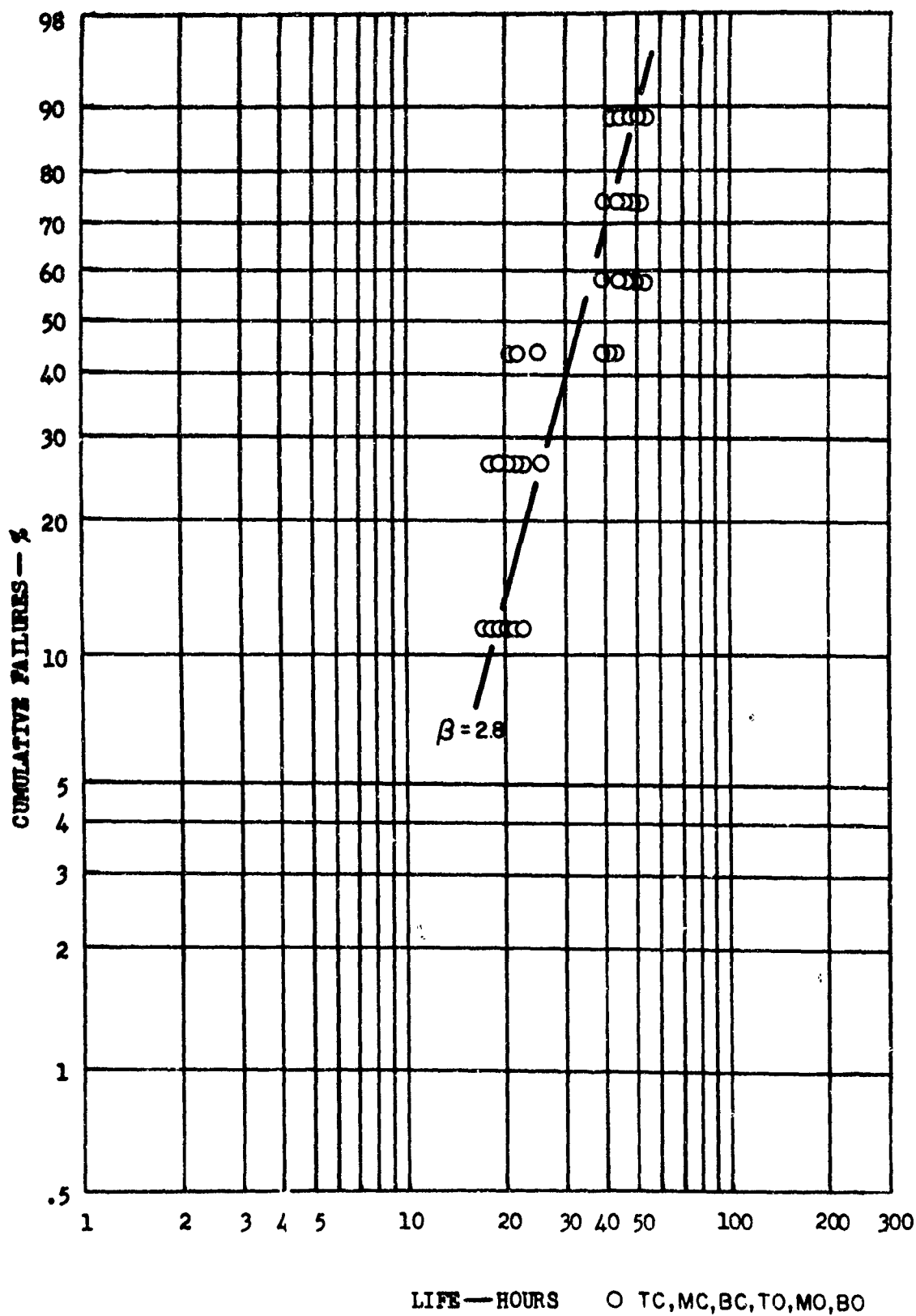
Percent Cumulative Failure vs. Cyclic Oxidation Life at 2700°F
for Specimens Coated in Module Run 3
Pack Position Breakout.



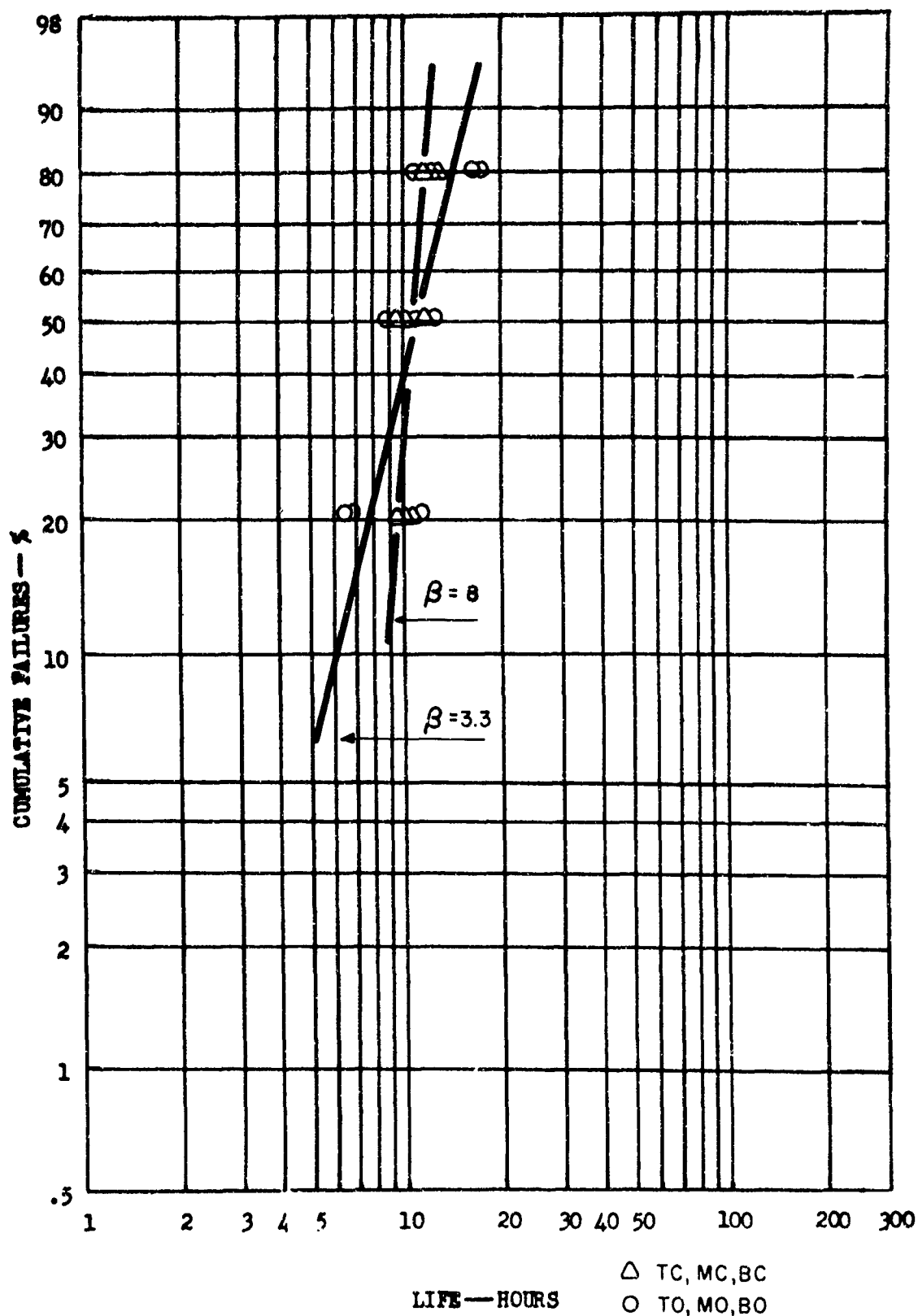
Percent Cumulative Failure Versus Cyclic Oxidation Life at 2700°F for Specimens Coated in Module Run 15. Pack Position Breakout.



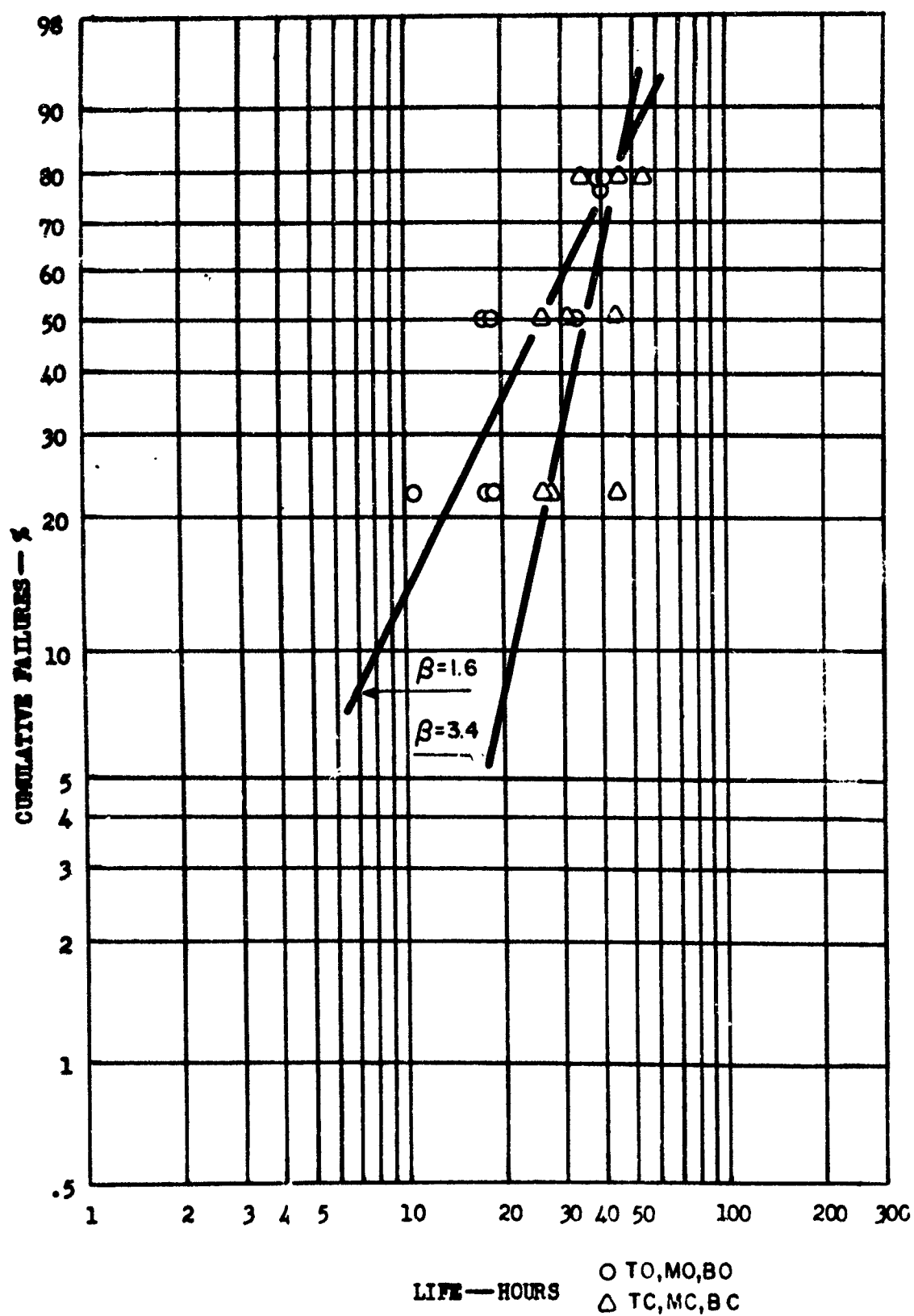
Percent Cumulative Failure Versus Cyclic Oxidation Life at 2700°F for Specimens Coated in Module Run #10, Pack Position Breakout.



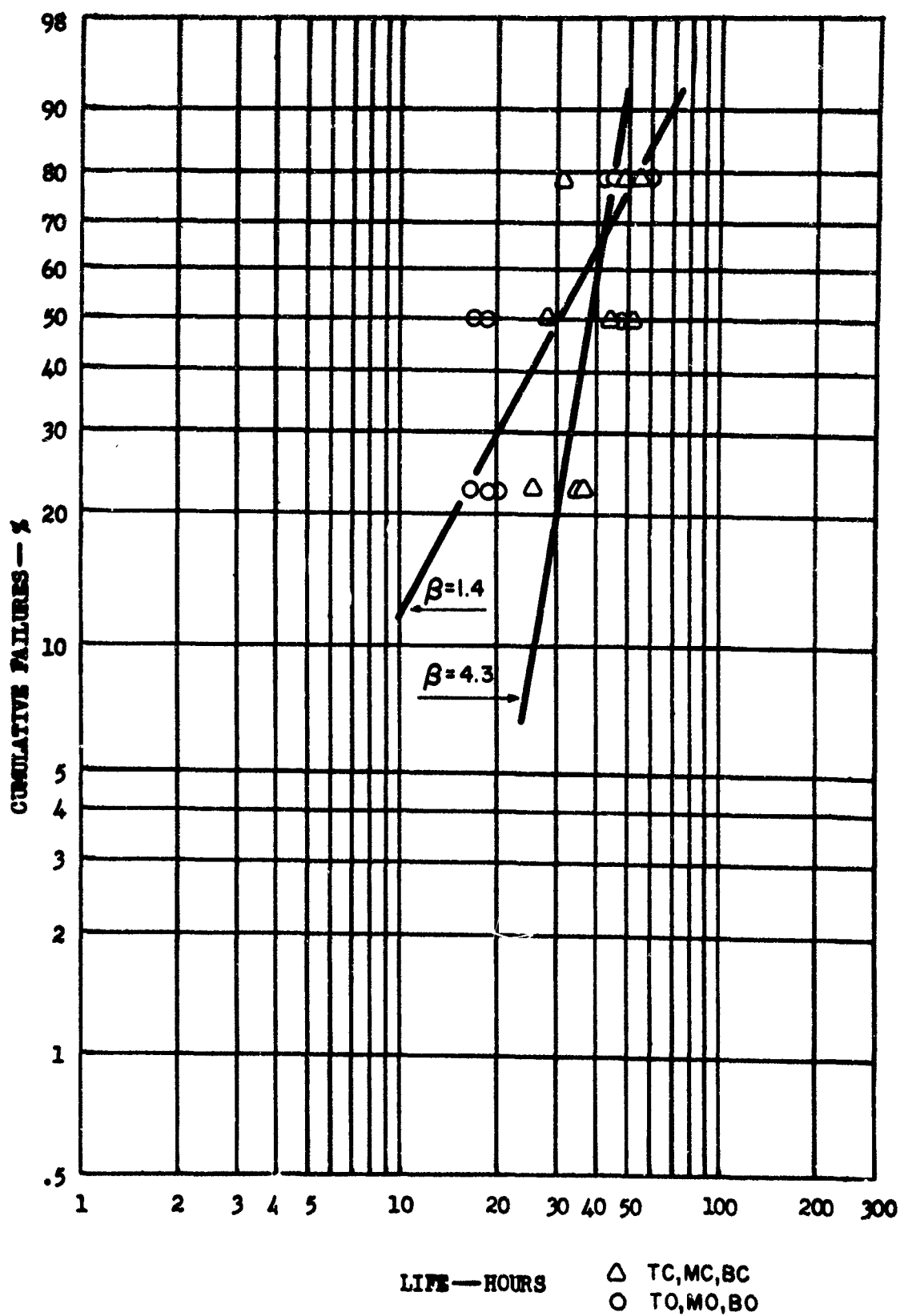
Percent Cumulative Failure Versus Cyclic Oxidation Life at 2700°F for Specimens Coated in Module Run #11, Pack Position Breakout.



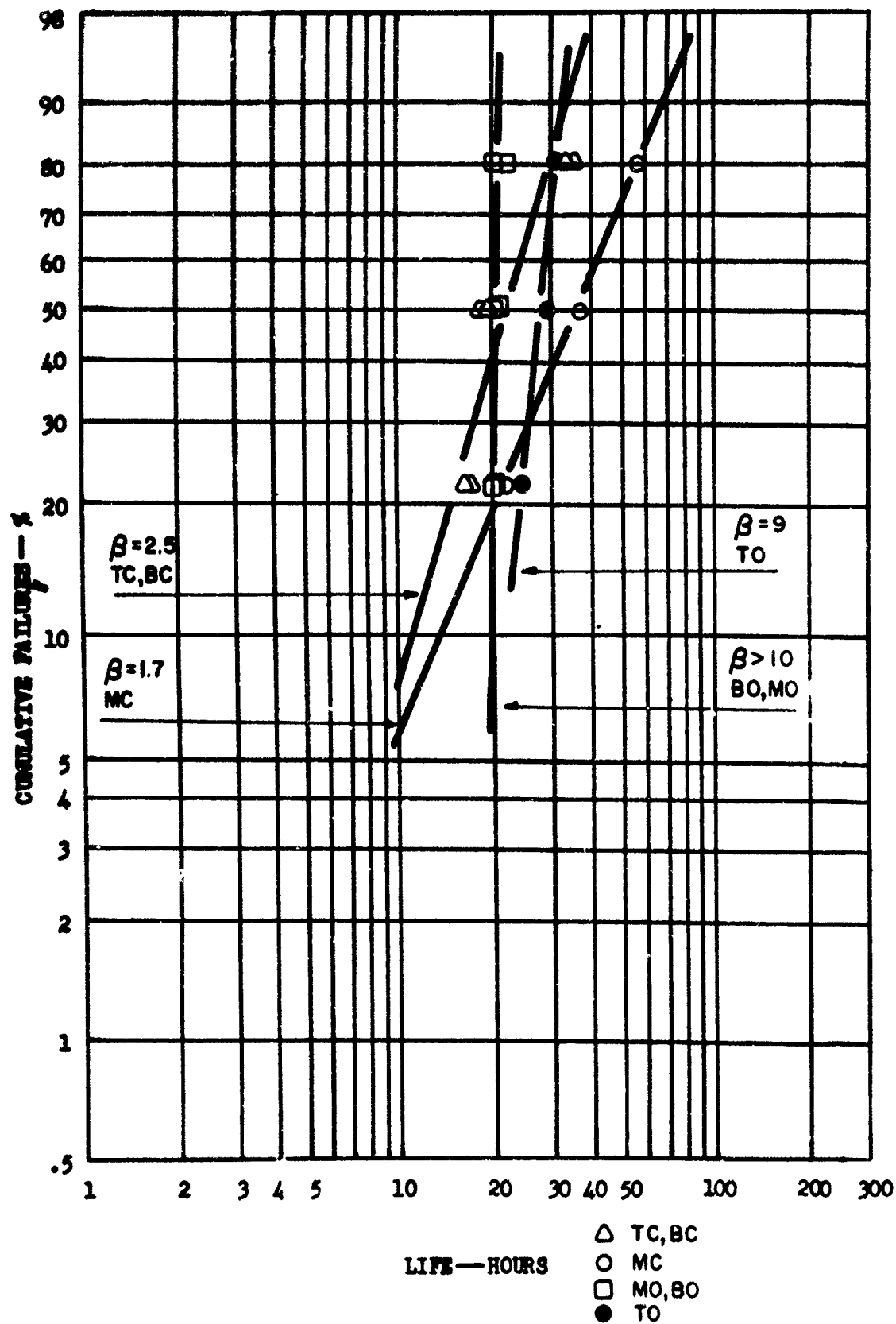
Percent Cumulative Failure vs. Cyclic Oxidation Life
At 2700°F For Specimens Coated In Module Run #12-
Pack Position Breakout



Percent Cumulative Failure vs. Cyclic Oxidation Life
At 2700°F For Specimens Coated In Module Run #13-
Pack Position Breakout



Percent Cumulative Failures vs. Cyclic Oxidation Life
 At 2700°F For Specimens Coated In Module Run #11-
 Pack Position Breakout



Percent Cumulative Failure vs. Cyclic Oxidation Life
At 2700°F For Specimens Coated In Module Run #15-
Pack Position Breakout

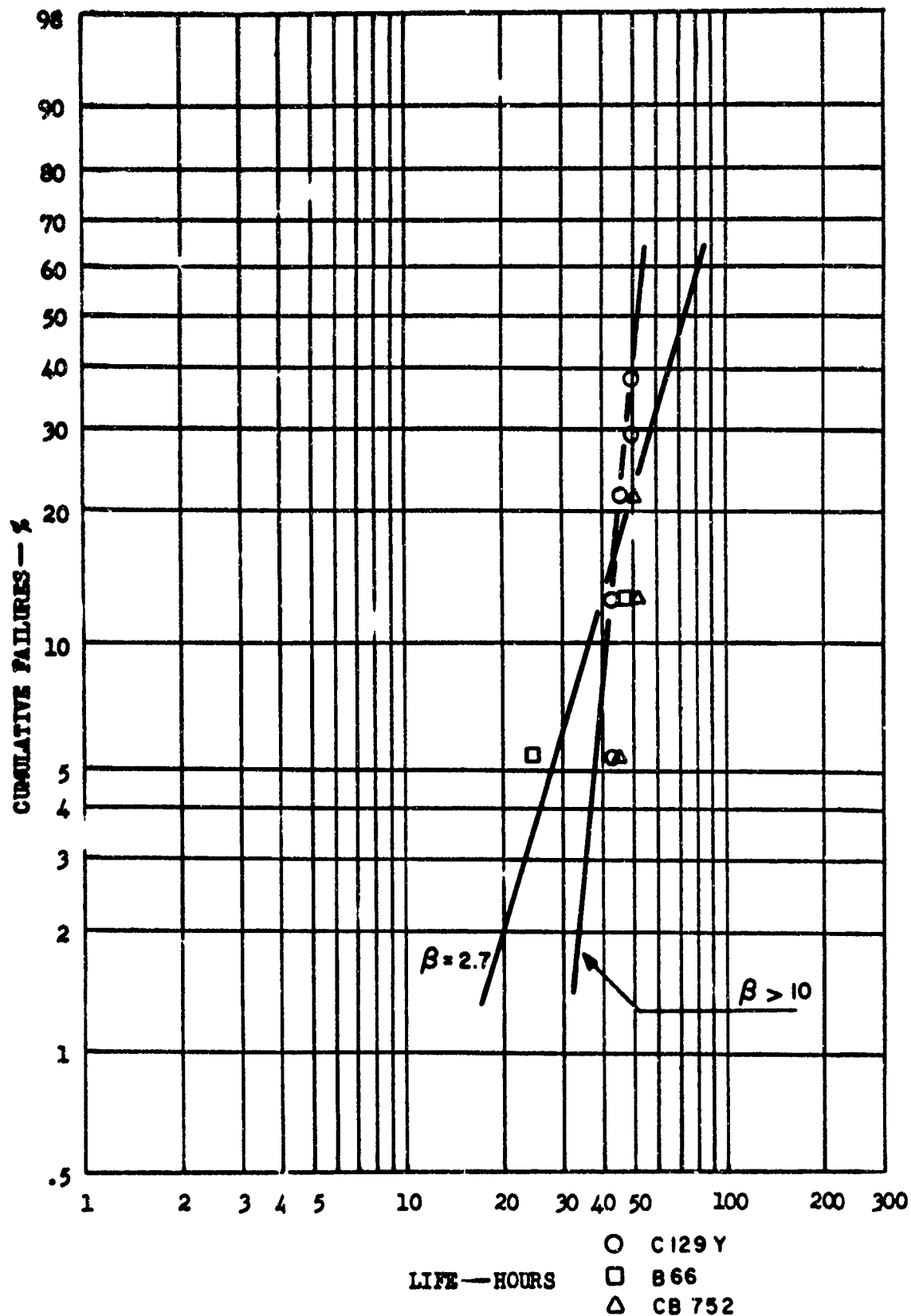
APPENDIX III - OXIDATION LIVES OF MODULE VACUUM-PACK COATED
COUPONS AS A FUNCTION OF ALLOY COMPOSITION

Performance of the following modules was not included because the number of coupons which failed at each temperature was not sufficient to permit a meaningful analysis:

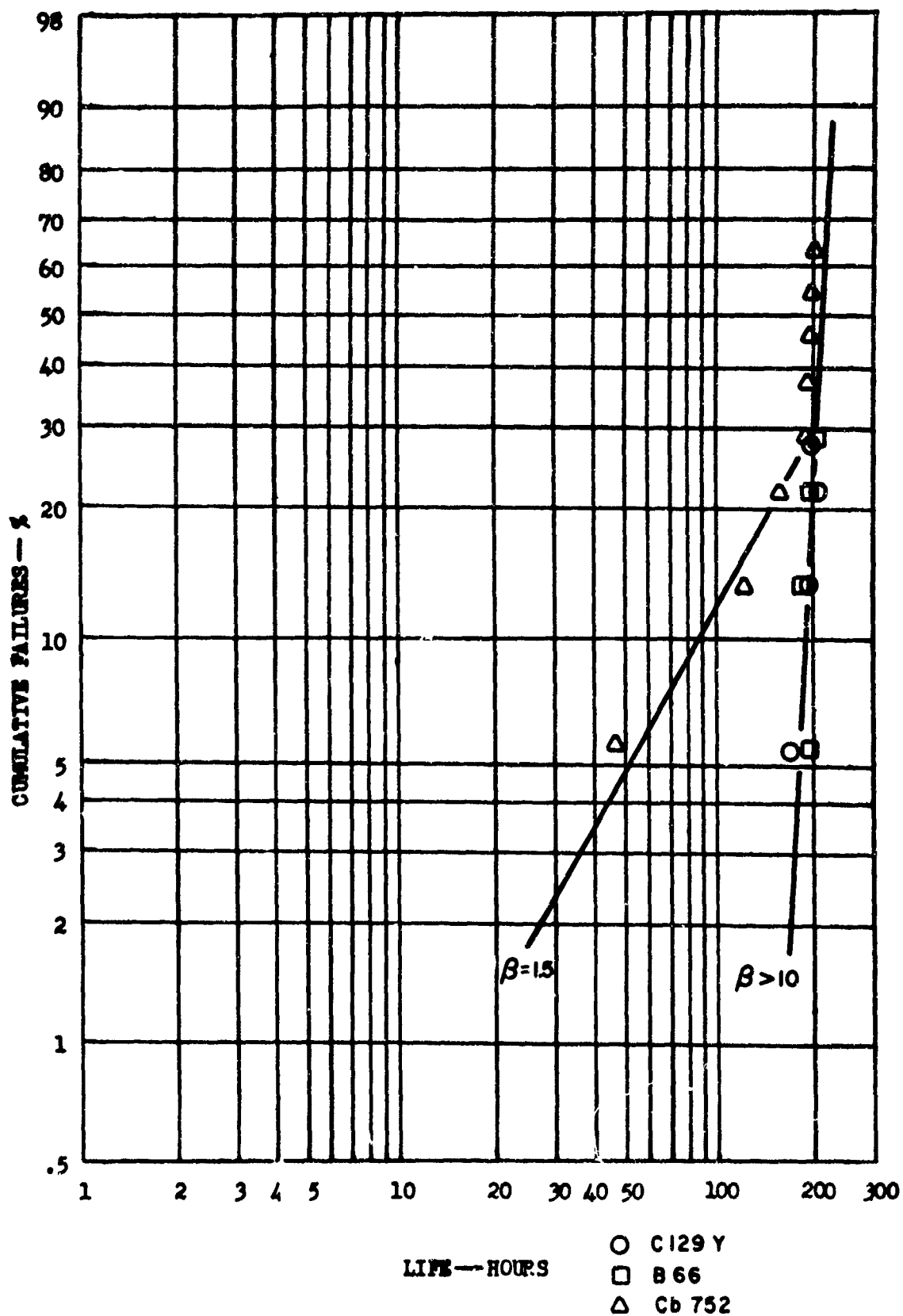
1800°F Modules 1,4,8,9,15

2500°F Modules 4,6,7,8,9,12

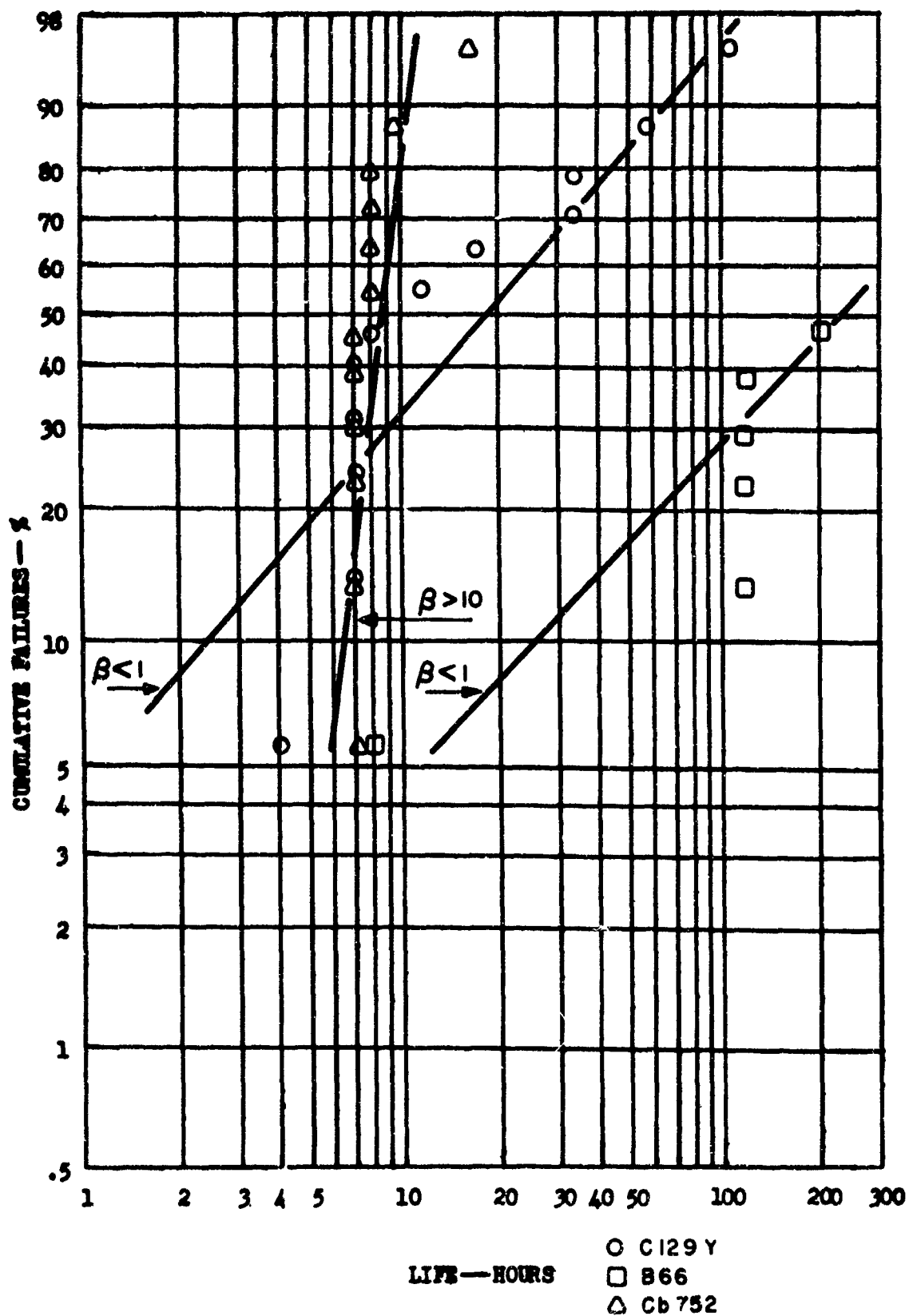
2700°F Modules 2,6,7,8,9



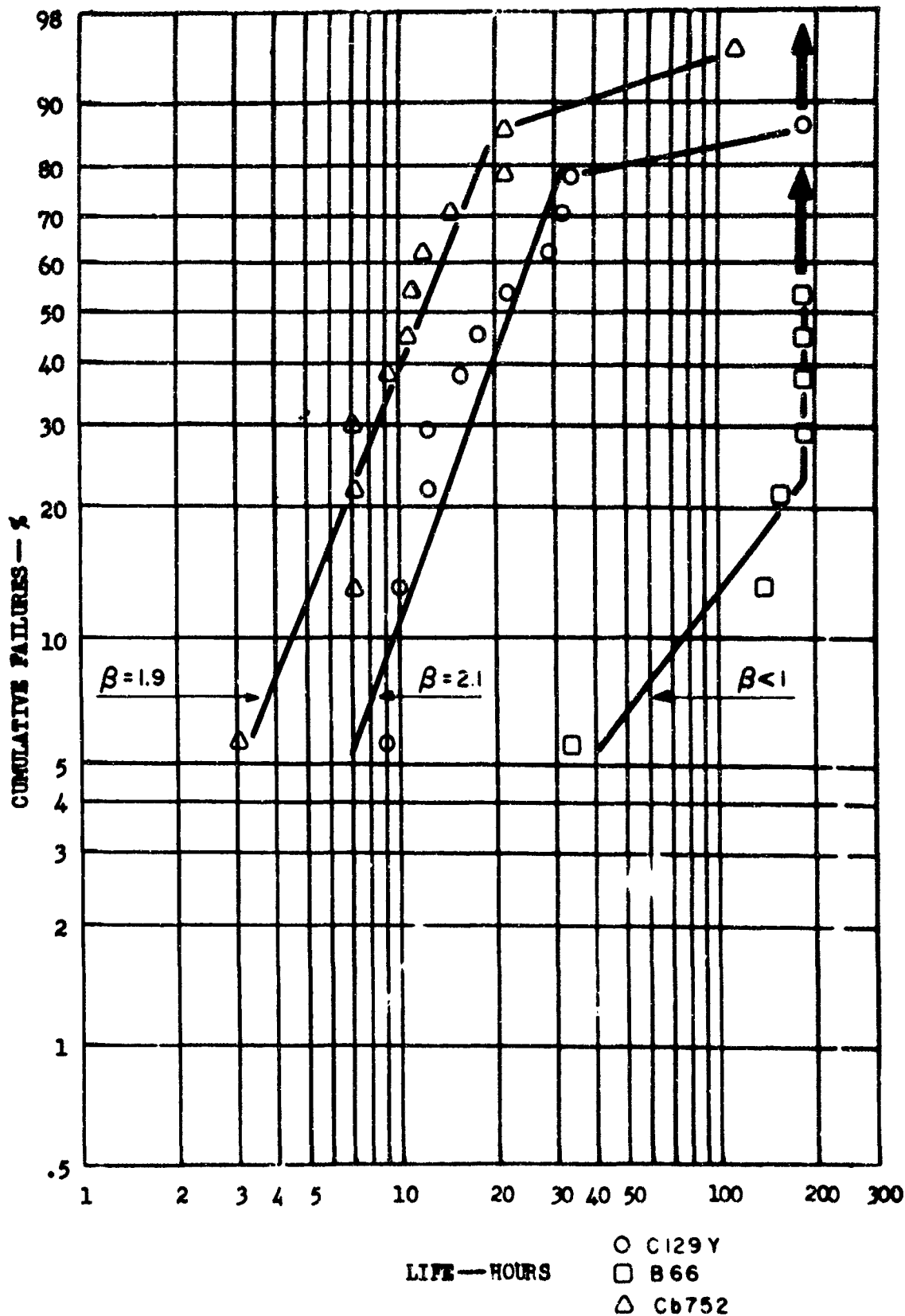
Percent Cumulative Failure vs. Cyclic Oxidation Life at 1800°F
for Specimens Coated in Module Run #2
Alloy Breakout



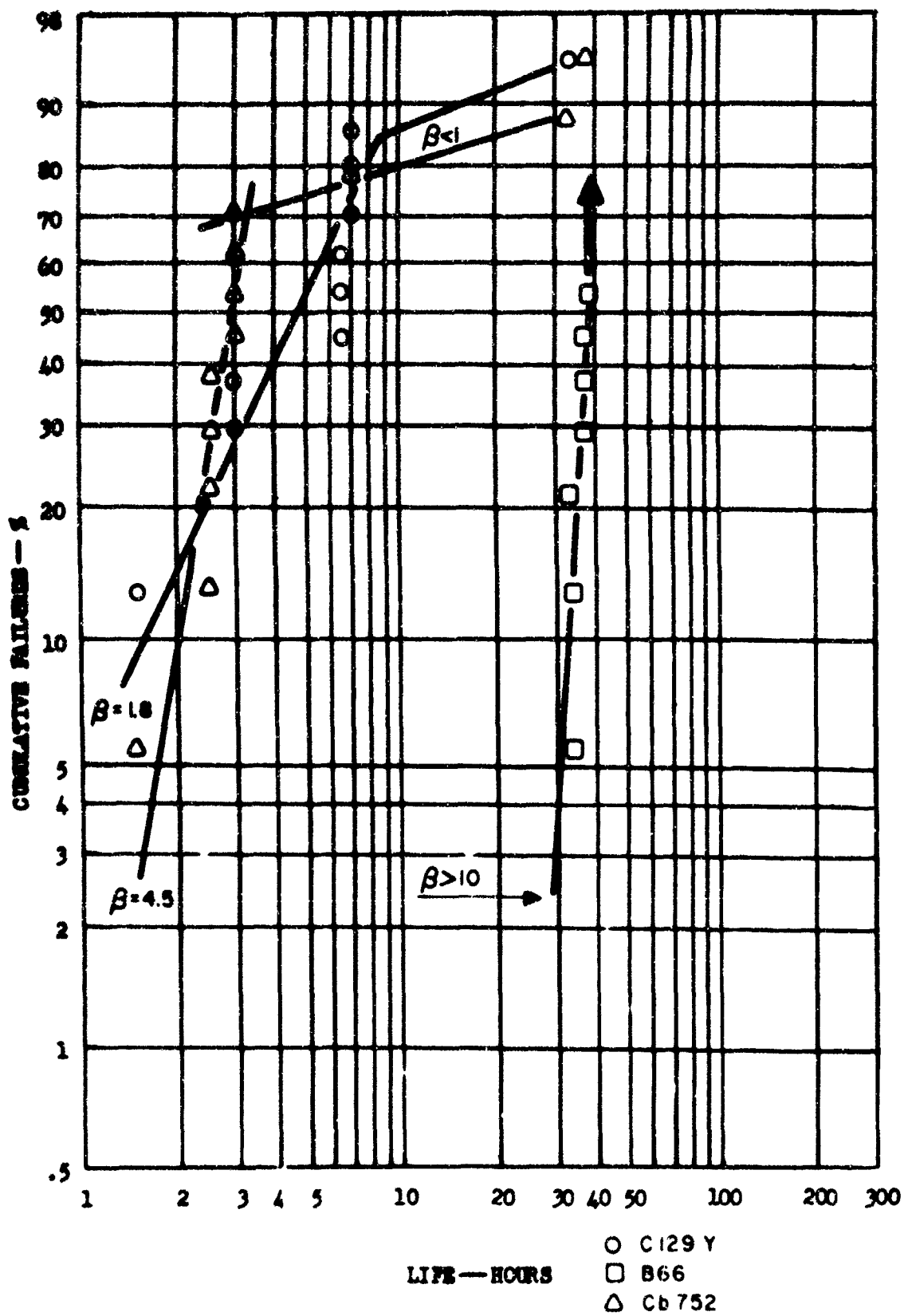
Percent Cumulative Failure vs. Cyclic Oxidation Life at 1800°F
 for Specimens Coated in Module Furn. 3
 Alloy Breakout



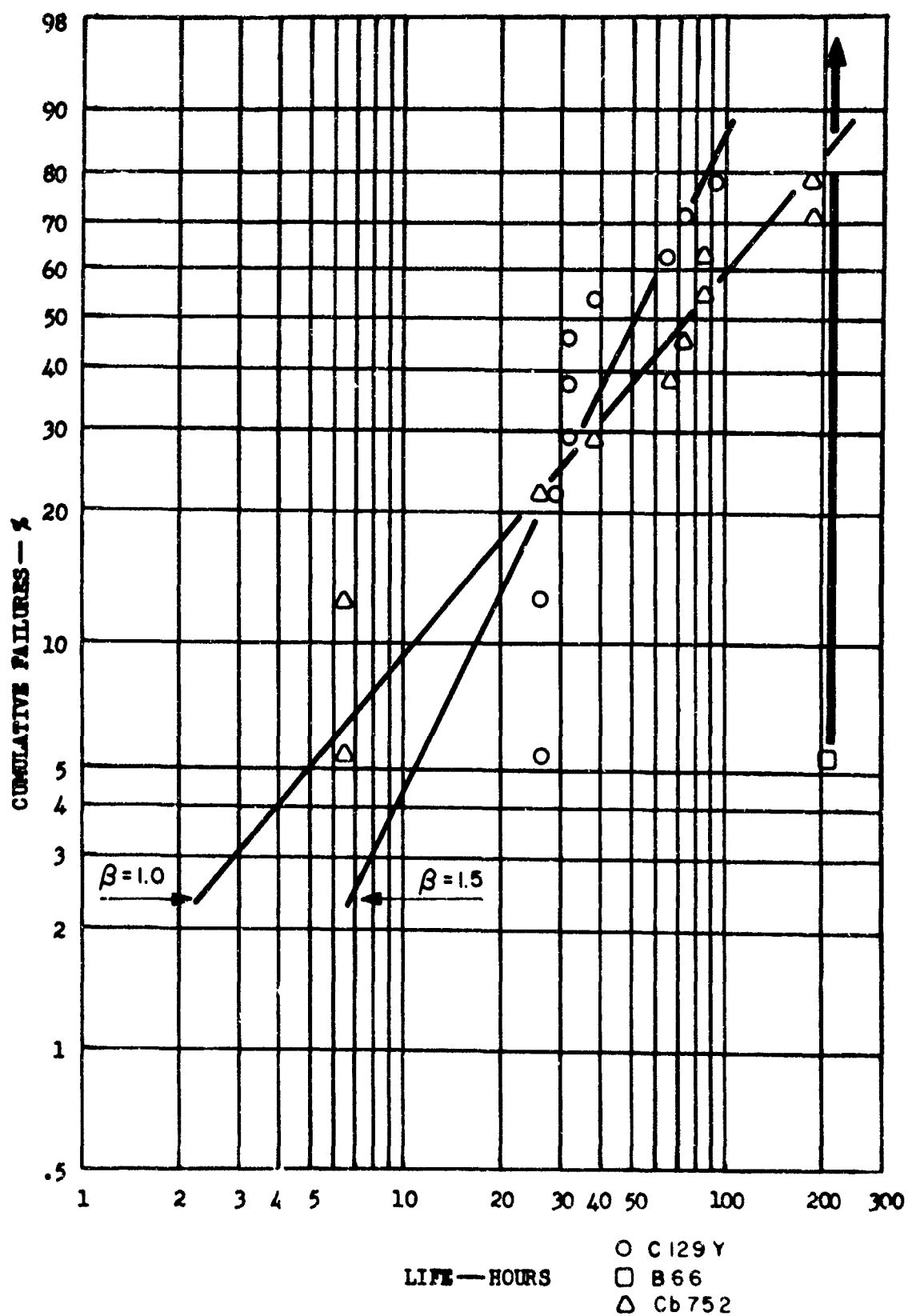
Percent Cumulative Failure Versus Cyclic Oxidation Life at 1800°F for Specimens Coated in Module Run #5, Alloy Breakout.



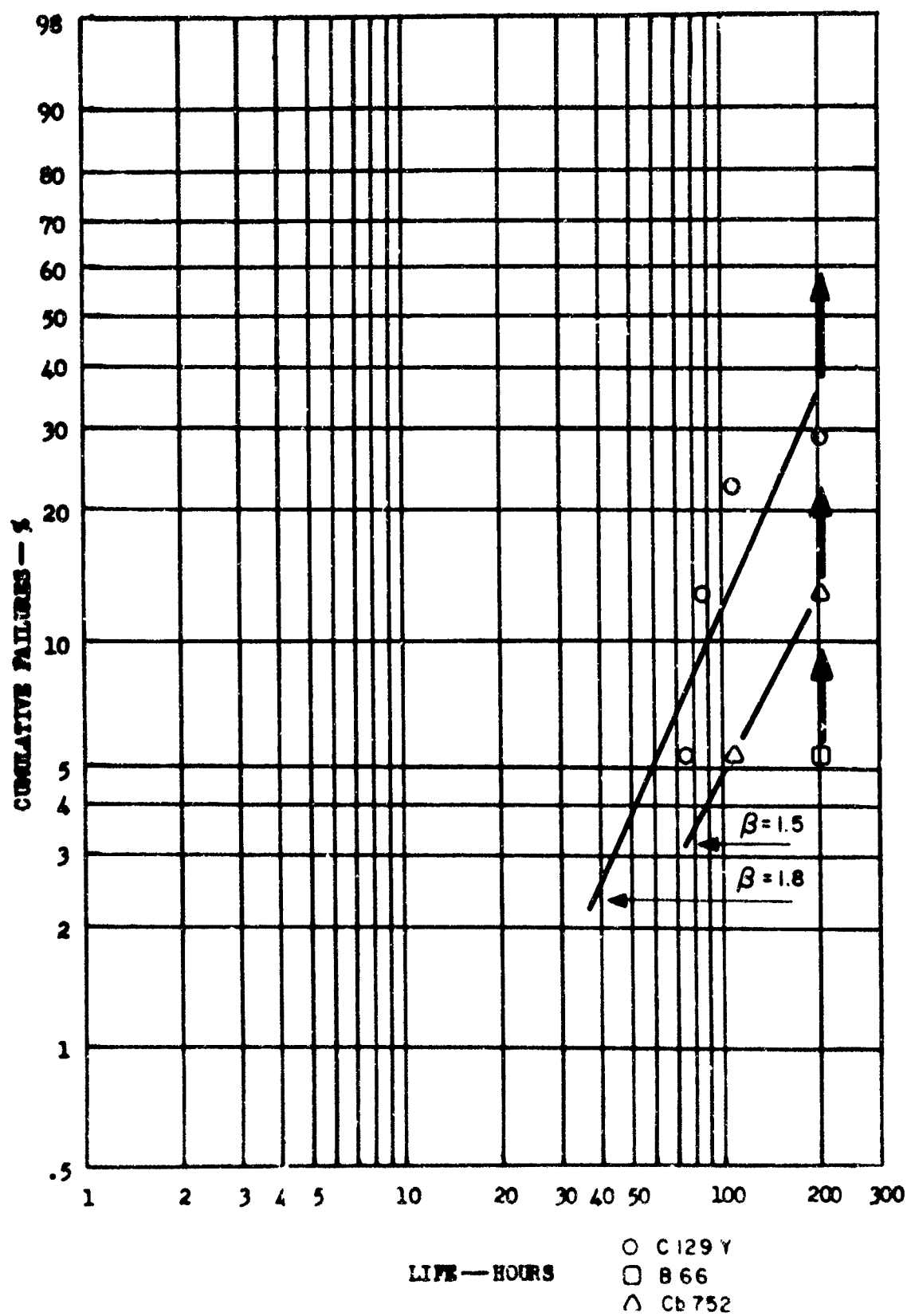
Percent Cumulative Failure Versus Cyclic Oxidation Life at 1800°F for Specimens Coated in Module Run #6, Alloy Breakout.



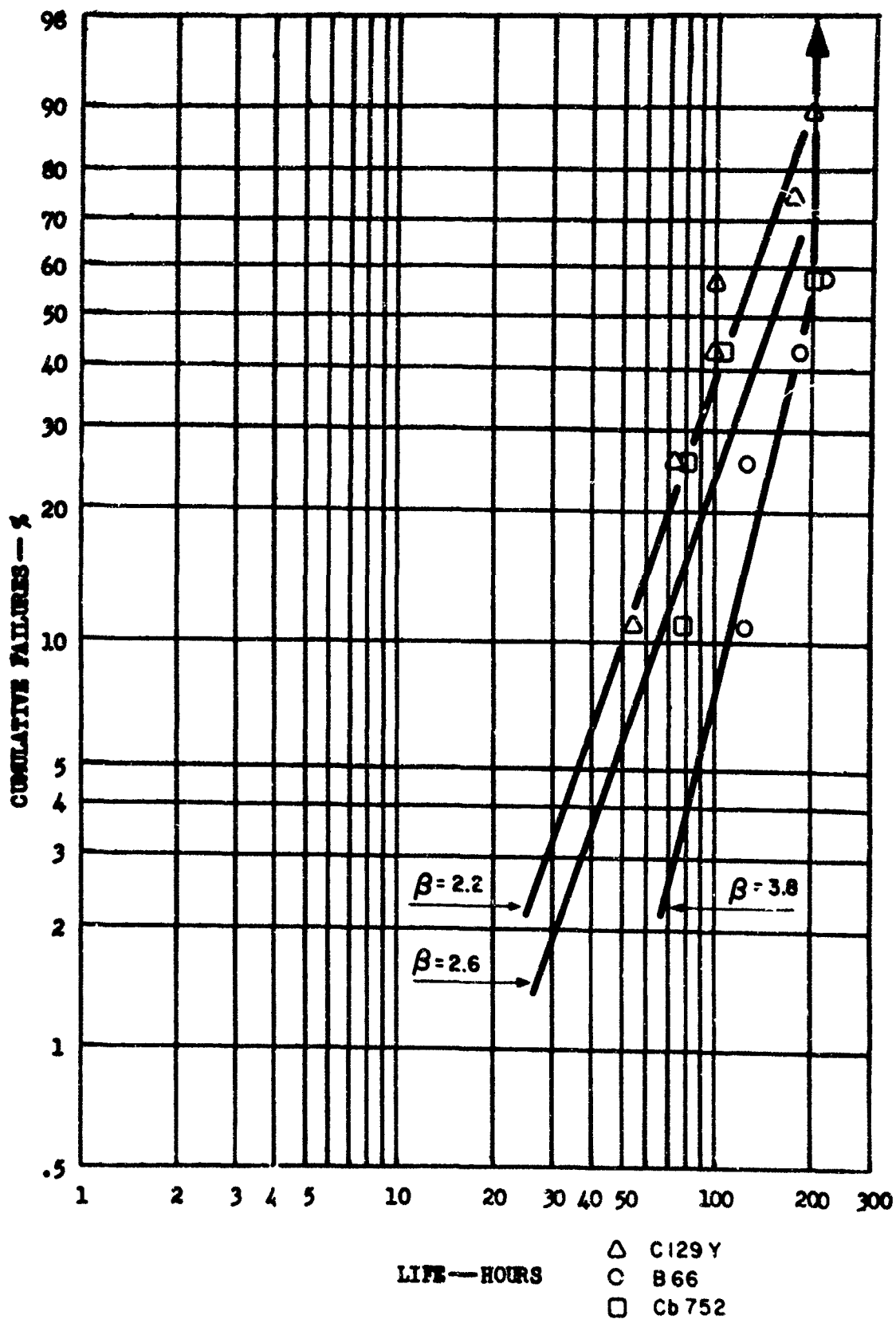
Percent Cumulative Failure Versus Cyclic Oxidation Life at 1800°F for Specimens Coated in Module Run #7, Alloy Breakout.



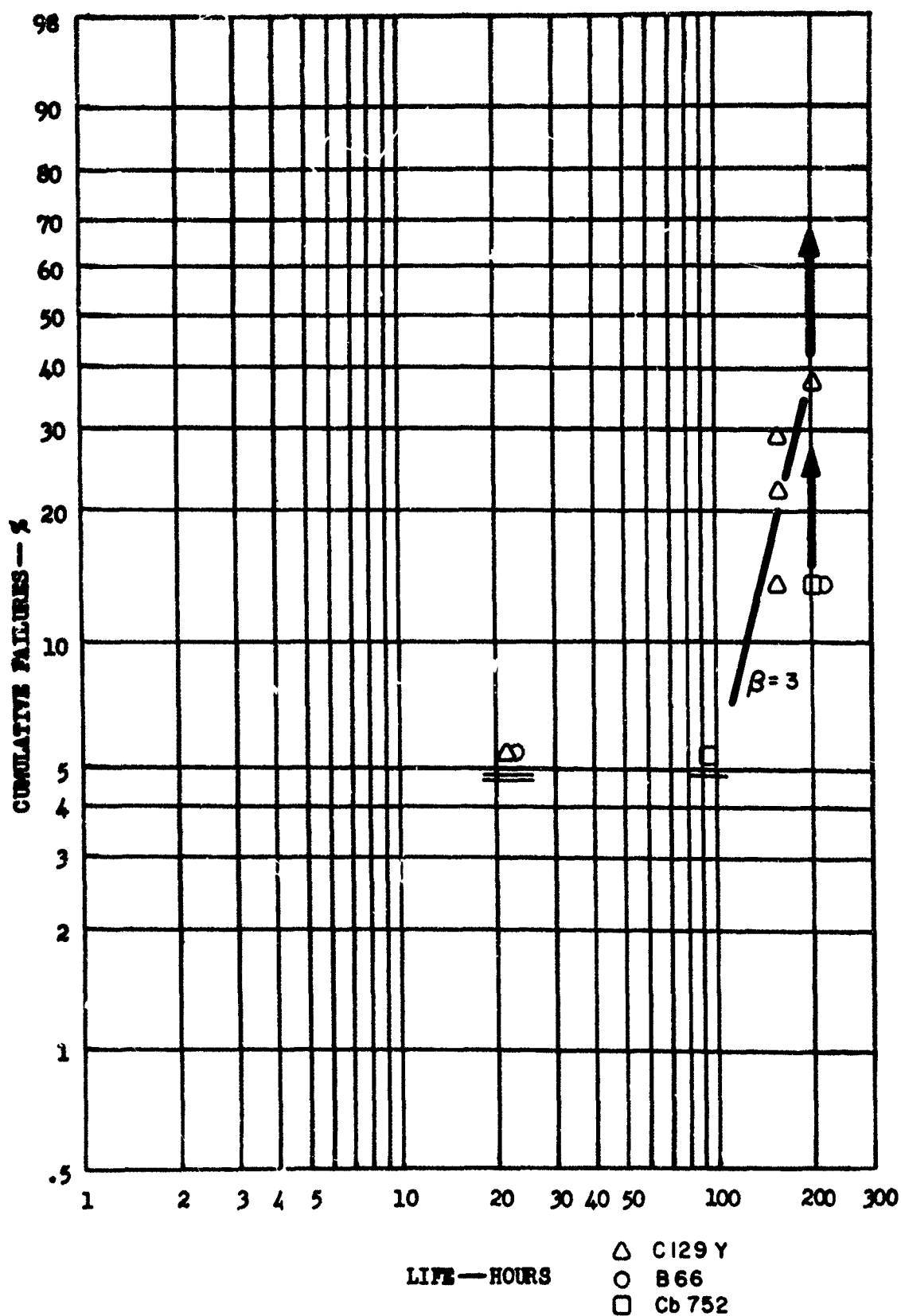
Percent Cumulative Failure Versus Cyclic Oxidation Life at 1800°F for Specimens Coated in Module Run #10, Alloy Breakout.



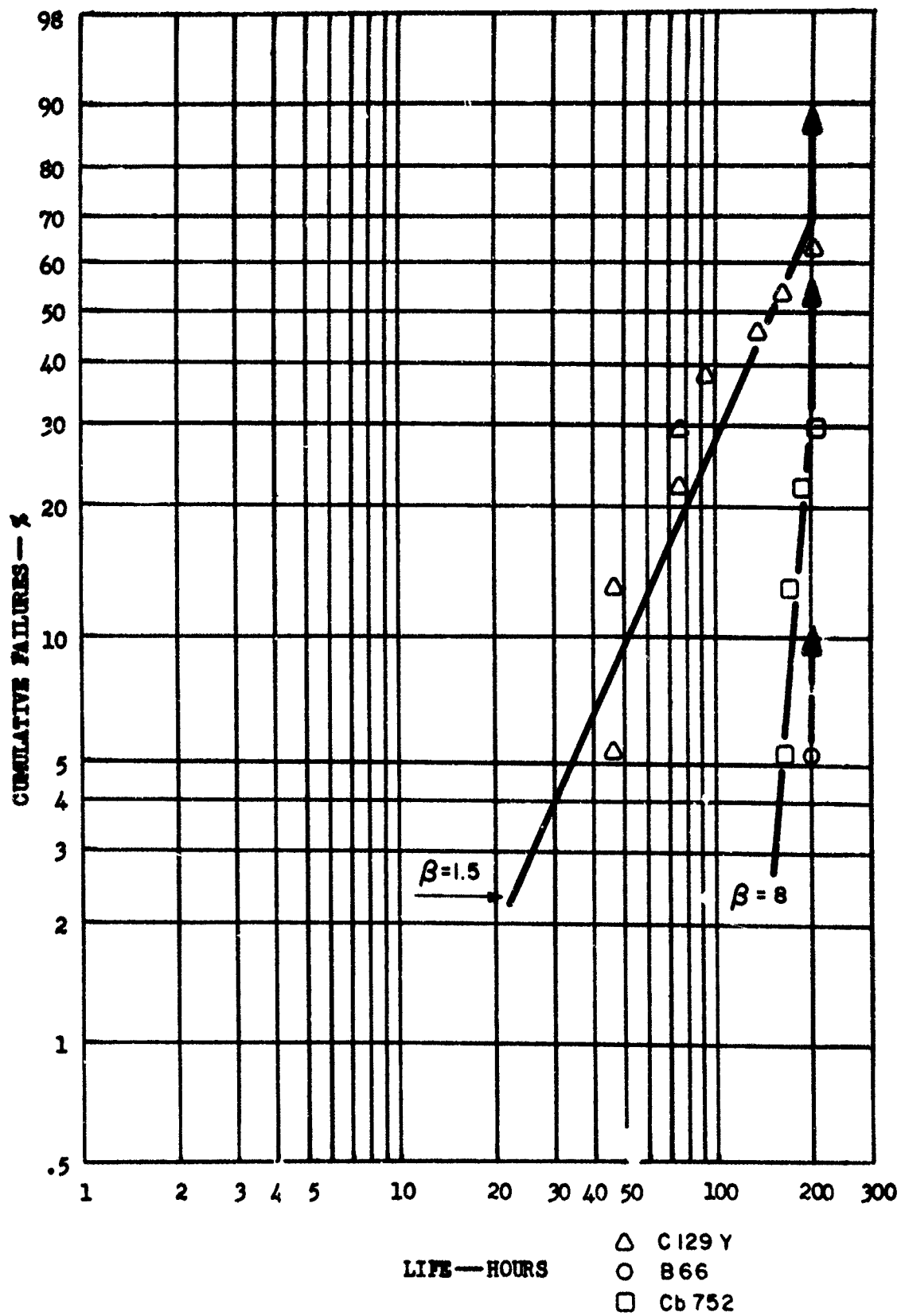
Percent Cumulative Failure Versus Cyclic Oxidation Life at 1800°F for Specimens Coated in Module Run #11, Alloy Breakcut.



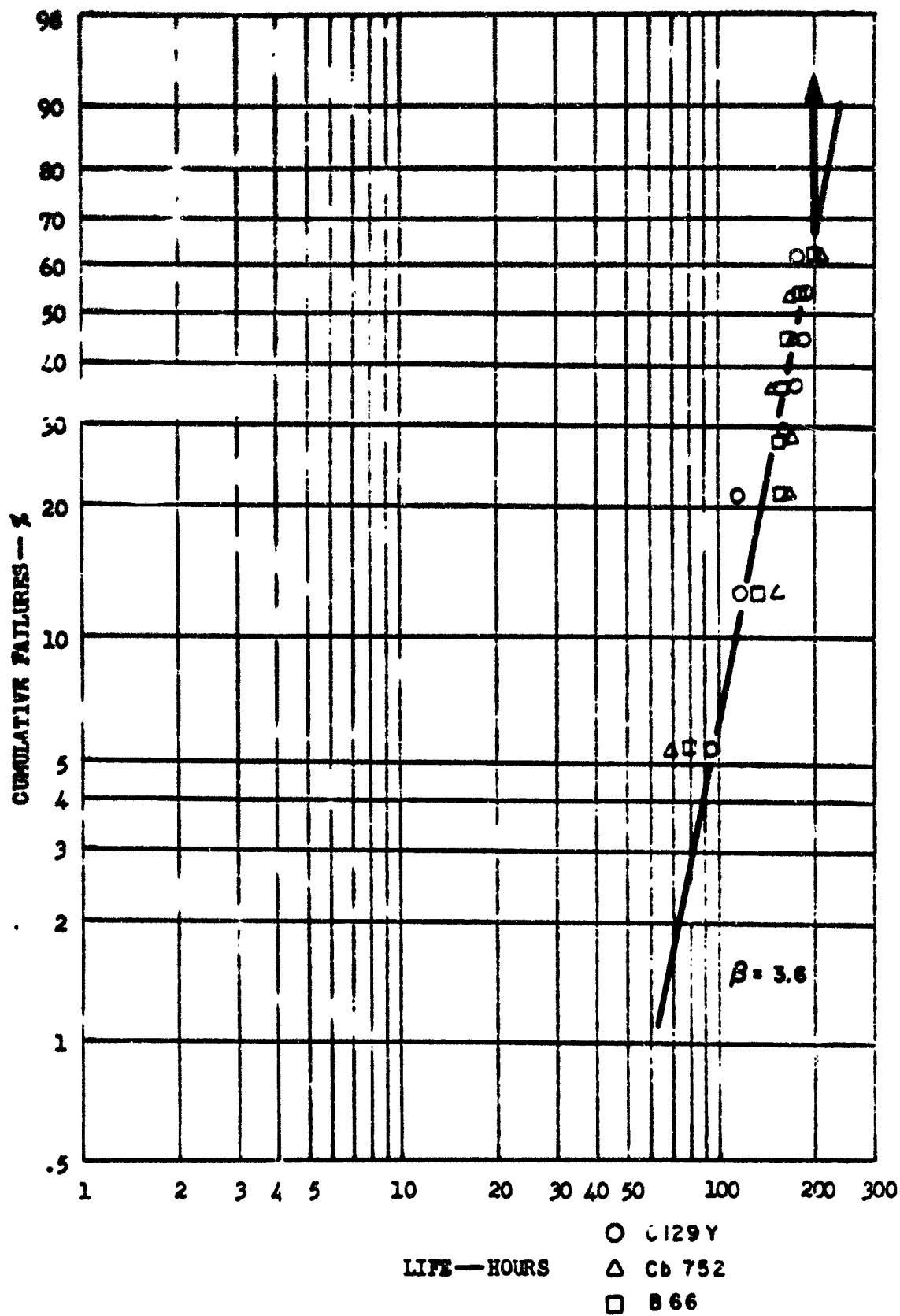
Percent Cumulative Failure vs. Cyclic Oxidation Life
 At 1800°F For Specimens Coated In Module Runs #12-
 Alloy Breakout



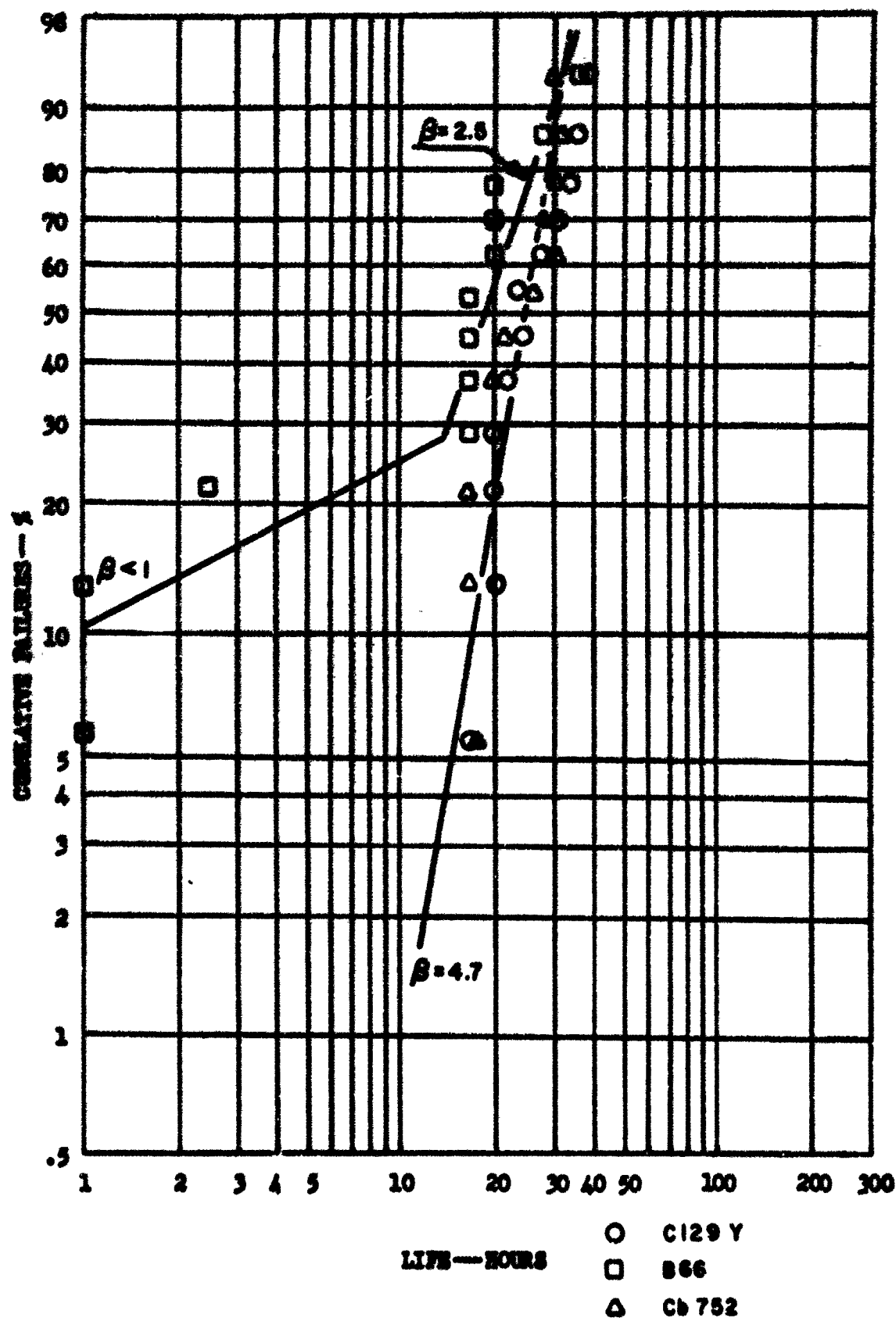
Percent Cumulative Failure vs. Cyclic Oxidation Life
At 1800°F For Specimens Coated In Module Run #13-
Alloy Breakout



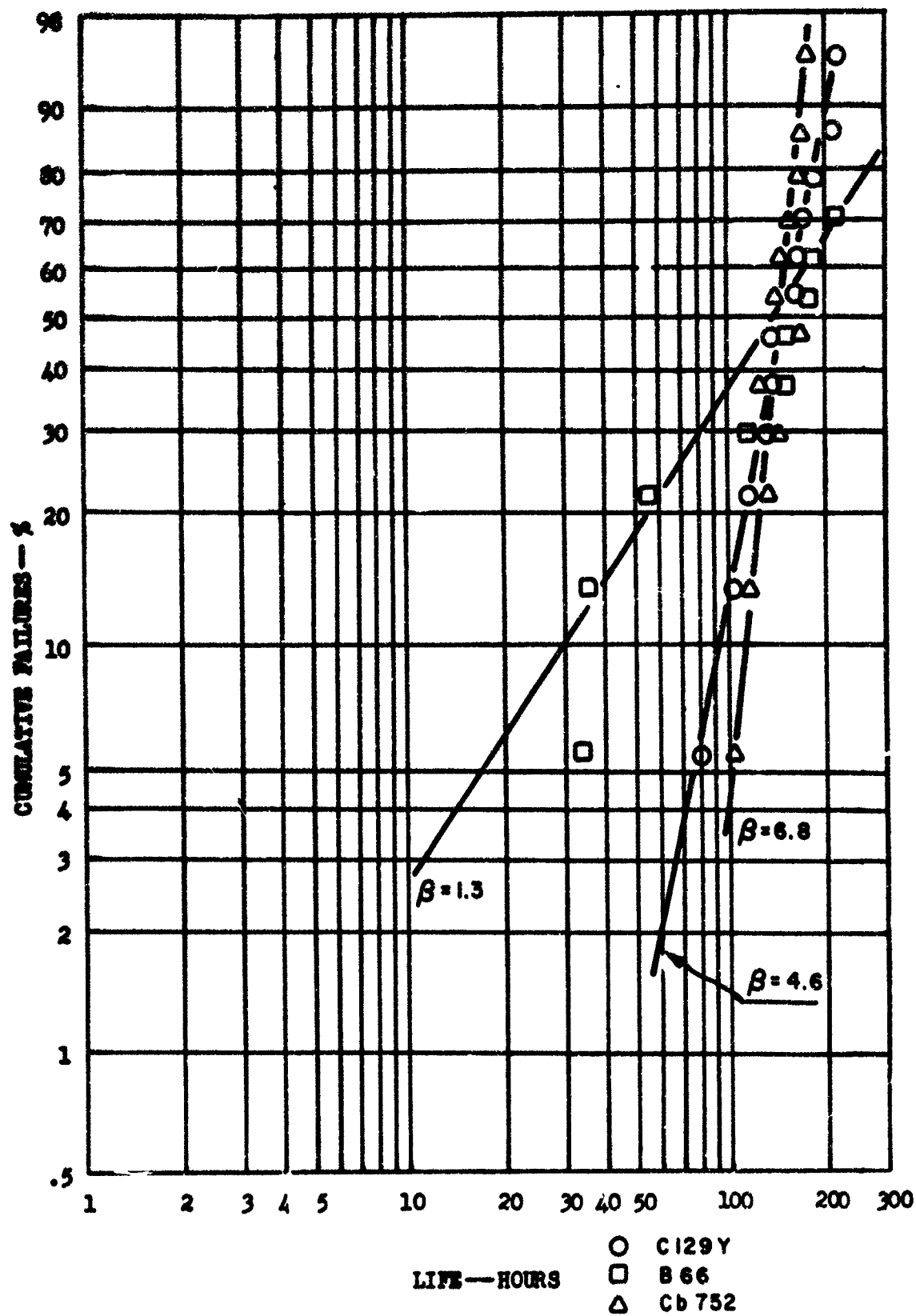
Percent Cumulative Failure vs. Cyclic Oxidation Life
At 1800°F For Samples Coated In Module Run #14-
Alloy Breakout



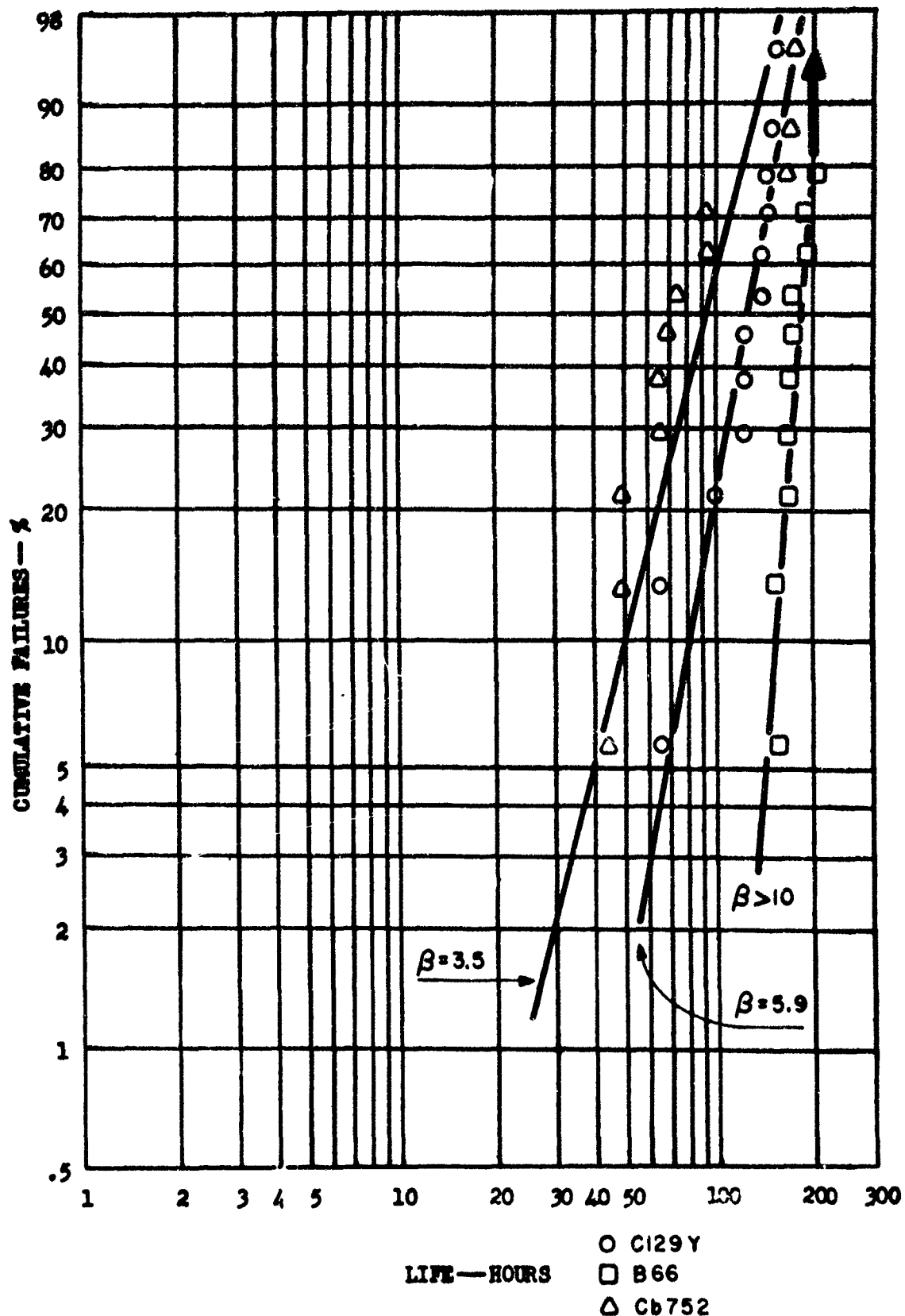
Percent Cumulative Failure vs. Cyclic Oxidation Life at 2500°F
 for Specimens Coated in Module Run #1
 Alloy Breakout



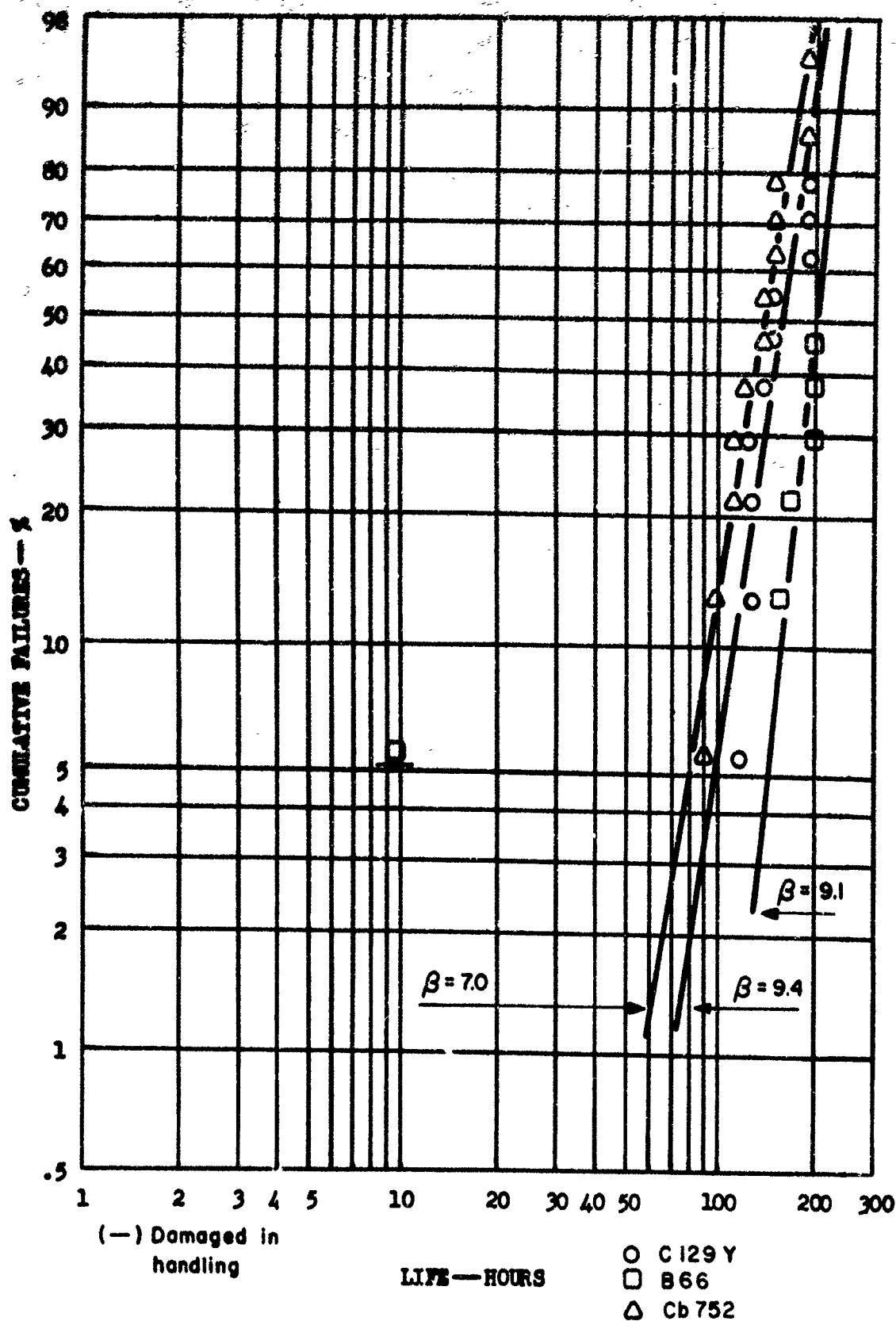
Percent Cumulative Failure vs. Cyclic Oxidation Life at 2500°F
 for Specimens Coated in Model Run 2
 Alloy Breakout



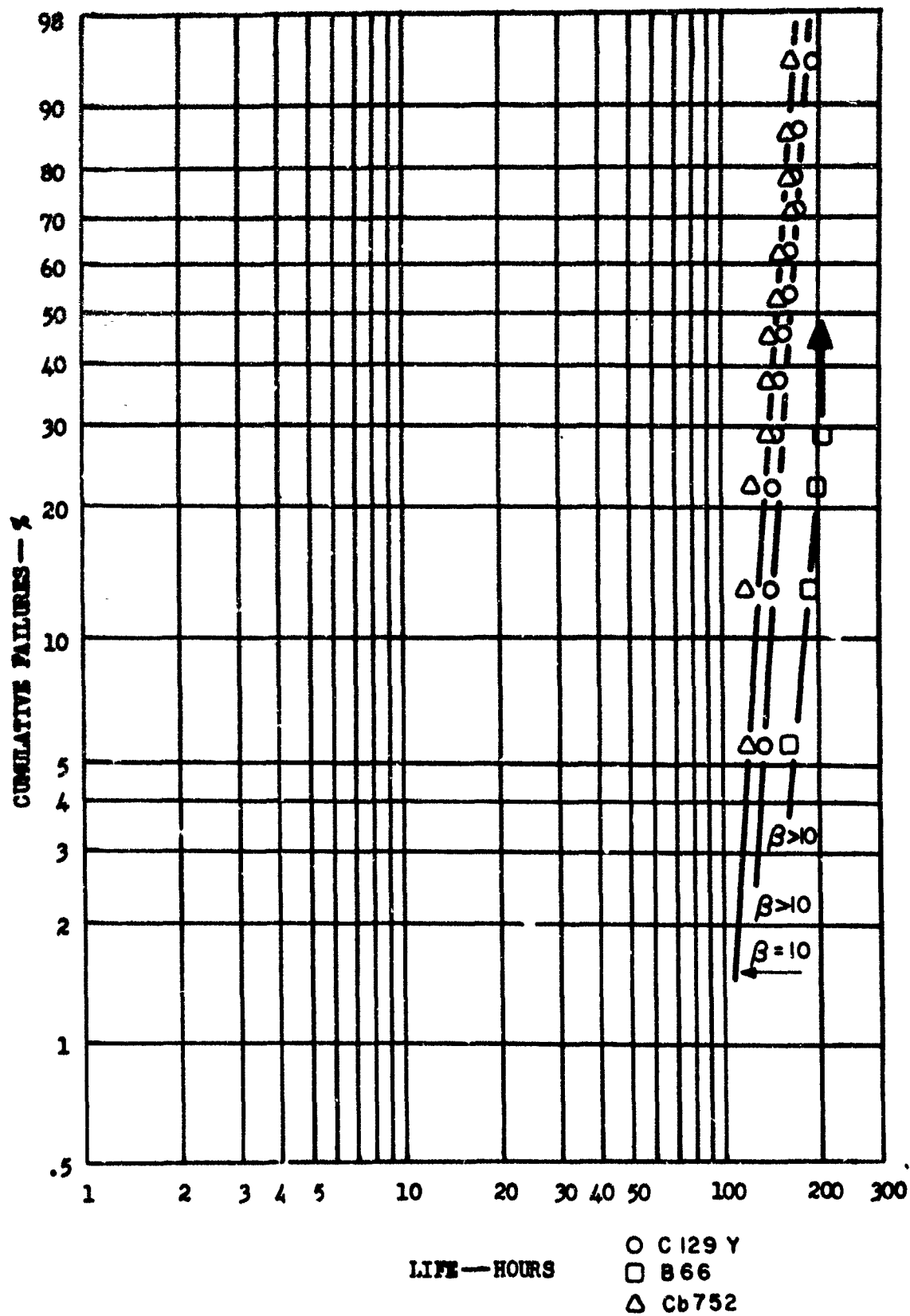
Percent Cumulative Failure vs. Cyclic Oxidation Life at 2500°F
for Specimens Coated in Module Run #3
Alloy Breakout



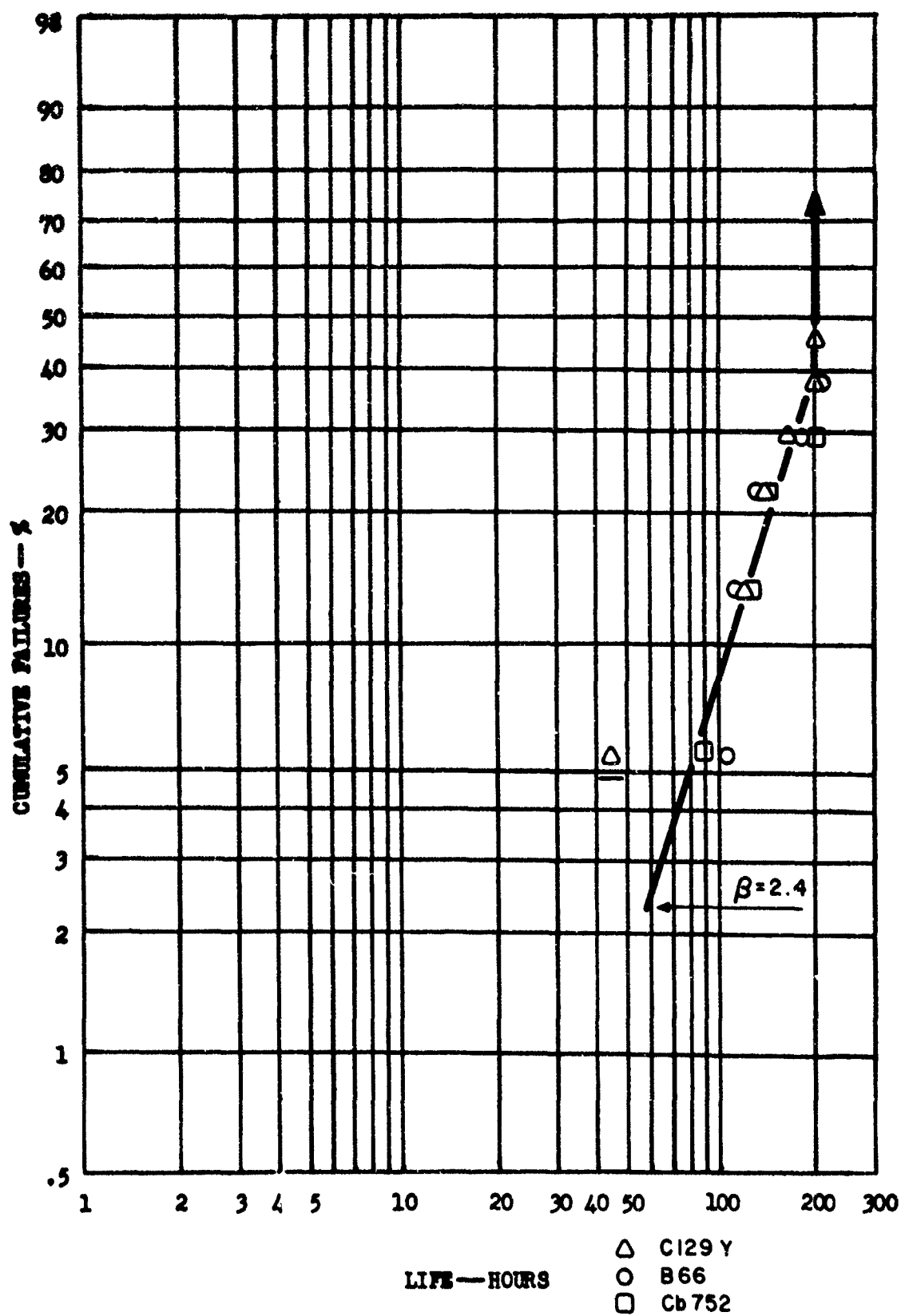
Percent Cumulative Failure Versus Cyclic Oxidation Life at 2500°F for Specimens Coated in Module Run #5, Alloy Breakout.



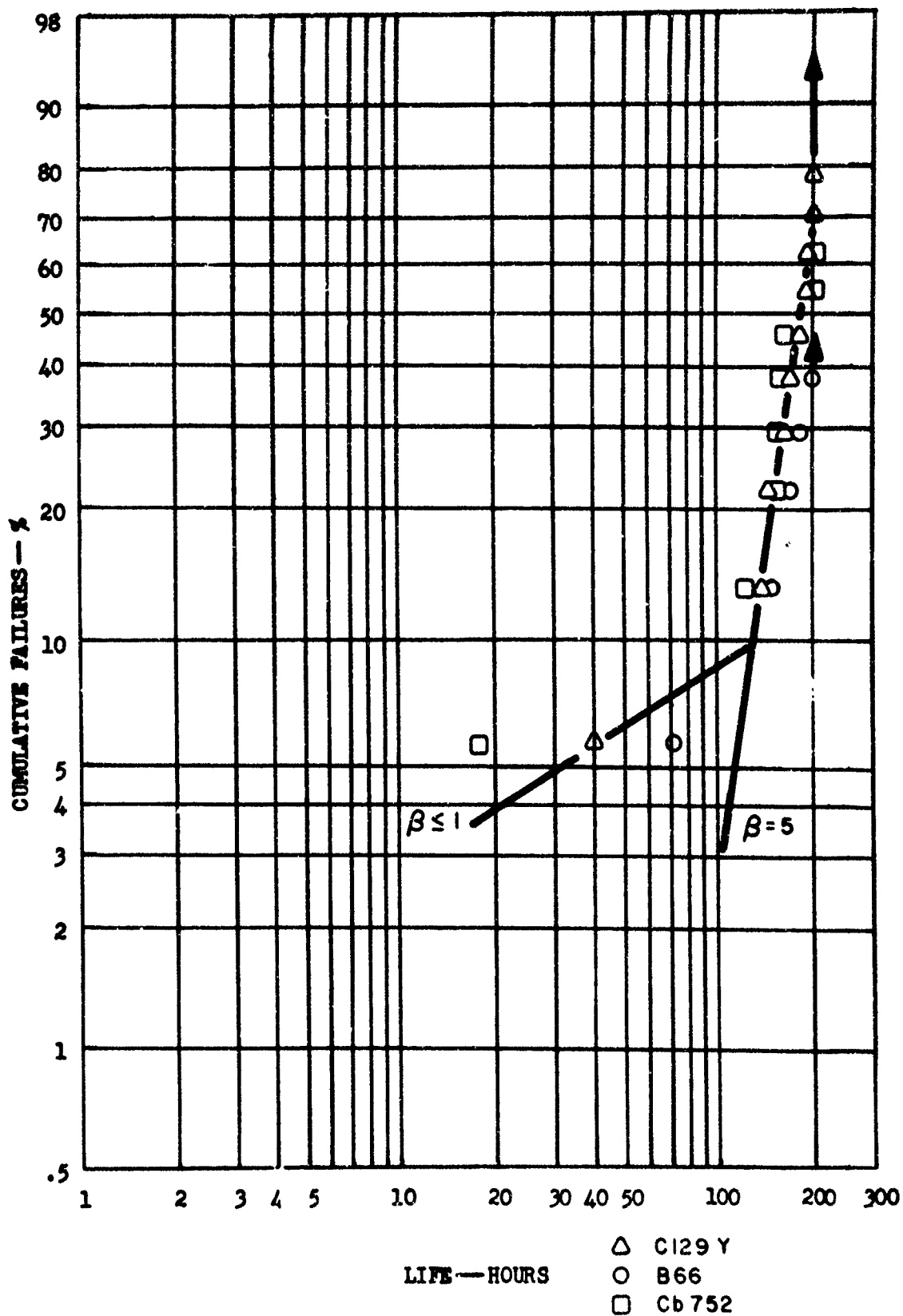
Percent Cumulative Failure Versus Cyclic Oxidation Life at 2500°F for Specimens Coated in Module Run #10, Alloy Breakout.



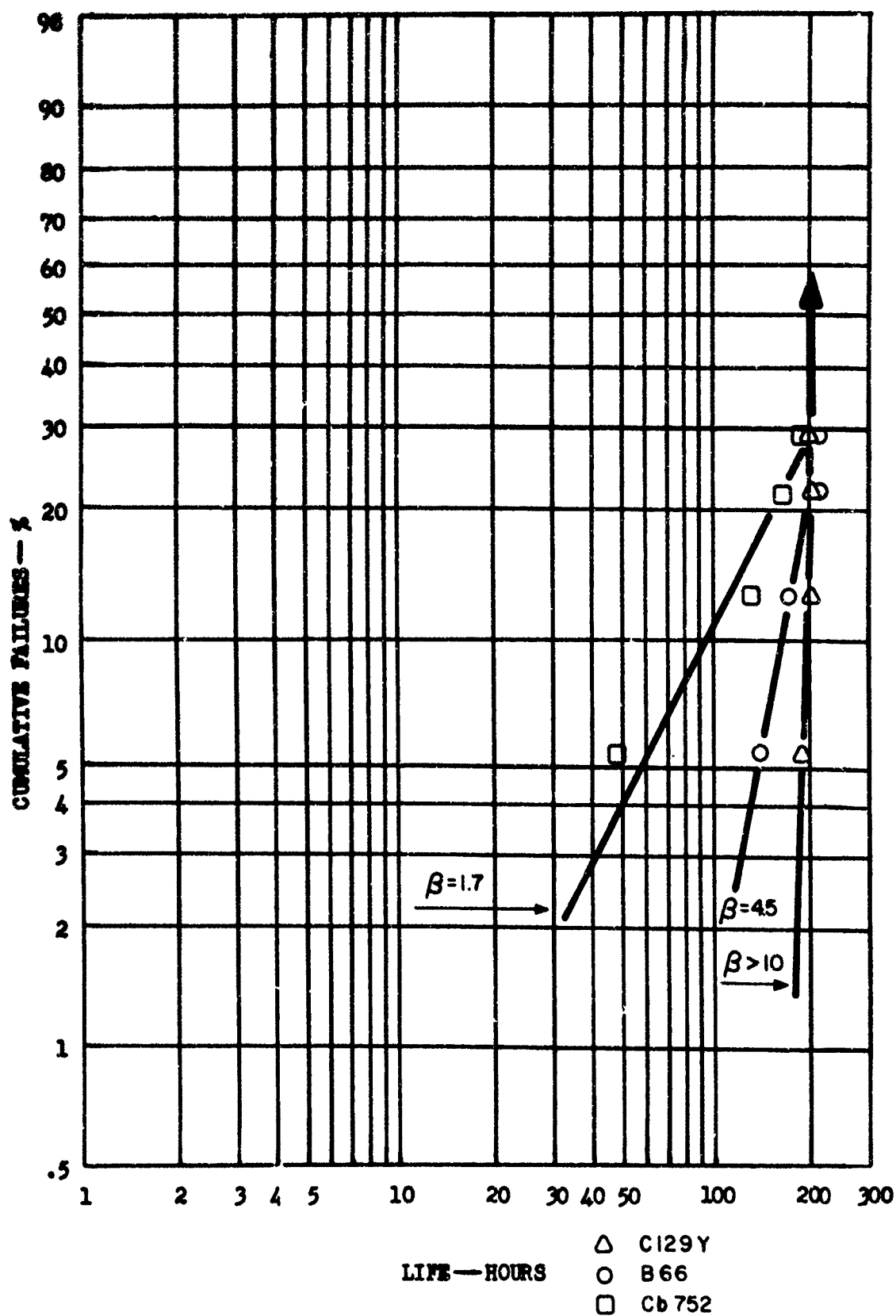
Percent Cumulative Failure Versus Cyclic Oxidation Life at 2500°F for Specimens Coated in Module Run #11, Alloy Breakout.



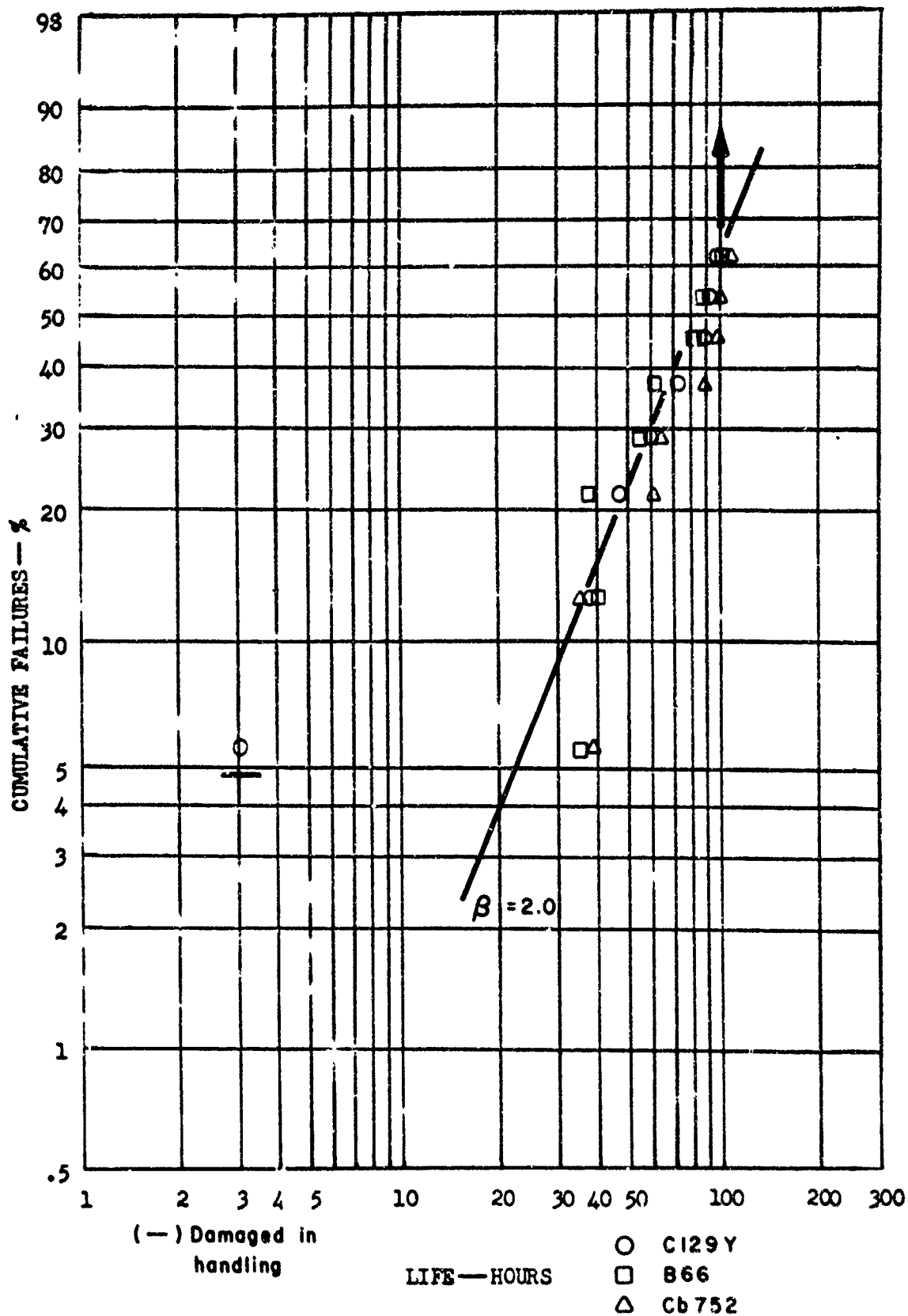
Percent Cumulative Failure vs. Cyclic Oxidation Life
At 2500°F For Specimens Coated In Module Run #13-
Alloy Breakout



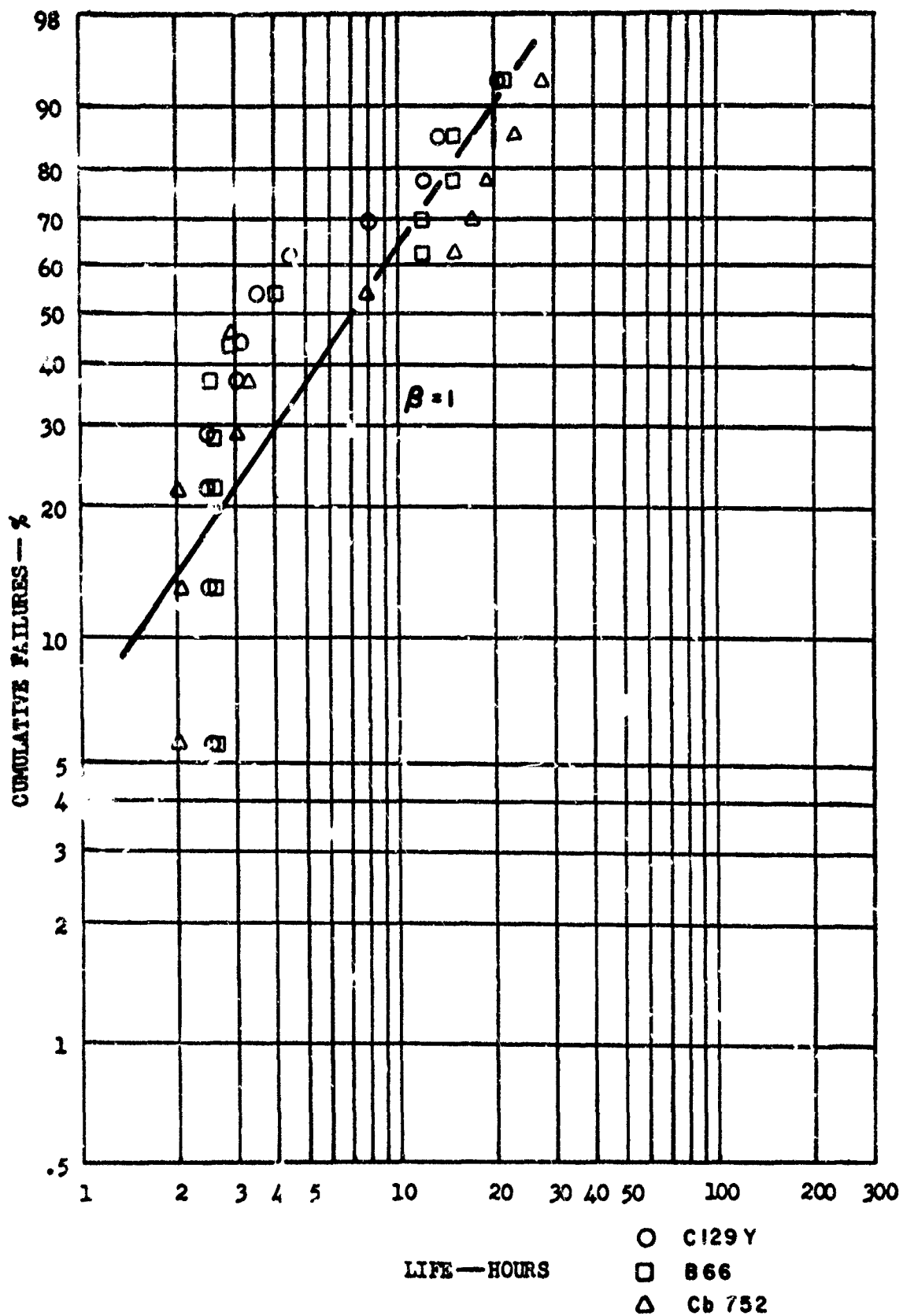
Percent Cumulative Failure vs. Cyclic Oxidation Life
At 2500°F For Specimens Coated In Module Run #14-
Alloy Breakout



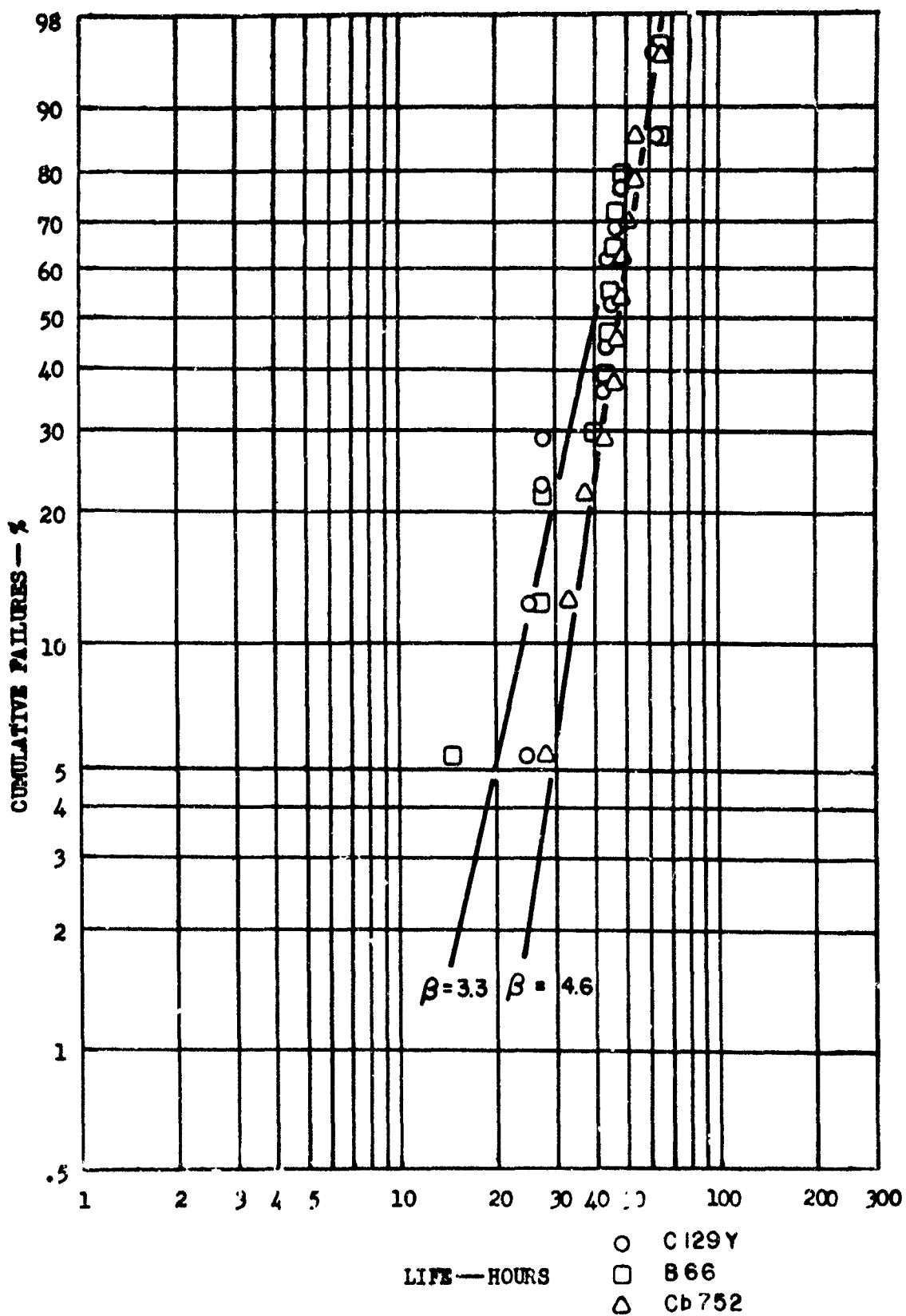
Percent Cumulative Failure vs. Cyclic Oxidation Life
At 2500°F For Specimens Coated In Module Run #15-
Alloy Breakout



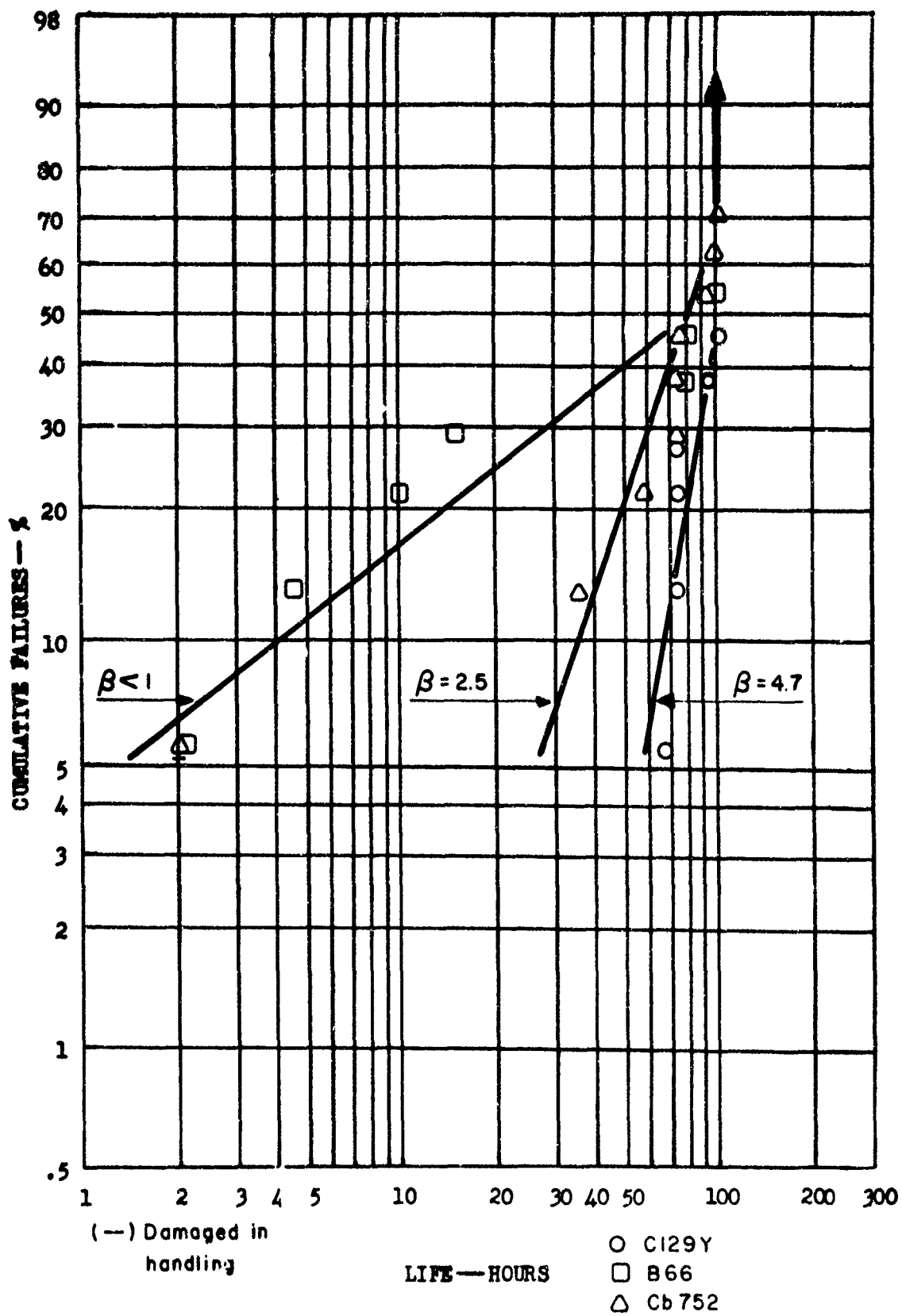
Percent Cumulative Failure vs. Cyclic Oxidation Life at 2700°F
for Specimens Coated in Module Run #1
Alloy Breakout



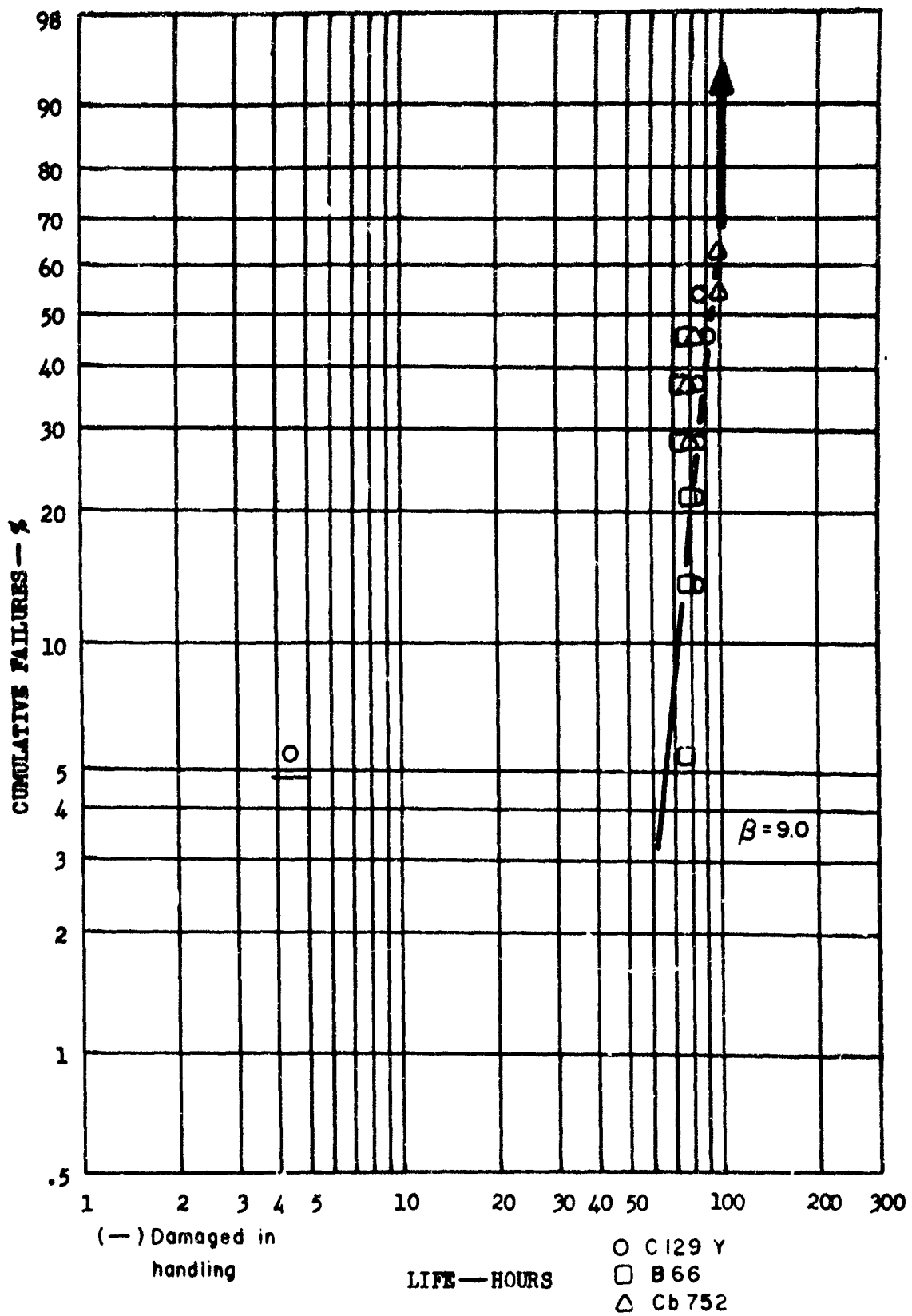
Percent Cumulative Failure vs. Cyclic Oxidation Life at 2700°F
for Specimens Coated in Module Run #3
Alloy Breakout



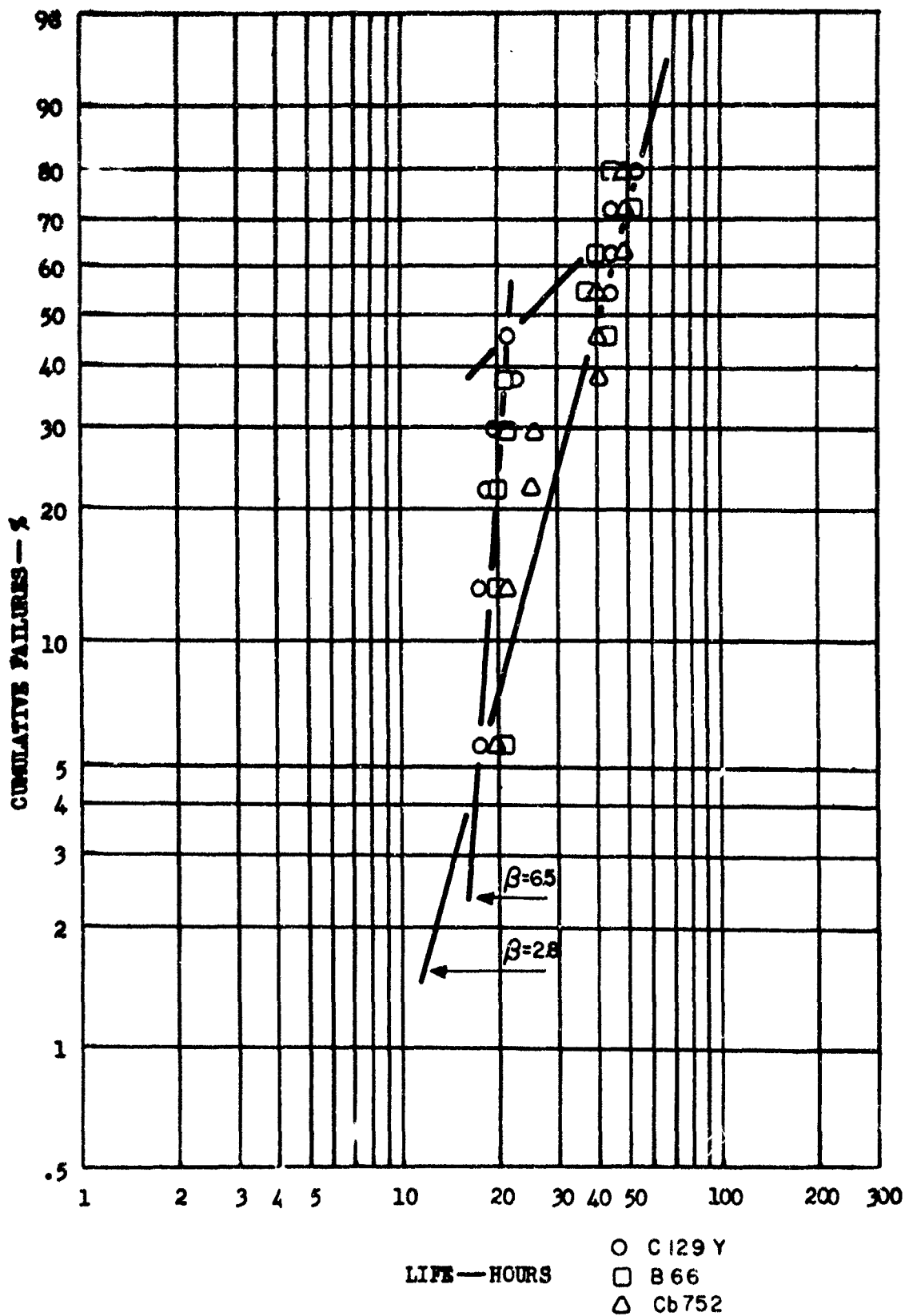
Percent Cumulative Failure Versus Cyclic Oxidation Life at 2700°F for Specimens Coated in Molybdenum Run #4, Alloy Breakout.



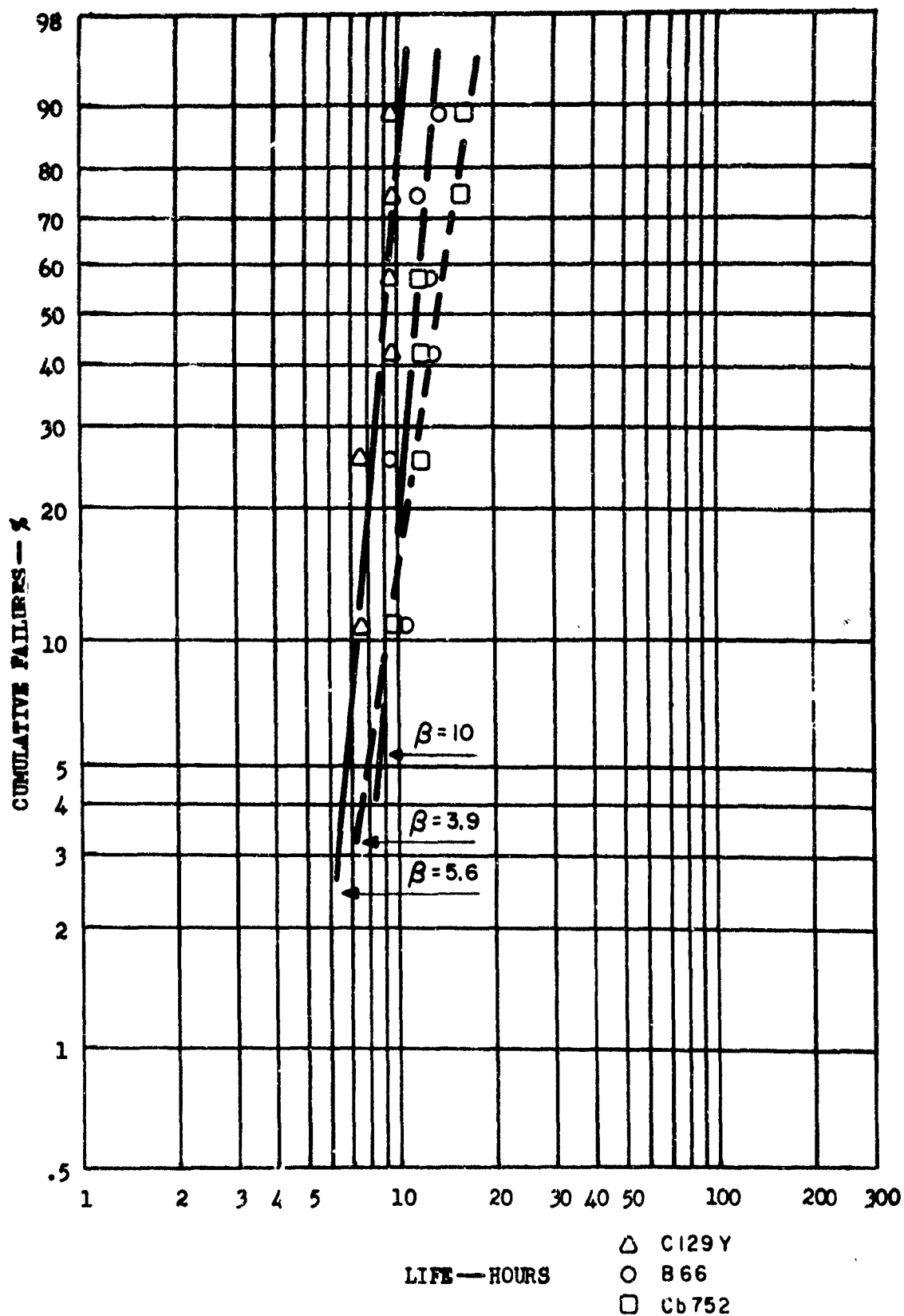
Percent Cumulative Failure Versus Cyclic Oxidation Life at 2700°F for Specimens Coated in Module Run #5, Alloy Breakout.



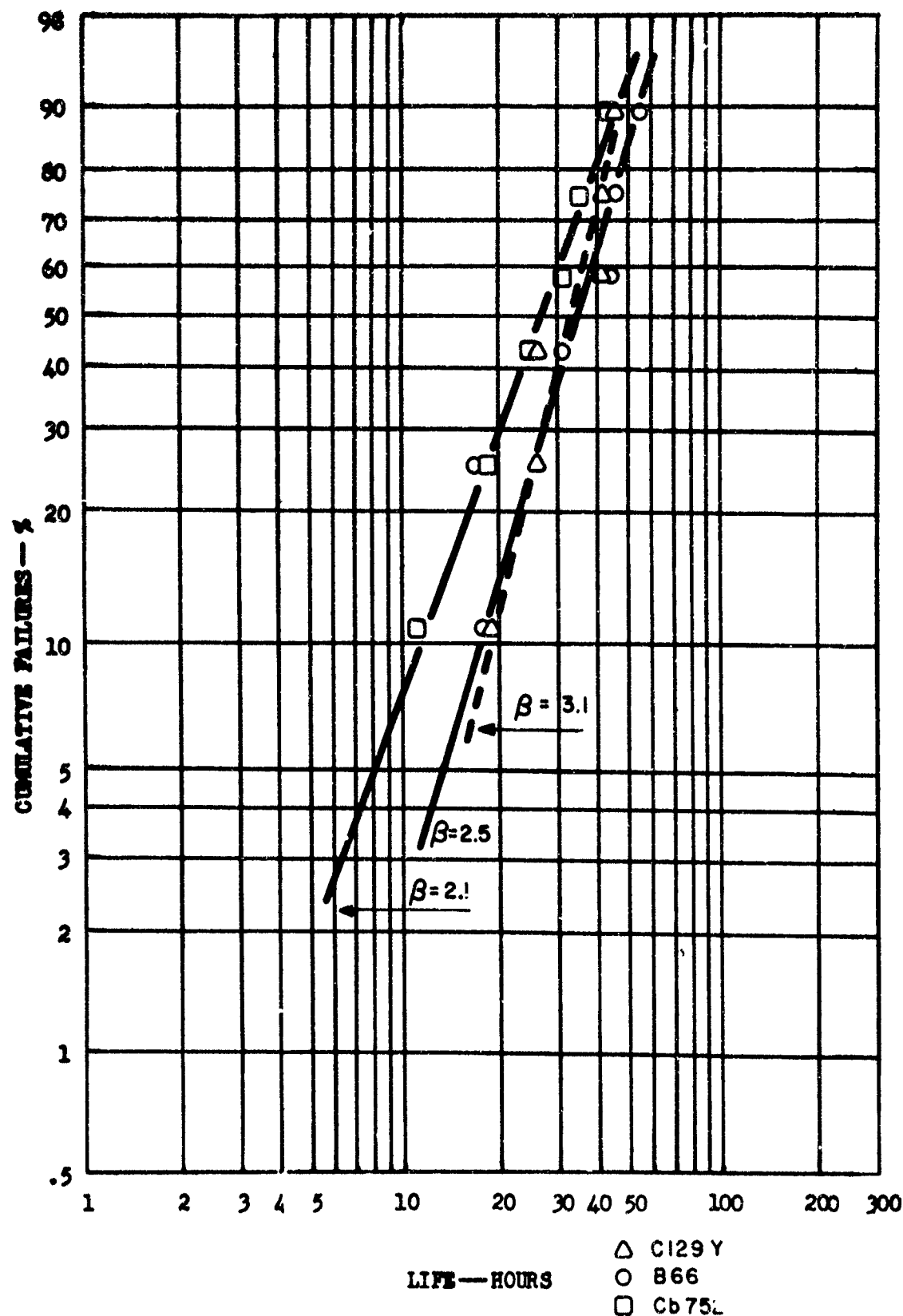
Percent Cumulative Failure Versus Cyclic Oxidation Life at 2700°F for Specimens Coated in Module Run #10, Alloy Breakout.



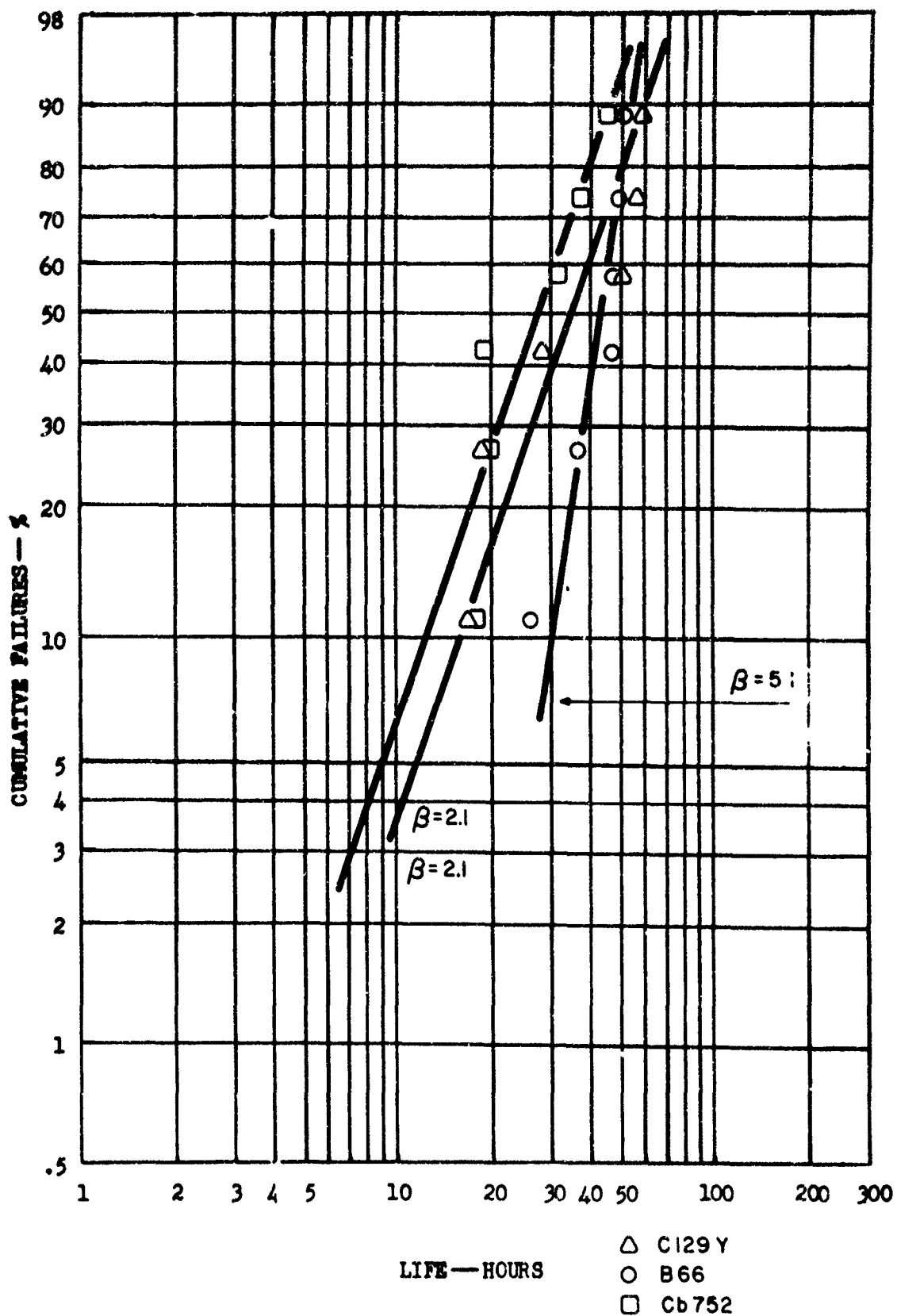
Percent Cumulative Failure Versus Cyclic Oxidation Life at 2700°F for Specimens Coated in Module Run #11, Alloy Breakout.



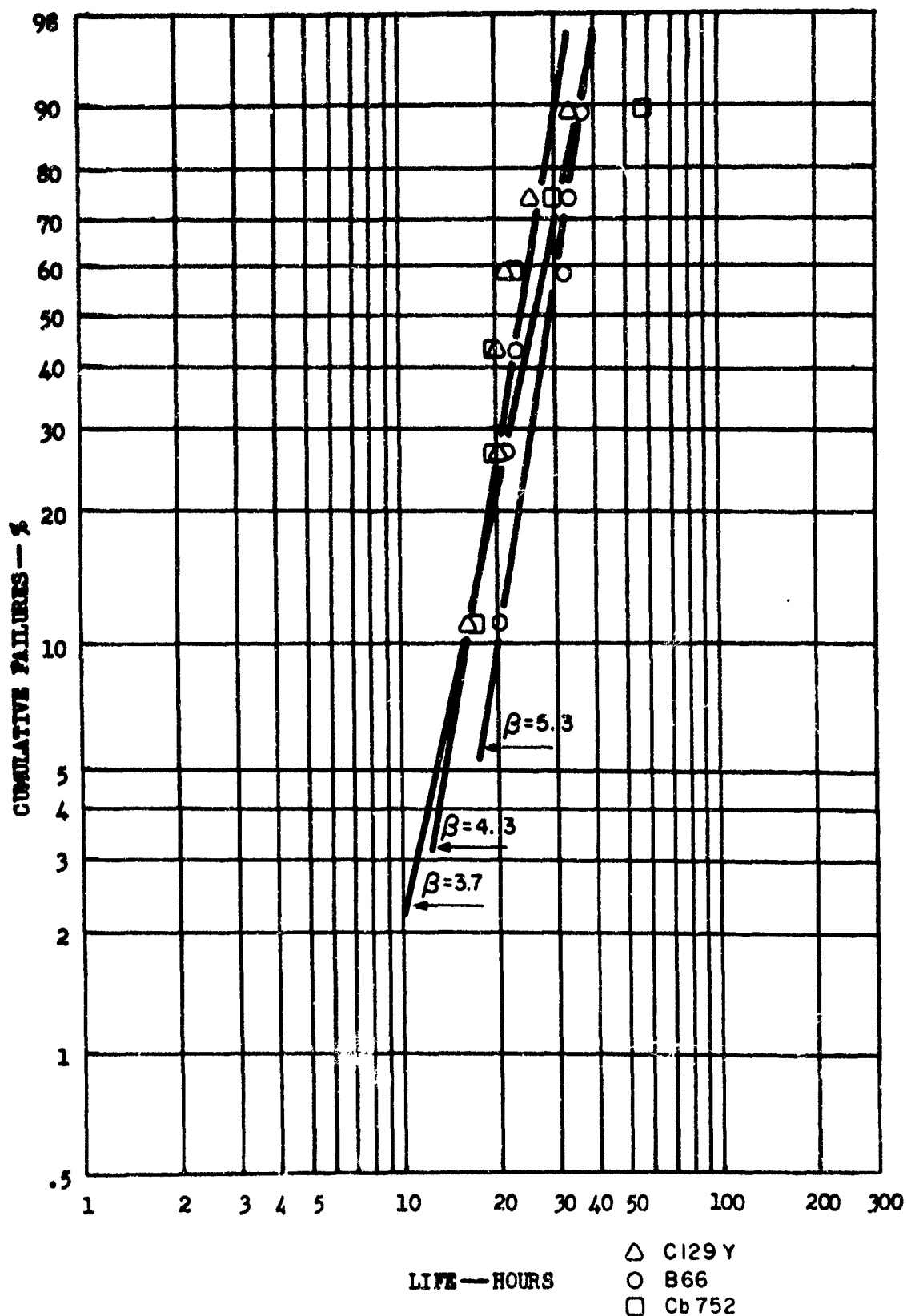
Percent Cumulative Failure vs. Cyclic Oxidation Life
At 2700°F For Specimens Coated In Module Run #12-
Alloy Breakout



Percent Cumulative Failure vs. Cyclic Oxidation Life
At 2700°F For Specimens Coated In Module Run #13-
Alloy Breakout



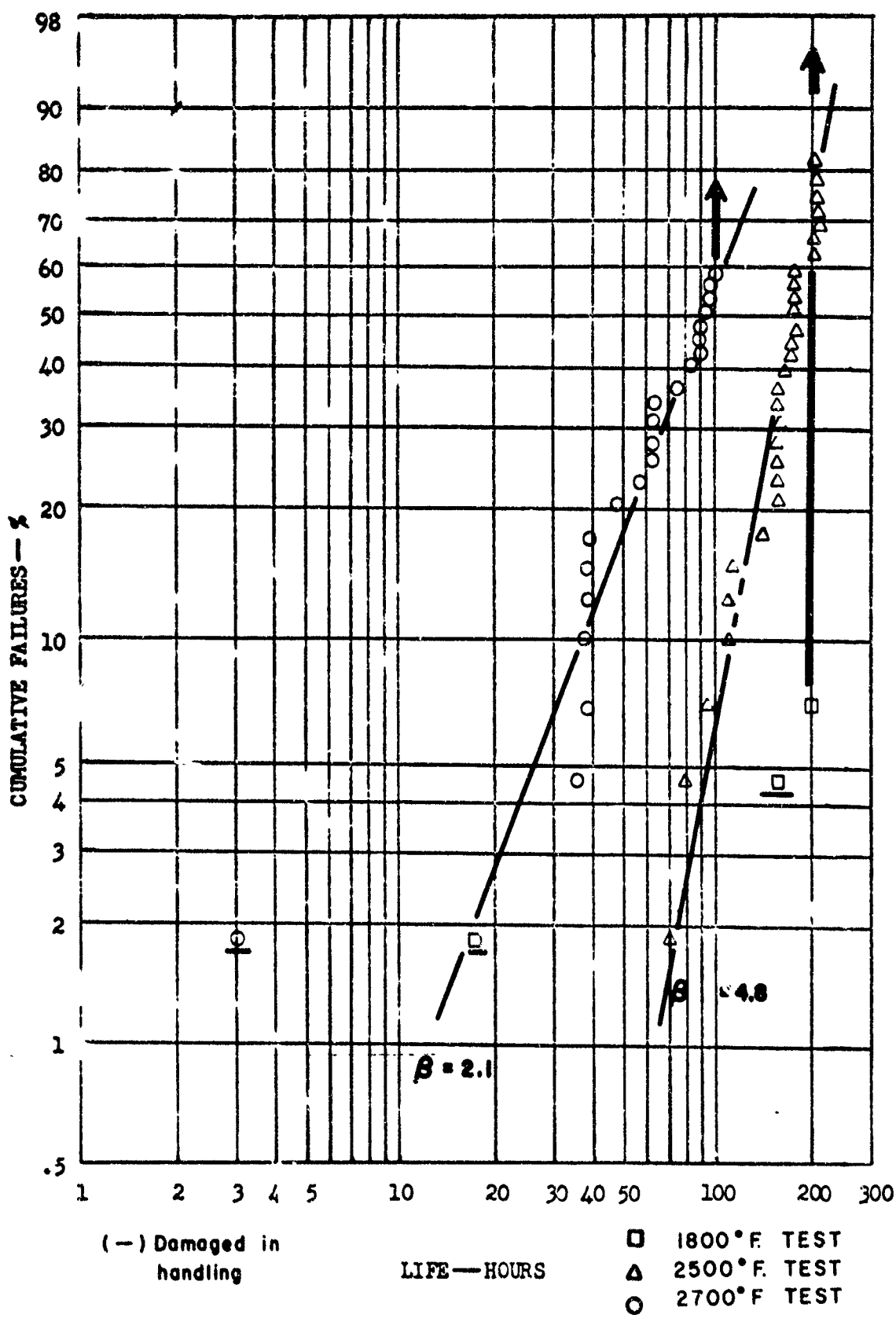
Percent Cumulative Failure vs. Cyclic Oxidation Life
 At 2700°F For Specimens Coated In Module Run #14-
 Alloy Breakout



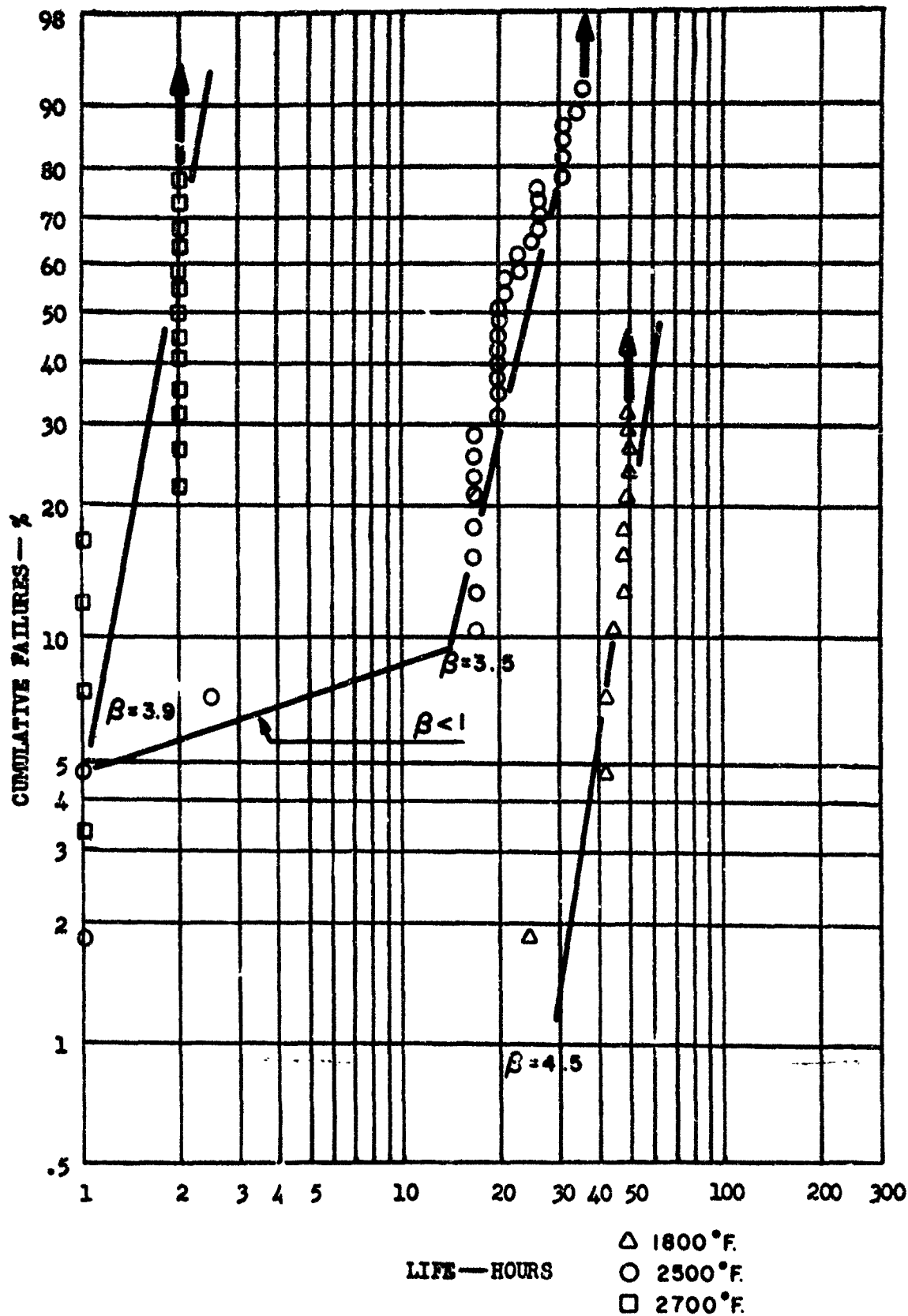
Percent Cumulative Failure vs. Cyclic Oxidation Life
At 2700°F For Specimens Coated In Module Run #15-
Alloy Breakout

APPENDIX IV SUMMARY OF OXIDATION LIVES OF COUPONS
COATED IN MODULE RUNS 1-15

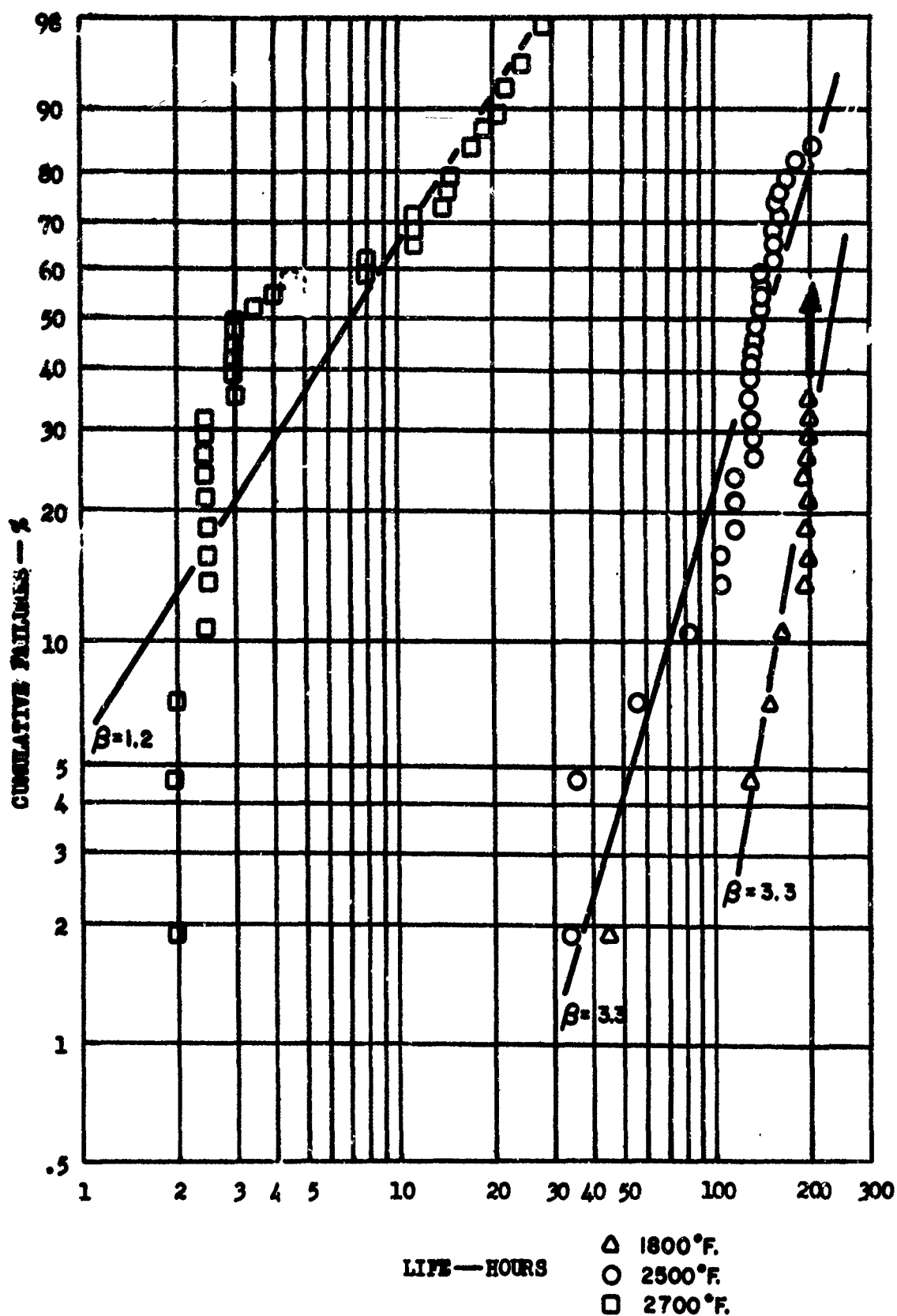
Coupons coated in Modules 8 and 9 were not oxidation tested.



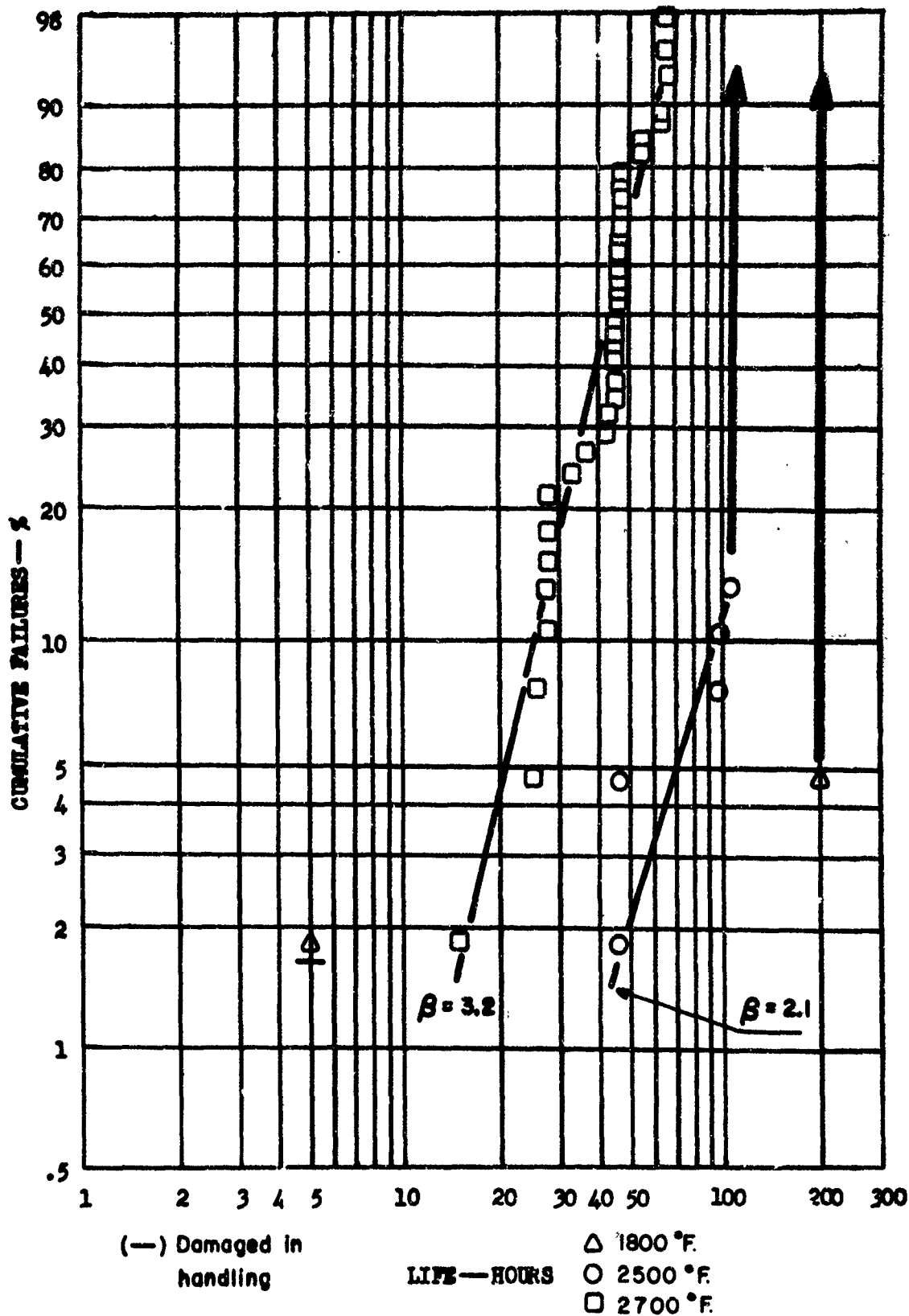
Percent Cumulative Failure vs. Cyclic Oxidation Life for All Specimens Coated in Module Run #1



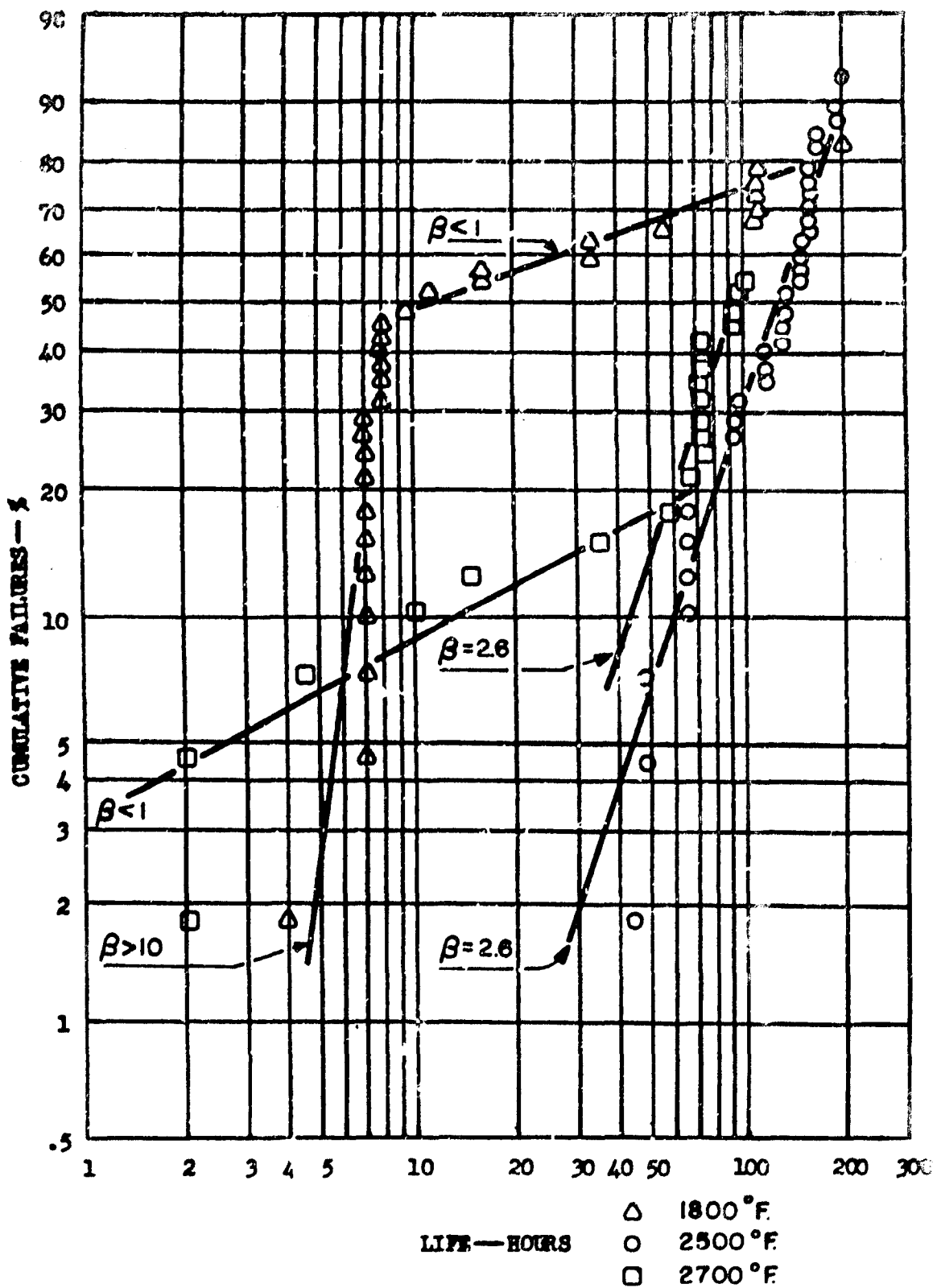
Percent Cumulative Failure vs. Cyclic Oxidation Life for All Specimens Coated in Module Run #2



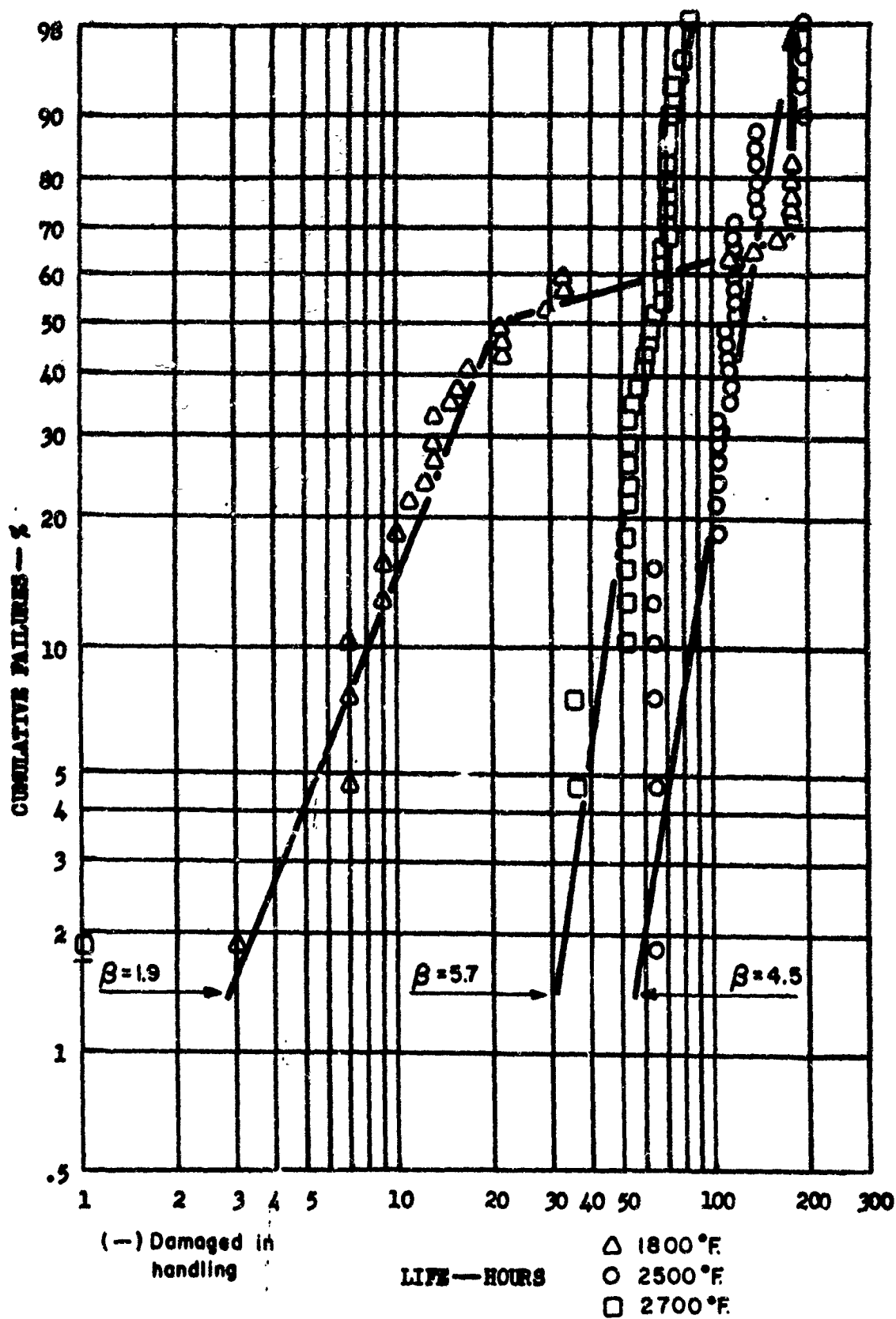
Percent Cumulative Failure vs. Cyclic Oxidation Life for All Specimens Coated in Module Run #3



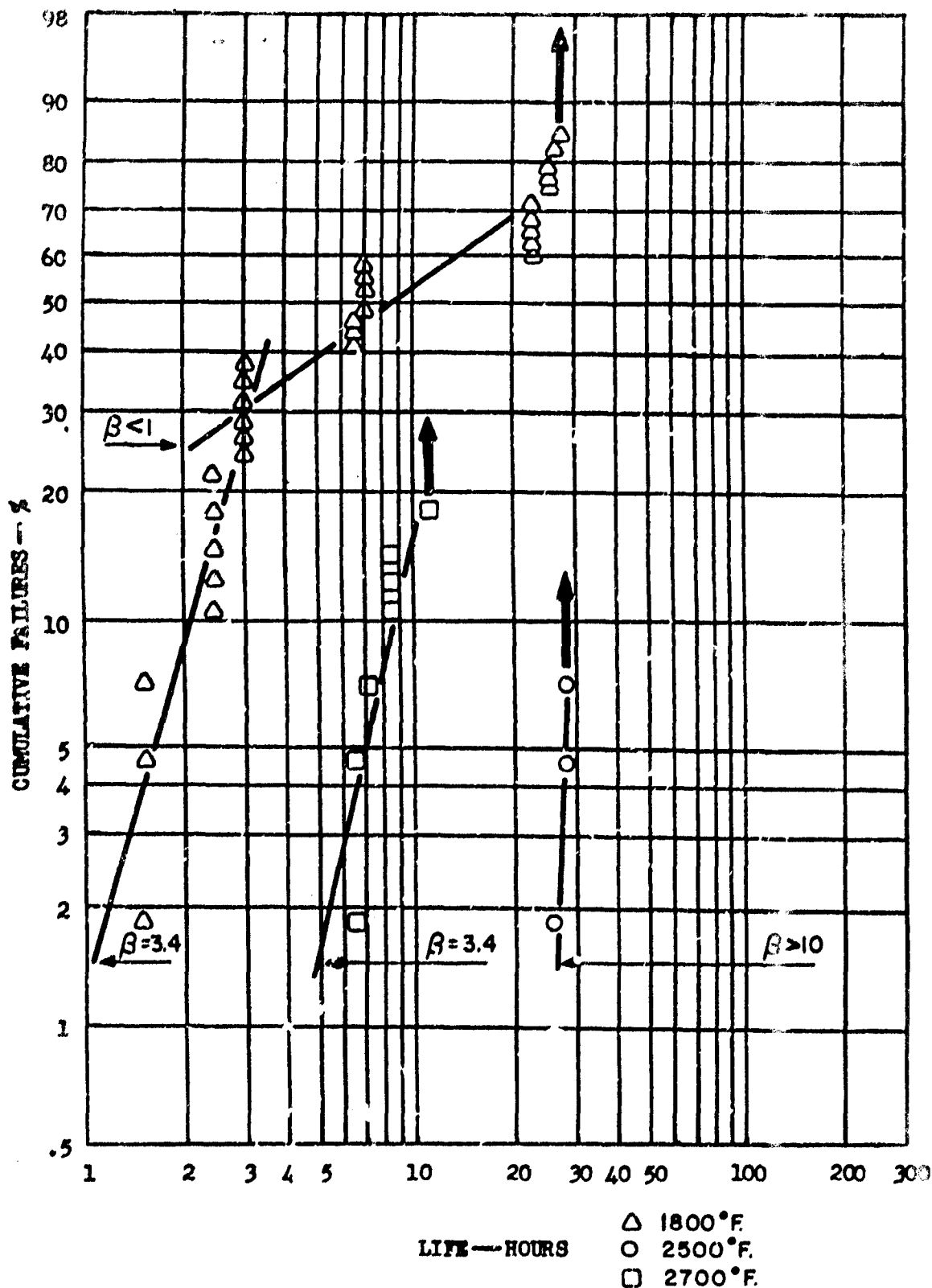
Percent Cumulative Failure Versus Cyclic Oxidation Life for All Specimens Coated in Module Run #4.



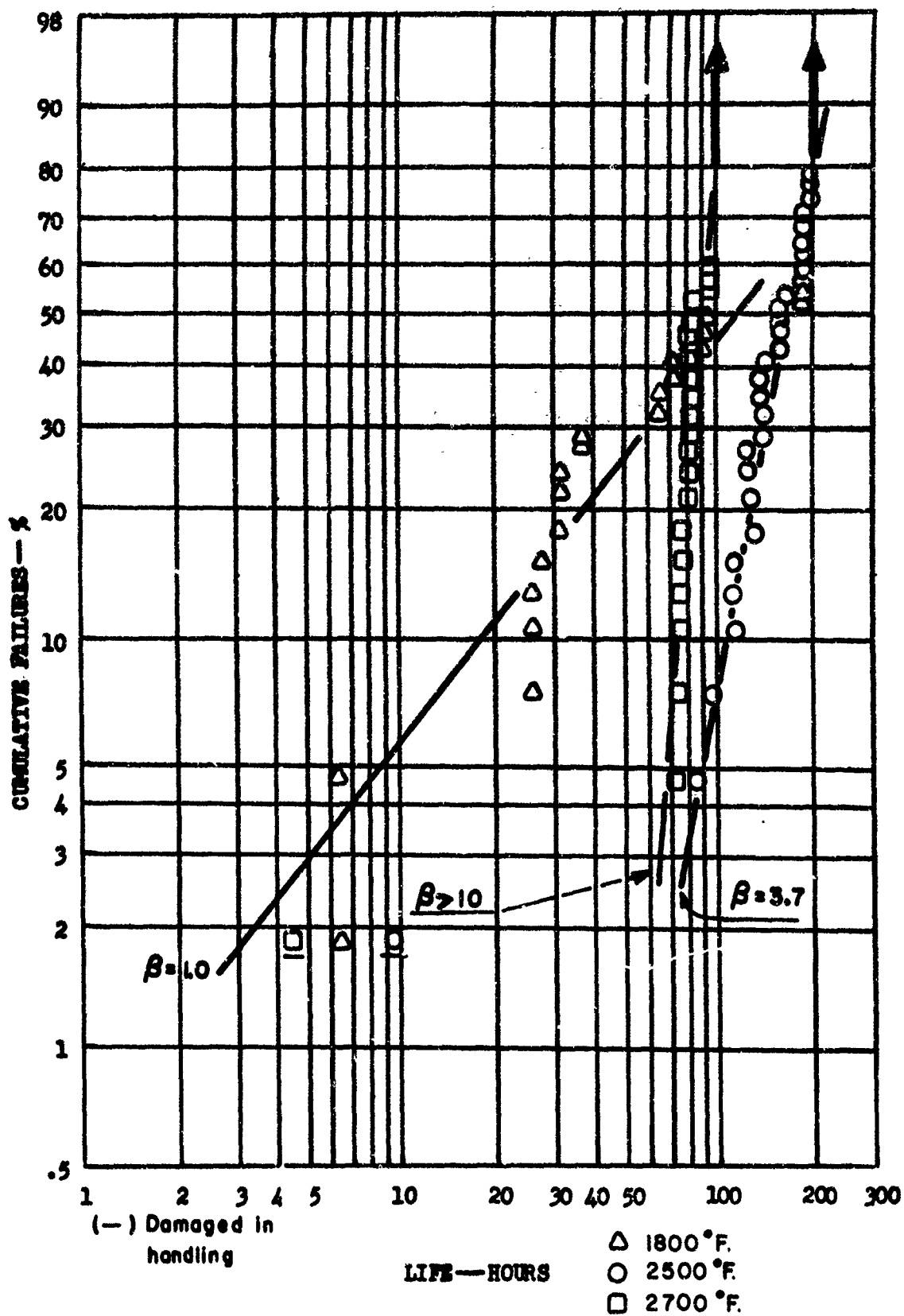
Percent Cumulative Failure Versus Cyclic Oxidation Life for All Specimens Coated in Module Run #5.



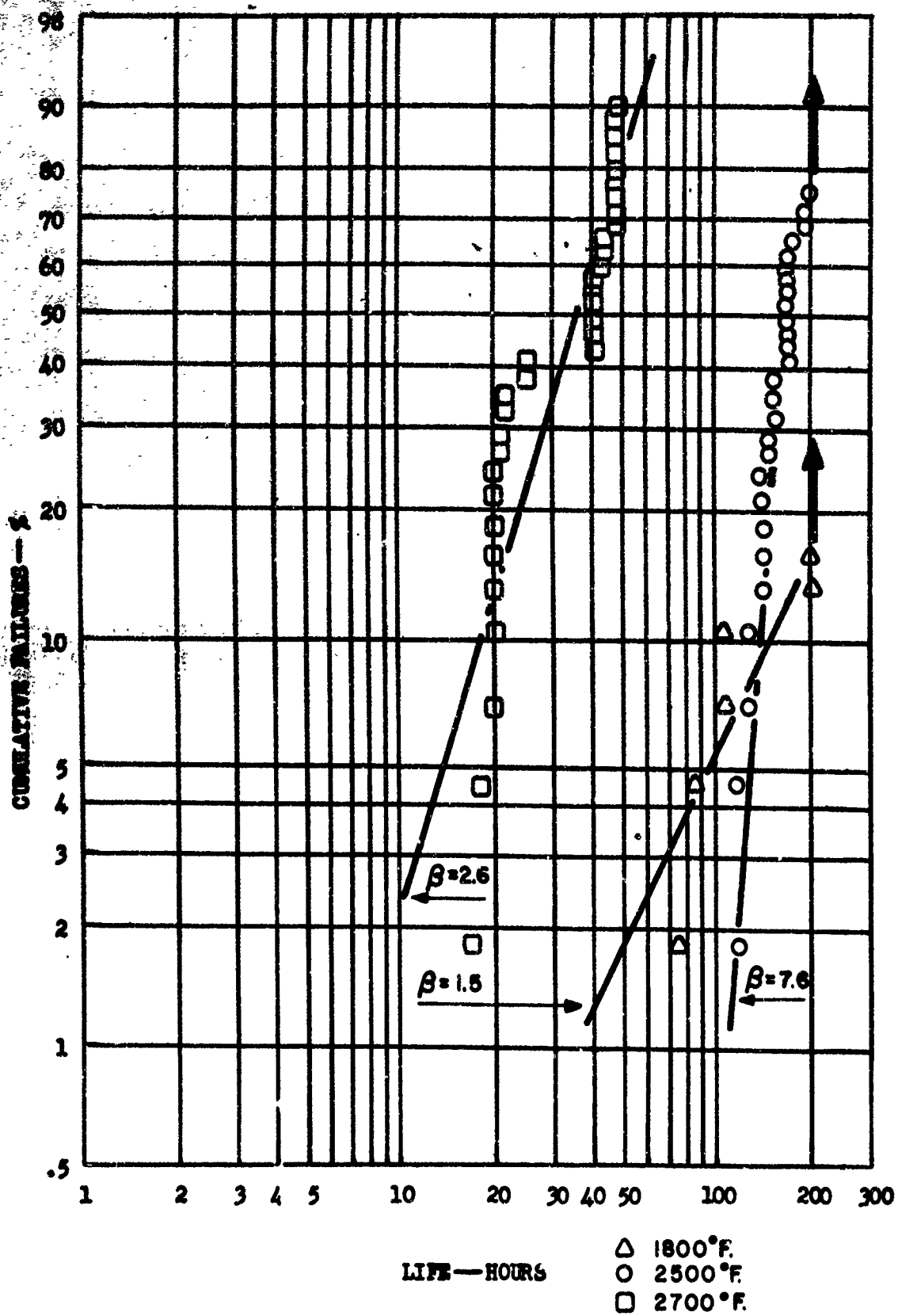
Percent Cumulative Failure Versus Cyclic Oxidation Life for All Specimens Coated in Module Run #6.



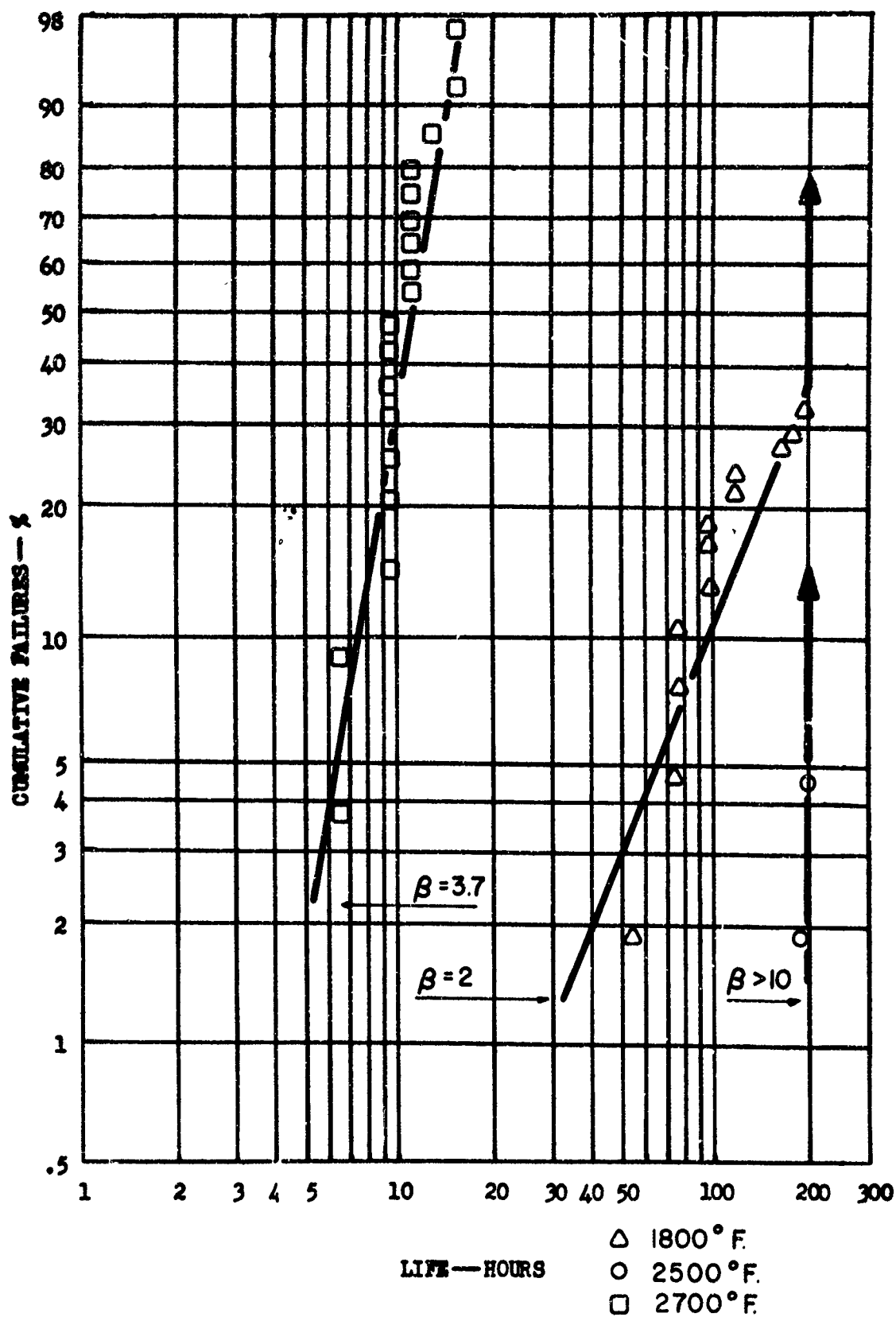
Percent Cumulative Failure Versus Cyclic Oxidation Life for All Specimens Coated in Module Run #7.



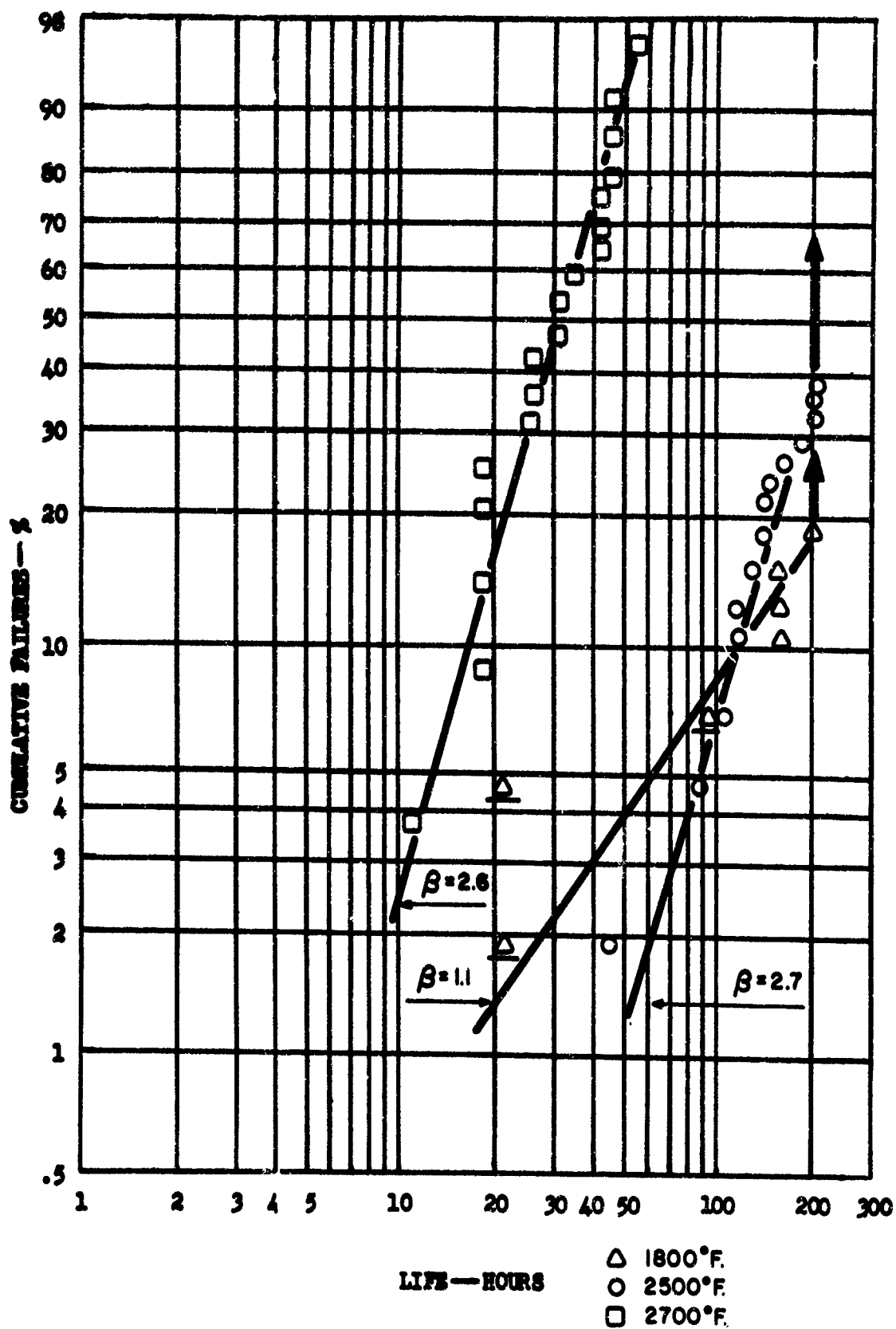
Percent Cumulative Failure Versus Cyclic Oxidation Life for All Specimens Coated in Module Run #10.



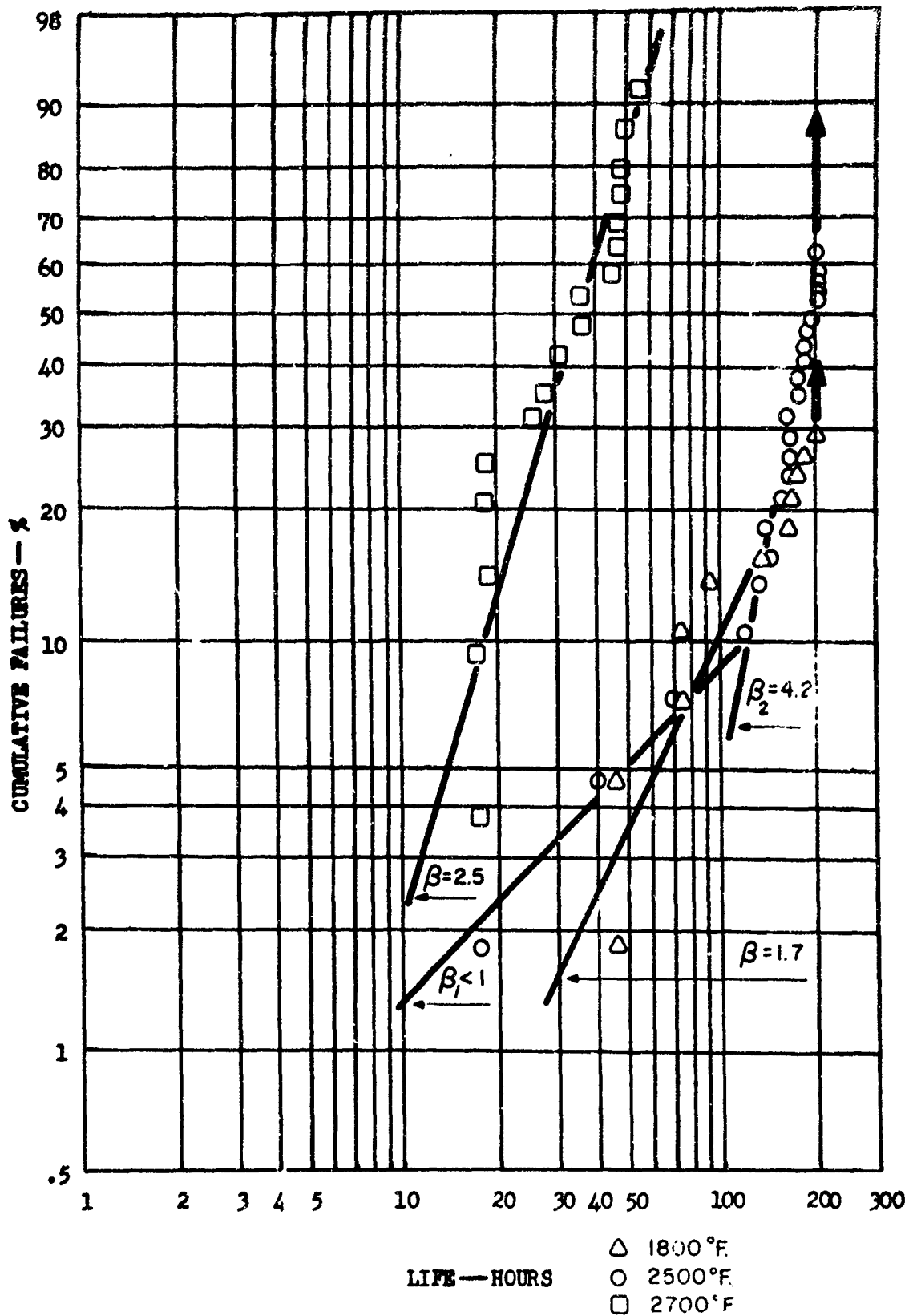
Percent Cumulative Failure Versus Cyclic Oxidation Life for All Specimens Coated in Module Run #11.



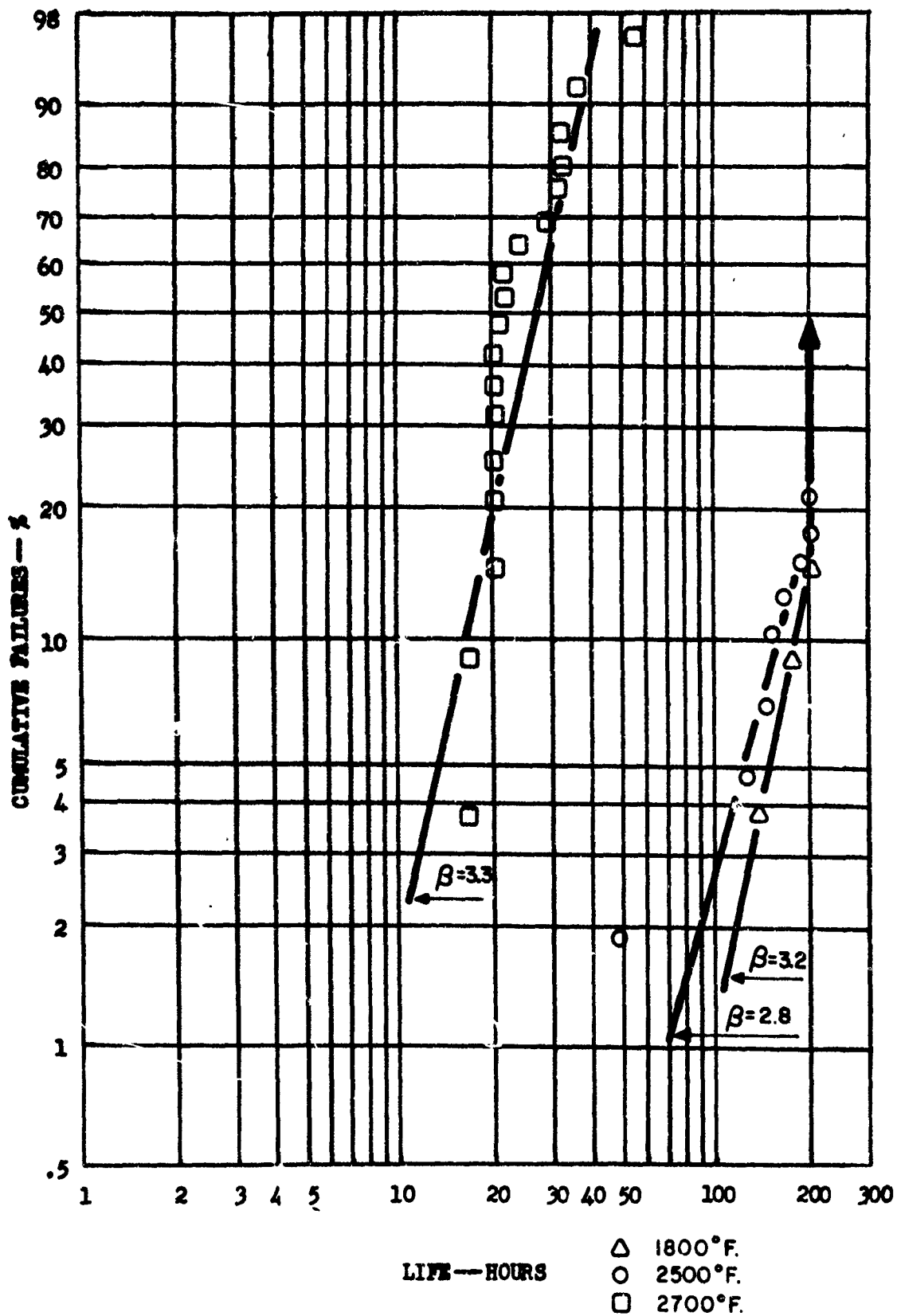
Percent Cumulative Failure vs. Cyclic Oxidation Life
For All Specimens Coated In Module Run #12



Percent Cumulative Failure vs. Cyclic Oxidation Life
For All Specimens Coated In Module Run #13

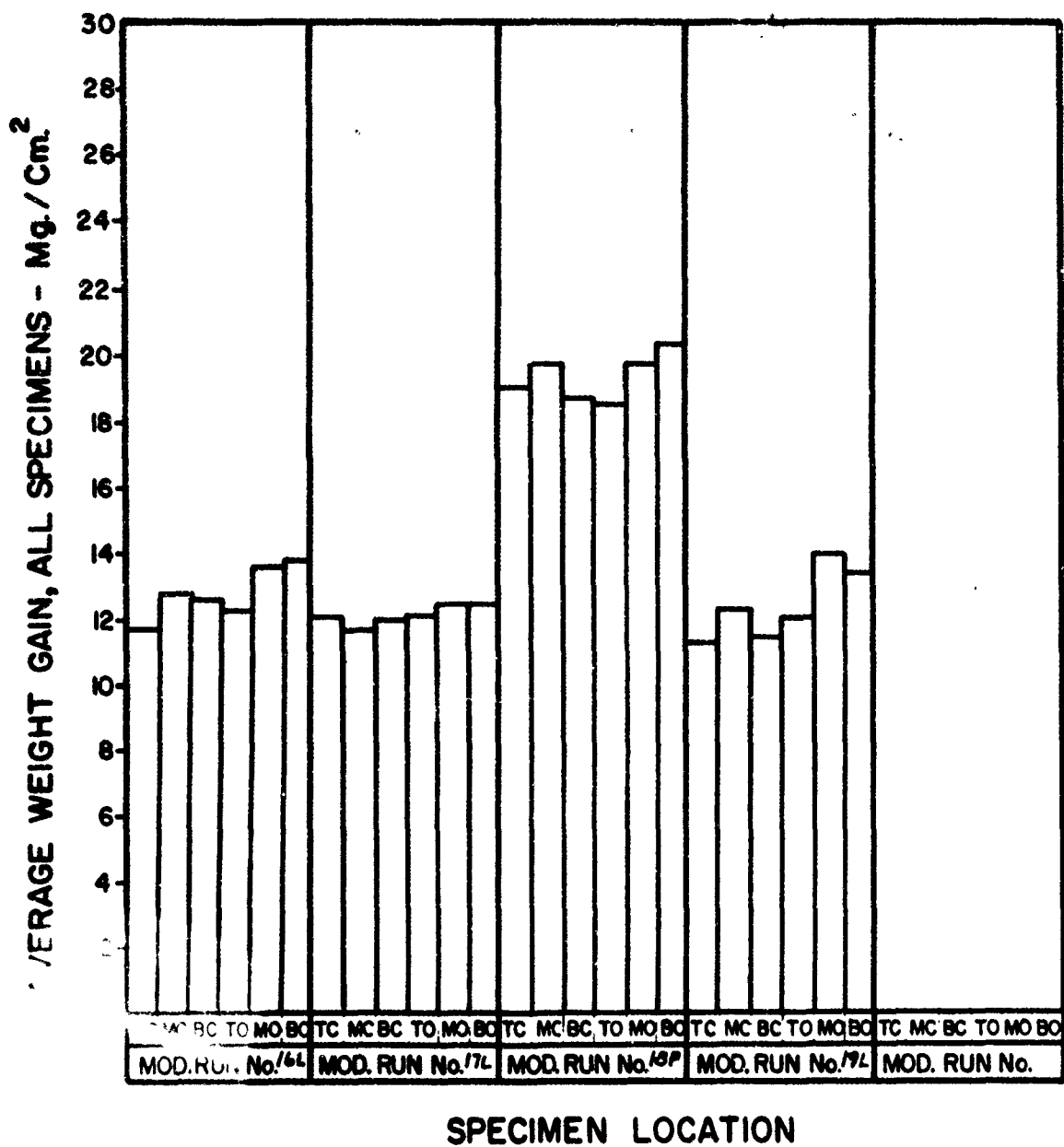


Percent Cumulative Failure vs. Cyclic Oxidation Life
For All Specimens Coated In Module Run #14

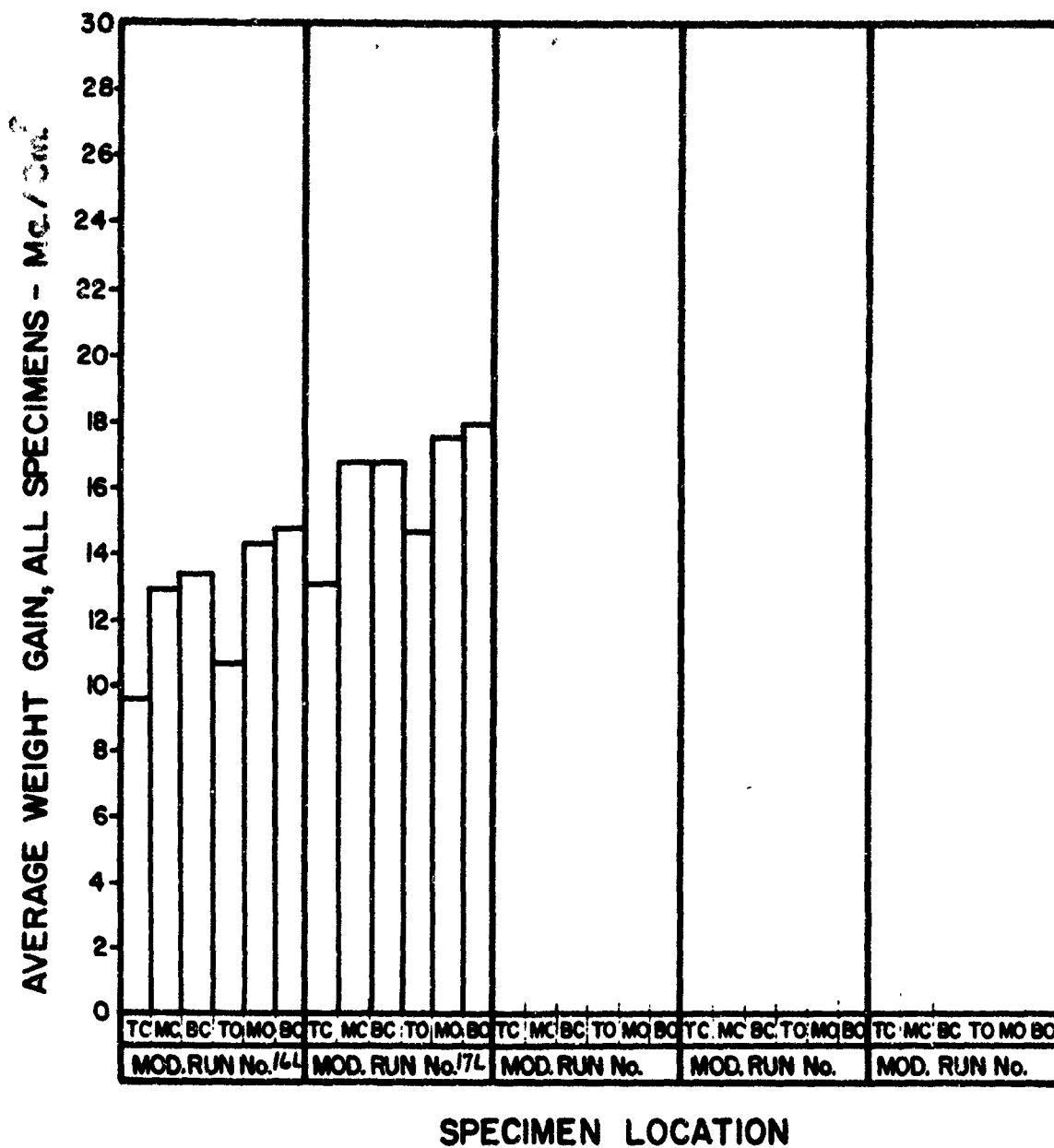


Percent Cumulative Failure vs. Cyclic Oxidation Life
Of All Specimens Coated In Module Run #15

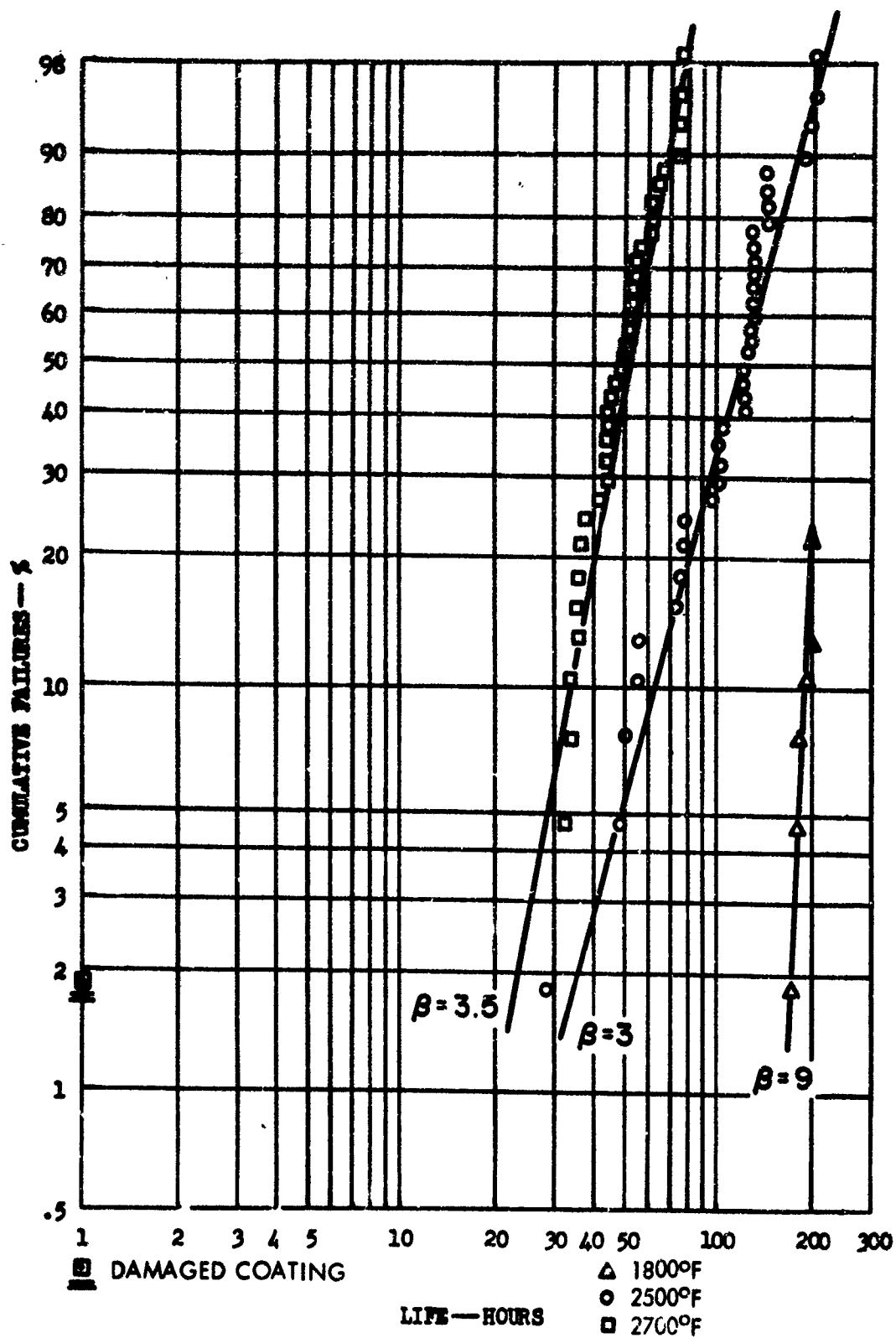
APPENDIX V RESULTS OF MODULE STUDIES CONDUCTED IN THE
PRODUCTION SCALE FURNACE-COATING WEIGHT GAIN AND OXIDATION TEST DATA



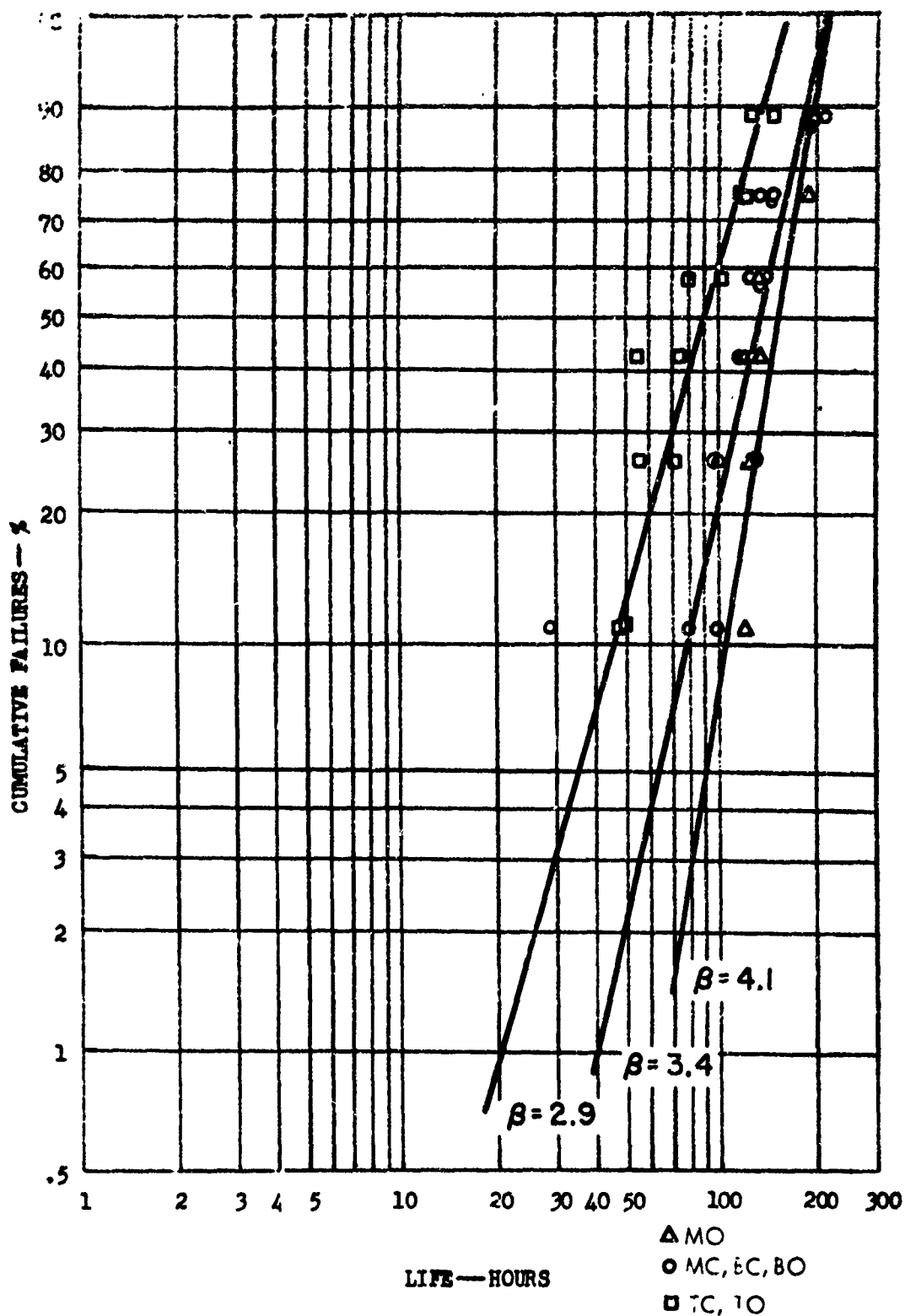
Average Weight Gains Resulting from Cr-Ti Coating Columbium Alloy Specimens



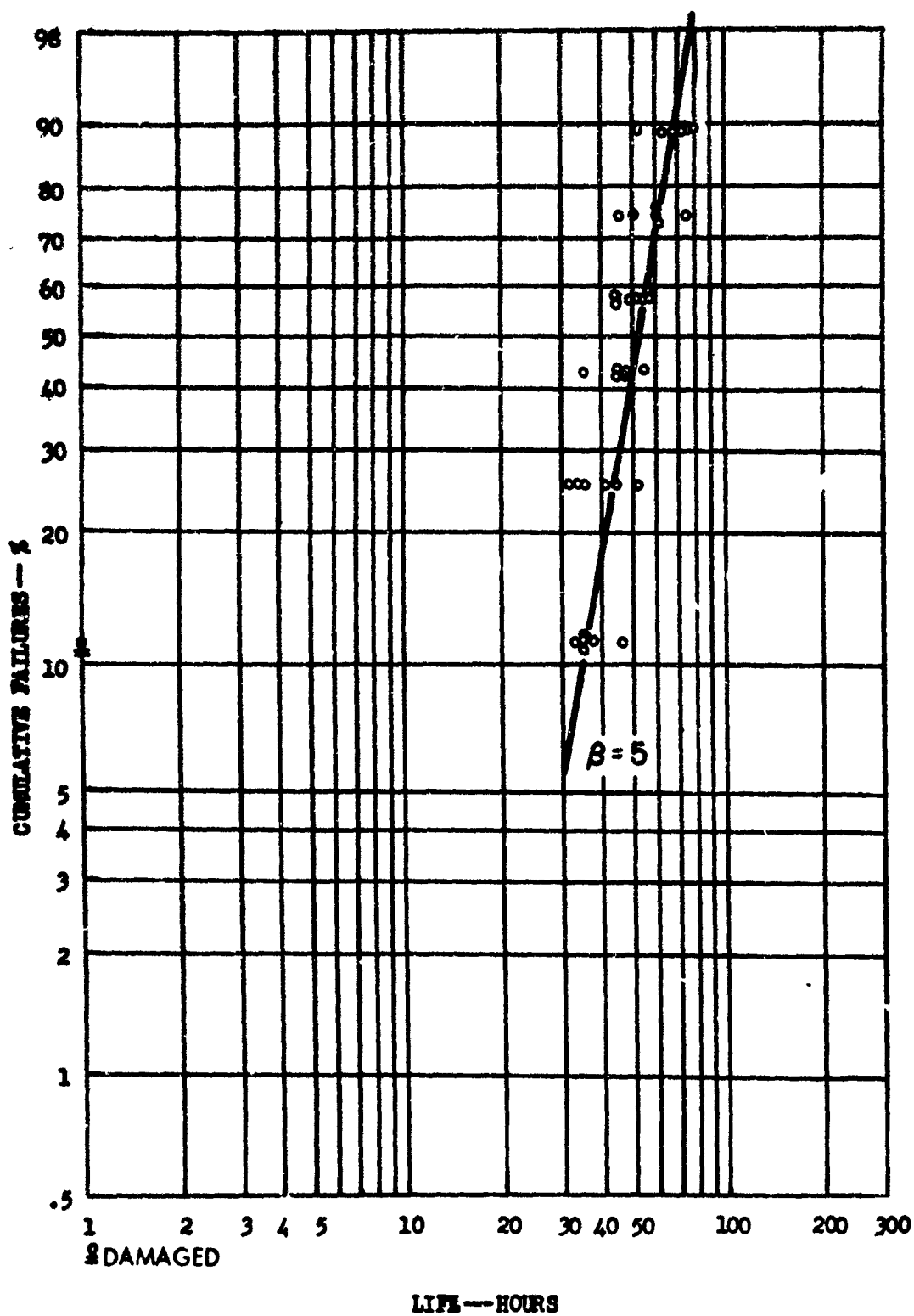
Average Weight Gains Resulting from Silicon Coating Cr-Ti Coated Columbium Alloy Specimens



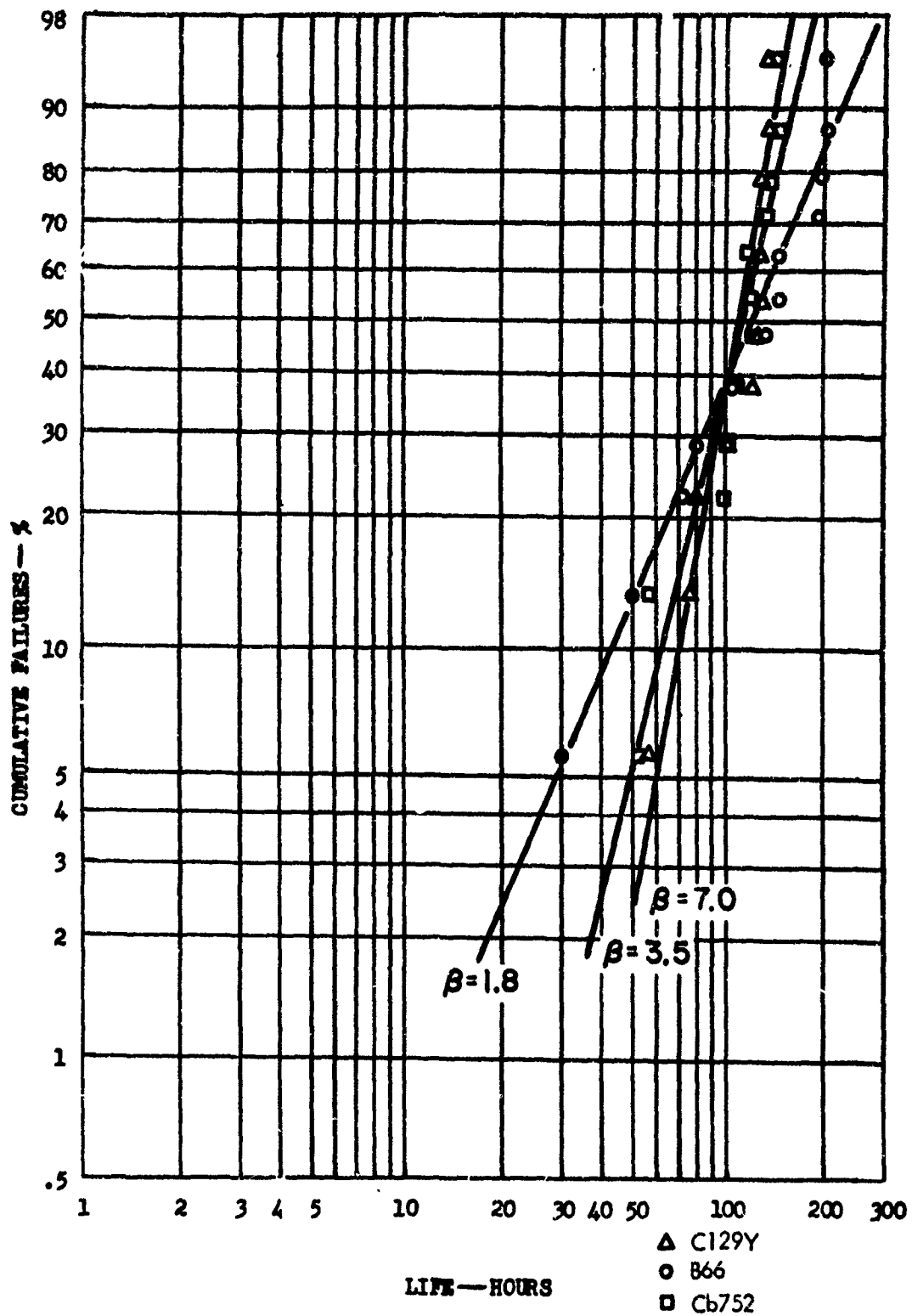
Percent Cumulative Failure Vs. Cyclic Oxidation Life for All Specimens Coated in Module Run 16L



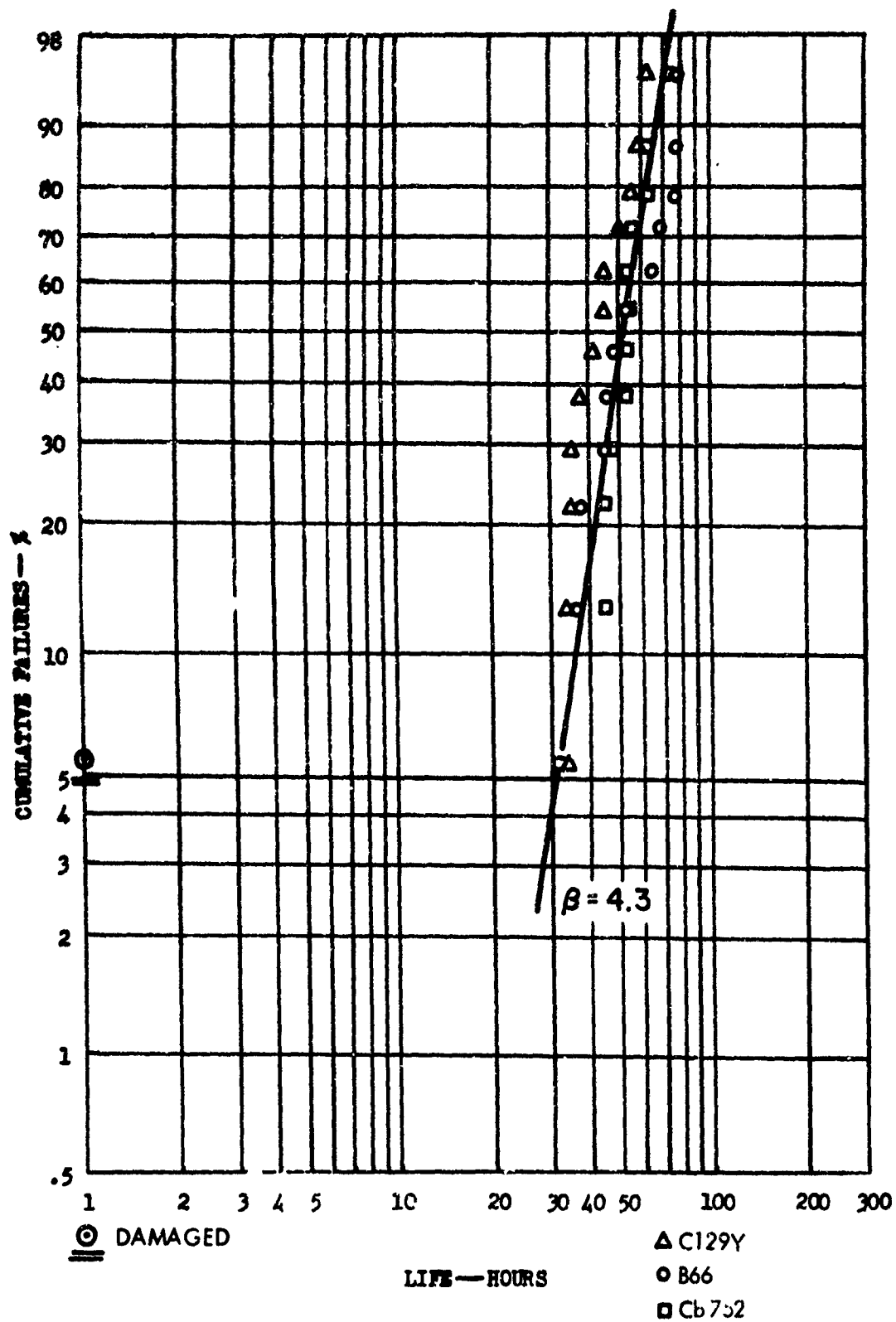
Percent Cumulative Failure Vs. Cyclic Oxidation Life at 2500°F
for Specimens Coated in Modulo Run 16L
Jack Position Breakout



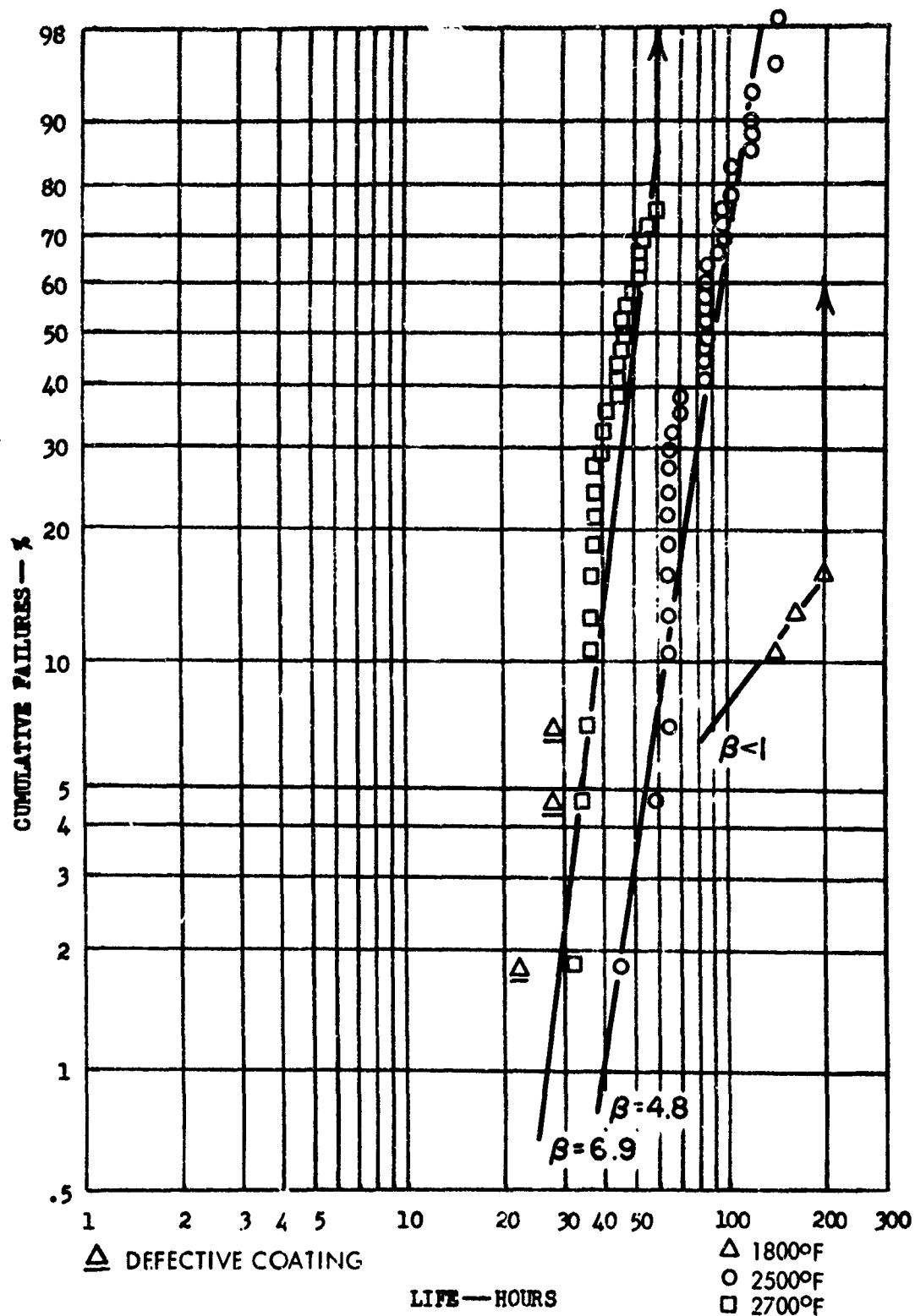
Percent Cumulative Failure Vs. Cyclic Oxidation Life at 2700°F
for Specimens Coated in Module Run 16L
Pack Position Breakout



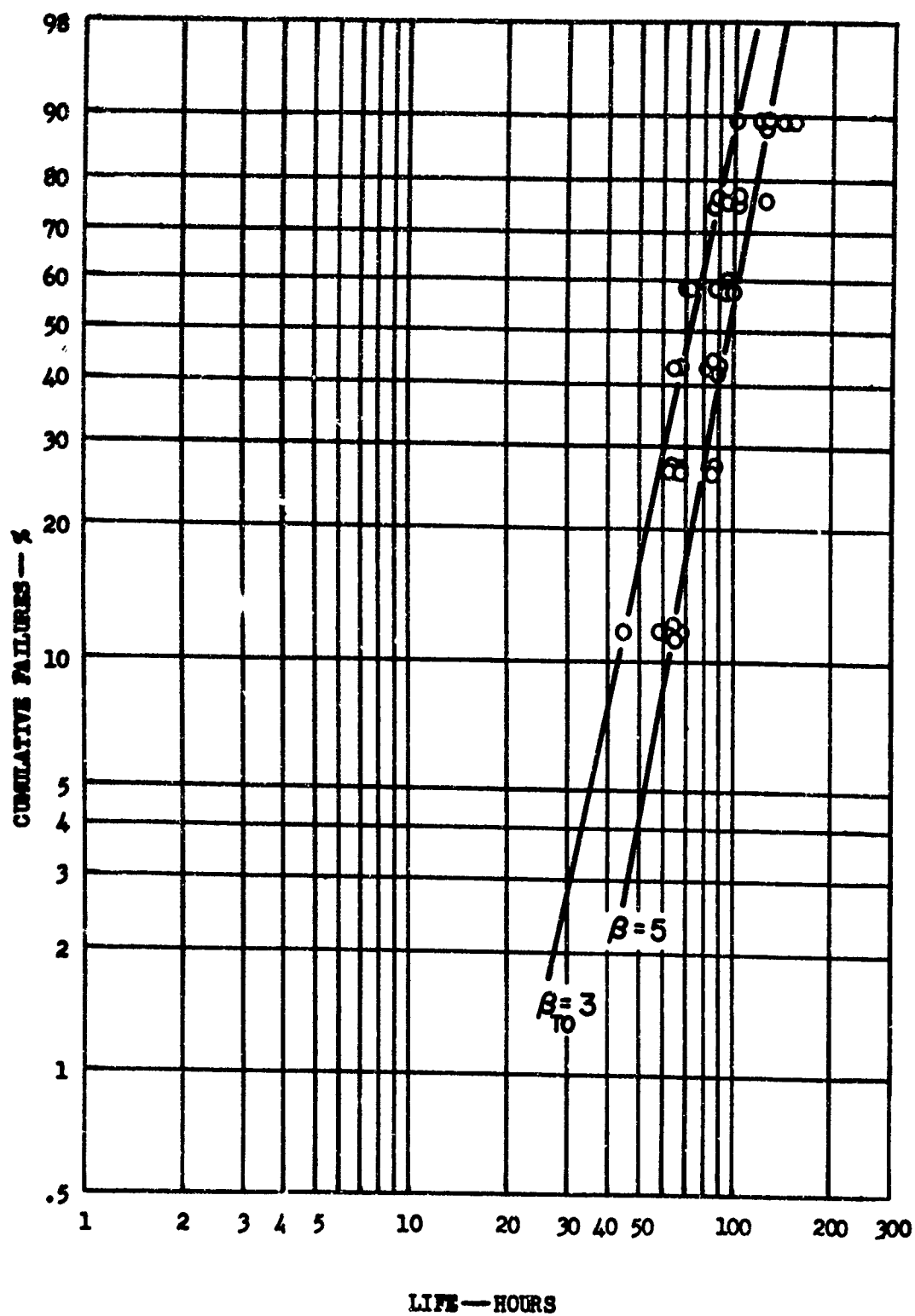
Percent Cumulative Failure Vs. Cyclic Oxidation Life at 2500°F
for Specimens Coated in Module Run 16L
Alloy Breakout



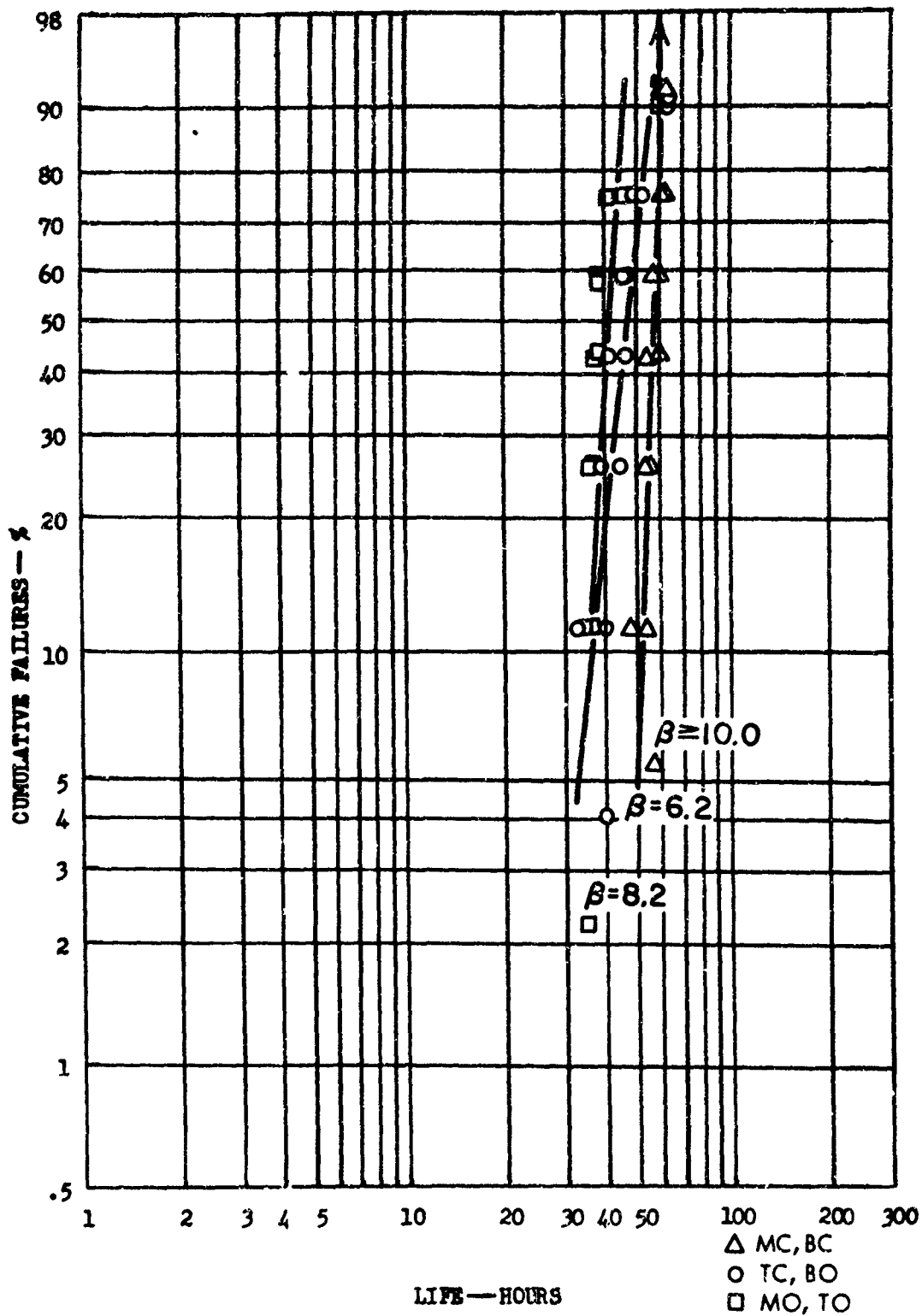
Percent Cumulative Failure Vs. Cyclic Oxidation Life at 2700°F
for Specimens Coated in Module Run 16L
Alloy Breakout



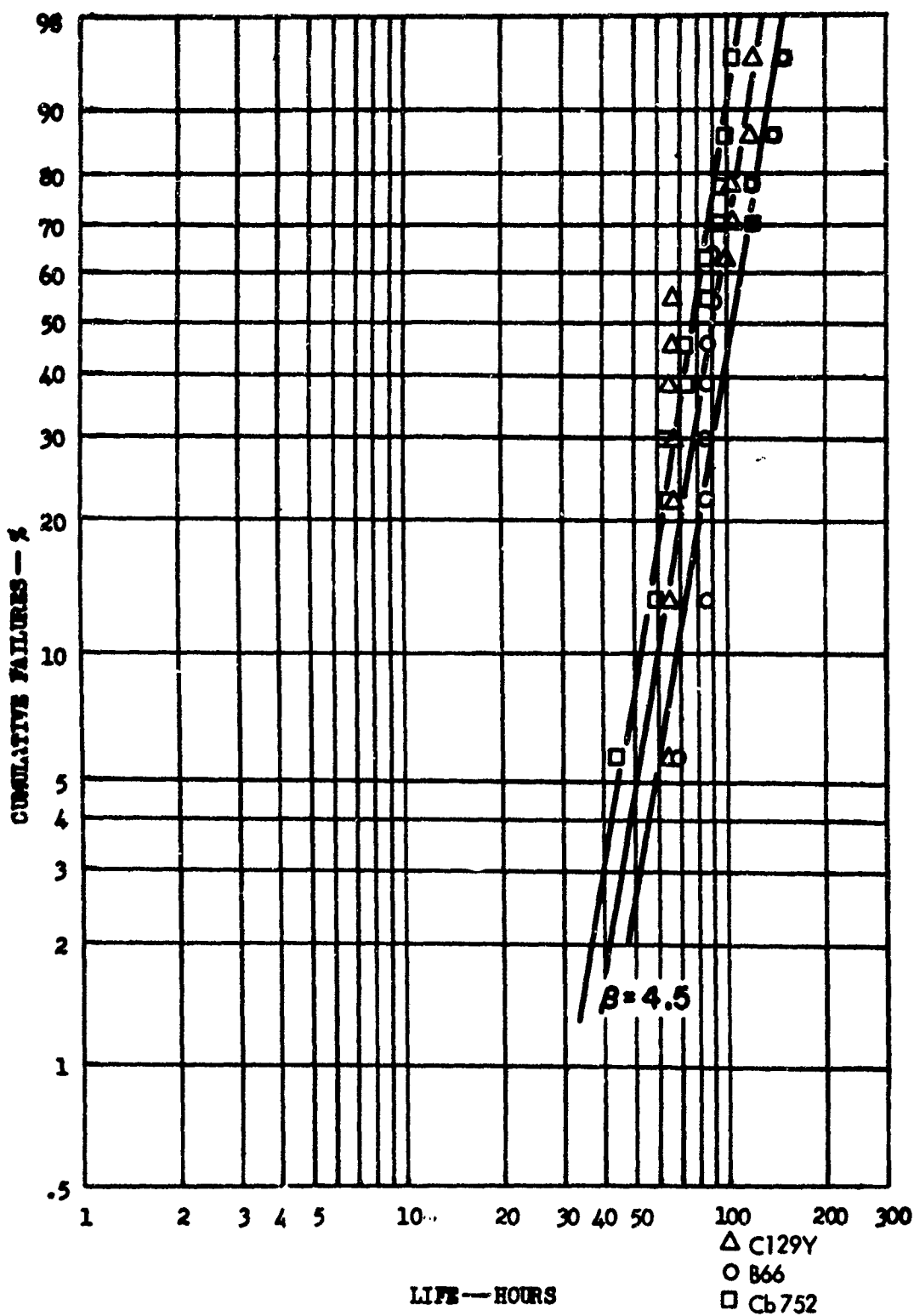
Percent Cumulative Failure Vs. Cyclic Oxidation Life for All Specimens Coated in Module Run 17L



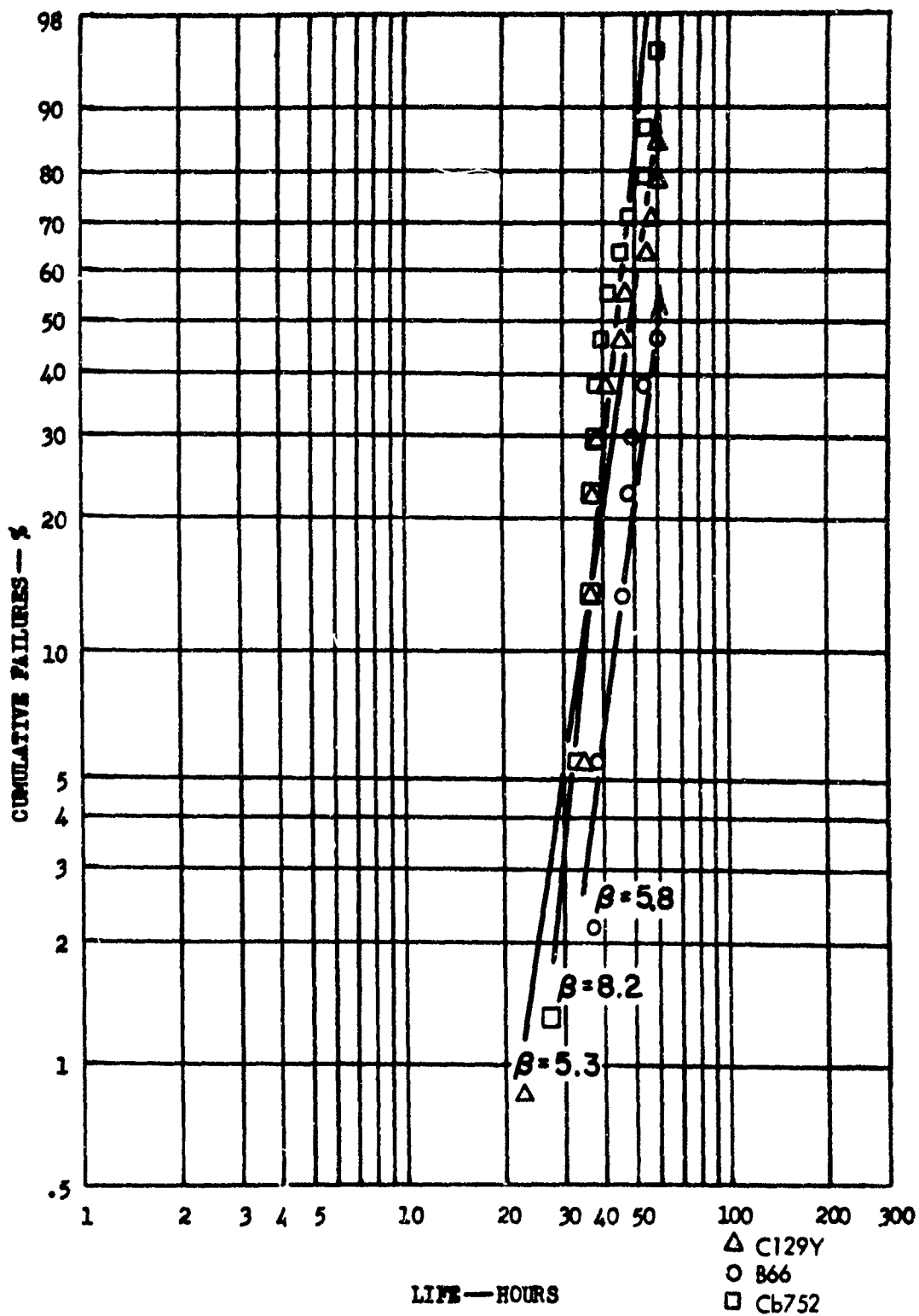
Percent Cumulative Failure Vs. Cyclic Oxidation Life at 2500°F
for Specimens Coated in Module Run 17L
Pack Position Breakout



Percent Cumulative Failure Vs. Cyclic Oxidation Life at 2700°F
for Specimens Coated in Module Run 17L
Pack Position Breakout

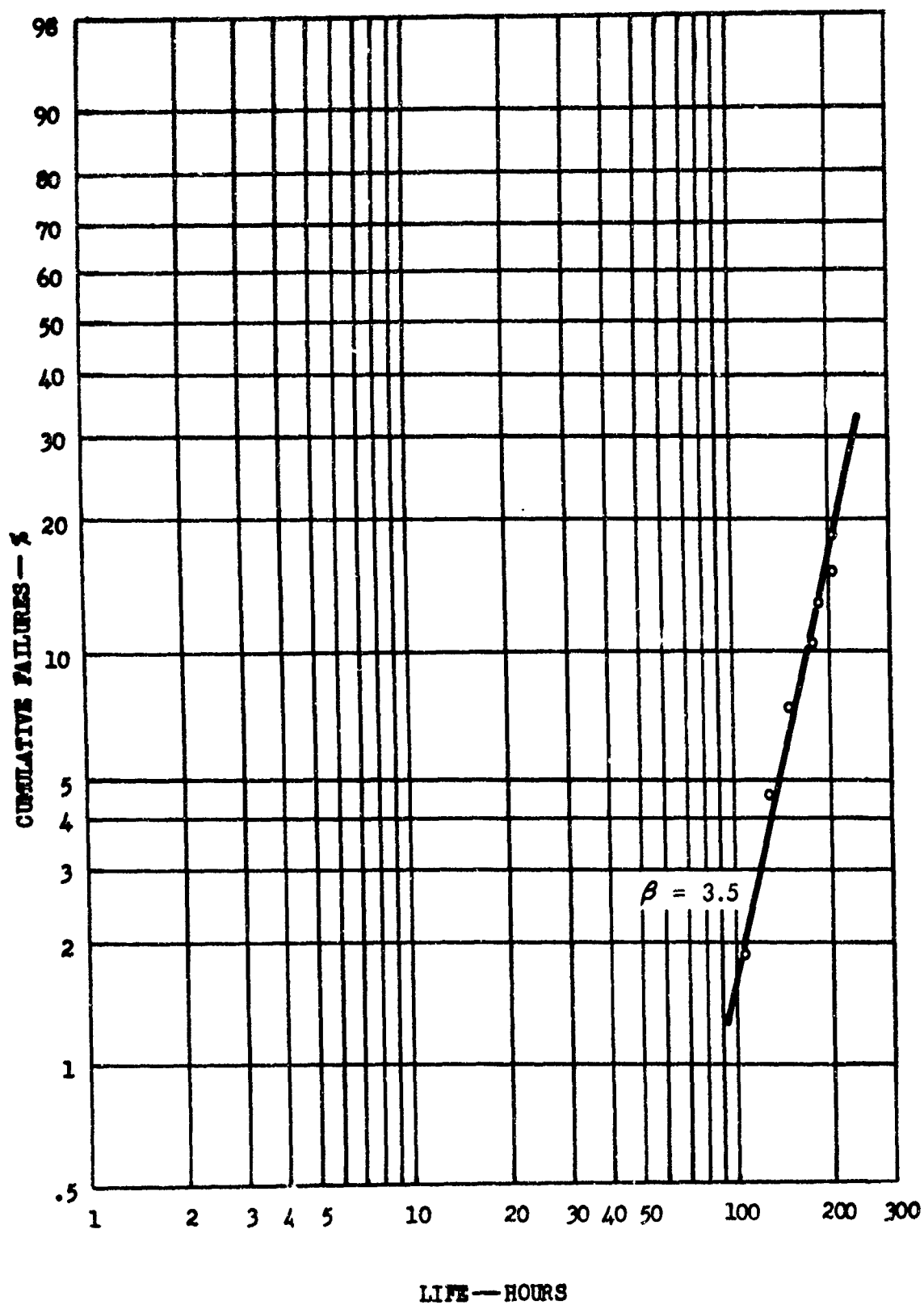


Percent Cumulative Failure Vs. Cyclic Oxidation Life at 2500°F
for Specimens Coated in Module Run 17L
Alloy Breakout

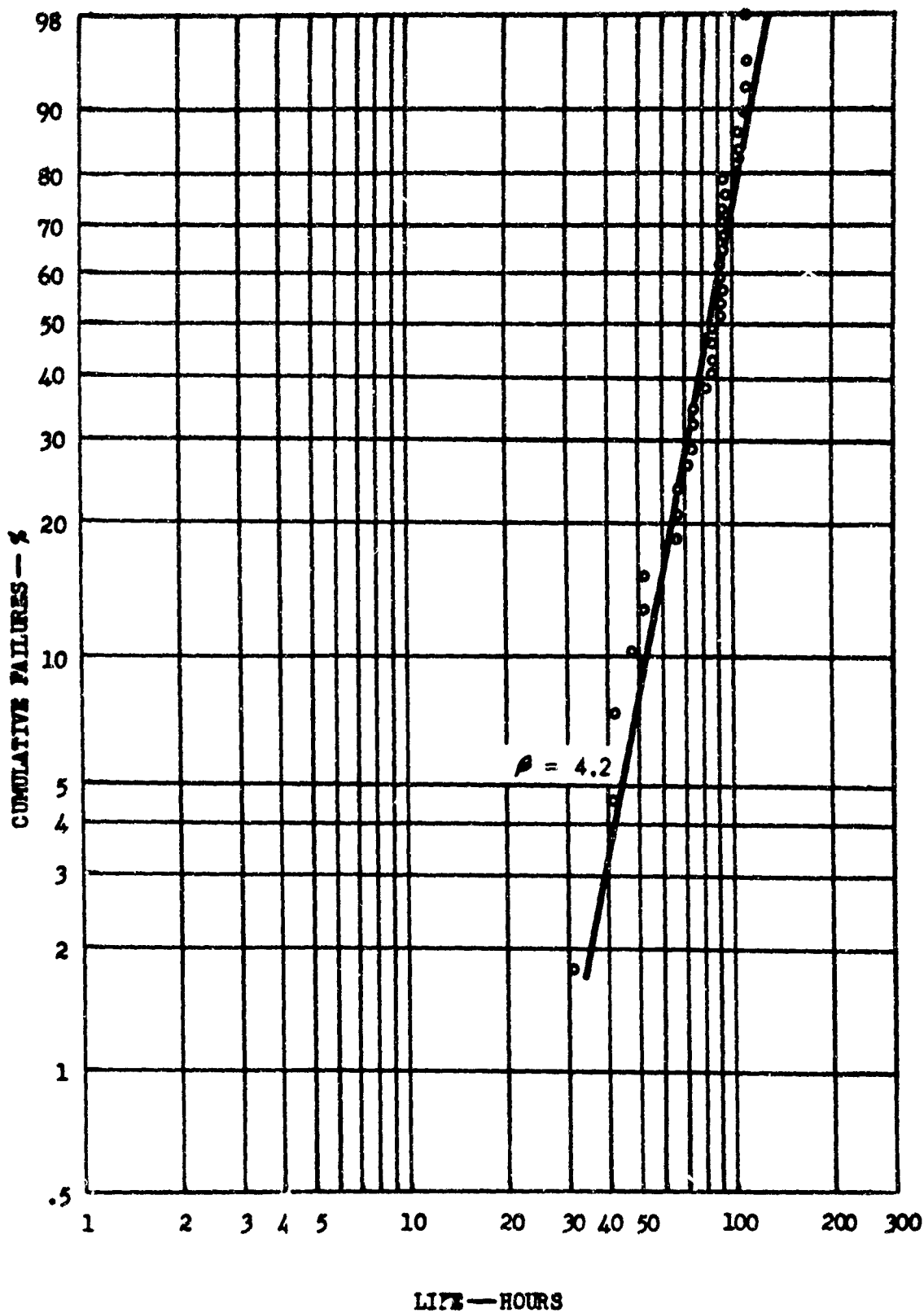


Percent Cumulative Failure Vs. Cyclic Oxidation Life at 2700°F
for Specimens Coated in Module Run 17L
Alloy Breakout

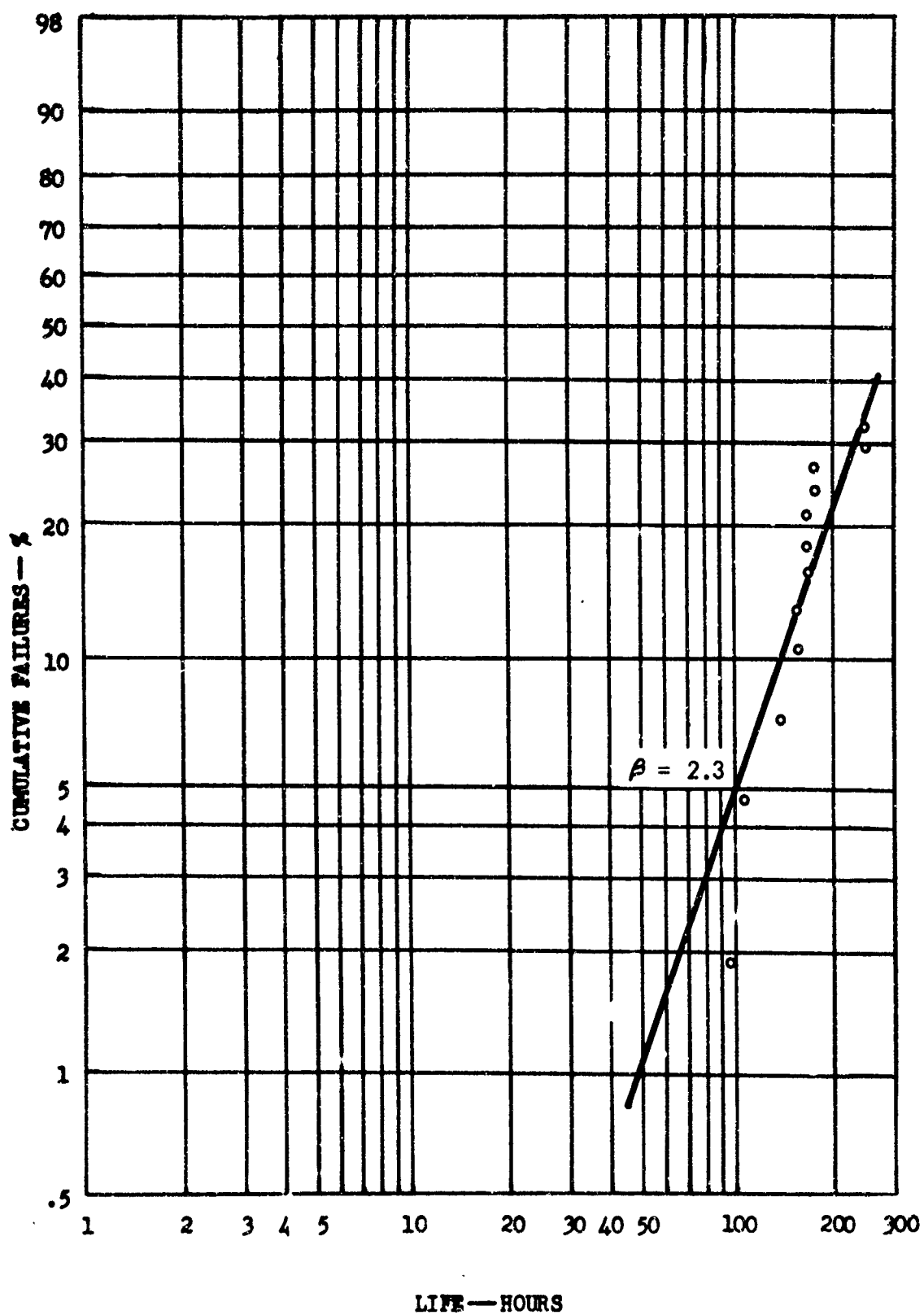
APPENDIX VI OXIDATION TEST RESULTS FROM
THE VACUUM PACK REPRODUCIBILITY STUDY



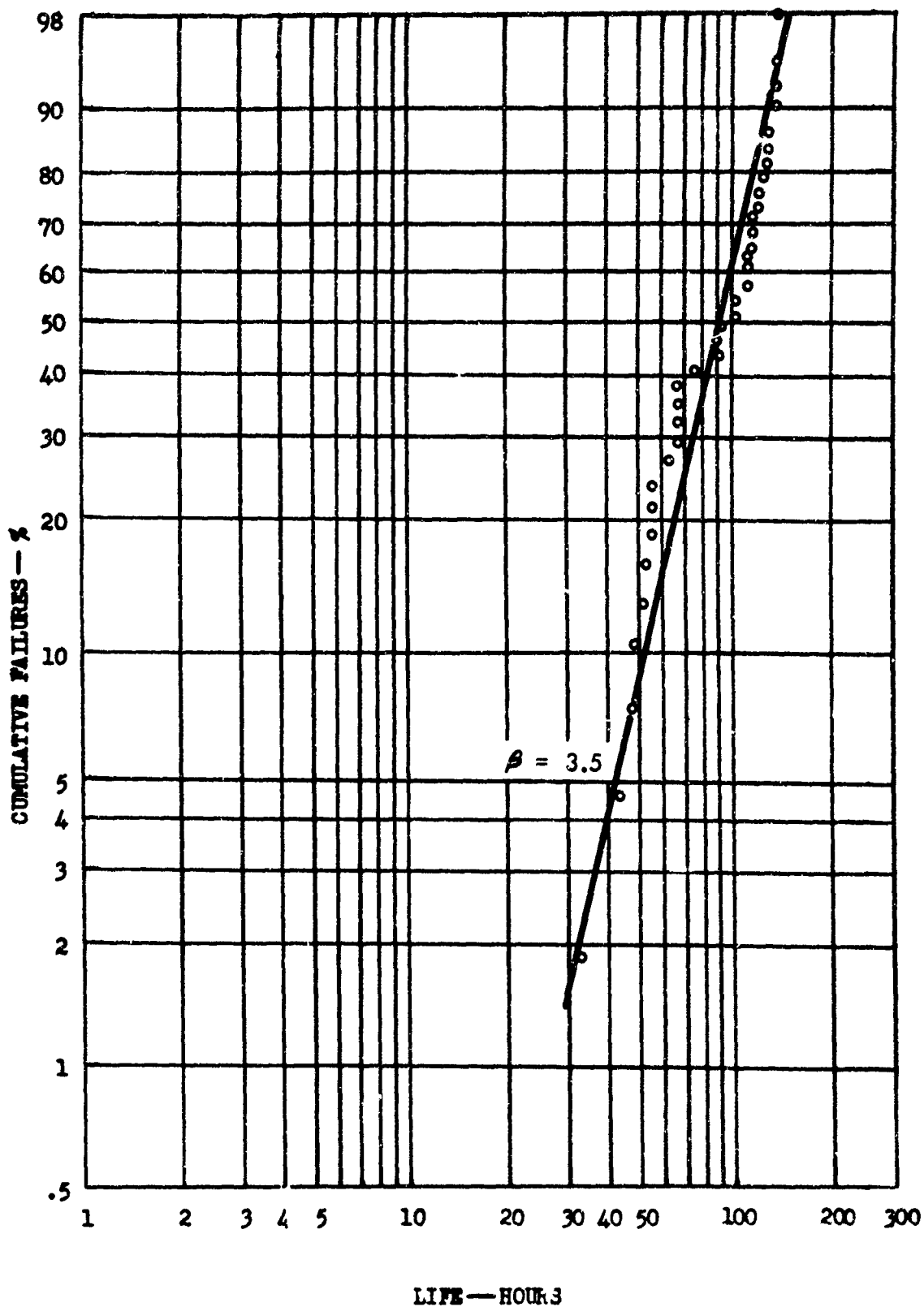
Percent Cumulative Failure vs. Cyclic Oxidation Life at 1800°F
for Specimens Coated in Reproducibility Run A



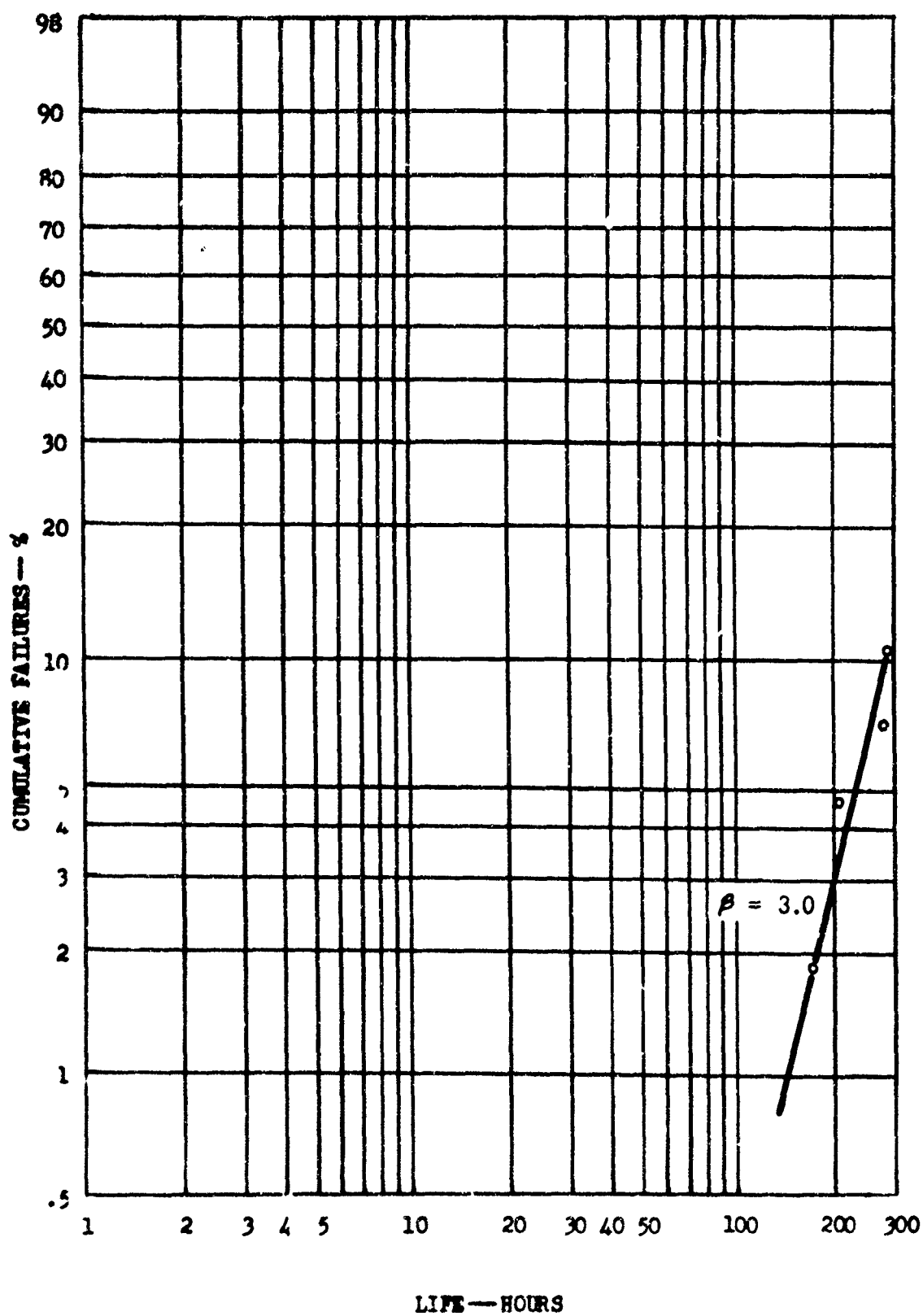
Percent Cumulative Failure vs. Cyclic Oxidation Life at 2600°F for Specimens Coated in Reproducibility Run A



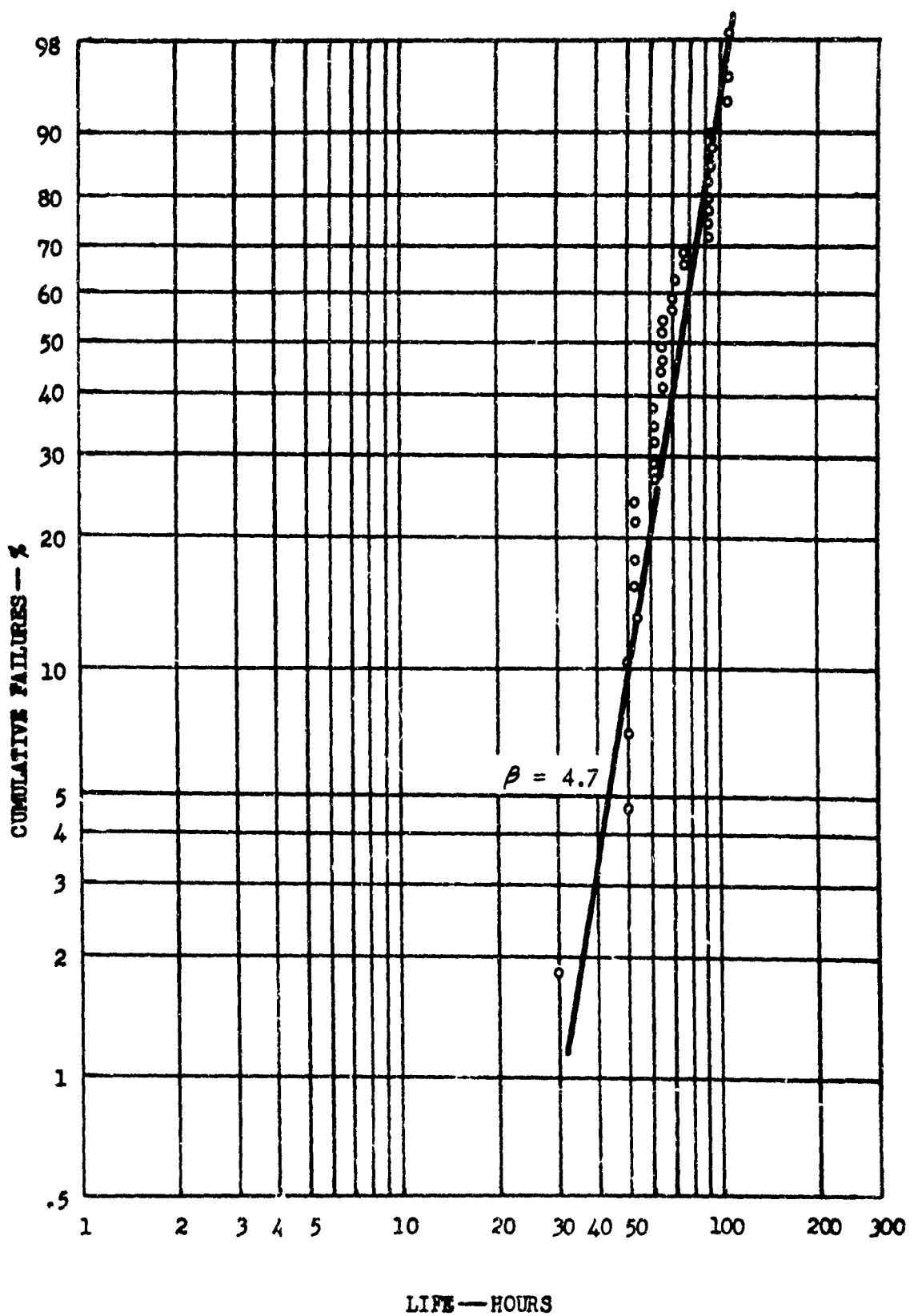
Percent Cumulative Failure vs. Cyclic Oxidation Life at 1800°F for Specimens Coated in Reproducibility Run B



Percent Cumulative Failure vs. Cyclic Oxidation Life at 2600°F for Specimens Coated in Reproducibility Run B



Percent Cumulative Failure vs. Cyclic Oxidation Life at 1800°F for Specimens Coated in Reproducibility Run C



Percent Cumulative Failure vs. Cyclic Oxidation Life at 2600°F for Specimens Coated in Reproducibility Run C

APPENDIX VII OXIDATION PERFORMANCE DATA OF SLURRY-DIFFUSION
COATED COUPONS EVALUATED IN THE FACTORIAL EXPERIMENTS.

Compilation of Weight Gain and Oxidation Performance for Specimens Coated in Factorial Run A

Cr-Ti Cycle				Si Cycle			
Activator	Quantity	Temperature	Pressure	Time	Activator	Quantity	Temperature
NaF	2 w/o	2350° F	100 torr	10 hours		2 w/o	2100° F
							10 torr
							8 hours

Run No. A

Cr-Ti Cycle											
-250 + 325 mesh						-170 + 250 mesh					
50Cr-50Ti						60Cr-40Ti					
50Cr-50Ti						60Cr-40Ti					
-250 + 325 mesh						-170 + 250 mesh					
Si Cycle						Si Cycle					

Compilation of Weight Gain and Oxidation Performance for Specimens Coated in Factorial Run B

Cr-Ti Cycle				S1 Cycle			
Activator	Activator Quantity	Temperature	Pressure	Time	Activator Quantity	Temperature	Pressure
NaF-CrCl ₃	2 w/o	2250° F	10 torr	6 hours	2 w/o	2000° F	100 torr
							8 hours

Run No. B

Cr-Ti Cycle											
-250 + 325 mesh						-170 + 250 mesh					
50Cr-50Ti						60Cr-40Ti					
Weight Gain			Oxidation			Weight Gain			Oxidation		
No.	Gr-Ti	S1	Ratio	1800°	2600°	No.	Gr-Ti	S1	Ratio	1800°	2600°
11	7.2	20.6	0.35			21	7.0	22.7	0.31		
12	7.0	20.8	0.34			22	6.7	22.8	0.29		
13	6.8	20.9	0.33			23	6.6	22.6	0.29		
14	7.1	20.4	0.35			24	6.3	22.9	0.28		
15	6.9	19.9	0.35			25	6.9	22.4	0.31		
16	6.4	19.6	0.33			26	6.5	21.7	0.30		
17	6.6	20.3	0.33			27	6.4	21.4	0.30		
18	6.2	20.4	0.30			28	5.8	21.9	0.27		
Avg.	6.8	20.4	0.33			Avg.	6.5	22.3	0.29		
19	7.2	20.8	0.35			29	6.5	20.1	0.32		
20	6.9	19.8	0.35			30	6.1	21.7	0.28		
21	7.1	20.8	0.34			31	6.6	21.6	0.31		
22	9.6	18.2	0.53			32	6.2	21.7	0.29		
23	7.2	10.3				33	5.9	22.2	0.27		
24	6.5	17.2	0.38			34	6.6	21.9	0.30		
25	6.9	19.8	0.35			35	6.6	21.9	0.30		
26	6.9	17.9	0.49			36	5.9	20.9	0.28		
27	7.5	19.0	0.40			37	6.1	21.5	0.28		
Avg.	7.5	19.0	0.40			Avg.	6.1	21.5	0.28		

All Specimens Failed at less than 5 minutes.

Compilation of Weight Gain and Oxidation Performance for Specimens Coated in Factorial Run C

Cr-Ti Cycle				Si Cycle			
Activator	Activator Quantity	Temperature	Pressure	Time	Activator Quantity	Temperature	Pressure
NaF-Cr-Cl ₃	6 w/o	2250° F	10 torr	10 hours	2 w/o	2000° F	10 torr
							4 hours

Run No. C

Cr-Ti Cycle											
-250 + 325 mesh						-170 + 250 mesh					
50Cr-50Ti						50Cr-50Ti					
60Cr-40Ti						60Cr-40Ti					
No.	Cr-Ti	Si	Ratio	1800°	2600°	No.	Cr-Ti	Si	Ratio	1800°	2600°
11	8.9	15.4	0.58	> 317		41	8.0	14.8	0.54	> 317	
12	7.7	15.1	0.51	> 317		42	8.4	14.6	0.58	> 317	
13	9.4	14.6	0.64	> 317		43	8.0	13.2	0.61	> 317	
14	8.9	13.1	0.68	> 317		44	7.6	14.8	0.51	> 317	
15	9.2	14.3	0.64		79	45	7.8	14.8	0.53		77
16	9.5	14.3	0.67		79	46	8.3	15.1	0.55		77
17	9.8	13.4	0.73		79	47	8.9	14.2	0.63		79
18	7.9	13.9	0.57		79	48	8.9	14.2	0.63		79
Avg.	8.9	14.1	0.63			Avg.	8.2	14.5	0.57		
51	9.5	15.2	0.62	> 317		81	8.3	16.3	0.51	246	
52	9.1	15.4	0.59	> 317		82	7.7	16.8	0.46	90	
53	8.6	13.8	0.62	> 317		83	8.1	16.6	0.49	> 317	
54	7.8	13.7	0.57	80		84	8.5	14.8	0.57	246	
55	9.6	14.2	0.68		69	85	8.0	15.6	0.51		72
56	8.9	13.9	0.64		69	86	8.8	15.6	0.56		72
57	9.4	13.7	0.69		72	87	8.2	17.0	0.48		72
58	8.2	13.1	0.63		75	88	7.6	15.7	0.48		61
Avg.	8.9	14.1	0.63			Avg.	8.2	16.1	0.51		

Compilation of Weight Gain and Oxidation Performance for Specimens Coated in Factorial Run D

Cr-Ti Cycle									
31 Cycle					31 Cycle				
Activator	Quantity	Temperature	Pressure	Time	Activator	Quantity	Temperature	Pressure	Time
NaF	2 w/o	2250° F	10 torr	10 hours		6 w/o	2100° F	100 torr	8 hours

Run No. D									
Cr-Ti Cycle									
-250 + 325 mesh					-170 + 250 mesh				
50Cr-50Ti					60Cr-40Ti				
No.	Cr-Ti	SI	Ratio	Oxidation	No.	Cr-Ti	SI	Ratio	Oxidation
11	6.4	27.6	0.23	1800°	21	6.2	27.4	0.23	1800°
12	6.8	26.7	0.25	2500°	22	6.7	26.7	0.25	2500°
13	6.1	28.1	0.22		23	7.1	31.7	0.22	
14	6.2	26.7	0.23		24	5.2	23.0	0.22	
15	5.7	27.8	0.21		25	6.8	31.3	0.22	
16	6.4	27.0	0.24		26	6.6	31.3	0.21	
17	6.1	27.8	0.22		27	6.9	30.9	0.22	
18	6.0	27.7	0.22		28	6.8	31.5	0.22	
Avg.	6.2	27.4	0.23		Avg.	6.5	31.3	0.21	
51	7.9	28.5	0.28		61	8.3	31.9	0.26	
52	8.2	27.2	0.30		62	7.8	33.3	0.23	
53	8.5	33.0	0.26		63	8.0	32.3	0.25	
54	7.3	28.5	0.26		64	7.3	33.5	0.22	
55	7.2	27.9	0.26		65	8.0	3.25	0.25	
56	7.8	27.9	0.28		66	8.2	33.7	0.24	
57	7.8	27.0	0.29		67	7.5	32.9	0.23	
58	8.9	26.7	0.33		68	8.2	32.0	0.26	
Avg.	8.0	29.3	0.29		Avg.	7.9	32.7	0.27	

Million Cycle									
-250 + 325 mesh					-170 + 250 mesh				
No.	Cr-Ti	SI	Ratio	Oxidation	No.	Cr-Ti	SI	Ratio	Oxidation
41	6.4	30.6	0.21		81	8.1	32.7	0.25	
42	7.0	30.5	0.23		82	8.2	32.3	0.25	
43	7.4	33.2	0.22		83	7.8	33.1	0.24	
44	7.9	31.6	0.24		84	7.8	34.3	0.23	
45	7.7	31.5	0.24		85	7.8	33.5	0.23	
46	7.5	32.7	0.23		86	8.2	32.2	0.25	
47	7.2	32.6	0.22		87	7.1	32.1	0.22	
48	8.0	32.2	0.25		88	8.1	34.1	0.24	
Avg.	7.4	31.9	0.23		Avg.	7.9	33.0	0.24	

All Specimens tested in 1 atm.

Compilation of Weight Gain and Oxidation Performance for Specimens Coated in Factorial Run E

Cr-Ti Cycle				Si Cycle			
Activator	Quantity	Temperature	Pressure	Time	Activator	Quantity	Temperature
NaF	2 w/o	2350° F	10 torr	6 hours		2 w/o	2000° F
							100 torr
							4 hours

Run No. E

Cr-Ti Cycle											
-250 + 325 mesh						-170 + 250 mesh					
50Cr-50Ti						60Cr-40Ti					
No.	Cr-Ti	Si	Ratio	Oxidation	Weight Gain	No.	Cr-Ti	Si	Ratio	Oxidation	Weight Gain
11	13.9	17.7	0.78	> 120	21	11.6	31	12.7	17.9	> 120	41
12	14.0	19.1	0.73	> 120	22	12.6	32	12.7	17.3	> 120	42
13	13.6	16.7	0.73	> 120	23	12.8	33	12.9	18.3	> 120	43
14	13.1	19.5	0.67	> 120	24	13.1	34	12.5	16.9	> 120	44
15	13.5	18.9	0.71	> 297	25	13.4	35	12.8	17.8	252	45
16	13.7	18.8	0.73	> 297	26	12.2	36	13.6	17.7	> 297	46
17	13.1	18.8	0.70	> 297	27	13.0	37	13.8	18.3	> 245	47
18	12.8	18.1	0.71	> 261	28	12.4	38	13.9	17.7	117	48
AVG.	13.5	18.7	0.72		AVG.	12.8	35.0	13.1	17.7		AVG.
51	15.4	20.8	0.74	> 297	61	13.0	71	13.6	20.4	> 297	81
52	15.0	20.6	0.73	277	62	12.9	72	12.2	19.3	57	82
53	14.0	21.2	0.66	37	63	13.2	73	13.0	21.1	> 297	83
54	14.1	20.8	0.68	> 297	64	13.3	74	14.6	19.9	> 297	84
55	14.1	20.8	0.68		65	12.2	75	14.3	20.6	> 120	85
56	14.6	20.4	0.72		66	13.7	76	14.4	21.2	> 120	86
57	13.4	20.5	0.65		67	12.6	77	14.2	20.5	> 120	87
58	13.7	20.9	0.65		68	12.5	78	15.0	20.2	> 120	88
AVG.	14.3	20.8	0.69		AVG.	12.9	75.0	13.9	20.4		AVG.
-250 + 325 mesh											
50Cr-50Ti						60Cr-40Ti					
No.	Cr-Ti	Si	Ratio	Oxidation	Weight Gain	No.	Cr-Ti	Si	Ratio	Oxidation	Weight Gain
11	13.9	17.7	0.78	> 120	21	11.6	31	12.7	17.9	> 120	41
12	14.0	19.1	0.73	> 120	22	12.6	32	12.7	17.3	> 120	42
13	13.6	16.7	0.73	> 120	23	12.8	33	12.9	18.3	> 120	43
14	13.1	19.5	0.67	> 120	24	13.1	34	12.5	16.9	> 120	44
15	13.5	18.9	0.71	> 297	25	13.4	35	12.8	17.8	252	45
16	13.7	18.8	0.73	> 297	26	12.2	36	13.6	17.7	> 297	46
17	13.1	18.8	0.70	> 297	27	13.0	37	13.8	18.3	> 245	47
18	12.8	18.1	0.71	> 261	28	12.4	38	13.9	17.7	117	48
AVG.	13.5	18.7	0.72		AVG.	12.8	35.0	13.1	17.7		AVG.
51	15.4	20.8	0.74	> 297	61	13.0	71	13.6	20.4	> 297	81
52	15.0	20.6	0.73	277	62	12.9	72	12.2	19.3	57	82
53	14.0	21.2	0.66	37	63	13.2	73	13.0	21.1	> 297	83
54	14.1	20.8	0.68	> 297	64	13.3	74	14.6	19.9	> 297	84
55	14.1	20.8	0.68		65	12.2	75	14.3	20.6	> 120	85
56	14.6	20.4	0.72		66	13.7	76	14.4	21.2	> 120	86
57	13.4	20.5	0.65		67	12.6	77	14.2	20.5	> 120	87
58	13.7	20.9	0.65		68	12.5	78	15.0	20.2	> 120	88
AVG.	14.3	20.8	0.69		AVG.	12.9	75.0	13.9	20.4		AVG.
-170 + 250 mesh											
50Cr-50Ti						60Cr-40Ti					
No.	Cr-Ti	Si	Ratio	Oxidation	Weight Gain	No.	Cr-Ti	Si	Ratio	Oxidation	Weight Gain
11	13.9	17.7	0.78	> 120	21	11.6	31	12.7	17.9	> 120	41
12	14.0	19.1	0.73	> 120	22	12.6	32	12.7	17.3	> 120	42
13	13.6	16.7	0.73	> 120	23	12.8	33	12.9	18.3	> 120	43
14	13.1	19.5	0.67	> 120	24	13.1	34	12.5	16.9	> 120	44
15	13.5	18.9	0.71	> 297	25	13.4	35	12.8	17.8	252	45
16	13.7	18.8	0.73	> 297	26	12.2	36	13.6	17.7	> 297	46
17	13.1	18.8	0.70	> 297	27	13.0	37	13.8	18.3	> 245	47
18	12.8	18.1	0.71	> 261	28	12.4	38	13.9	17.7	117	48
AVG.	13.5	18.7	0.72		AVG.	12.8	35.0	13.1	17.7		AVG.
51	15.4	20.8	0.74	> 297	61	13.0	71	13.6	20.4	> 297	81
52	15.0	20.6	0.73	277	62	12.9	72	12.2	19.3	57	82
53	14.0	21.2	0.66	37	63	13.2	73	13.0	21.1	> 297	83
54	14.1	20.8	0.68	> 297	64	13.3	74	14.6	19.9	> 297	84
55	14.1	20.8	0.68		65	12.2	75	14.3	20.6	> 120	85
56	14.6	20.4	0.72		66	13.7	76	14.4	21.2	> 120	86
57	13.4	20.5	0.65		67	12.6	77	14.2	20.5	> 120	87
58	13.7	20.9	0.65		68	12.5	78	15.0	20.2	> 120	88
AVG.	14.3	20.8	0.69		AVG.	12.9	75.0	13.9	20.4		AVG.
-250 + 325 mesh											
50Cr-50Ti						60Cr-40Ti					
No.	Cr-Ti	Si	Ratio	Oxidation	Weight Gain	No.	Cr-Ti	Si	Ratio	Oxidation	Weight Gain
11	13.9	17.7	0.78	> 120	21	11.6	31	12.7	17.9	> 120	41
12	14.0	19.1	0.73	> 120	22	12.6	32	12.7	17.3	> 120	42
13	13.6	16.7	0.73	> 120	23	12.8	33	12.9	18.3	> 120	43
14	13.1	19.5	0.67	> 120	24	13.1	34	12.5	16.9	> 120	44
15	13.5	18.9	0.71	> 297	25	13.4	35	12.8	17.8	252	45
16	13.7	18.8	0.73	> 297	26	12.2	36	13.6	17.7	> 297	46
17	13.1	18.8	0.70	> 297	27	13.0	37	13.8	18.3	> 245	47
18	12.8	18.1	0.71	> 261	28	12.4	38	13.9	17.7	117	48
AVG.	13.5	18.7	0.72		AVG.	12.8	35.0	13.1	17.7		AVG.
51	15.4	20.8	0.74	> 297	61	13.0	71	13.6	20.4	> 297	81
52	15.0	20.6	0.73	277	62	12.9	72	12.2	19.3	57	82
53	14.0	21.2	0.66	37	63	13.2	73	13.0	21.1	> 297	83
54	14.1	20.8	0.68	> 297	64	13.3	74	14.6	19.9	> 297	84
55	14.1	20.8	0.68		65	12.2	75	14.3	20.6	> 120	85
56	14.6	20.4	0.72		66	13.7	76	14.4	21.2	> 120	86
57	13.4	20.5	0.65		67	12.6	77	14.2	20.5	> 120	87
58	13.7	20.9	0.65		68	12.5	78	15.0	20.2	> 120	88
AVG.	14.3	20.8	0.69		AVG.	12.9	75.0	13.9	20.4		AVG.
-170 + 250 mesh											
50Cr-50Ti						60Cr-40Ti					
No.	Cr-Ti	Si	Ratio	Oxidation	Weight Gain	No.	Cr-Ti	Si	Ratio	Oxidation	Weight Gain
11	13.9	17.7	0.78	> 120	21	11.6	31	12.7	17.9	> 120	41
12	14.0	19.1	0.73	> 120	22	12.6	32	12.7	17.3	> 120	42
13	13.6	16.7	0.73	> 120	23	12.8	33	12.9	18.3	> 120	43
14	13.1	19.5	0.67	> 120	24	13.1	34	12.5	16.9	> 120	44
15	13.5	18.9	0.71	> 297	25	13.4	35	12.8	17.8	252	45
16	13.7	18.8	0.73	> 297	26	12.2	36	13.6	17.7	> 297	46
17	13.1	18.8	0.70	> 297	27	13.0	37	13.8	18.3	> 245	47
18	12.8	18.1	0.71	> 261	28	12.4	38	13.9	17.7	117	48
AVG.	13.5	18.7	0.72		AVG.	12.8	35.0	13.1	17.7		AVG.
51	15.4	20.8	0.74	> 297	61	13.0	71	13.6	20.4	> 297	81
52	15.0	20.6	0.73	277	62	12.9	72	12.2	19.3	57	82
53	14.0	21.2	0.66	37	63	13.2	73	13.0	21.1	> 297	83
54	14.1	20.8	0.68	> 297	64	13.3	74	14.6	19.9	> 297	84
55	14.1	20.8	0.68		65	12.2	75	14.3	20.6	> 120	85
56	14.6	20.4	0.72		66	13.7	76	14.4	21.2	> 120	86
57	13.4	20.5	0.65		67	12.6	77	14.2	20.5	> 120	87
58	13.7	20.9	0.65		68	12.5	78	15.0	20.2	> 120	88
AVG.	14.3	20.8	0.69		AVG.	12.9	75.0	13.9	20.4		AVG.

Compilation of Weight Gain and Oxidation Performance for Specimens Coated in Factorial Run F

Cr-Ti Cycle				Si Cycle			
Activator	Activator Quantity	Temperature	Pressure	Time	Activator Quantity	Temperature	Pressure
NaF-CrCl ₃	2 w/o	2350° F	10 torr	10 hours	6 w/o	2100° F	100 torr
				4 hours			

Run No. F_o

Cr-Ti Cycle											
-250 +325 mesh						-170 +250 mesh					
50Cr-50Ti						50Cr-50Ti					
60Cr-40Ti						60Cr-40Ti					
No.	Cr-Ti	Si	Ratio	1800°	2600°	No.	Cr-Ti	Si	Ratio	1800°	2600°
11	17.5	30.4	0.56	> 248		41	15.2	30.7	0.49	19	
12	17.5	31.1	0.56	121		42	15.1	30.7	0.49	15	
13	17.7	30.3	0.58	> 248		43	14.6	30.3	0.48	15	
14	17.6	30.8	0.57	47		44	15.0	31.4	0.48	15	
15	17.0	31.3	0.54	102	106	45	15.2	30.6	0.50		
16	16.9	31.2	0.54	106	71	46	14.8	30.9	0.48		
17	16.4	29.4	0.56	102	71	47	15.3	29.9	0.51		
18	17.3	29.1	0.59	106	105	48	15.4	31.0	0.50		
Avg.	17.2	30.5	0.56			Avg.	15.1	30.7	0.49		
51	15.6	27.7	0.56	19		81	14.6	31.3	0.47	19	
52	17.0	29.9	0.57	23		82	14.4	31.3	0.46	19	
53	16.8	30.3	0.55	19		83	14.6	30.9	0.47	15	
54	16.8	27.9	0.60	30		84	13.6	30.9	0.44	15	
55	16.8	29.7	0.57			85	13.7	30.6	0.45		
56	13.1	29.7	0.44	> 115	78	86	13.6	30.7	0.44	43	
57	16.3	29.4	0.55	> 115	73	87	13.8	31.0	0.44	92	
58	18.2	29.4	0.62	> 115	72	88	13.3	28.6	0.46	89	
Avg.	16.3	29.3	0.56			Avg.	14.0	30.7	0.46	93	

Si Cycle
-170 + 250 mesh
-250 + 325 mesh

Compilation of Weight Gain and Oxidation Performance for Specimens Coated in Factorial Run G

Gr-Ti Cycle				Si Cycle			
Activator	Quantity	Temperature	Pressure	Time	Activator	Quantity	Pressure
NaF	6 w/o	2250° F	10 torr	6 hours		6 w/o	2100° F
							10 torr
							4 hours

Run No. G

Gr-Ti Cycle											
-250 +325 mesh						-170 +250 mesh					
50Cr-50Ti						60Cr-40Ti					
No.	Gr-Ti	Si	Ratio	Weight Gain	Oxidation	No.	Gr-Ti	Si	Ratio	Weight Gain	Oxidation
11	7.7	16.4	0.47	18.5	1800° 318	21	7.3	16.5	0.39	18.5	1800° 318
12	7.1	17.6	0.40	18.4	318	22	7.6	18.4	0.41	18.4	318
13	7.4	17.4	0.42	19.3	318	23	6.9	19.3	0.36	19.3	318
14	8.2	16.7	0.49	18.9	318	24	7.3	18.9	0.39	18.9	318
15	7.4	17.2	0.43	18.7	318	25	6.9	18.7	0.37	18.7	318
16	7.0	17.1	0.41	18.5	318	26	6.9	18.5	0.37	18.5	318
17	6.4	17.5	0.37	18.5	318	27	6.9	18.5	0.37	18.5	318
18	7.2	16.9	0.43	19.2	318	28	7.1	19.2	0.37	19.2	318
Avg.	7.3	17.1	0.43	18.8		Avg.	7.1	18.8	0.38	18.8	
29	7.7	18.2	0.42	18.5	25	61	6.8	18.5	0.37	18.5	25
31	6.4	18.2	0.35	17.4	29	62	7.4	18.7	0.40	18.7	29
32	7.4	17.4	0.42	17.7	29	63	6.9	17.7	0.39	17.7	29
33	7.5	17.8	0.42	17.4	29	64	7.2	17.4	0.41	17.4	29
34	8.2	18.0	0.45	17.4	318	65	6.3	17.4	0.36	17.4	318
35	8.0	17.3	0.46	19.1	318	66	7.2	19.1	0.38	19.1	318
36	8.3	17.1	0.48	18.1	318	67	6.9	18.1	0.38	18.1	318
37	7.5	17.7	0.42	18.0	318	68	7.2	18.0	0.40	18.0	318
Avg.	7.6	17.7	0.43	18.1		Avg.	7.0	18.1	0.39	18.1	
50Cr-50Ti											
-250 +325 mesh						60Cr-40Ti					
50Cr-50Ti						60Cr-40Ti					
No.	Gr-Ti	Si	Ratio	Weight Gain	Oxidation	No.	Gr-Ti	Si	Ratio	Weight Gain	Oxidation
41	6.9	18.8	0.37	18.8	1800° 318	41	6.9	18.8	0.37	18.8	1800° 318
42	7.2	18.0	0.40	18.0	318	42	7.2	18.0	0.40	18.0	318
43	7.6	19.5	0.39	19.5	318	43	7.6	19.5	0.39	19.5	318
44	7.5	19.1	0.39	19.1	318	44	7.5	19.1	0.39	19.1	318
45	7.3	18.5	0.39	18.5	318	45	7.3	18.5	0.39	18.5	318
46	7.2	18.9	0.38	18.9	318	46	7.2	18.9	0.38	18.9	318
47	7.8	18.7	0.42	18.7	318	47	7.8	18.7	0.42	18.7	318
48	7.0	19.0	0.37	19.0	318	48	7.0	19.0	0.37	19.0	318
Avg.	7.3	18.8	0.39	18.8		Avg.	7.3	18.8	0.39	18.8	
29	7.4	19.9	0.37	19.9	29	49	7.4	19.9	0.37	19.9	29
51	6.2	18.6	0.33	18.6	29	51	6.2	18.6	0.33	18.6	29
52	6.8	18.5	0.37	18.5	29	52	6.8	18.5	0.37	18.5	29
53	6.3	19.6	0.32	19.6	29	53	6.3	19.6	0.32	19.6	29
54	7.1	19.2	0.37	19.2	43	54	7.1	19.2	0.37	19.2	43
55	6.1	19.4	0.31	19.4	318	55	6.1	19.4	0.31	19.4	318
56	7.3	19.0	0.38	19.0	318	56	7.3	19.0	0.38	19.0	318
57	6.0	20.7	0.29	20.7	318	57	6.0	20.7	0.29	20.7	318
58	6.7	19.4	0.35	19.4	318	58	6.7	19.4	0.35	19.4	318
Avg.	6.7	19.4	0.35	19.4		Avg.	6.7	19.4	0.35	19.4	

Compilation of Weight Gain and Oxidation Performance for specimens Coated in Factorial Run H

Cr-Ti Cycle				Si Cycle			
Activator	Activator Quantity	Temperature	Pressure	Time	Activator Quantity	Temperature	Pressure
HaF-CrCl ₃	2 w/o	225° F	100 torr	6 hours	0 w/o	200° F	10 torr
							8 hours

Run No. H

Cr-Ti Cycle											
-250 + 325 mesh						-170 + 250 mesh					
50Cr-50Ti						50Cr-50Ti					
No.	Cr-Ti	Si	Ratio	Weight Gain	Oxidation	No.	Cr-Ti	Si	Ratio	Weight Gain	Oxidation
11	15.1	17.8	0.85	20.0	0.61	31	15.5	17.0	0.84	25.9	2600°
12	14.6	17.7	0.82	19.5	0.63	32	15.8	15.8	1.06	24.1	259
13	14.9	18.8	0.79	19.0	0.64	33	15.5	15.5	1.00	25.9	259
14	14.7	18.5	0.79	19.0	0.64	34	15.5	15.5	1.00	25.9	259
15	14.9	18.0	0.83	19.0	0.64	35	15.5	15.5	1.00	25.9	259
16	14.0	18.1	0.77	19.0	0.64	36	15.5	15.5	1.00	25.9	259
17	15.2	17.4	0.87	19.0	0.64	37	15.5	15.5	1.00	25.9	259
18	14.3	17.5	0.81	19.0	0.64	38	15.5	15.5	1.00	25.9	259
Avg.	14.5	17.7	0.81	19.0	0.64	Avg.	15.5	15.5	1.00	25.9	259
51	14.5	17.7	0.81	19.0	0.64	71	15.5	15.5	1.00	25.9	259
52	14.6	17.8	0.82	19.0	0.64	72	15.5	15.5	1.00	25.9	259
53	14.6	17.9	0.87	19.0	0.64	73	15.5	15.5	1.00	25.9	259
54	14.5	17.7	0.87	19.0	0.64	74	15.5	15.5	1.00	25.9	259
55	14.9	18.5	0.80	19.0	0.64	75	15.5	15.5	1.00	25.9	259
56	14.2	17.8	0.81	19.0	0.64	76	15.5	15.5	1.00	25.9	259
57	14.2	17.4	0.86	19.0	0.64	77	15.5	15.5	1.00	25.9	259
58	14.0	18.0	0.88	19.0	0.64	78	15.5	15.5	1.00	25.9	259
Avg.	14.5	17.7	0.81	19.0	0.64	Avg.	15.5	15.5	1.00	25.9	259

Compilation of Weight Gain and Oxidation Performance for Specimens Coated in Factorial Run I

Cr-Ti Cycle				Si Cycle			
Activator	Quantity	Temperature	Pressure	Time	Activator	Quantity	Temperature
NaF-CrCl ₃	2 w/o	2250° F	100 torr	10 hours		2 w/o	2100° F
							10 torr
							4 hours

Run No. I

Cr-Ti Cycle											
-250 + 325 mesh						-170 + 250 mesh					
50Cr-50Ti						50Cr-50Ti					
No.	Cr-Ti	Si	Ratio	Oxidation	Weight Gain	No.	Cr-Ti	Si	Ratio	Oxidation	Weight Gain
11	9.4	1.3	0.50	1800°	2600°	41	9.5	18.3	0.52	1800°	2600°
12	9.4	1.3	0.50	1800°	2600°	42	9.5	18.3	0.52	1800°	2600°
13	9.4	1.3	0.50	1800°	2600°	43	9.5	18.3	0.52	1800°	2600°
14	9.4	1.3	0.50	1800°	2600°	44	9.5	18.3	0.52	1800°	2600°
15	9.4	1.3	0.50	1800°	2600°	45	9.5	18.3	0.52	1800°	2600°
16	9.4	1.3	0.50	1800°	2600°	46	9.5	18.3	0.52	1800°	2600°
17	9.4	1.3	0.50	1800°	2600°	47	9.5	18.3	0.52	1800°	2600°
18	9.4	1.3	0.50	1800°	2600°	48	9.5	18.3	0.52	1800°	2600°
AVE.	9.4	1.3	0.50			AVE.	9.5	18.3	0.52		
51	1.3	9.4	0.50	1800°	2600°	81	8.8	18.9	0.53	1800°	2600°
52	1.3	9.4	0.50	1800°	2600°	82	8.8	18.9	0.53	1800°	2600°
53	1.3	9.4	0.50	1800°	2600°	83	8.8	18.9	0.53	1800°	2600°
54	1.3	9.4	0.50	1800°	2600°	84	8.8	18.9	0.53	1800°	2600°
55	1.3	9.4	0.50	1800°	2600°	85	8.8	18.9	0.53	1800°	2600°
56	1.3	9.4	0.50	1800°	2600°	86	8.8	18.9	0.53	1800°	2600°
57	1.3	9.4	0.50	1800°	2600°	87	8.8	18.9	0.53	1800°	2600°
58	1.3	9.4	0.50	1800°	2600°	88	8.8	18.9	0.53	1800°	2600°
AVE.	1.3	9.4	0.50			AVE.	8.8	18.9	0.53		

511208 Cycle

Cr-XI Cycle						Si Cycle			
Activator	Activator Quantity	Temperature	Pressure	Time		Activator Quantity	Temperature	Pressure	Time
NaF	6 w/o	2350° F	100 torr	6 hours		2 w/o	2100° F	100 torr	4 hours

293

Compilation of Weight Gain and Oxidation Performance for Specimens Coated in Factorial Run K

Cr-Ti Cycle				Si Cycle			
Activator	Quantity	Temperature	Pressure	Time	Activator	Quantity	Temperature
NaF-CrCl ₃	6 w/o	2350°F	10 torr	6 hours		6 w/o	2100°F
							10 torr
							8 hours

Run No. 1

Cr-Ti Cycle											
-250 + 325 mesh						-170 + 250 mesh					
50Cr-50Ti						60Cr-40Ti					
No.	Cr-Ti	Si	Ratio	1800°	2600°	No.	Cr-Ti	Si	Ratio	1800°	2600°
11	11.1	22.8	0.49	1	20	41	9.5	23.7	0.40	20	20
12	11.1	23.4	0.47	1	26	42	9.5	23.7	0.41	20	20
13	11.4	23.7	0.45	48	20	43	9.3	24.7	0.38	46	17
14	11.7	23.0	0.51	69	20	44	9.4	25.0	0.37	17	30
15	11.1	23.9	0.46		30	45	9.2	25.0	0.37	30	30
16	11.4	23.6	0.48	1	27	46	9.6	25.4	0.38	24	24
17	11.2	23.5	0.48	41	27	47	9.3	23.9	0.39	24	24
18	11.2	25.0	0.45	46	27	48	9.7	24.4	0.41	24	24
Avg.	11.3	23.6	0.48			Avg.	9.4	24.3	0.39		
11	11.0	25.0	0.44	49	30	51	9.7	24.9	0.39	38	38
52	11.2	22.0	0.49	41	27	52	9.5	24.2	0.39	30	30
53	10.9	22.3	0.48	41	27	53	9.0	24.5	0.37	30	30
54	11.6	22.5	0.51	50	30	54	10.8	22.1	0.49	10	10
55	11.5	24.0	0.45	27	26	55	9.3	24.7	0.38	13	13
56	11.5	24.2	0.47	13	23	56	11.0	24.1	0.46	17	17
57	11.1	23.1	0.48	48	26	57	9.9	24.1	0.41	17	17
58	11.5	24.6	0.48	40	17	58	9.3	24.5	0.38	17	17
Avg.	11.1	23.6	0.48			Avg.	9.8	24.1	0.41		

L. Specimens lost during test.

Compilation of Weight Gain and Oxidation Performance for Specimens Coated in Factorial Run L

Cr-Ti Cycle				Si Cycle			
Activator	Activator Quantity	Temperature	Pressure	Time	Activator Quantity	Temperature	Pressure
NaF	2 w/o	2250° F	100 torr	6 hours	6 w/o	2000° F	10 torr
							4 hours

Run No. L

Cr-Ti Cycle											
-250 +325 mesh						-170 +250 mesh					
50Cr-50Ti						50Cr-50Ti					
60Cr-40Ti						60Cr-40Ti					
No.	Cr-Ti	Si	Ratio	1800°	2600°	No.	Cr-Ti	Si	Ratio	1800°	2600°
11	9.0	15.5	0.58	21	7.1	16.8	8.0	14.6	0.55	44	41
12	7.7	15.5	0.53	22	6.9	16.6	8.1	15.0	0.54	20	42
13	8.6	16.4	0.50	23	7.8	16.0	8.3	15.2	0.58	216	43
14	8.1	14.5	0.56	24	7.1	16.6	8.3	14.4	0.58	86	44
15	9.2	16.1	0.57	25	7.9	17.9	7.7	15.6	0.49		45
16	9.7	16.6	0.55	26	7.3	17.0	8.3	15.0	0.55		46
17	8.0	15.6	0.51	27	7.4	17.4	8.2	16.0	0.51		47
18	9.1	15.3	0.61	28	7.3	17.9	8.7	15.8	0.55		48
Avg.	8.8	15.7	0.56	Avg.	7.4	17.0	Avg.	15.2	0.55		Avg.
19	9.2	15.0	0.61	35	7.5	17.3	8.3	15.2	0.55		47
20	7.9	15.2	0.57	50	7.8	17.6	7.1	16.0	0.44		48
21	8.7	14.7	0.59	50	7.9	17.3	7.0	15.6	0.45		49
22	8.8	14.7	0.62	50	7.9	17.3	7.9	15.1	0.52		50
23	7.9	15.4	0.51	50	7.3	17.0	7.4	14.8	0.50		50
24	7.6	16.0	0.47	21	7.3	17.9	7.7	15.8	0.49	15	84
25	9.1	15.2	0.60	28	7.4	17.7	8.4	15.2	0.55	37	85
26	7.8	15.5	0.50	68	8.3	17.6	7.8	15.0	0.52	15	86
27	8.4	15.1	0.56	Avg.	7.7	17.5	7.3	15.2	0.48	20	87
Avg.	8.4	15.1	0.56	Avg.	7.7	17.5	Avg.	15.3	0.50	Avg.	Avg.

Stillcon Cycle
-250 +325 mesh
-170 +250 mesh

Compilation of Weight Gain and Oxidation Performance for Specimens Coated in Factorial Run M

Gr-Ti Cycle				S1 Cycle			
Activator	Activator Quantity	Temperature	Pressure	Time	Activator Quantity	Temperature	Pressure
NaF	6 w/o	2250° F	100 torr	10 hours	6 w/o	2000° F	100 torr
							8 hours

Run No. M													
Gr-Ti Cycle													
-250 +325 mesh													
-170 +250 mesh													
60Gr-40Ti													
50Gr-50Ti													
-170 + 250 mesh													
-250 +325 mesh													
Silicon Cycle													
-170 + 250 mesh													
-250 +325 mesh													
60Gr-40Ti													
50Gr-50Ti													
-170 + 250 mesh													
-250 +325 mesh													
Silicon Cycle													
-170 + 250 mesh													
-250 +325 mesh													
60Gr-40Ti													
50Gr-50Ti													
-170 + 250 mesh													
-250 +325 mesh													
Silicon Cycle													
-170 + 250 mesh													
-250 +325 mesh													
60Gr-40Ti													
50Gr-50Ti													
-170 + 250 mesh													
-250 +325 mesh													
Silicon Cycle													
-170 + 250 mesh													
-250 +325 mesh													
60Gr-40Ti													
50Gr-50Ti													
-170 + 250 mesh													
-250 +325 mesh													
Silicon Cycle													
-170 + 250 mesh													
-250 +325 mesh													
60Gr-40Ti													
50Gr-50Ti													
-170 + 250 mesh													
-250 +325 mesh													
Silicon Cycle													
-170 + 250 mesh													
-250 +325 mesh													
60Gr-40Ti													
50Gr-50Ti													
-170 + 250 mesh													
-250 +325 mesh													
Silicon Cycle													
-170 + 250 mesh													
-250 +325 mesh													
60Gr-40Ti													
50Gr-50Ti													
-170 + 250 mesh													
-250 +325 mesh													
Silicon Cycle													
-170 + 250 mesh													
-250 +325 mesh													
60Gr-40Ti													
50Gr-50Ti													
-170 + 250 mesh													
-250 +325 mesh													
Silicon Cycle													
-170 + 250 mesh													
-250 +325 mesh													
60Gr-40Ti													
50Gr-50Ti													
-170 + 250 mesh													
-250 +325 mesh													
Silicon Cycle													
-170 + 250 mesh													
-250 +325 mesh													
60Gr-40Ti													
50Gr-50Ti													
-170 + 250 mesh													
-250 +325 mesh													
Silicon Cycle													
-170 + 250 mesh													
-250 +325 mesh													
60Gr-40Ti													
50Gr-50Ti													
-170 + 250 mesh													
-250 +325 mesh													
Silicon Cycle													
-170 + 250 mesh													
-250 +325 mesh													
60Gr-40Ti													
50Gr-50Ti													
-170 + 250 mesh													
-250 +325 mesh													
Silicon Cycle													
-170 + 250 mesh													
-250 +325 mesh													
60Gr-40Ti													
50Gr-50Ti													
-170 + 250 mesh													
-250 +325 mesh													
Silicon Cycle													
-170 + 250 mesh													
-250 +325 mesh													
60Gr-40Ti													
50Gr-50Ti													
-170 + 250 mesh													
-250 +325 mesh													
Silicon Cycle													
-170 + 250 mesh													
-250 +325 mesh													
60Gr-40Ti													
50Gr-50Ti													
-170 + 250 mesh													
-250 +325 mesh													
Silicon Cycle													
-170 + 250 mesh													
-250 +325 mesh													
60Gr-40Ti													
50Gr-50Ti													
-170 + 250 mesh													
-250 +325 mesh													
Silicon Cycle													
-170 + 250 mesh													
-250 +325 mesh													
60Gr-40Ti													
50Gr-50Ti													
-170 + 250 mesh													
-250 +325 mesh													
Silicon Cycle													
-170 + 250 mesh													
-250 +325 mesh													
60Gr-40Ti													
50Gr-50Ti													
-170 + 250 mesh													
-250 +325 mesh													
Silicon Cycle													
-170 + 250 mesh													
-250 +325 mesh													
60Gr-40Ti													
50Gr-50Ti													
-170 + 250 mesh													
-250 +325 mesh													
Silicon Cycle													
-170 + 250 mesh													
-250 +325 mesh													
60Gr-40Ti													
50Gr-50Ti													
-170 + 250 mesh													
-250 +325 mesh													
Silicon Cycle													
-170 + 250 mesh													
-250 +325 mesh													
60Gr-40Ti													
50Gr-50Ti													
-170 + 250 mesh													
-250 +325 mesh													
Silicon Cycle													
-170 + 250 mesh													
-250 +325 mesh													
60Gr-40Ti													
50Gr-50Ti													
-170 + 250 mesh													
-250 +325 mesh													
Silicon Cycle													
-170 + 250 mesh													
-250 +325 mesh													
60Gr-40Ti													
50Gr-50Ti													
-170 + 250 mesh													
-250 +325 mesh													
Silicon Cycle													
-170 + 250 mesh													
-250 +325 mesh													
60Gr-40Ti													
50Gr-50Ti													
-170 + 250 mesh													
-250 +325 mesh													
Silicon Cycle													
-170 + 250 mesh													
-250 +325 mesh													
60Gr-40Ti													
50Gr-50Ti													
-170 + 250 mesh													
-250 +325 mesh													
Silicon Cycle													
-170 + 250 mesh													
-250 +325 mesh													
60Gr-40Ti													
50Gr-50Ti													
-170 + 250 mesh													
-250 +325 mesh													
Silicon Cycle													
-170 + 250 mesh													
-250 +325 mesh													
60Gr-40Ti													
50Gr-50Ti													
-170 + 250 mesh													
-250 +325 mesh													
Silicon Cycle													
-170 + 250 mesh													
-250 +325 mesh													
60Gr-40Ti													
50Gr-50Ti													
-170 + 250 mesh													
-250 +325 mesh													
Silicon Cycle													
-170 + 250 mesh													
-250 +325 mesh													
60Gr-40Ti													
50Gr-50Ti													
-170 + 250 mesh													
-250 +325 mesh													
Silicon Cycle													
-170 + 250 mesh													
-250 +325 mesh													
60Gr-40Ti													
50Gr-50Ti													
-170 + 250 mesh													
-250 +325 mesh													
Silicon Cycle													
-170 + 250 mesh													
-250 +325 mesh													
60Gr-40Ti													
50Gr-50Ti													
-170 + 250 mesh													
-250 +325 mesh													
Silicon Cycle													
-170 + 250 mesh													
-250 +325 mesh													
60Gr-40Ti													
50Gr-50Ti													
-170 + 250 mesh													
-250 +325 mesh													
Silicon Cycle													
-170 + 250 mesh													
-250 +325 mesh													
60Gr-40Ti													
50Gr-50Ti													
-170 + 250 mesh													
-250 +325 mesh													
Silicon Cycle													
-170 + 250 mesh													
-250 +325 mesh													
60Gr-40Ti													
50Gr-50Ti													
-170 + 250 mesh													
-250 +325 mesh													
Silicon Cycle													
-170 + 250 mesh													
-250 +325 mesh													
60Gr-40Ti													
50Gr-50Ti													
-170 + 250 mesh													
-250 +325 mesh													
Silicon Cycle													
-170 + 250 mesh													
-250 +325 mesh													
60Gr-40Ti													
50Gr-50Ti													
-170 + 250 mesh													
-250 +325 mesh													
Silicon Cycle													
-170 + 250 mesh													
-250 +325 mesh													
60Gr-40Ti													
50Gr-50Ti													
-170 + 250 mesh													
-250 +325 mesh													
Silicon Cycle													
-170 + 250 mesh													
-250 +325 mesh													
60Gr-40Ti													
50Gr-50Ti													
-170 + 250 mesh													
-250 +325 mesh													
Silicon Cycle													
-170 + 250 mesh													
-250 +325 mesh													
60Gr-40Ti													
50Gr-50Ti													
-170 + 250 mesh													
-250 +325 mesh													
Silicon Cycle													
-170 + 250 mesh													
-250 +325 mesh													
60Gr-40Ti													
50Gr-50Ti													
-170 + 250 mesh													
-250 +325 mesh													
Silicon Cycle													
-170 + 250 mesh													
-250 +325 mesh													
60Gr-40Ti													
50Gr-50Ti													
-170 + 250 mesh													
-250 +325 mesh													
Silicon Cycle													
-170 + 250 mesh													
-250 +325 mesh													
60Gr-40Ti													
50Gr-50Ti													
-170 + 250 mesh													
-250 +325 mesh													
Silicon Cycle													
-170 + 250 mesh													
-250 +325 mesh													
60Gr-40Ti													
50Gr-50Ti													
-170 + 250 mesh													
-250 +325 mesh													
Silicon Cycle													
-170 + 250 mesh													
-250 +325 mesh													
60Gr-40Ti													
50Gr-50Ti													
-170 + 250 mesh													
-250 +325 mesh													
Silicon Cycle													
-170 + 250 mesh													
-250 +325 mesh													
60Gr-40Ti													
50Gr-50Ti													
-170 + 250 mesh													
-250 +325 mesh													
Silicon Cycle													
-170 + 250 mesh													
-250 +325 mesh													
60Gr-40Ti													
50Gr-50Ti													
-170 + 250 mesh													
-250 +325 mesh													
Silicon Cycle													
-170 + 250 mesh													
-250 +325 mesh													
60Gr-40Ti													
50Gr-50Ti													
-170 + 250 mesh													
-250 +325 mesh													
Silicon Cycle													
-170 + 250 mesh													
-250 +325 mesh													
60Gr-40Ti													
50Gr-50Ti													
-170 + 250 mesh													
-250 +325 mesh													
Silicon Cycle													
-170 + 250 mesh													
-250 +325 mesh													
60Gr-40Ti													
50Gr-50Ti													
-170 + 250 mesh													
-250 +325 mesh													
Silicon Cycle													
-170 + 250 mesh													
-250 +325 mesh													
60Gr-40Ti													
50Gr-50Ti													
-170 + 250 mesh													
-250 +325 mesh													
Silicon Cycle													
-170 + 250 mesh													
-250 +325 mesh													
60Gr-40Ti													
50Gr-50Ti													
-170 + 250 mesh													
-250 +325 mesh													
Silicon Cycle													
-170 + 250 mesh													
-250 +325 mesh													
60Gr-40Ti													
50Gr-50Ti													
-170 + 250 mesh													
-250 +325 mesh													
Silicon Cycle													
-170 + 250 mesh													
-250 +325 mesh													
60Gr-40Ti													
50Gr-50Ti													
-170 + 250 mesh													
-250 +325 mesh													
Silicon Cycle													
-170 + 250 mesh													
-250 +325 mesh													
60Gr-40Ti													
50Gr-50Ti													
-170 + 250 mesh													
-250 +325 mesh													
Silicon Cycle													
-170 + 250 mesh													
-250 +325 mesh													
60Gr-40Ti													
50Gr-50Ti													
-170 + 250 mesh													
-250 +325 mesh													
Silicon Cycle													
-170 + 250 mesh													
-250 +325 mesh													
60Gr-40Ti													
50Gr-50Ti													
-170 + 250 mesh													
-250 +325 mesh													
Silicon Cycle													
-170 + 250 mesh													
-250 +325 mesh													
60Gr-40Ti													
50Gr-50Ti													
-170 + 250 mesh													
-250 +325 mesh													
Silicon Cycle													
-170 + 250 mesh													
-250 +325 mesh													
60Gr-40Ti													
50Gr-50Ti													
-170 + 250 mesh													
-250 +325 mesh													
Silicon Cycle													
-170 + 250 mesh													
-250 +325 mesh													
60Gr-40Ti													
50Gr-50Ti													
-170 + 250 mesh													
-250 +325 mesh													
Silicon Cycle													
-170 + 250 mesh													
-250 +325 mesh													
60Gr-40Ti													
50Gr-50Ti													
-170 + 250 mesh													
-250 +325 mesh													
Silicon Cycle													
-170 + 250 mesh													
-250 +325 mesh													
60Gr-40Ti													
50Gr-50Ti													
-170 + 250 mesh													
-250 +325 mesh													
Silicon Cycle													
-170 + 250 mesh													
-250 +325 mesh													
60Gr-40Ti													
50Gr-50Ti													
-170 + 250 mesh													
-250 +325 mesh													
Silicon Cycle													
-170 + 250 mesh													
-250 +325 mesh													
60Gr-40Ti													
50Gr-50Ti													
-170 + 250 mesh													
-250 +325 mesh													
Silicon Cycle													
-170 + 250 mesh													
-250 +325 mesh													
60Gr-40Ti													
50Gr-50Ti													
-170 + 250 mesh													
-250 +325 mesh													
Silicon Cycle													
-170 + 250 mesh													
-250 +325 mesh													
60Gr-40Ti													
50Gr-50Ti													
-170 + 250 mesh													
-250 +325 mesh													
Silicon Cycle													
-170 + 250 mesh													
-250 +325 mesh													
60Gr-40Ti													
50Gr-50Ti													
-170 + 250 mesh													
-250 +325 mesh													
Silicon Cycle													
-170 + 250 mesh													
-250 +325 mesh													
60Gr-40Ti													
50Gr-50Ti													
-170 + 250 mesh													
-250 +325 mesh													
Silicon Cycle													
-170 + 250 mesh													
-250 +325 mesh													
60Gr-40Ti													
50Gr-50Ti													
-170 + 250 mesh													
-250 +325 mesh													
Silicon Cycle													
-170 + 250 mesh													
-250 +325 mesh													
60Gr-40Ti													
50Gr-50Ti													
-170 + 250 mesh													
-250 +325 mesh													
Silicon Cycle													
-170 + 250 mesh													
-250 +325 mesh													
60Gr-40Ti													
50Gr-50Ti													
-170 + 250 mesh													
-250 +325 mesh													
Silicon Cycle													
-170 + 250 mesh													
-250 +325 mesh													
60Gr-40Ti													
50Gr-50Ti													
-170 + 250 mesh													
-250 +325 mesh													
Silicon Cycle													
-170 + 250 mesh													
-250 +325 mesh													
60Gr-40Ti													
50Gr-50Ti													
-170 + 250 mesh													
-250 +325 mesh													
Silicon Cycle													
-170 + 250 mesh													
-250 +325 mesh													
60Gr-40Ti													
50Gr-50Ti													
-170 + 250 mesh													
-250 +325 mesh													
Silicon Cycle													
-170 + 250 mesh													
-250 +325 mesh													
60Gr-40Ti													
50Gr-50Ti													
-170 + 250 mesh													
-250 +325 mesh													
Silicon Cycle													
-170 + 250 mesh													
-250 +325 mesh													
60Gr-40Ti													
50Gr-50Ti													
-170 + 250 mesh													
-250 +325 mesh													
Silicon Cycle													
-170 + 250 mesh													
-250 +325 mesh													
60Gr-40Ti													
50Gr-50Ti													
-170 + 250 mesh													
-250 +325 mesh													
Silicon Cycle													
-170 + 250 mesh													
-250 +325 mesh													
60Gr-40Ti													
50Gr-50Ti													
-170 + 250 mesh													
-250 +325 mesh													
Silicon Cycle													
-170 + 250 mesh													
-250 +325 mesh													
60Gr-40Ti													
50Gr-50Ti													
-170 + 250 mesh													
-250 +325 mesh													
Silicon Cycle													
-170 + 250 mesh													
-250 +325 mesh													
60Gr-40Ti													
50Gr-50Ti													
-170 + 250 mesh													
-250 +325 mesh													
Silicon Cycle													
-170 + 250 mesh													
-250 +325 mesh													
60Gr-40Ti													
50Gr-50Ti													
-170 + 250 mesh													
-250 +325 mesh													
Silicon Cycle													
-170 + 250 mesh													
-250 +325 mesh													
60Gr-40Ti													
50Gr-50Ti													
-170 + 250 mesh													
-250 +325 mesh													
Silicon Cycle													
-170 + 250 mesh													
-250 +325 mesh													
60Gr-40Ti													
50Gr-50Ti													
-170 + 250 mesh													
-250 +325 mesh													
Silicon Cycle													
-170 + 250 mesh													
-250 +325 mesh													
60Gr-40Ti													
50Gr-50Ti													
-170 + 250 mesh													
-250 +325 mesh													
Silicon Cycle													
-170 + 250 mesh													
-250 +325 mesh													
60Gr-40Ti													
50Gr-50Ti													

Compilation of Weight Gain and Oxidation Performance for Specimens Coated in Factorial Run N

Cr-Ti Cycle				Si Cycle			
Activator	Activator Quantity	Temperature	Pressure	Time	Activator Quantity	Temperature	Pressure
NaF-CrCl ₃	6 w/o	2350° F	100 torr	10 hours	6 w/o	2000° F	100 torr
							4 hours

Run No. N

Cr-Ti Cycle											
-250 +325 mesh						-170 +250 mesh					
50Cr-50Ti						60Cr-40Ti					
No.	Cr-Ti	Si	Ratio	Oxidation	Weight Gain	No.	Cr-Ti	Si	Ratio	Oxidation	Weight Gain
11	17.9	24.6	0.73	1800°	2600°	21	15.2	26.3	0.58	1800°	2600°
12	17.7	24.4	0.72	17		22	15.1	25.7	0.59	11	
13	16.9	23.7	0.71	108		23	15.7	25.8	0.61	17	
14	18.7	24.2	0.71	26		24	15.1	26.0	0.58	11	
15	16.5	24.7	0.67			25	16.5	25.8	0.64	17	
16	16.9	25.2	0.67	120		26	16.2	25.8	0.63	168	
17	17.4	24.4	0.71	160		27	15.5	26.6	0.58	168	
18	18.2	24.9	0.73	144		28	15.7	26.0	0.60	144	
Avg.	17.5	24.5	0.71			Avg.	15.6	26.0	0.60		
31	15.9	24.4	0.65	136		61	14.2	25.4	0.56	144	
32	16.1	24.0	0.67	144		62	14.1	25.0	0.56	144	
33	16.3	24.6	0.66	144		63	13.8	25.6	0.54	136	
34	18.2	24.4	0.75	136		64	13.8	25.0	0.55	136	
35	18.3	25.4	0.72	13		65	14.4	25.1	0.57	10	
36	18.1	23.8	0.76	26		66	14.3	25.7	0.56	11	
37	16.5	24.0	0.69	13		67	15.8	25.1	0.63	10	
38	16.4	25.0	0.66	29		68	14.9	25.0	0.60	13	
Avg.	17.0	24.5	0.69			Avg.	14.4	25.2	0.57		
60Cr-40Ti						50Cr-50Ti					
No.	Cr-Ti	Si	Ratio	Oxidation	Weight Gain	No.	Cr-Ti	Si	Ratio	Oxidation	Weight Gain
41	17.5	25.0	0.70	10		31	17.5	25.0	0.70	1800°	2600°
42	14.8	25.0	0.59	13		32	18.1	25.2	0.72	19	
43	14.9	25.6	0.58	17		33	18.8	25.1	0.75	19	
44	14.5	26.4	0.55	10		34	19.4	24.8	0.78	17	
45	17.3	28.0	0.62	144		35	17.5	25.9	0.68	147	
46	15.0	24.7	0.61	144		36	18.0	24.4	0.74	144	
47	15.4	26.1	0.59	120		37	18.1	26.7	0.68	120	
48	14.8	27.4	0.54	144		38	18.1	24.7	0.73	120	
Avg.	15.2	26.0	0.58			Avg.	18.2	25.2	0.72		
81	16.0	25.8	0.62	136		71	17.8	25.2	0.71	136	
82	15.7	25.8	0.61	168		72	16.8	25.6	0.66	168	
83	16.4	25.8	0.64	160		73	16.4	25.6	0.64	160	
84	16.5	25.3	0.65	144		74	17.3	26.0	0.66	144	
85	16.2	26.5	0.61	29		75	17.6	25.1	0.70	17	
86	16.2	26.2	0.62	22		76	17.9	25.0	0.72	19	
87	16.5	25.6	0.64	29		77	17.9	25.4	0.70	17	
88	15.2	25.3	0.60	17		78	16.6	25.9	0.64	17	
Avg.	16.1	25.8	0.62			Avg.	17.3	25.5	0.68		

811000 Cycle
-170 + 250 mesh
-250 + 325 mesh

Compilation of Weight Gain and Oxidation Performance for Specimens Coated in Factorial Run 0

Gr-Ti Cycle				Si Cycle			
Activator	Quantity	Temperature	Pressure	Time	Activator	Quantity	Temperature
NaF-CrCl ₃	6 w/o	2250°F	100 torr	6 hours	2 w/o	2100°F	100 torr
				8 hours			

Run No. 0

Gr-Ti Cycle											
-250 + 325 mesh						-170 + 250 mesh					
500r-50Ti						500r-50Ti					
600r-40Ti						600r-40Ti					
No.	Gr-Ti	Si	Ratio	1800°	2600°	No.	Gr-Ti	Si	Ratio	1800°	2600°
11	6.4	27.9	0.23	5		41	7.6	28.7	0.26	64	
12	6.8	27.3	0.25	3		42	7.1	29.0	0.24	5	
13	6.6	29.4	0.22	22		43	6.9	31.0	0.22	13	
14	6.6	28.3	0.23	3		44	7.4	30.2	0.24	5	
15	7.7	26.4	0.29		9	45	7.9	30.0	0.26		68
16	.2	28.1	0.26		23	46	7.4	30.0	0.25		11
17	7.3	27.8	0.26		23	47	7.4	30.6	0.24		91
18	6.5	27.2	0.24		23	48	7.6	30.5	0.25		80
Avg.	6.9	27.8	0.25			Avg.	7.4	30.0	0.25		
51	6.1	27.3	0.22		51	81	7.2	29.8	0.24		51
52	6.8	26.5	0.26		9	82	7.3	29.3	0.25		12
53	6.9	28.5	0.24		13	83	7.2	29.6	0.24		91
54	6.6	28.5	0.23		91	84	6.5	30.7	0.21		80
55	.9	27.6	0.24		5	85	6.5	30.0	0.22		5
56	7.0	26.0	0.27		3	86	7.0	29.0	0.24		22
57	7.5	27.0	0.28		3	87	7.1	29.5	0.25		7
58	7.1	27.4	0.27		3	88	7.0	29.9	0.23		17
Avg.	6.9	27.4	0.25			Avg.	7.0	29.7	0.24		

Billson Cycle
-170 + 250 mesh
-250 + 325 mesh

Compilation of Weight Gain and Oxidation Performance for Specimens Coated in Factorial Run P

Gr-Ti Cycle				S1 Cycle			
Activator	Quantity	Temperature	Pressure	Time	Activator	Quantity	Pressure
NaF	6 w/o	2350° F	10 torr	10 hours		2 w/o	2000° F
							10 torr
							6 hours

Run No. P													
Gr-Ti Cycle													
-250 +325 mesh							-170 +250 mesh						
500r-50Ti							60r-40Ti						
Weight Gain							Weight Gain						
No.	Gr-Ti	S1	Ratio	Oxidation	No.	Gr-Ti	S1	Ratio	Oxidation	No.	Gr-Ti	S1	Ratio
11	17.4	29.2	0.49	1800°	29	21	15.2	31.2	0.49	22	31	15.9	29.9
12	16.3	29.1	0.56	13	22	22	14.5	30.1	0.48	36	32	16.5	30.1
13	16.3	28.9	0.56	191	23	23	15.4	29.7	0.52	47	33	16.6	29.6
14	15.4	28.7	0.54	22	24	24	16.1	29.3	0.55	10	34	17.3	28.8
15	16.3	28.7	0.57		25	25	13.2	30.2	0.44		35	16.1	29.6
16	15.0	28.7	0.52	150	26	26	14.7	29.3	0.50	150	36	16.5	29.6
17	15.3	27.5	0.56	134	27	27	14.1	28.8	0.49	150	37	16.2	28.2
18	15.7	24.2	0.54	189	28	28	15.6	30.8	0.51	230	38	15.8	28.6
AVG.	15.6	28.8	0.54	191	AVG.	14.9	29.9	0.50		AVG.	16.4	29.2	0.55
19	16.1	29.4	0.55	158	61	15.2	29.9	0.50		71	16.3	28.5	0.56
20	16.8	28.0	0.60	128	62	15.0	30.2	0.50	150	72	17.6	27.6	0.57
21	17.0	28.1	0.60	170	63	16.7	32.2	0.52	99	73	16.6	27.8	0.60
22	16.4	29.2	0.56	187	64	14.3	29.2	0.49	251	74	15.5	28.8	0.54
23	17.1	28.8	0.59		65	14.5	28.9	0.50	13	75	17.3	28.1	0.62
24	15.8	27.9	0.57	22	66	14.0	29.0	0.48	13	76	17.5	28.4	0.62
25	14.4	27.2	0.53	104	67	12.0	29.8	0.40	13	77	19.3	28.4	0.65
26	14.9	23.4	0.52	17	68	19.8	30.4	0.65	13	78	16.8	28.9	0.55
AVG.	16.1	28.4	0.57		AVG.	15.2	30.0	0.51		AVG.	17.1	28.3	0.60

500r-50Ti

60r-40Ti

500r-50Ti

60r-40Ti

500r-50Ti

60r-40Ti

500r-50Ti

60r-40Ti

500r-50Ti

60r-40Ti

500r-50Ti

60r-40Ti

500r-50Ti

60r-40Ti

500r-50Ti

60r-40Ti

500r-50Ti

60r-40Ti

500r-50Ti

60r-40Ti

500r-50Ti

60r-40Ti

500r-50Ti

60r-40Ti

500r-50Ti

60r-40Ti

500r-50Ti

60r-40Ti

UNCLASSIFIED

Security Classification

DOCUMENT CONTROL DATA - R&D		
(Security classification of title, body of abstract and indexing annotation must be entered when the overall report is classified)		
1 ORIGINATING ACTIVITY (Corporate author) Equipment Laboratories TRW, INC. 23555 Euclid Avenue, Cleveland, Ohio 44117		2a REPORT SECURITY CLASSIFICATION UNCLASSIFIED
		2b GROUP
3 REPORT TITLE Manufacturing Methods for High Temperature Coating of Large Columbium Parts.		
4 DESCRIPTIVE NOTES (Type of report and inclusive dates) Final Technical Report 1 December 1964 to 1 April 1968		
5 AUTHOR(S) (Last name, first name, initial) Fisch, Herbert A. Gadd, John D.		
6 REPORT DATE May 1968	7a. TOTAL NO. OF PAGES 299	7b. NO. OF REFS 14
8a CONTRACT OR GRANT NO. AF 33(615)-2018	9a. ORIGINATOR'S REPORT NUMBER(S) ER-7268	
b PROJECT NO 8-183	9b. OTHER REPORT NO(S) (Any other numbers that may be assigned this report) AFML-TR-68-134	
10 AVAILABILITY/LIMITATION NOTICES This document is subject to special export controls and each transmittal to foreign governments or foreign nationals may be made only with prior approval of the Air Force Materials Laboratory (MATC), Wright-Patterson Air Force Base, Ohio 45433		
11 SUPPLEMENTARY NOTES Qualified requesters may obtain copies of this report from DDC.	12. SPONSORING MILITARY ACTIVITY Air Force Materials Laboratory Air Force Systems Command Wright-Patterson Air Force Base, Ohio	
13 ABSTRACT A program was conducted to develop a manufacturing method for producing the high temperature oxidation resistant Cr-Ti-Si coating on large columbium parts. The program was accomplished in three principle development areas: 1) scale-up of the diffusion pack process for producing the Cr-Ti-Si coatings, 2) scale-up of the slurry diffusion process for producing this coating, and 3) production proof of the slurry diffusion process. A vacuum furnace with hearth dimensions of 42" diameter X 48" high was constructed and successfully adapted to application of the Cr-Ti-Si coating. Cr-Ti-Si coatings formed in the production-scale furnace by both the vacuum pack and slurry-diffusion methods reliably protected columbium alloys from oxidation for times greater than 125 hours at 1800°F and 50 hours at 2600°F. Three secondary areas of investigation were also undertaken: 1) an investigation of the effects of edge preparation and edge radius on the protection offered by the Cr-Ti-Si coating system; 2) a development using fused silicides, locally applied and fired either in argon or air, for repairing defects in unoxidized and oxidized coatings, and 3) an evaluation of the effect of the Cr-Ti-Si coatings system on the tensile properties of 0.018 inch Cb752 alloy sheet. This document is subject to special export controls and each transmittal to foreign governments or foreign nationals may be made only with prior approval of the Air Force Materials Laboratory (MATC), Wright-Patterson Air Force Base, Ohio. 45433		

DD FORM 1473
1 JAN 64

UNCLASSIFIED

Security Classification

14 KEY WORDS	LINK A		LINK B		LINK C	
	ROLE	WT	ROLE	WT	ROLE	WT
Chromium-Titanium-Silicon Coatings Coatings - Niobium Alloys Oxidation - Niobium Alloys Manufacturing Methods - Coatings						

INSTRUCTIONS

1. **ORIGINATING ACTIVITY:** Enter the name and address of the contractor, subcontractor, grantee, Department of Defense activity or other organization (*corporate author*) issuing the report.

2a. **REPORT SECURITY CLASSIFICATION:** Enter the overall security classification of the report. Indicate whether "Restricted Data" is included. Marking is to be in accordance with appropriate security regulations.

2b. **GROUP:** Automatic downgrading is specified in DoD Directive 5200.10 and Armed Forces Industrial Manual. Enter the group number. Also, when applicable, show that optional markings have been used for Group 3 and Group 4 as authorized.

3. **REPORT TITLE:** Enter the complete report title in all capital letters. Titles in all cases should be unclassified. If a meaningful title cannot be selected without classification, show title classification in all capitals in parenthesis immediately following the title.

4. **DESCRIPTIVE NOTES:** If appropriate, enter the type of report, e.g., interim, progress, summary, annual, or final. Give the inclusive dates when a specific reporting period is covered.

5. **AUTHOR(S):** Enter the name(s) of author(s) as shown on or in the report. Enter last name, first name, middle initial. If military, show rank and branch of service. The name of the principal author is an absolute minimum requirement.

6. **REPORT DATE:** Enter the date of the report as day, month, year, or month, year. If more than one date appears on the report, use date of publication.

7a. **TOTAL NUMBER OF PAGES:** The total page count should follow normal pagination procedures, i.e., enter the number of pages containing information.

7b. **NUMBER OF REFERENCES:** Enter the total number of references cited in the report.

8a. **CONTRACT OR GRANT NUMBER:** If appropriate, enter the applicable number of the contract or grant under which the report was written.

8b, 8c, & 8d. **PROJECT NUMBER:** Enter the appropriate military department identification, such as project number, subproject number, system numbers, task number, etc.

9a. **ORIGINATOR'S REPORT NUMBER(S):** Enter the official report number by which the document will be identified and controlled by the originating activity. This number must be unique to this report.

9b. **OTHER REPORT NUMBER(S):** If the report has been assigned any other report numbers (either by the originator or by the sponsor), also enter this number(s).

10. **AVAILABILITY/LIMITATION NOTICES:** Enter any limitations on further dissemination of the report, other than those

imposed by security classification, using standard statements such as:

- (1) "Qualified requesters may obtain copies of this report from DDC."
- (2) "Foreign announcement and dissemination of this report by DDC is not authorized."
- (3) "U. S. Government agencies may obtain copies of this report directly from DDC. Other qualified DDC users shall request through _____."
- (4) "U. S. military agencies may obtain copies of this report directly from DDC. Other qualified users shall request through _____."
- (5) "All distribution of this report is controlled. Qualified DDC users shall request through _____."

If the report has been furnished to the Office of Technical Services, Department of Commerce, for sale to the public, indicate this fact and enter the price, if known.

11. **SUPPLEMENTARY NOTES:** Use for additional explanatory notes.

12. **SPONSORING MILITARY ACTIVITY:** Enter the name of the departmental project office or laboratory sponsoring (paying for) the research and development. Include address.

13. **ABSTRACT:** Enter an abstract giving a brief and factual summary of the document indicative of the report, even though it may also appear elsewhere in the body of the technical report. If additional space is required, a continuation sheet shall be attached.

It is highly desirable that the abstract of classified reports be unclassified. Each paragraph of the abstract shall end with an indication of the military security classification of the information in the paragraph, represented as (TS), (S), (C), or (U).

There is no limitation on the length of the abstract. However, the suggested length is from 150 to 225 words.

14. **KEY WORDS:** Key words are technically meaningful terms or short phrases that characterize a report and may be used as index entries for cataloging the report. Key words must be selected so that no security classification is required. Identifiers, such as equipment model designation, trade name, military project code name, geographic location, may be used as key words but will be followed by an indication of technical context. The assignment of links, rules, and weights is optional.